UNIVERSITY *of the*
WESTERN CAPE

Development of a Bismuth-Silver Nanofilm Sensor for the Determination of
Platinum Group Metals in Environmental Samples

By

Charlton van der Horst

MSc (Chemistry)

Submitted in fulfilment of the requirements for the degree

DOCTOR OF PHILOSOPHY

in the

Department of Chemistry

Faculty of Science

University of the Western Cape

February, 2015

Supervisors: **Dr V.S. Somerset**
Prof. E.I. Iwuoha

Declaration

I declare that:

Development of a Bismuth-Silver Nanofilm Sensor for the Determination of Platinum Group Metals in Environmental Samples

is my own work, that is has not been submitted for any degree or examination in any other university, and that all the sources I have used or quoted have been indicated and acknowledged by complete references.

Charlton van der Horst

Signature: ………………………….

Date: ………………………….

Summary

Nowadays, the pollution of surface waters with chemical contaminants is one of the most crucial environmental problems. These chemical contaminants enter rivers and streams resulting in tremendous amount of destruction, so the detection and monitoring of these chemical contaminants results in an ever-increasing demand. This thesis describes the search for a suitable method for the determination of platinum group metals (PGMs) in environmental samples due to the toxicity of mercury films and the limitations with methods other than electroanalytical methods. This study focuses on the development of a novel bismuth-silver bimetallic nanosensor for the determination of PGMs in roadside dust and soil samples. Firstly, individual silver, bismuth and novel bismuth-silver bimetallic nanoparticles were chemically synthesised. The synthesised nanoparticles was compared and characterised by cyclic voltammetry (CV), electrochemical impedance spectroscopy (EIS), ultraviolet-visible spectroscopy (UV-Vis), Fourier-transformed infrared spectroscopy (FT-IR), Raman spectroscopy, and transmission electron microscopy (TEM) analysis to interrogate the electrochemical, optical, structural, and morphological properties of the nanomaterials. The individual silver, bismuth, and bismuth-silver bimetallic nanoparticles in the high resolution transmission electron microscopy results exhibited an average particle size of 10-30 nm. The electrochemical results obtained have shown that the bismuth-silver bimetallic nanoparticles exhibit good electro-catalytic activity that can be harnessed for sensor construction and related applications. The ultraviolet-visible spectroscopy, Fourier-transformed infrared spectroscopy, and Raman spectroscopy results confirmed the structural properties of the novel bismuth-silver bimetallic nanoparticles. In addition the transmission electron microscopy and selected area electron diffraction morphological characterisation confirmed the nanoscale nature of the bismuth-silver bimetallic nanoparticles.

Secondly, a sensitive adsorptive stripping voltammetric procedure for palladium, platinum and rhodium determination was developed in the presence of dimethylglyoxime (DMG) as the chelating agent at a glassy carbon electrode coated with a bismuth-silver bimetallic nanofilm. The nanosensor further allowed the adsorptive stripping voltammetric detection of PGMs without oxygen removal in solution. In this study the factors that influence the stripping performance such as composition of supporting electrolyte, DMG concentration, deposition potential and time studies, and pH have been investigated and optimised. The bismuth-silver bimetallic nanosensor was used as the working electrode with

0.2 M acetate buffer (pH = 4.7) solution as the supporting electrolyte. The differential pulse adsorptive stripping peak current signal was linear from 0.2 to 1.0 ng/L range (60 s deposition), with limit of detections for Pd (0.19 ng/L), Pt (0.20 ng/L), Rh (0.22 ng/L), respectively. Good precision for the sensor application was also obtained with a reproducibility of 4.61% for Pd(II), 5.16% for Pt(II) and 5.27% for Rh(III), for three measurements. Investigations of the possible interferences from co-existing ions with PGMs were also done in this study. The results obtained for the study of interferences have shown that Ni(II) and Co(II) interfere with Pd(II), Pt(II) and Rh(III) at high concentrations. The interference studies of Cd(II), Pb(II), Cu(II) and Fe(III) showed that these metal ions only interfere with Pd(II) and Pt(II) at high concentrations, with no interferences observed for Rh(III). Phosphate and sulphate only interfere at high concentrations with Pt(II) and Rh(III) in the presence of DMG with 0.2 M acetate buffer (pH = 4.7) solution as the supporting electrolyte.

Based on the experimental results, this bismuth-silver bimetallic nanosensor can be considered as an alternative to common mercury electrodes, carbon paste and bismuth film electrodes for electrochemical detection of PGMs in environmental samples.

Thirdly, this study dealt with the development of a bismuth-silver bimetallic nanosensor for differential pulse adsorptive stripping voltammetry (DPAdSV) of PGMs in environmental samples. The nanosensor was fabricated by drop coating a thin bismuth-silver bimetallic film onto the active area of the SPCEs. Optimisation parameters such as pH, DMG concentration, deposition potential and deposition time, stability test and interferences were also studied. In 0.2 M acetate buffer (pH = 4.7) solution and DMG as the chelating agent, the reduction signal for PGMs ranged from 0.2 to 1.0 ng/L. The detection limit for Pd(II), Pt(II) and Rh(III) was found to be 0.07 ng/L, 0.06 ng/L and 0.2 ng/L, respectively. Good precision for the sensor application was also obtained with a reproducibility of 7.58% for Pd(II), 6.31% for Pt(II) and 5.37% for Rh(III), for three measurements. In the study of possible interferences, the results have shown that Ni(II), Co(II), Fe(III), Na^+, SO_4^{2-} and PO_4^{3-} does not interfere with Pd(II) in the presence of DMG with sodium acetate buffer as the supporting electrolyte solution. These possible interference ions only interfere with Pt(II) and Rh(III) in the presence of DMG with 0.2 M acetate buffer (pH = 4.7) as the supporting electrolyte solution.

Dedication

This thesis is dedicated to my father, the late Nicolaas Jacobus van der Horst
and my grandmother, the late Wilhelmina Sauls (R.I.P).

Acknowledgement

I am grateful to my supervisor Dr. Vernon Somerset for his positive attitude, help, support, encouragement, his valuable ideas, assistance and sharing his enormous amount of knowledge and practical experience throughout this project. Thanks to Professor Emmanuel Iwuoha, who was my supervisor at the SensorLab, University of the Western Cape, it is much appreciated. The assistance provided by the Council for Scientific and Industrial Research (CSIR) in Stellenbosch where I was based during my studies, and financial support from the Department of Science and Technology (DST) / National Research Foundation (NRF) Professional Development Programme (PDP) is also gratefully acknowledged.

Special thanks to my colleague Bongiwe Silwana for a warm social working environment. I thank you for being friendly, cheerful, and helpful throughout my B.Tech, MSc and PhD studies. I also thank the staff of the Analytical Laboratory (CAS, CSIR, Stellenbosch) for their advice, encouragement, support and friendship.

I am very grateful to my family for their support and encouragement. Special thanks to my mother for being positive and believing in me. Thanks to my sisters, my brother, brother and sister in law for their support and also believing in me. Thanks to my son, Kimi for helping me understand the important things in my life, giving me new perspectives, making my every day special and my life meaningful. I am grateful to Hakeem, Manesia, Ilne, Cia, Nigel, Melbourne, Yada for their support.

To all my friends Ferdinand Daniels, Colin Goliath, Eddie Goliath, Warren Klazen, Edgar van Rooyen, Ricardo Manus for their friendship and support.

Finally I would like to thank our mighty God who gave me the opportunity and power to fulfil my dreams.

Acronyms and Abbreviations

AAS	Atomic absorption spectroscopy
AdSV	Adsorptive stripping voltammetry
AE	Amalgam electrodes
AFM	Atomic force microscopy
AFS	Atomic fluorescence spectroscopy
Ag/AgCl	Silver silver chloride
$AgBiS_2$	Silver bismuth sulphide
Ag/GCE	Silver glassy carbon electrode
Ag/MFGC	Mercury-doped silver nanoparticle film glassy carbon
$AgNO_3$	Silver nitrate
AgSAE	Silver solid amalgam electrode
Al_2O_3	Alumina
AMS	Accelerator mass spectrometry
ANDO	Acenaphthenequinone dioxime
ASSWV	Anodic stripping square wave voltammetr
ASV	Anodic stripping voltammetry
AuSAE	Gold solid amalgam electrode
Bi-Ag	Silver bismuth bimetallic
Bi-AgFE	Bismuth-silver bimetallic film electrode
Bi-Ag NPs	Bismuth-silver bimetallic nanoparticles
BiF	Bismuth film
BiFEs	Bismuth film electrodes
$Bi(NO_3)_3\ 5H_2O$	Bismuth nitrate pentahydrate
CILE	Carbon ionic liquid electrode
CMEs	Chemical modified electrodes

CNS	Central nervous system
CNTs	Carbon nanotubes
CPEs	Carbon paste electrodes
CRTs	Cathode ray tubes
CSV	Cathodic stripping voltammetry
CuSAE	Copper solid amalgam electrode
CV	Cyclic voltammetry
DCV	Direct current voltammetry
DLS	Dynamic light scattering
DMF	*N,N*-dimethylformamide
DMG	Dimethylglyoxime
DNA	Deoxyribonucleic acid
DPAdSV	Differential pulse adsorptive stripping voltammetry
DPP	Differential pulse polarography
DPV	Differential pulse voltammetry
EDTA	Ethylenediaminetetraacetic acid
EIS	Electrochemical impedance spectroscopy
ESRS	Electron spin resonance
FT-IR	Fourier transforms infrared spectroscopy
GC	Gas condensation
GCEs	Glassy carbon electrodes
GC/Bi-AgFE	Glassy carbon bismuth-silver film electrode
GC/BiFE	Glassy carbon bismuth silver film electrode
GFAAS	Graphite furnace atomic absorption spectrometry
Hg(Ag)FE	Silver amalgam film electrode
HMDE	Hanging mercury drop electrode
HMTA	Hexamethylene tetramine
H_2NaPO_4	Sodium phosphate

HPLC-ICP-MS	High performance liquid chromatography-inductive coupled plasma mass spectrometry
HR-ICP-MS	High resolution inductive coupled plasma mass spectrometry
HRTEM	High resolution transmission electron microscopy
ICP	Inductively coupled plasma
ICP-AES	Inductive coupled plasma atomic emission spectrometry
ICP-MS	Inductive coupled plasma mass spectrometry
ICP-OES	Inductively coupled plasma-optical emission spectrometry
INAA	Instrumental neutron activation analysis
LODs	Limits of detections
LSV	Linear stripping voltammetry
Me(HDMG)$_2$	Metal complexes
MeSAEs	Metallic solid amalgam electrode
MFE	Mercury film electrode
M-O	Metal-oxygen
MRSI	Magnetic resonance spectroscopic imaging
MS	Mass spectrometer
NaBH$_4$	Sodium boronhydride
NaOAc	Sodium acetate
Na$_2$SO$_4$	Sodium sulphate
NH$_3$	Ammonia
NH$_4$Cl	Ammonium chloride
NMR	Nuclear magnetic resonance
NPs	Nanoparticles
p-AgSAE	Polished silver solid amalgam electrode
PANI	Poly-aniline
Pd-DMG	Palladium dimethylglyoxime complex
PGMs	Platinum group metals
PIXE	Particle induced X-ray excitation

PSA	Potentiometric stripping analysis
Pt-DMG	Platinum dimethylglyoxime complex
PVA	Polyvinyl alcohol
PZT	Piezoelectric
Rh-DMG	Rhodium dimethylglyoxime complex
SAED	Selected area diffraction patterns
SEM	Scanning electron microscopy
SIMS	Secondary ion mass spectrometry
SPCEs	Screen-printed carbon electrodes
SPC/Bi-AgFE	Screen-printed carbo bismuth-silver film electrode
SPC/BiFE	Screen-printed carbon electrode bismuth-silver film electrode
SPEs	Screen-printed electrodes
SPR	Surface plasmon resonance
SWV	Square wave voltammetry
SWASV	Square wave anodic stripping voltammograms
TEM	Transmission electron microscopy
TXRF	Total reflection X-ray fluorescence spectrometry
UV-Vis	Ultraviolet visible spectroscopy
XPS	X-ray photoelectron spectroscopy
XRD	X-ray diffraction
XRF	X-ray fluorescence spectroscopy

List of Publications and Presentations

Publications

1. **Charlton van der Horst**, Bongiwe Silwana, Emmanuel Iwuoha and Vernon Somerset. (**2015**). Synthesis and characterisation of bismuth-silver bimetallic nanoparticles for electrochemical sensor applications. *Analytical Letters*, 48(8). (Accepted).

2. **Charlton van der Horst**, Bongiwe Silwana, Emmanuel Iwuoha and Vernon Somerset. (**2015**). Modified glassy carbon electrode bismuth-silver bimetallic nanosensor characterisation for the voltammetric analysis of dust and soil samples. *Journal of Electroanalytical Chemistry*. (Submitted).

3. **Charlton van der Horst**, Bongiwe Silwana, Emmanuel Iwuoha and Vernon Somerset. (**2015**). Spectroscopic and voltammetric analysis of platinum group metals in environmental samples. Comparative analysis of roadside soil and dust samples. *Chemosphere*. (Prepared).

Oral and Poster Presentations at Conferences

1. **Charlton van der Horst**, Bongiwe Silwana, Vernon Somerset, Emmanuel Iwuoha. Adsorptive stripping voltammetric determination of palladium, platinum and rhodium as dimethylglyoxime complexes. Paper presented at the WISA 2012 Biannual Conference, CTICC, Cape Town, South Africa, 6 – 10 May 2012. [Poster presentation]

2. Chavon Walters, Vernon Somerset, **Charlton van der Horst**, Bongiwe Silwana, Shirley Le Roux and Emmanuel Iwuoha. Spatial distribution of trace metals in water resources impacted by PGM activities. Paper presented at the WISA 2012 Biannual Conference, CTICC, Cape Town, South Africa, 6 – 10 May 2012. [Poster presentation]

3. **Charlton van der Horst**, Bongiwe Silwana, Emmanuel Iwuoha and Vernon Somerset. Stripping voltammetric determination of palladium, platinum and rhodium in freshwater and sediment samples from South African water resources. Paper presented at the 2nd International Symposium on Electrochemistry, Electrochemistry for Energy, University of the Western Cape, Bellville, South Africa, 19 – 20 July 2012. [Poster presentation]

4. Chavon Walters, **Charlton van der Horst**, Bongiwe Silwana, Emmanuel Iwuoha and Vernon Somerset. Spatial distribution of metal concentrations in water resources closely situated to mining activities. Paper presented at the 13th WaterNet/WARFSA/GWP-SA International Symposium on Integrated Water Resource Management, Birchwood Hotel and OR Tambo Conference Centre, Johannesburg, South Africa, 31 October – 2 November 2012. [Poster presentation]

5. **Charlton Van der Horst**, Emmanuel Iwuoha, Bongiwe Silwana and Vernon Somerset. Synthesis and characterisation of bismuth-silver amalgam nanoparticles for electrochemical sensor applications. Paper presented at the 13th Topical Meeting of the International Society of Electrochemistry (ISE). Theme: Advances in Electrochemical Materials, Science and Manufacturing. CSIR International Conference Centre, Pretoria, South Africa, 7 – 10 April, 2013. [Poster presentation]

6. **Charlton van der Horst**, Bongiwe Silwana, Emmanuel Iwuoha and Vernon Somerset. Construction and application of a bismuth-silver amalgam nanoparticles sensor in environmental analysis. Paper presented at the Third Regional Conference of the Southern African Young Water Professionals. Konservatorium, University of Stellenbosch, Stellenbosch, South Africa, 16 – 18 July, 2013 [Poster presentation]

7. **Charlton van der Horst**, Bongiwe Silwana, Emmanuel Iwuoha and Vernon Somerset. Analysis of platinum group metals in environmental sediment samples. Paper presented at the SANCIAHS2014 Conference, School of Public Health Building, University of Western Cape, Bellville, Cape Town, 01 – 03 September 2014. [Poster presentation

Reports

1. V Somerset, **C van der Horst**, B Silwana, C Walters, E Iwuoha, S le Roux. (**2012**). Development of Analytical Sensors for the Identification and Quantification of Metals in Environmental Samples. Water Research Commission (WRC). *Report Number: 2013/1/12.*

UNIVERSITY *of the*

WESTERN CAPE

Table of Contents

UNIVERSITY *of the*

WESTERN CAPE

List of Figures

List of Tables

Chapter 1

Introduction

1.1. Introduction

Heavy and platinum group metal (PGM) contaminations at trace levels in water resources presents a major current environmental threat, so the detection and monitoring of these metal contaminants results in an ever-increasing demand. In the simultaneous determination of heavy metal ions in water, sediment and biota samples, several methods have been established such as atomic absorption spectroscopy (AAS), inductive coupled plasma-mass spectroscopy (ICP-MS), and atomic fluorescence spectroscopy (AFS) and X-ray fluorescence spectroscopy (XRF). These methods are highly sensitive and efficient but require sophisticated and expensive instruments, highly qualified technicians and tedious sample pre-treatments. These methods are also not suitable for field analysis of multiple samples and are very time consuming. The problems with these methods are the demand for more sensitive methods such as electro-analytical techniques that are inexpensive, rapid, reproducible and accurate in environmental sample monitoring. A wide range of inorganic and organic substances can be detected by electro-analytical techniques because it a very efficient, versatile and highly sensitive (Liu *et al*., 2008; Hildebrandt *et al*., 2008; Raman, *et al*., 2009; Heitzmann *et al*., 2005; Wang 1994).

In electro-analytical techniques, the technique of anodic stripping voltammetry (ASV) is now widely used in heavy and platinum group metal analysis in environmental samples. The technique offers low limits of detection of sub-ppb-concentrations and is based on the controlled electrolytical accumulation of metal ions of interest.

In this study a working electrode of bismuth-silver bimetallic was constructed to determine platinum, palladium and rhodium in environmental samples. The study will start with the synthesis and characterisation of a novel true metallic film for stripping analysis and to differentiate between single Ag, Bi, and Bi-Ag bimetallic nanoparticles for electrochemical sensor application. The novel bismuth-silver bimetallic nanoparticles will be drop-coated

onto glassy carbon electrodes (GCEs) and screen-printed carbon electrodes (SPCEs) for the analysis of PGMs in roadside soil and dust samples using acetate buffer (pH = 4.7) solution as the supporting electrolyte. The novelty of this study lies in the construction of a Bi-Ag bimetallic nanosensor that can be applied in stripping voltammetric analysis for the determination of metal ions in environmental samples.

1.2. Electrochemical sensors

The mercury film electrode (MFE) and hanging mercury drop electrode (HMDE) was known as the traditional working electrode materials for the simultaneous determination of heavy metals in anodic stripping voltammetry (ASV) measurements. Nowadays, many researchers request alternative working electrodes because in some countries the use of mercury for sensor platforms is completely banned due to its considerable toxicity. The search is therefore ongoing to find new alternative sensing materials with suitable recognition elements that can be used for the detection of heavy and platinum group metals (PGMs). Various types of mercury-free working electrodes including silver electrodes, glassy carbon electrodes (GCEs), bismuth film electrodes (BiFEs), carbon nanotubes (CNTs), screen-printed carbon electrodes (SPCEs) or carbon paste electrodes (CPEs) has been used for heavy metal determination (Khezri *et al*., 2008; Senthilkumar and Saraswathi, 2009; Abdollah and Fatemeh, 2009; Li *et al*., 2009; Somerset *et al*., 2010; Maiti *et al*., 2009).

Figure 1 is a good illustration of a chemical sensor.
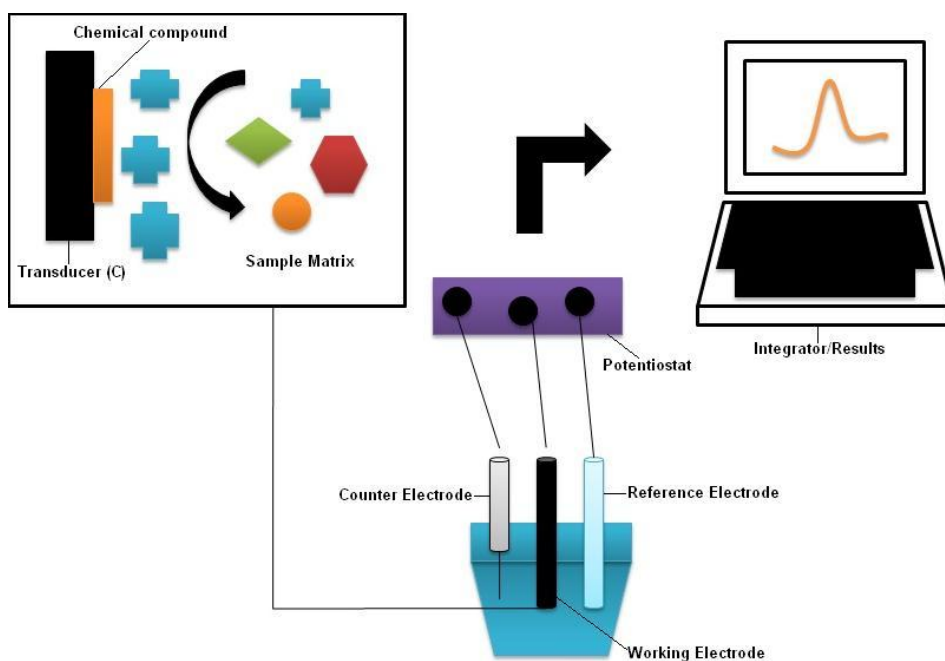
Figure 1.   **Illustration of a chemical sensor (Prakash *et al*., 2012).**

The noble nanoparticles (NPs) especially silver and gold NPs have attracted a great deal of attention as chemical modifiers in the construction of electrochemical or optical sensors due to their small sizes, unique electronic, catalytic and optical properties. In these electrochemical sensors the overpotentials of many analytes can be decreased at common unmodified electrodes (Rena *et al*., 2005; Zheng *et al*., 2002; Yantasee *et al*., 2005; Ordeig *et al*., 2006).

1.3. Electrochemical characterisation

Electrochemical characterisation has been proven to determine trace metals, polymers and nanoparticles (NPs) in various samples of environmental, clinical and industrial origin. In electrochemical characterisation different techniques are used to determined analytes, e.g. electrolysis, voltammetry, polarography, amperometry, potentiometry, and coulometry.

Voltammetry is widely used in inorganic, physical and biological chemistry for non-analytical purposes including fundamental studies of redox processes, effect of solvent on electrode reaction, adsorption processes on surfaces and electron transfer mechanisms at

chemically modifies electrode. Voltammetry and particularly classical polarography was the main method for determining inorganic and certain organic species in aqueous solutions, in the 1950s. It is used in determining a variety of analytes, particularly those of pharmaceutical interest. Voltammetry can also be coupled with chromatographic techniques for analysis of complex matrices (Somerset, 2010).

In electrochemical characterisation cyclic voltammetry will be used to characterise the redox activity of the bismuth, silver and bismuth-silver nanoparticles in different electrolytes. In the construction of thin-film sensors, adsorptive stripping voltammetry will be used to determine the analyte of interest.

1.4. Platinum Group Metals

The excellent performance of platinum group metals (PGMs) in many catalytic processes results in a minimal release of these pollutants into the environment. Platinum group metals are very difficult to determined at low concentration levels, mainly due to their tendency to hydrolyse, the formation of poly-nuclear complexes and the ability of these PGMs to form many species in a given oxidation state. In the determination of PGMs some of the critical steps are the complete dissolution of the PGMs, quantitative conversion into stable complexes and their pre-concentration before final detection (Cordonna et al., 1989; Hartley, 1991; Rao and Reddi, 2000).

The world consumption of platinum is growing steadily and at present time the application of this precious metal is not only in jewelleries, healthcare and equipment, but also in the chemical industry. Together with rhodium and platinum, it serves as a compound for automotive catalyst and is used as a catalyst for organic synthesis (Zolotov et al., 2003; Buyanov and Pakhomov, 2001; Buslaeva, 1999).

In the field of analytical chemistry the determination of platinum must be accurate, sensitive and selective in many studies. Various methods have been described for the determination of platinum in different environmental samples. Adsorptive stripping voltammetry (AdSV) is a very good sensitive, selective method and is relatively cheap for the determination of platinum. According to those advantages AdSV is extremely useful for

platinum determination in the environmental samples (Begerow *et al*., 1997; Beinrohr *et al*., 1993; Elle *et al*., 1989; Lee *et al*., 1993).

1.5. Nanomaterials

Nowadays, nanoparticles (NPs) have become the platform for many sensing schemes in the field of analytical chemistry; especially NPs with different properties have found broad application in many kinds of analytical methods. The study, manipulation, creation and use of materials, devices and systems typically with dimensions smaller than 100 nm are known as nanotechnology or nanoscience. In the development of smarter chemical and biosensors, nanotechnology plays an increasingly important role. The design of new and improved sensing devices makes NPs very suitable for electrochemical and biosensors due to their unique chemical and physical properties. Many types of NPs of different sizes and compositions are now available, which facilitate their application in electro-analysis (Penn *et al*., 2003). According to Luo *et al*. (2005) the construction of electrochemical and biosensors, many kind of NPs such as semiconductor, oxide and metal NPs have been used and these NPs play different roles in different sensing systems and configurations.

Tunable optical properties of metal nanostructures can practically be applied as materials for optical filters, plasmonic device, surface-enhanced spectroscopy and sensors. The strong UV-Vis absorption band exhibited by these metal NPs is not present in the spectrum of the bulk metal and is the so called surface plasmon resonance (SPR) band. This surface plasmon resonance band arises from the surface plasmon oscillation modes of conduction band electrons in metal particles and strongly influences the linear and non-linear optical response of these metal NPs. The excellent conductivity and catalytic properties of metal NPs makes them suitable for acting as "electronic wires" to enhance the electron transfer between redox centers in proteins and electrode surfaces and as catalysts to increase electrochemical reactions (Shipway *et al*., 2000).

The preparation of metal NPs can be done by two routes, physical approach is the first one and it utilizes several methods such as laser ablation and condensation or evaporation. The second one is a chemical approach in which the metal ions in solution is reduced in

conditions favouring the subsequent formation of small metal clusters or aggregates (Oliveira *et al*., 2005; Egorova and Revina, 2000; Khomutov and Gubin, 2002).

1.6. Chelating agents for PGMs

The formation or presence of two or more separate bindings between a polydentate (multiple bonds) ligand and a single central atom is known as a chelation. Chelants, chelators, chelating agents or sequestering agents are usually organic compounds. The formation of a chelating complex results between the ligand and the substrate. Chelate complexes are contrasted with coordination complexes with monodentate ligands, which form only one bond with the central atom. Due to their high selectivity and sensitivity towards various metal ions dioximes such as dimethylglyoxime (DMG), a-furil dioxime, a-bend dioxime, cyclohexane-1.2-dione dioxime (Nioxime) and cycloheptane- 1.2-dione dioxinie (heptoxime), have received considerable attention in adsorptive stripping voltammetry. These dioximes have been used widely as reagents for the determination of transition metals, especially palladium and nickel. According to many studies, palladium and nickel form stable water-insoluble complexes with all dioximes (Girolami and Rauchfuss, 1999).

1.7. Research hypothesis

The development of a bismuth-silver nanofilm sensor can be an attractive alternative to the hanging mercury drop electrode (HDME) and common mercury film electrode (MFE) for the determination of platinum group metals in environmental samples.

1.8. Research Design / Methodology

1.8.1. Objectives of the Study

The following aims and objectives were identified:

(i)   The main aim of this investigation was the development and application of an electrochemical bimetallic nanosensor for the determination of platinum, palladium and rhodium in environmental samples.

(ii)   To characterise the synthesised bismuth, silver and bismuth-silver bimetallic nanoparticles by Raman spectroscopy, UV-Vis, FT-IR, SEM, TEM, EIS and cyclic voltammetry.

(iii)   The development and construction of the bimetallic nano electrochemical sensor involved the investigation, incorporation and optimisation of various nanoparticles and chelating materials (e.g. bismuth, silver, bismuth-silver bimetallic and dimethylglyoxime) for low level detection of these metal ions in environmental samples.

(iv)   The development, integration, testing and optimisation of screen-printed chemical sensor formats coated with the bimetallic NPs for sensor evaluation and determination of PGMs in environmental samples.

1.8.2. Approach

Certain key research questions and approaches for this study were identified, which included:

(i)   The chemical synthesis of individual silver, bismuth and bismuth-silver bimetallic nanoparticles and compare these silver and bismuth nanoparticles with novel bismuth-silver bimetallic nanoparticles.

(ii)   Characterisation of chemically synthesised nanoparticles using various analytical techniques such as cyclic voltammetry, spectroscopy techniques (e.g. FT-IR, UV-Vis, EIS, Raman), transmission electron microscopy (TEM) and scanning electron microscopy (SEM).

(iii)   The modification of GCE and SPCE surfaces with bismuth-silver bimetallic nanoparticle films, characterisation of these surfaces with various techniques and application of the sensor surfaces in stripping voltammetry measurements for PGMs determination.

(iv)   The detection of PGMs in appropriate model standard solutions.

(vi)   Application of the constructed chemical sensors to road-side dust and soil environmental samples for PGMs determination, including optimisation of pre-treatment steps of environmental samples to minimise interferences.
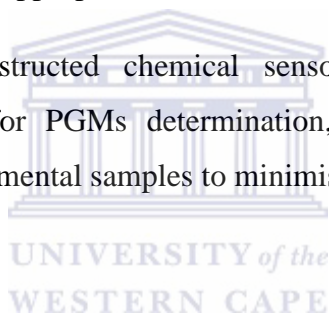
1.9. Layout of the Thesis

The thesis is divided into the following chapters:

Chapter 1   An introduction on the study of nanoparticles (NPs) for the construction of chemical sensors for the determination of platinum group metals (PGMs) in environmental samples are given with the main objectives, research hypothesis, research methodology and the layout of the thesis.

Chapter 2   A review of literature on the application of electrochemical sensors for the determination of platinum group metals in different environmental matrices are presented.

Chapter 3   Experimental methods and analytical techniques for characterisation of the synthesised metal NPs such as cyclic voltammetry, differential pulse voltammetry (DPV), and electrochemical impedances spectroscopy (EIS) are discussed. Other spectroscopic microscopic techniques such as scanning electron, transmission electron, FT-IR, UV-Vis and Raman spectroscopy are discussed.

Chapter 4   Nanoparticles synthesis and characterisation (e.g. bismuth, silver and bismuth-silver bimetallic) are presented and discussed.

Chapter 5   Optimisation and application of Bi-Ag bimetallic nanosensor is discussed, displaying the results obtained for cyclic voltammetry, the effect of chelating agent concentration, pH, deposition potential and time upon the peak current influence. The studies of sensor stability, interferences of different ions and application of the sensor to environmental samples are presented.

Chapter 6   PGMs analysis using screen-printed electrodes in roadside dust and soil samples is discussed.

Chapter 7   Summary, Conclusions, Recommendation and Future work.

Chapter 8   References

Appendices

Chapter 2

Review of literature on the application of electrochemical sensors for the determination of platinum group

2.1. Introduction

Water is one of the essentials enablers of life and has been central to the evolution of human civilisations from the beginning with the origin of the earliest form of life in seawater (Anshup, 2009). On the other hand noble metals have been similarly associated with the prosperity of human civilisations due to their prominent applications such as medicine and jewellery. The minimal reactivity at the bulk scale is the most important reason for the use of noble metals, which can explained by a number of concepts such as molecular orbital theory, electrochemical potential, relativisitic contraction, etc. The water quality has been associated with the development index of society and the quality of drinking water has been endangered by a number of chemical and biological contaminants (Anshup, 2009).

Platinum Group Metals (PGMs) contamination becomes more serious in the last decades due to dramatic growth in electronic and chemical industries, healthcare and equipment, jewelleries and as catalyst in exhaust converters (Ravindra *et al*., 2004). The analysis of PGMs is very cumbersome and is widely known that the results obtained often vary according to the analytical technique chosen. This, the determination of PGMs is of high interest. In environmental compartments such as sediments, biota and water, the concentration of these PGMs are relatively low. Bioaccumulation creates harmful levels of these PGMs towards the top of the food chain. Consumption of species near the top of the chain can result in high levels of PGMs within important organs in the human body causing asthma, allergy, rhino-conjunctivitis and other serious health problems (Zereini and Alt, 2000; Merget, 2000; Merget and Rosner, 2001).

Some researchers have conducted research work by using the hanging drop mercury electrode (HDME) and mercury film electrode (MFE) for the determination of PGMs in environmental samples (Khezri *et al*., 2008; Senthilkumar and Saraswathi, 2009). The use of

these working electrodes has been considered as undesirable by many researchers due to the toxicity of mercury. The use various mercury-free electrodes including gold-coated electrodes, silver electrodes, carbon paste electrodes (CPEs), glassy carbon electrodes (GCEs) and bismuth film electrodes (BiFEs) for sensitive PGMs determinations have been developed. The search to find new sensing materials with suitable recognition elements that can respond selectively and reversibly to specific metal ions is therefore ongoing (Abdollah and Fatemeh, 2009; Li *et al*., 2009; Somerset *et al*., 2010; Maiti *et al*., 2009).

According to Do Carmo *et al*. (2003) chemical modification of electrodes is a field of growing interest in analytical chemistry. The construction and application of chemical modified electrodes (CMEs) have received great attention in recent years due to its ability to accumulate metal ions on the basis of the interaction of these metal ions with functional group on the electrode surface. Chemical modified electrodes can be easily prepared, regenerate and modified with various modifiers and offer renewable and modified surfaces, including low background current interferences and are very cheap. The most common modifiers used for the determination of a specific analyte of interest are ligands, organic polymers, as well as inorganic ion-exchangers such as clays (Švancara *et al*., 2001; Fanjul-Bolado *et al*., 2008; Mojica and Merca, 2005; Raoof *et al*., 2007; Arrigan, 1994).

In the literature several studies report the determination of Pt, Pd and Rh in environmental samples (soil, sediments, air particulate matter, superficial water and vegetables) generally by spectroscopic techniques in the last decade (Barefoot and Van Loon, 1999; Barefoot, 1997; Djingova *et al*., 2003; Vlašánkova *et al*., 1999; Kanitsar *et al*., 2003; Lesniewska *et al*., 2004). The present review intends to highlight PGMs in environmental matrices and their different health effects to humans and aquatic life. The different electro-analytical techniques used for the analysis of PGMs, recent applications of electrochemical sensors for monitoring PGMs in sediments and surface waters will be discussed. Also to summarise the importance, construction and application of nanoparticle-based electrochemical sensors to PGMs determination.

2.2. Platinum group metals

Platinum group metals (PGMs) consisting of platinum (Pt), palladium (Pd), rhodium (Rh), ruthenium (Ru), iridium (Ir) and osmium (Os) are the most valuable metals. They have been described in a wide range of geotectonic setting but they are also associated with primary magmatic sulphides. These PGMs accumulate in different environmental samples such as water, sediment and biota, soil, airborne particulate matter and road dust at very low concentrations. The economic mineralisation of Pt and Pd are hosted in well-defined stratiform reefs of large layered intrusions such as the Stillwater Complex (USA), the Bushveld Complex (South Africa) and the Great Dyke (Zimbabwe). The Bushveld Complex in South Africa is the largest layered igneous complex in the world (Ravindra *et al*., 2004; Naldrett, 2010).

Heavy metals such as lead (Pb) or cadmium (Cd) plays a major role among pollutants of environmental concern and are well studied in respect of their effects on living organisms. Information on metals such as platinum group metals Pt, Pd, and Rh, which have been predominantly released in the last few decades as a consequence of anthropogenic activities, are scarce. These PGMs are release into the environment by mining, industries, hospitals (especially Pt, because it is used in anticancer drugs and dentistry), and other medical institutions. Automobile traffic are the greatest contributor of PGMs emissions due to the use of these metals in catalytic converters for purification of exhaust fumes from hydrocarbons, carbon monoxide, and nitrogen oxides (Kominkova *et al*., 2014; Merian *et al*., 2004; Rauch and Morrison, 2008; Sures *et al*., 2005; Ek *et al*., 2004).

Palladium are extensively used as artificial fibres, a feedstock in the manufacturing of packaging materials, jewellery, dental appliances and for industrial catalyst in the production of vinyl acetate monomer, or for production of terephthalic acid (PTA). These PGMs are used as thick-film resistors or conductors and also needed for passive electronic components such as very small multilayer ceramic capacitors. Palladium is also used in electrical equipment as Pd metal or palladium-silver pastes for active components such as transistors, hybrid circuits, diodes, semiconductor memories and integrated circuits (WHO, 2002).

Platinum has been extensively using as a catalyst in the chemical and petroleum industries in hydrogenation, cyclisation, dehalogenation, isomerisation, oxidation and

dehydration. It's also used in the catalytic upgrading of the octane rating of gasoline, in ammonia oxidation and in the production of nitric acid. Platinum has many high-temperature uses in the electrical industry such as platinum resistance thermometers, in electrochemical platinum electrodes, thermocouples and strain gauges, in printed circuits and in platinum resistance thermometers. This PGM is used in jewellery industry for rings and settings for gems and in the glassmaking industry and in the production of fibreglass. In medicine and dentistry it is also used in neurological and dental prostheses, for pacemaker electrodes and for recording electrical activity (Mason, 1966; Loebenstein, 1988).

Rhodium is extensively used in automotive catalysts due to its special catalytic activity to reduce nitrogen oxides (NO_x) to nitrogen (N_2). This PGM has a high and relatively uniform reflectivity and it produces hard, bright electrodeposits that easily led to the widespread use of rhodium in electrical contacts, jewellery, searchlight reflectors (Colombo, 2008; Stwertka, 2002; Raub, 1994).
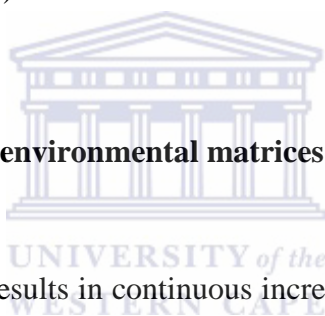
2.2.1. Platinum group metals in environmental matrices

Anthropogenic activities results in continuous increase in the amount of heavy metals and accumulation in the environment. Due to the toxicity of platinum group metals (PGMs) these PGMs can be dangerous to human health as a result of inhalation of fine particulate matter (aerodynamic diameter <10 µm), through food and water and direct contact with the dust. The concentrations of Pt(II), Pd(II) and Rh(III) has consequently increased in surface water, in vegetation and soil surfaces at sites next to roadways with high traffic density. In aqueous matrices (fresh and sea water) the concentrations are generally below 0.1 μg/L and in solid matrices (soil, plant and particulate matter) the concentrations are below 50 μg/kg (Pyrzynska, 2000; Sternbeck *et al*., 2002; Gomez *et al*., 2002; Hees *et al*., 1998; Palacios *et al*., 2000; Merian, 1991; Moldovan *et al*., 2002; Ravindra *et al*., 2004; Wayne, 1997).

It is known that the determination of airborne PGMs is very complicated. The most reliable, sensitive and accurate method for determination of these airborne PGMs is neutron activation analysis (NAA). According to the obtained data it is difficult to estimate the current level of Pt, Pd or Rh concentrations in air or to know the size of the particles that contain the PGMs. Since the introduction of exhaust gas catalysts, higher concentrations of

airborne PGMs were obtained and clearly correlated with a higher traffic density. Several authors (Renner and Schmuckler, 1991; Alt *et al*., 1993; Mukai *et al*., 1990) have conducted measurements of platinum in airborne particulate matter. Platinum concentrations in roadside dust collected on vegetation were determined in a range of 0.037 to 0.68 mg/kg by Hodge and Stellard (1986). In Japan the Pt concentrations were ranging from 0.073 to 0.184 mg/kg in samples of airborne particles. The use of neutron activation analysis for the analysis particles collected in Belgium and Italy, have shown platinum concentrations to be below the detection limit of 100 μg/kg (Gómez, 2002; Hodge and Stallard, 1986; Schutyser *et al*., 1977).

The deposition of platinum along roadways (on adjacent soils) might enter the vegetation and then the food cycle. Platinum may dispersed in water, silt, and soil, also accumulate in plants and a rapid accumulation in the environment was observed. This accumulation was determined between 1999 and 2005, observed along heavy traffic roads with enrichment factors between 2.1 and 8.9. A factor of 15 was also found and parallel to these findings elevated concentrations of Pt and Rh were found in airborne dust. In the north of Graz, near Kapfenberg (Styria, Austria) two studies were carried out on road dust collected in the ventilation shaft of a highway tunnel. The first study was a feasibility one and the second was a certification study. The results they obtained with 4 years in time difference between the studies, showed the average concentration of Pt increased from 55 ± 8 to 81 ± 6 *n*g/g (Moore *et al*., 2008; Zimmermann *et al*., 2004; Calamari *et al*., 1991; Whiteley and Murray, 2003; Schafer and Pulchet, 1998; Gomez *et al*., 1998; Wichmann *et al*., 2007; Liu *et al*., 2003; Yongming *et al*., 2006; Pacepac, 1998).

During rain events the deposited platinum on the road can be washed out and transported to urban rivers by means of storm-water outfalls and can be a threat to the freshwater ecosystem. In Göteborg (Sweden) specimens of *Asellus aquaticus* were sampled in urban rivers in order to determine the occurrence of platinum (Moldovani *et al*., 2001). For the urban river Mölndalsån water and sediment was also analysed and the experiments was used to evaluate the bioaccumulation of platinum under defined conditions (Wei and Morrison, 1994; Lashka *et al*., 1996; Rauch and Morrison, 1999).

2.2.2. Health effects

Dental alloys such as palladium and mercury releases cations continuously and they accumulate in the liver, thyroid, kidneys, central nervous system (CNS) and brain. The galvanic current densities of mercury and palladium are very high when they are near other metals, with the current densities of Pd alloys approximately 10 times higher than for high noble alloys. This galvanic current density causes extensive migration of mercury and palladium to tooth roots, saliva, gums, jaw and other parts of the body (Schedle *et al*., 1995; Bieger *et al*., 1996; Bonnig *et al*., 1990).

Many cases of palladium poisoning have result in the banning of palladium in dental alloys in Switzerland due to its toxicity and high mobility. Dentists in Germany have been warned by the German Health Ministry since 1993 not to use palladium-copper alloys. Palladium is cytotoxic and kills or damages cells and causes considerable damage and degradation of DNA and exacerbates hydroxyl radical damage. Palladium inhibits enzyme activity and function due to the damages of cell mitochondria (Kolesova *et al*., 1979; Spikes *et al*., 1969; Shultz *et al*., 1995; Kawata *et al*., 1981; Liu *et al*., 1997; Pillai *et al*., 1977).

Many studies on the toxicity of palladium were done in Germany and early symptoms of palladium toxicity include pain in teeth and jaw, cold feeling in mouth, fungus like coating in throat and sore throat, migraine headaches, swollen lymph nodes in the neck, extreme nervousness, extreme tiredness, confusion, memory loss, dizziness, burning of eyes, allergies, impairment of immune system, and blisters on body (Al-roubaie, 1986; Downey, 1989; Marcusson, 1996; Vilaplana *et al*., 1994).

The platinum halide salt complexes and the antitumour agent, *cis*-platin and its analogues are toxic to humans. The adverse health effects of the halide salt complexes are characterised by sensitisation and are known to be the most potent sensitisers. Studies on these sensitizers were done in occupational environments; the reports described irritation of the nose and throat with difficulty in breathing in workers in a photographic studio handling paper treated with complex platinum salts (Hunter *et al*., 1945).

Many studies on the toxicity of platinum were done in four British refineries and workers exposed to complex platinum salts exhibited repeated sneezing, rhinorrhoea, chest tightness, wheezing, shortness of breath and cyanosis, while a proportion of these also developed scaly

erythematous dermatitis with urticaria (Ravindra *et al*., 2004; Hunter *et al*., 1945). In the environment rhodium compounds are encountered relatively rarely by most people. There are almost no reported cases of human being affected by this element in any way. All rhodium compounds should be regarded as highly toxic and as carcinogenic and compounds of rhodium stain the skin very strongly. For rhodium no health effects of exposure investigations have been done to date. There are thus insufficient data available on the effect of rhodium on human health so special care must be taken with this substance (http://www.lenntech.com/periodic/elements/rh.htm#ixzz1vEl3Zy3P).

2.3. Electrochemical determination of platinum group metals

The most frequently used electroanalytical methods are voltammetry and amperometry. These electroanalytical methods are especially suitable for large scale of environmental monitoring of electrochemically active pollutants in various types of matrices (water, sediment, biota, etc.). They present an independent alternative to so far prevalent spectrometric and separation techniques, suitable for speciation, extremely sensitive and inexpensive (Wang, 2006).

Anodic stripping voltammetry (ASV) and adsorptive stripping voltammetry (AdSV) are the two most important voltammetric techniques used in water analysis. Cathodic stripping voltammetry (CSV) and potentiometric stripping analysis (PSA) are the other stripping techniques. Voltammetric techniques also include linear sweep voltammetry (LSV), differential pulse voltammetry (DPV), and square wave voltammetry (SWV), which are fast but not very sensitive techniques. Cyclic voltammetry (CV) is not sensitive enough for determination of trace metals in natural waters but is used to study electrode processes and finding optimum analytical conditions (Buffle *et al*., 2000).

According to Locatelli, (2007) voltammetric techniques with its great versatilities (high sensitivity, multicomponent analysis and low instrument cost) has allowed its application in a large number of analytical problems relevant to clinical, environmental, industrial and food matrices. The illustration of a typical electrochemical cell for voltammetric measurements is shown in Figure 2.
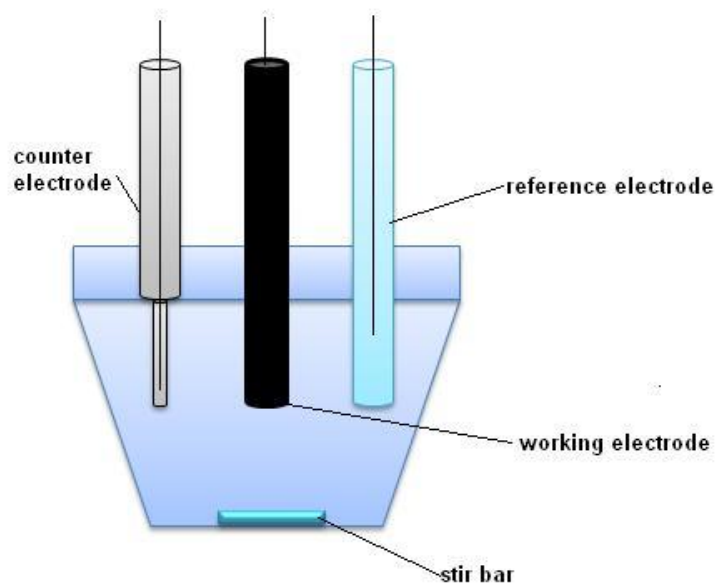
Figure 2. **An electrochemical cell used in different voltammetric techniques consisting of a working electrode, reference electrode and a counter electrode (Zhang, 2006).**

2.3.1. Electroanalytical techniques
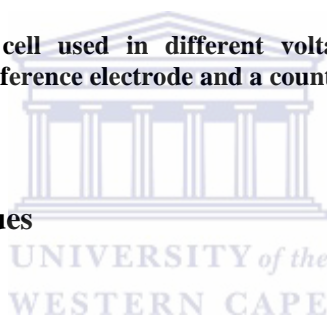
During the past two decades the use of stripping voltammetry has grown rapidly due to its low cost, its remarkable sensitivity with extremely low detection limits, can analyze non-metals such as anions or organics, suitability to on-line measurements, and its multiple elements, speciation capabilities and differentiates between free and complexed metal ions. Stripping voltammetry with its unique features of trace analysis has been reviewed. The development of multi-purpose instruments, the introduction of reliable working electrodes, modulated stripping modes (aimed at rejection the charging current) and a wide range of applications were done during the 1970s (Wang, 1985; Florence, 1984).

Adsorptive stripping voltammetry (AdSV) is the technique which involves the accumulation of the analyte of interest onto the electrode surface by adsorption, generally without electrolysis, followed by differential pulse, square wave or direct current voltammetric determination of the surface adsorbed species. The surface active species is formed during trace metal analysis by either reaction of the metal ion with a suitable reagent giving a complex which is then adsorbed on the electrode surface or by reaction of the metal

40

ion with the reagent adsorbed on the electrode surface. The reduction of the metal or ligand in the adsorbed complex or the catalytic evolution of hydrogen produced a current during the cathodic scan. According to the literature the adsorbed layer can be reduced during the cathodic scan giving low limits of detection. This AdSV results in procedures for measuring more than 25 trace metals, coupled with conventional stripping schemes, and about 45 elements are now measurable by stripping analysis. It also allows the simultaneous determination of 2-3 metals, based on the metal chelates peak potentials separations. In the presence of dissolved oxygen adsorptive stripping chronopotentiometry metal analysis are also possible (Maxwell and Smyth, 1996; Wang *et al*., 1989; Adeloju *et al*., 1984).

A powerful analytical method such as AdSV is used for the determination of ppb level of PGMs. This method is based on adsorptive deposition and stripping of PGM ion complex with a suitable ligand at the electrode surface. The low instrumentation and running costs with high sensitivity are the advantageous of AdSV and therefore becoming a widely accepted technique for the determination of trace amount of PGM ions (Cha *et al*., 2000; Wang, 1987; Brihaye and Dugckaerts, 1983; Staray and Kopanica, 1984; Hong *et al*., 1997).

2.3.2. Use of different electrodes
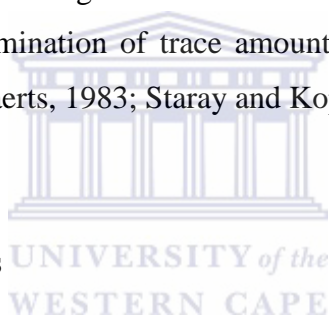
The different approaches and techniques that have been reported in the development of different environmental sensors are discussed and listed below in Table 1. Platinum group metal concentration was determined in superficial water, fresh water, vegetables, Waste water, aqueous, rice, tea and human hair. The hanging mercury drop electrode was the most popular electrode compares with chemically modified carbon paste electrode, mixed binder carbon paste electrode, glassy carbon bismuth film electrode and silver amalgam film electrode. Square wave adsorptive stripping voltammetry is the stripping mode that was used in the determination of PGMs.

Table 1. Determination of Platinum Group Metals in different environmental samples using different working electrodes (Locatelli, 2007; Somerset *et al.*, 2011).

Environmental matrix	Analyte of intrest [a]	Sample treatment [b]	Stripping mode [c]	Working electrode [d]	References
Superficial water	Pt(II)−Rh(III)	−	LSAdSV	HMDE	Dalvi *et al.*, 2008
Fresh water	Pd(II)	−	SWAdSV	Hg(Ag)FE	Bobrowski *et al.*, 2009
Superficial water	Pt(II), Pd(II), Rh(III)	−	SWAdSV	HMDE	Locatelli, 2006
Vegetables	Pt(II), Pd(II), Rh(III)	DD	SWAdSV	HMDE	Locatelli *et al.*, 2005
Fresh water, sediments	Pt(II), Pd(II), Rh(III)	WD	DPAdSV	GC/BiFE	Van der Horst *et al.*, 2012
Waste water	Pt(IV), Ir(III), Os(IV)	−	DPCSV	CMCPE	Svancara *et al.*, 2007
Aqueous	Pd(II)	−	AdSV	HMDE	Ramirez & Gordillo, 2009
Surface water	Pt(II), Rh(III), Pd(II)	WD	SWASV	HMDE	Locatelli, 2006
Rice, tea, human hair	Pd	WD	CSV	MBCPE	Zhang *et al.*, 1996

[a] Pt − platinum; Pd − palladium; Rh − rhodium; Os − osmium; Ir − iridium.

[b] DD − dry digestion; WD − wet digestion.

[c] SWAdSV − square wave adsorptive stripping voltammetry; DPAdSV − differential pulse adsorptive stripping voltammetry; DPCSV − differential pulse cathodic stripping voltammetry; AdSV − adsorptive stripping voltammetry; SWASV − square wave anodic stripping voltammetry; CSV − cathodic stripping voltammetry.

[d] HMDE − hanging mercury drop electrode; GC/BiFE − glassy carbon bismuth film electrode; CMCPE − chemically modified carbon paste electrode; MBCPE − mixed binder carbon paste electrode; Hg(Ag)FE − silver amalgam film electrode.

2.3.2.1. Metal film electrodes

The mercury film electrode (MFE) has been develop to replace the mercury drop electrode and can be formed by in-situ plating of Hg on glassy carbon, silver and gold electrodes or by preliminary deposition. This electrode is robust and has an excellent sensitivity due to a high surface area to volume ratio. Mercury film electrodes consist of a very thin mercury layer or many small mercury droplets on a conducting surface. These electrodes were traditionally used as working electrodes for the simultaneous voltammetric determination of heavy metals in different environmental samples due to their, reliability and reproducibly. Due to the toxicity of mercury alternative working electrodes has been developed by many researchers since mercury toxicity has been highlighted and the use of it been considered undesirable (Somerset *et al*., 2011; Airey, 1947; Florence, 1970).

The bismuth film electrodes (BiFEs) was introduced in 2000 as a favourable replacement for mercury film electrodes (MFEs) and has been widely accepted due to the fact that bismuth is environmental friendly, since the toxicity of bismuth and its salts is negligible. Nowadays, BiFEs is extensively used in numerous electrochemical laboratories worldwide; the analytical properties of BFEs in voltammetric analysis are comparable to those of MFEs due to the property of bismuth to form fused alloys with other heavy metals (Wang *et al*., 2000; Long *et al*., 1978; Economou and Fielden, 1998).

Table 2 presents analytical parameters for the determination of PGMs in environmental samples using different metal film electrodes. The excellent analytical capabilities of metal film electrodes for different metal ions were demonstrated such as Pd(II), Pt(II), and Rh(III). Platinum group analysis was done in different supporting electrolytes such as ammonia, hydrochloric acid, sulphuric acid and acetate buffer solutions. Very good limit of detection were obtained, in the micrograms and nanograms per liter range for deposition times between 30 and 300 s.

Van der Horst *et al*. (2012) developed an analytical sensor for the detection and characterisation of PGMs in environmental samples. A bismuth film was coated onto a GCE and differential pulse adsorptive stripping voltammetric measurements for PGMs were used in the presence of dimethylglyoxime (DMG) as chelating agent. In this study the parameters

affecting the peak currents of PGMs were optimised. Well defined peaks were obtained with the bismuth film with highly linear behaviour between concentrations ranging from 0.5 to 20 µg/L of Pd, Pt and Rh, respectively. This bismuth film electrode coated on a GCE, exhibited good reproducibility. In Figure 3 the differential pulse adsorptive stripping voltammogram for the simultaneous determination of Pd-Rh-(HDMG)$_n$ and Pt-Rh-(HDMG)$_n$ complexes at a bismuth film electrode is shown.
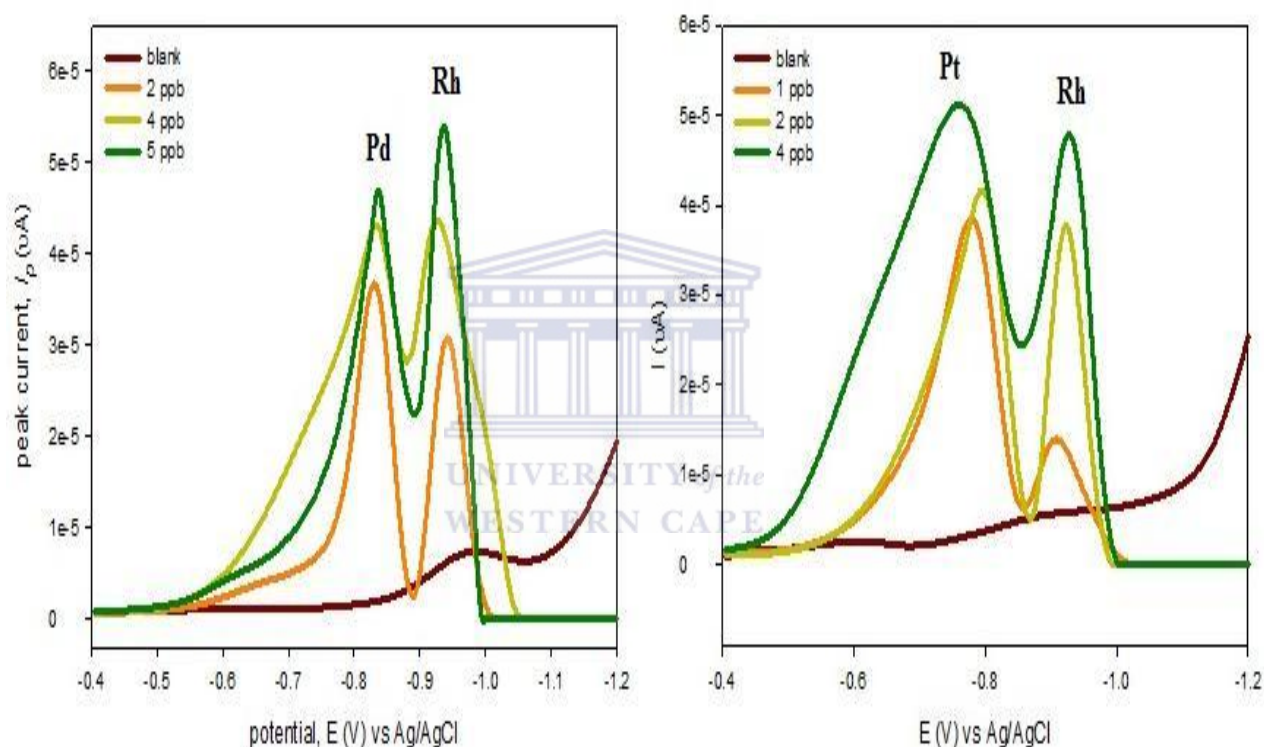
Figure 3.   **Differential pulse adsorptive stripping voltammetry for increasing concentration of Pd(II)−Rh(II) and Pt(II)−Rh(II) at a Bismuth film electrode. The solutions of 0.01 M ammonia buffer (pH 9.0) containing 2 to 5 ppb Pd(II)−Rh(II) and Pt(II)−Rh(II) with 5 × 10^{-4} M DMG; deposition potential was -0.6 V and deposition time 150 s (Van der Horst *et al*., 2012).**

The work done by Dalvi *et al*. (2008) described the characteristics of the adsorption/electro-reduction of Pt/Rh hexamethylene tetramine (HMTA) complex on static mercury drop electrode surface. In this study cyclic voltammetry was used to get the insight about the mechanistic behaviour of the catalytic current of Pt/Rh HMTA complex in acidic solution. For the determination of Pt/Rh adsorptive stripping voltammetry using HMTA as

the complexing agent was found to be highly sensitive method. The working electrode was the hanging mercury drop electrode (HMDE), a glassy carbon rod as the counter and an Ag/AgCl/KCl$_{saturated}$ as the reference electrode in the present voltammetric measurements. The optimisation of various electrochemical parameters such as concentration of the ligand, deposition potential, supporting electrolyte, deposition time, etc. was done. For a deposition time of 30 s the limit of detection for Pt and Rh was found to be 4.38 pML^{-1} and 2.80 pML^{-1} respectively and the simultaneous determination of Pt(II) and Rh(III) in water samples was possible. The linear sweep voltammogram for the simultaneous determination of increasing concentration of Pt(II) and Rh(III) at a HDME are illustrated in Figure 4.
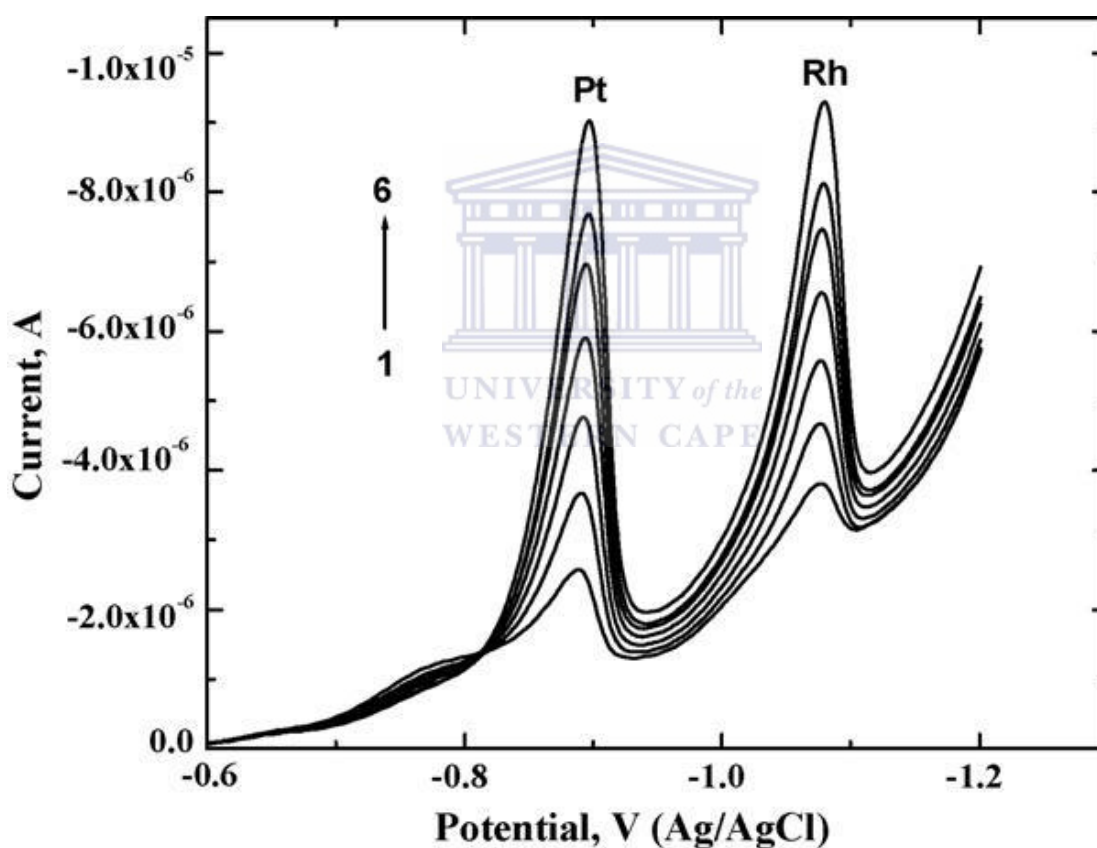
Figure 4.   **Linear sweep voltammetry for increasing concentrations of Pt(II) and Rh(III) at a HDME. The solution of 2.5 M sulphuric acid containing 8, 16, 24, 32, 40 and 48 pM Pd(II) and Rh(II) with 2 mM HMTA; deposition potential was -0.5 V (vs. Ag/AgCl) and deposition time 30 s (Dalvi *et al.*, 2008).**

Locatelli *et al*. (2005) constructed a analytical procedure for the voltammetric sequential determination of Pt(II), Pd(II), and Rh(III), by squarewave adsorption stripping voltammetry (SWAdSV), and Pb(II), by square-wave anodic stripping voltammetry

(SWASV) in environmental samples. In this study the relative standard deviation and relative error were always less than 6% respectively and the limits of detection (LOD) for each element were below 0.096 µg/g. the voltammetric results was compared with the spectroscopic measurements.

The work done by Kim and Cha (2002) described the determination of palladium(II) complexed with α-(2-benzimidazolyl)-α',α"-(N-5-nitro-2-pyridiylhydrazone)-toluene (BINPHT) was investigated by adsorptive cathodic stripping voltammetry using hanging mercury drop electrode. In this analytical procedure, the supporting electrolyte was sodium acetate buffer (0.01 M) at pH 5.0 with a 2×10^{-5} M concentration of BINPHT. Accumulation is achieved by adsorption of Pd(II)–BINPHT complex on a hanging mercury drop electrode with accumulation potential of −590 mV versus Ag/AgCl, accumulation time of 180 s and scan rate of 50 mV/s. A detection limit ($S/N = 3$) of 2 ng/mL was obtained with good relative standard deviation.

Table 2.   **Determination of Platinum Group Metals in different environmental samples using different working electrodes.**

Analyte determined [a]	Detection limit	Deposition time	Deposition potential	Dynamic range	Working electrode [b]	Electrolyte [c]	References
Pd(II); Pt(II); Rh(II)	0.12 μg/L − Pd(II); 0.04 μg/L − Pt(II); 0.23 μg/L − Rh(II)	90 s for Pd (II); 150 s for Pt(II); 150 s for Rh (II)	-0.7 V − Pd(II); -0.7 V − Pt(II); -0.5 V − Rh(II)	0−3.5 μg/L	BiFE	NH_3	Van der Horst *et al.*, 2012
Pt(II); Rh(III)	4.38 pM/L − Pt(II); 2.80 pM/L − Rh(III)	30 s	-0.5 V	−	HMDE	H_2SO_4	Dalvi *et al.*, 2008
Pt(II); Pd(II); Rh(III)	0.096 μg/g	240 s − Pd(II); 270 s − Pt(II); 270 s − Rh(III)	-0.05 V − Pd(II); -0.7 V − Pt(II); -0.7 V − Rh(III)	−	HMDE	HCl	Locatelli *et al.*, 2005
Pd(II)	5 *n*g/mL	180 s	-0.59 V	20-100 *n*g/mL	HMDE	HAc−NaAc	Kim and Cha, 2002

[a] Pt − platinum; Pd − palladium; Rh − rhodium.

[b] BiFE – bismuth film electrode; HMDE – hanging mercury drop electrode.

[c] NH_3 – amaonia buffer; HCl – hydrochloric acid; H_2SO_4 – sulphuric acid; HAc−NaAc – acetate buffer.

2.3.2.2. Carbon based electrodes

Due to its toxicity, mercury drop and film electrodes are being progressively replaced by various forms of carbon electrodes or carbon electrode substrates (carbon paste, glassy carbon, carbon nanotubes, carbon screen printed electrodes, etc.). In voltammetric analysis glassy carbon has played an important role due to its good positive potential range, hardness, low porosity, low permeability to gases and good electrical conductivity. For several years carbon paste electrodes (CPEs) have received considerable attention under the field of chemically modified electrodes (CMEs) due to its ability to accumulate metal ions on the basis of the interaction of these ions with a functional group on the electrode surface. The preparation, regeneration and modification of CPEs can be easy with the mixing of various ligands depending on the application. A disadvantage of these carbon or carbon substrate electrodes are they tend to become blocked over time when employed in voltammetric analysis in natural media, due to irreversible adsorption of electroactive and other chemical species, leading to a decrease in response and difficulties in the analysis of untreated samples (McCreery, 1991; Brett, 1999). An illustration of carbon based electrodes is shown in Figure 5.
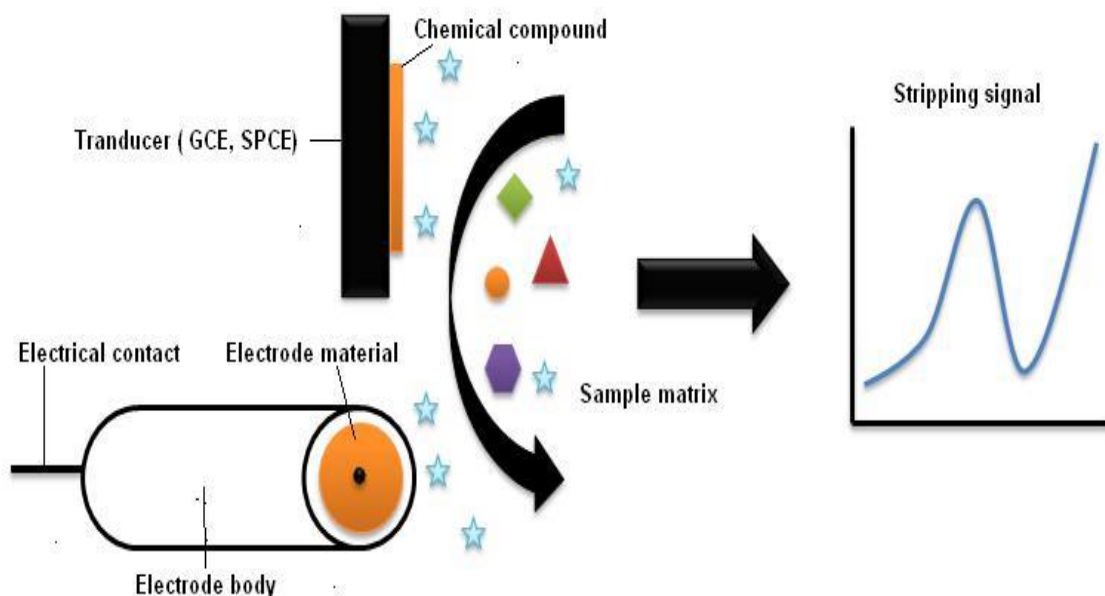
Figure 5.   **Illustration of carbon based electrodes (Navratill and Barek, 2009; Stetter *et al.*, 2003).**

The work done by Švancara *et al*. (2007) described a novel method for the determination of platinum metals. In this method a carbon paste electrode modified *in situ* with cationic surfactants and the pre-concentration step is based on a specific accumulation mechanism involving ion-pair formation. Cathodic scanning differential pulse voltammetric mode was applied for the detection of three heavy platinum metals in the form of Pt(IV), Ir(III) and Os(IV). It was found that this method was almost inapplicable for the detection of Ru, Rh, and Pd. For both platinum and iridium the stripping signals were proportional to the concentration in a range of $1-10 \times 10^{-6}$ M Pt(IV) and Ir(III) and for osmium the response being linear within 0.1 to 6×10^{-7} M Os(IV) with a detection limit of about 5×10^{-9} mol/L. This developed method showed both in model solutions and real samples of industrial waste water satisfactory analytical performance. Figure 6 depicted the differential pulse cathodic stripping voltammogram for the simultaneous determination of Ir(III), Pt(IV), Os(IV) at a carbon paste electrode modified with Septonex.
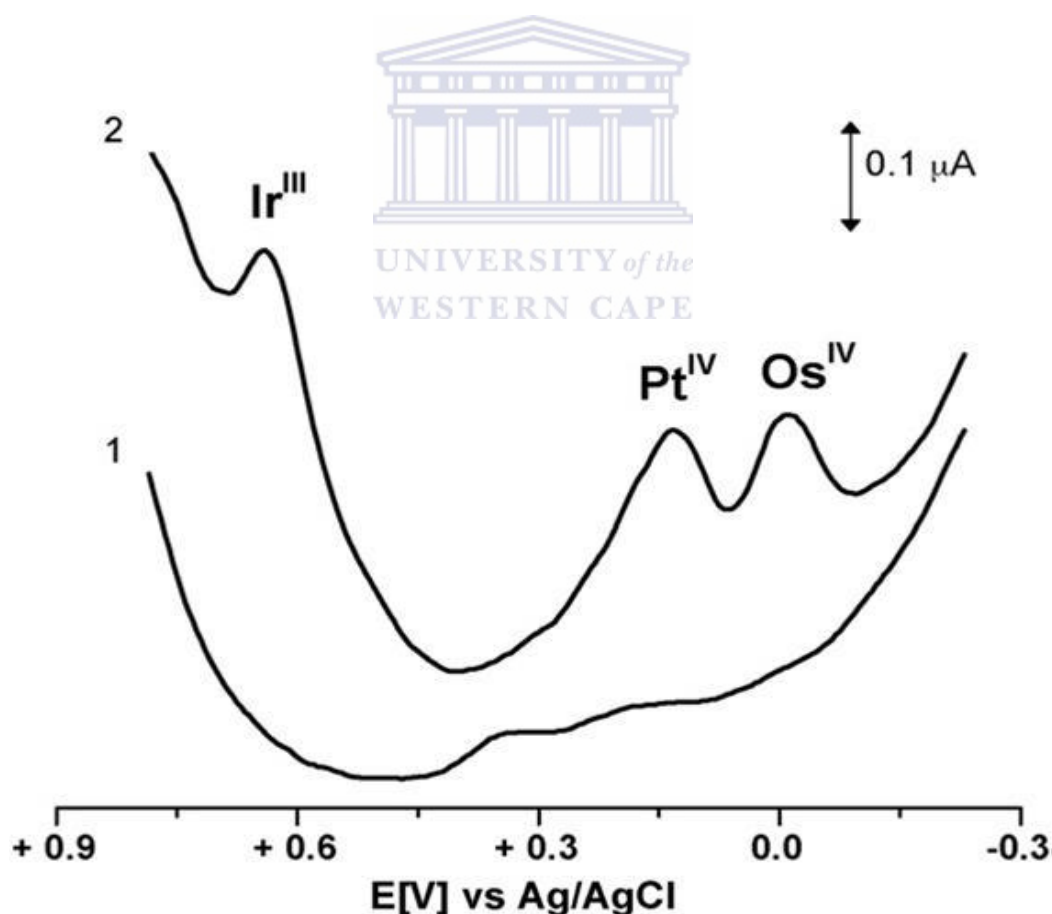
Figure 6.   **Differential pulse cathodic stripping voltammetry for 5×10^{-7} M Pt(IV), 3.5×10^{-6} M Ir(III) and 5×10^{-8} Os(IV) with a carbon paste electrode modified with Septonex. The solution of 0.10 M acetate buffer, 0.15 M KCl, 1×10^{-5} M Septonex (pH 4.5) deposition potential was +0.8 V (Švancara *et al*., 2007).**

Galík *et al*. (2006) developed a method for the determination of osmium at a carbon paste electrode (CPE) modified with cationic surfactants such as cetyltrimethylammonium bromide (CTAB) and 1-(ethoxycarbonyl)-pentadecyltrimethyl-ammonium bromide (Septonex). Electrochemical detection of osmium was performed by cathodic scanning in the differential pulse voltammetric mode with both salts were added in situ and serving for preconcentration of osmium via its hexachloroosmate(IV) anion. The supporting electrolyte was chloride/acetate buffer with Septonex as the modifier of choice. The reduction signal for osmium was found to be proportional to the Os(IV) concentration in a range from 5×10^{-9} to 5×10^{-7} mol/L with a limit of detection close to 5×10^{-9} mol/L (with preconcentration for 60 s). The analytical procedure was capable to determine Os(IV) in the presence of both Pt(IV) and Ir(III) was tested on model solutions and real sample of industrial waste water.

UNIVERSITY *of the*

WESTERN CAPE

Table 3. **Determination of Platinum Group Metals in different environmental samples using carbon based working electrodes.**

Analyte determined [a]	Detection limit	Deposition time	Deposition potential	Dynamic range	Working electrode [b]	Electrolyte [c]	References
Pd(II)	10^{-8} M	120 s − Pd(II)	-0.7 V − Pd(II)	−	MBCPE	HAc−NaAc	Zhang *et al*., 1996
Pt(IV); Ir(III); Os(IV)	7×10^{-7} M − Pt(IV); 9×10^{-9} M − Ir(III); 5×10^{-9} M − Os(IV)	30 s − Pt(IV); 60 s − Ir (III); 30 s − Os(IV)	+0.9 V − Pt(IV); +0.8 V − Ir(III); +0.8 V − Os(IV)	1-10 × 10^{-6} M − Pt(IV); 0.1-6 × 10^{-7} M − Os(IV)	CPE	HAc−NaAc	Švancara *et al*., 2007
Os(IV)	5×10^{-9} mol/L	30 s	+0.7 V	$5 \times 10^{-9} - 5 \times 10^{-7}$ mol/L	CPE	HAc−NaAc	Galík *et al*., 2006

[a] Pt − platinum; Rh − rhodium; Os − osmium; Ir − iridium.

[b] MBCPE − mixed binder carbon paste electrode; CPE − carbon paste electrode.

[c] HAc−NaAc − acetate buffer solution.
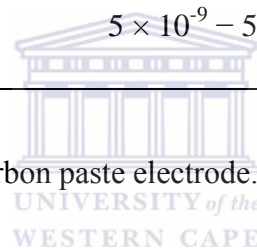
2.3.2.3. Metal based nanosensors (MBNSs)

Nanoparticles are extremely suitable for designing new and improved sensing devices, especially electrochemical sensors and biosensors due to its unique chemical (catalytic) and physical (structural, electronic and optical) properties. The constructing of these electrochemical sensors and biosensors are done by using many kinds of nanoparticles such as metal, oxide and semiconductor nanoparticles which plays different roles in different sensing systems (Luo *et al*., 2006). According to Hernandez-Santos *et al*. (2002) there is no universally agreed upon definition of when a small particle qualifies as a nanoparticle. Physical and chemical methods are used to prepare metal nanoparticles. The properties of all nanoparticles depend on their size, shape and stabilising agents which are controlled by the preparation conditions. The chemical methods which involve reduction of metal ions to metal atoms followed by controlled aggregation of atoms. Physical methods starts from vapour deposition consist in principle of subdividing bulk precursors to nanoparticles. The different metal based nanosensors (MBNSs) that were developed for the determination of heavy metals and other analytes are discussed and listed below in Table 4.

2.3.2.3.1. Synthesis of bismuth nanoparticles

In recent years bismuth has gained much attention in metallurgical and pharmaceutical additives and is suggested to replace mercury in environmental sensor application (Rodilla *et al*., 1998; Sun *et al*., 1999; Guo *et al*., 2005). The ability of bismuth to form alloy with different metals are one of the advantageous analytical properties and its alloys are used as high-temperature heat-transfer agents (Wang *et al*., 2006; Hocevar *et al*., 2002; Kefala *et al*., 2006). Bismuth which has semi-metal properties must have semiconductor properties in response to decreasing crystallite size. The applications of bismuth are also expanded by the magnetoresistance effect observed in single crystals and thin films. Due to its high electron mobility, high anisotropic electronic behavior and low conduction-band effectively mass makes semi-metal bismuth an interesting material for electronics (Gallo *et al*., 1963).

52

The preparation of bismuth nanoparticles are done by an extremely simple one step solution dispersion method modification starting from bulk metal described by Zhao *et al*. (2004) Solid bismuth granules were added to paraffin oil and the vessel was sealed. The bismuth mixture was heated and the bismuth has melted under vigorous stirring. Centrifugation was done to the supernatant after cooling. The bismuth particles residue was washed several times with chloroform to eliminate any paraffin, and finally dried under N_2 stream. A dark grey powder was obtained and stored in a sealed vial at room temperature.

Zhang *et al*. (2010) synthesised bunch-like bismuth nanostructures for the development of a chemical sensor via an electrochemical two step deposition. Due to its unique three-dimensional structures and strong ability of adsorbing the heavy metal ions, this designed bunch-like Bi electrode has very high sensitivity to detect heavy metal ions in aqueous solutions.

In the work done by Lee *et al*. (2010) nano-sized bismuth (Bi) binding technology has been developed to improve the electrochemical characterisation of Bi(III) for heavy metals detection. Gas condensation method was used to synthesise Bi nanopowder and exhibits nanoparticles with size smaller than 100 nm. Strong chemical bonding by Nafion solution was used to distribute the Bi nanoparticles uniformly on a carbon surface. The phase stability and dispersion stability of the Bi nanoparticles is suggested by an optimum additional amount of Nafion.

The work of Rico *et al*. (2009) reports a simple procedure for the chemical synthesis of bismuth nanoparticles and the subsequent adsorption on commercial screen-printed carbon electrodes for the reliable quantitation of trace zinc, cadmium and lead by anodic stripping square wave voltammetry (ASSWV) in non deareated water samples. Various experimental variables and the influence of the two hydrodynamic configurations (convective cell and flow cell) are explored upon the stripping signals at the bismuth-coated sensor.

Malakhova *et al*. (2010) developed a procedure for the immobilisation of bismuth nanoparticles prepared by the method of gas condensation on inert supports manufactured by screen printing method using carbon containing inks. The conditions of the electrochemical activation are found by investigate the electrochemical behaviour of the immobilised bismuth nanoparticles. The optimisation of the composition of the modified suspension "bismuth nanoparticles-liquid" is done. Similar results are obtained for the analytical parameters of the elaborated thick film carbon containing electrode modified by bismuth nanoparticles compare

to the commercially available thick film carbon containing electrode premodified by calomel and substantially exceeds carbon containing electrodes with electrolytically deposited bismuth films in its properties.

2.3.2.3.2. Synthesis of silver nanoparticles

In recent years nanosized silver colloids have received a great deal of attention for various potential applications, such as catalysts, chemical sensors and conductors due to its excellent thermal, optical, catalytic and electrical properties. These special and unique properties could be attributed to their small sizes and large specific surface area (Haes and Van Duyne, 2003; Magdassi *et al*., 2003; Nie and Emory, 1997; Pradhan *et al*., 2002; Ye *et al*., 1999). According to Sun and Xia, 2002; Cuenya, 2010, the size, shape and surface morphology play pivotal roles in controlling the electronic, chemical, optical and physical properties of these nanoscopic materials. Many research works were done on the synthesis and characterisation of silver nanoparticles with different morphologies. In the synthesis of these nanoparticles the catalytical activity is also dependent on their size as well as their shape, structure, size distribution and chemical−physical environment. Thus, control over the size and size distribution is an important task. According to many publication specific control of shape, size and size distribution is often achieved by varying the synthesis methods, reducing agents and stabilizers (Zhang *et al*., 2004; Zhang *et al*., 2006; He *et al*., 2004; Chimentao *et al*., 2004; Yeo *et al*., 2003).

In anodic stripping voltammetry (ASV) the application of metallic silver electrodes is not so common and higher interest was devoted to the cathodic polarization of these electrodes. Differences between the voltammetric behaviour of metallic and composite silver electrodes were illustrated in the results obtained by cyclic voltammetry and by anodic stripping voltammetry (Ishiyama and Tanaka, 1996; Miva *et al*., 1982; Shain and Perone, 1961).

The formation of silver nanoparticles can be obtained by various techniques but the wet chemical method is probably the most popular due to the ability to produce large quantities, its simplicity and low cost. Strong reducing agent such as sodium borohydride ($NaBH_4$) or hydrazine (N_2H_4) is added to silver nitrate ($AgNO_3$) in an aqueous reaction

medium. Sodium chloride (NaCl) is added and the nanoparticles aggregate and the suspension turns cloudy gray. The addition of a small amount of polyvinyl pyrrolidone will prevent aggregation. To obtain silverparticles the solution can be left to evaporate or put in a toaster oven for 30 minutes. When formaldehyde is used which act as a moderate reducing agent silver particles with a mean size of 27.8 nm and standard deviation of 9.9 nm are obtained (Chou and Lai, 2004; Chou and Lu, 2005; Nersisyan *et al*., 2003; Pradhan *et al*., 2002).

Li *et al*. (2005) constructed a novel mercury-doped silver nanoparticle film glassy carbon (Ag/MFGC) electrode to investigate the electrochemical behaviours of cysteine on the Ag/MFGC electrode by electrochemical impedance spectroscopy (EIS) and cyclic voltammetry (CV). Due to strong adsorption of cysteine thin layer of cysteine are formed at the surface of the Ag/MFGC electrode. In an acetate buffer solution (pH = 5.0) the doped electrode catalysed the electrode reaction process of cysteine, and the cysteine displayed a pair of well defined and nearly reversible CV peaks at the electrode.

The work of Šebková *et al*. (2003) indicates the examination of new types of silver composite electron prepared from silver, graphite powder and methacrylyte. The determination of 2-nitronaphtalene was done by using differential pulse voltammetry (DPV) and direct current voltammetry (DCV) at electrodes with varied content of silver (10, 15, 20%). The application of this electrode in differential pulse cathodic stripping voltammetry enables the direct determination of nitrocompounds without elimination of the presence of dissolved oxygen. The most advantageous electrode for the determination of 2-nitronaphtalene was the electrode consisting of 15% of silver, 25% of graphite and 60% of metacrylate resin.

In the work done by Safavi *et al*. (2009) a two-step potentiostatic method was used to electrodeposited silver nanoparticles (narrowly dispersed in diameter) on a carbon ionic liquid electrode (CILE) surface. The size and morphologies controls for electrodeposited silver nanoparticles on a CILE were done by using a suitable and simple potentiostatic double pulse technique. The obtained silver nanoparticles deposited on CILE surface showed excellent electrocatalytic activity (low overpotential of -0.35 V vs. Ag/AgCl) towards reduction of hydrogen peroxide.

According to Shukla *et al*. (2012) the "green" synthesis of nanosilver is an efficient, easy-going, fast, renewable, inexpensive, eco-friendly and non-toxic approach which offers

numerous benefits over physiochemical approaches. The formation and crystallinity of nanosilver are proved by the X-ray diffraction (XRD) patterns. Transmission electron microscopy (TEM) confirmed the average particle size of silver nanoparticles (8.25 ± 1.37 nm). The UV-Vis absorption spectrum shows a characteristic absorption peak of silver nanoparticles at 410 nm. Azadirachtin the reducing and stabilizing agent for nanosilver formation was confirmed by FTIR. In addition excellent electro-catalytic activity toward the reduction of hydrogen peroxide (H_2O_2) was exhibited by the nanosilver modified glassy carbon electrode (Ag/GC). The produced nanosilver is stable and comparable in size which shows potential applications in the field of fuel cells, catalysis, nanodevices and sensors.

2.3.2.3.3. Silver bimetallic sensor

New types of electrodes based on amalgamation of soft metal powder (MeSAE–metal solid amalgam electrodes) were designed by Prague research group several years ago (Novotny and Yosypchuk, 2000). The Trondheim research group developed a solid dental amalgam electrode at the same time (Mikkelsen and Schroder, 2000). The construction of these electrodes was prepared simply by placing the dental amalgam paste in a cavity of the electrode holder and was used for the analysis of heavy metals. A variety of metals was used for amalgam electrodes preparation (e.g., silver, copper, gold, and thallium) by the Prague group. After the modification of their surfaces by mercury film (MF-MeSAE) or after polishing of solid amalgam disc (p-MeSAE) they can be used as mercury-free electrodes. The application of these solid amalgam electrodes and the results achieved are fully comparable with those obtained using hanging mercury drop electrode (HMDE) or dropping mercury electrode (DME). In many cases the solid amalgam electrodes do not reach the quality of HMDE but they approach it and it was proved by a variety of analytical applications, including many inorganic anions as well as organic species and the voltammetric determination of heavy metal cations. At amalgam electrodes the value of the hydrogen overvoltage is as high as at liquid mercury. The field of their application is similar to this of HMDE or DME and easiness, universality of their surface regeneration belong to advantages of amalgam electrodes (Novotny and Yosypchuk, 2000; Mikkelsen and Schroder, 2000; Mikkelsen and Schroder, 2002; Yosypchuk and Novotny, 2002; Selesovska-Fadrna *et al*., 2007; Fadrna, 2004).

In electro-analytical research the development of solid electrodes has been one of the long term trends. The most electrochemical measurements are done by some solid electrodes such as pure metallic (silver, platinum, gold, etc.) or metallic composite electrodes (carbon composites, silver composites or gold composites). The greatest advantage of these electrodes is the high oxygen overvoltage and makes it possible to observe electrode reactions at positive potentials (Kolb, 1978; Navrátil and Kopanica, 2002; Navrátil and Kopanica, 2002; Navrátil *et al*., 2004; Šebková *et al*., 2003; Navrátil *et al*., 2003; Šebková *et al*., 2005).

Based on amalgamation of soft metal powders the designed and of nontoxic electrodes of solid amalgams especially the silver solid amalgam electrode AgSAE was introduced a few years ago. The dental amalgams with the same composition as the polished AgSAE were suggested at a later stage. However, lower sensitivity and narrower range of working potentials was achieved by these dental amalgams (Novotńy and Yossypchuk, 2000; Polaro-Sensors, 1997; Yossypchuk and Novotńy, 2001; Mikkelsen and Schroder, 2000; Mikkelsen and Schroder, 2001). The construction of a solid amalgam electrode is illustrated in Figure 7.
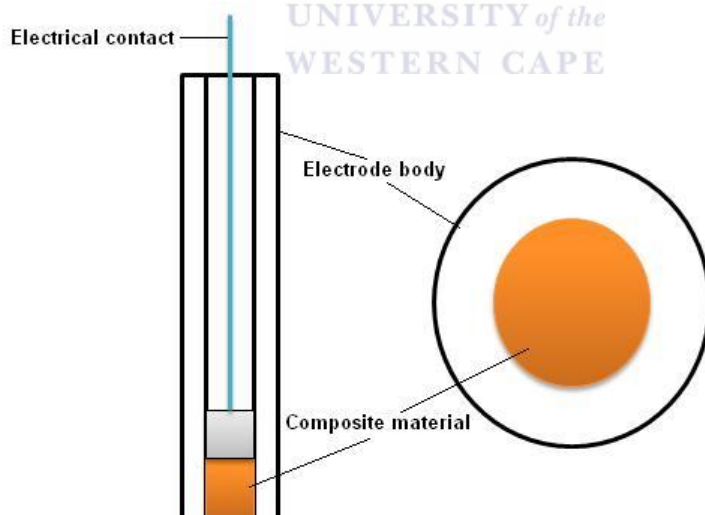
Figure 7.   **Illustration of the construction of a solid amalgam electrode (Šebková *et al*., 2004).**

Due to its low mechanical stability and because of unsubstantiated fears of toxicity this complicating the used of mercury electrodes and avoid the use of mercury in flowing systems and in portable devices. The work done by Yosypchuk and Novotńy (2002), clearly

shown that amalgam electrodes (AE) can, in many cases, successfully substitute mercury electrodes. When compared with the HMDE some of the MeSAEs exhibit narrower range of working potentials which is the base of similar applicability.

Bobrowski *et al*. (2009) constructed an amalgam film electrode of mercury and silver (Hg(Ag)FE) for the determination of palladium(II) in the presence of dimethylglyoxime (DMG). This described sensitive method is based on adsorptive stripping voltammetric protocol and the procedure is based on the adsorptive preconcentration of the Pd(II)-dimethylglyoxime complex onto the (Hg(Ag)FE) at -0.45 V followed by a negatively going square-wave voltammetric scan. The investigation and optimisation of factors affecting the stripping performance such as deposition potential, deposition time, pH, composition of DMG concentration, the supporting electrolyte, including different ligands and SW frequency have been done.

The work done by Fadrná (2005), shown that polished silver solid amalgam electrode (p-AgSAE) appears to be a good alternative to hanging mercury drop electrode (HMDE). Analysis was done on the electrode material and of the working electrode surface. In this study inorganic electrochemical measurement for the determination of metal cations, thiocyanates and nitrates was successfully demonstrated using this electrode.
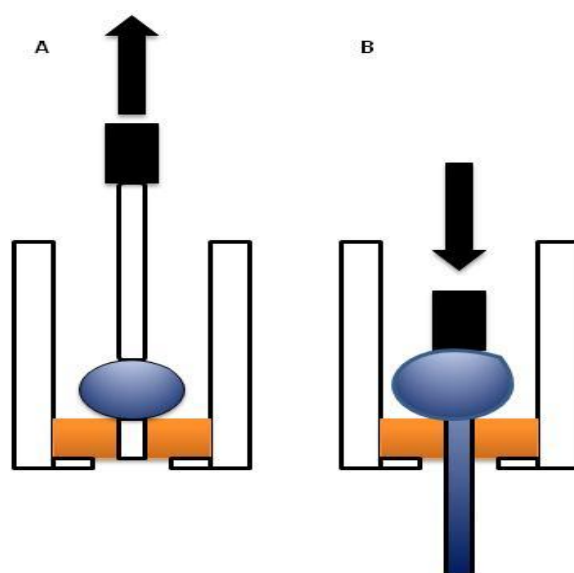
Figure 8. **Illustration of the mechanical refreshing of the mercury film silver based electrode. The construction shown a Hg(Ag)FE: (A) refreshing configuration, (B) configuration ready for voltammetric measurement (Piech *et al*., 2008).**

Table 4.   **Determination of different analytes in environmental samples using metal based nanosensors (MBNSs).**

Analyte determined	Detection limit	Deposition time	Deposition potential	Dynamic range	Working electrode	Electrolyte	References
Pb(II); Cd(II); Hg(II); Cu(II)	2.5−50 μg/L	60 s	-1.1 V	2.5−50 μg/L	BiFE	HAc−NaAc	Zhang *et al*., 2010
Zn, Cd, Pb	0.15 *ng*/mL for Cd; 0.07 *ng*/mL for Pb	120 s	-1.4 V	0.9−4.9 *ng*/mL	Bi-film SPCEs	HAc−NaAc	Rico *et al*., 2009
As(III)	1.2 ppb	120 s	-0.6 V	10−100 ppb	AgNPs/CT/GC	HNO$_3$	Prakash *et al*., 2012
Pd(II)	0.15 mg/L	60 s	-0.45 V	1.0−50 mg/L	Hg(Ag)FE	HAc−NaAc	Bobrowski *et al*., 2009
Co; Ni	0.0035 μg/L for Co; 0.013 μg/L for Ni	60 s	-0.7 V	0.01−7 μg/L − Co; 0.1−10 μg/L − Ni	Hg(Ag)FE	NH$_3$	Kapturski and Bobrowski, 2008
Pb; Cd; Zn	0.55 μg/L − Pb; 0.40 μg/L − Cd; 0.38 μg/L − Zn	180 s	-1.4 V	1−8 μg/L	TCE/Bi$_{nano}$	HAc−NaAc -Cl	Malakhova *et al*. 2010
H$_2$O$_2$	1 μM	9 s	-0.42 V	0.25−1.4 μM	Ag/GC	HAc−NaAc	Shukla *et al*., 2012

[a] HAc−NaAc − acetate buffer; HAc−NaAc−Cl − acetate chloride; NH$_3$ − ammonia buffer; HNO$_3$ – nitric acid.

[b] Ag/MFGCE − mercury doped silver nanoparticles film glassy carbon electrode; Hg(Ag)FE − silver amalgam film electrode; TCE/Bi$_{nano}$ − thick-film carbon-containing electrode bismuth nanoparticles; Bi-film SPCEs−bismuth film screen printed carbon electrodes; BiFE − bismuth film electrode; AgNPs/CT/GC – silver nanoparticles bult-in chitosan modified glassy carbon electrode; Ag/GC – silver nanoparticles modified glassy carbon electrode.

[c] Pb – lead; Cd − cadmium; Zn − zinc; Co − cobalt; Pd − palladium; Hg − mercury; Ni − nickel; Cu – copper; As – arsenic; H$_2$O$_2$ – hydrogen peroxide.

2.3.3. Chelating agents

Chemicals that form soluble, complex molecules with certain metal ions, inactivating the ions so that they cannot normally react with other elements or ions to produce precipitates or scale are called chelants. The most common chelates known are dimethylglyoximes (DMG), Hexamethylene tetramine (HMTA) and ethylenediaminetetraacetic acid (EDTA). Georgieva (2002) investigated the electrochemical behavior of Pt(IV) ions in the presence of dimethylglyoxime using adsorptive stripping voltammetric method. The obtained results in this study indicated that the platinum is reduced from its adsorbed state as bis-dimethylglyoxi-mate platinum (IV) complex. This study showed that the reduction process of platinum dimethylglyoximate complex in acidic media is possible and gave highly linear response.

The applications of chelators have been proposed and listed below:

- used in the production of nutritional supplements,
- chemical analysis,
- fertilizers,
- as water softeners,
- industrial applications,
- medicine,
- food preservatives,
- heavy metal detox,
- and commercial products such as shampoo.

(Ashmead, *et al*., 1986; Doja and Roberts, 2006; U.S. Centers for Disease Control, 2006; Furia, 1964; Lanigan and Yamarik, 2002).

2.3.3.1. Dimethylglyoxime

Dimethylglyoxime is a common laboratory reagent and has been mostly used in the spectrophotometric analysis. Dimethylglyoxime (DMG), acenaphthenequinone dioxime

(ANDO) and their mixed ligands (DMG−ANDO) supported on naphthalene are solid chelating compounds which provide rapid and economical route to the pre-concentration of nickel in alloys and biological and natural water samples. In the determination of platinum group metals (PGMs) by ASV a number of ligands such as dimethylglyoxime, the derivatives of phenolthiozine have been studied. A detection limit of 1 ng/L was obtained for the dimethylglyoxime-base and phenolthiozine-base methods but those methods have an interfering ions, such as Ag(II) and Zn(II) (Wang and Varughese, 1987; Sanke Gowda *et al*., 1975; Sanke Gowda and Thimmaiah, 1976).

For the separation and preconcentration of palladium at trace level (DMG) was chosen as the complexing agent. Palladium forms a stable complex with DMG having a stability constant log $\beta 2$ = 34.3. The application of DMG has been very little for the separation and preconcentration of palladium by solid phase extraction (Daniel *et al*., 2003; Oymak, 2003; Usami *et al*., 1990). Figure 9 is a good illustration of the general structure for dimethylglyoxime.
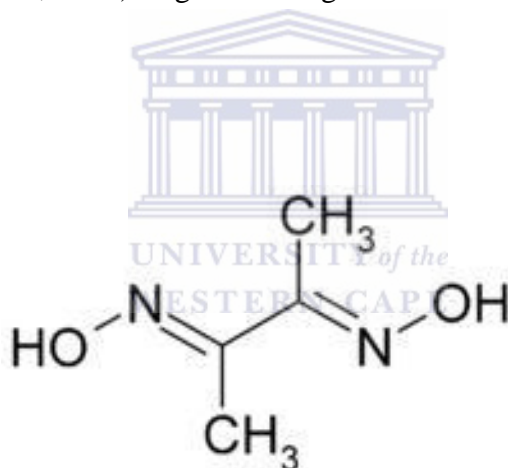
Figure 9.   **General structure of Dimethylglyoxime (Semon and Damerell, 1943).**

2.3.3.2. Hexamethylene tetramine

Hexamethylene tetramine (HMTA) is a heterocyclic organic compound and has got excellent adsorbing properties at the mercury surface. According to Figure 10 this compound has a cage-like structure similar to adamantane and contains N' donor atoms. Hexamethylene tetramine is a white crystalline compound and is highly soluble in water and polar organic solvents. Due to its sensitivity and stability HMTA is used as the complexing agent in

adsorptive stripping voltammetric determination of platinum group metals. Hexamethylene tetramine is also useful in the synthesis of chemical compounds such as pharmaceuticals, rubber additives and plastics (Eller *et al*., 2005; Dalvi *et al*., 2008). The general structure of hexamethylene tetramine is shown in Figure 10.
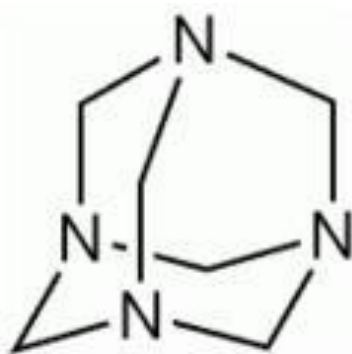
Figure 10. **General structure of Hexamethylene tetramine (Butlerow, 1859).**

The work of Dalvi *et al*. (2008), illustrates the adsorption or reduction of Pt/Rh hexamethylene tetramine (HMTA) complexes on a hanging mercury drop electrode (HMDE) surface. In this study, the mechanistic behaviour of the catalytic current was obtained in the voltammetric scan of Pt/Rh HMTA complex in acidic solution using cyclic voltammetry. Various electrochemical parameters like deposition time, deposition potential, supporting electrolyte and concentration of the ligand were optimized. For a deposition time of 30 s the detection limit of Pt and Rh was found to be 4.38 pM/L and 2.80 pM/L. tap and sea water samples were spiked and the determination of Pt and Rh were also carried out.

2.3.3.3. Ethylenediaminetetraacetic acid

The chelating agent ethylenediaminetetraacetic (EDTA) acid is a colourless and water soluble polyamino carboxylic acid. Ethylenediaminetetraacetate is the conjugate base of EDTA and is applied to dissolve limescale. It's a hexadentate (six-toothed) ligand and chelating agent and its usefulness arises due to its ability to sequester metal ions such as Fe^{3+} and Ca^{2+}. The metal ions remain in solution after being bound by EDTA but exhibit

diminished reactivity. In 1935 Ferdinand Munz described the compound from the reaction between ethylenediamine and chloroacetic acid. The synthesis of EDTA is from formaldehyde, ethylenediamine and sodium cyanide. The sodium salt is obtained from this synthesise method and can be converted in a subsequent step into the acid forms (Harris, 2007; Lanigan and Yamarik, 2002; Hart, 2005). Figure 11 is a good illustration of the general structure for ethylenediaminetetraacetic acid.
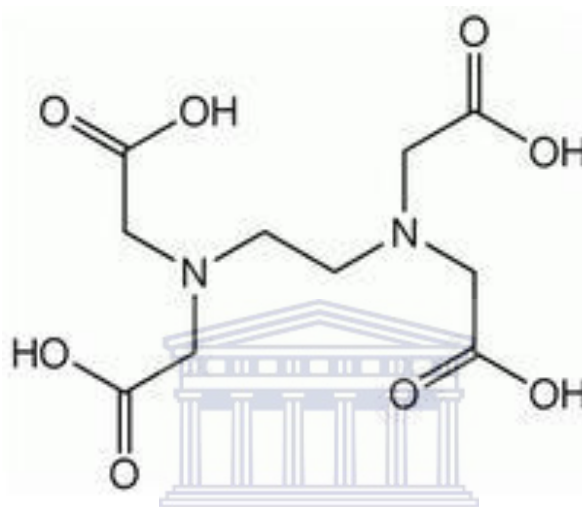
Figure 11.   **General structure of Ethylenediaminetetraacetic acid (Hart, 2005).**

Ethylenediaminetetraacetic acid is used for the spectrophotometric determination of palladium and it is found that the EDTA reagent with the palladium cation formed a yellow complex. Palladium is one of the 32 cations that give no visible reaction with EDTA. According to Pfibil *et al*. (1953) the reduction of silver ion by the ferrous complex of EDTA are disturb by palladium. Palladium forms a stable complex with EDTA which has a maximum absorbance in the near ultraviolet (Hynes *et al*., 1950).

In Table 5 the different complexing agents with their limits of detection in the determination of PGMs are summarised. The work summarised in Table 5 illustrates some work relavant to the simultaneous determination of PGMs such as Pt(II), Pd(II), and Rh(III) (Van der Horst *et al*., 2012; Dalvi *et al*., 2008; Locatelli, 2006; Locatelli, 2006). These develop electro-analytical procedures show to have very low limits of detection for the concentration of these PGMs in real samples, like environmental matrices.

Table 5. **Determination of trace levels of Platinum group metals using different complexing agents (Locatelli, 2007).**

Analyte of intrest	Complexing agent	Limit of detection	Reference
Pt(II), Pd(II), Rh(II), Pt(II)-Rh(II), Pd(II)-Rh(II)	Dimethylglyoxime in ammonia buffer (pH = 9.1)	0.12 μg/L Pd(II); 0.04 μg/L Pt(II); 0.23 μg/L Rh(II)	Van der Horst *et al*., 2012
Pt(II), Rh(III)	Hexamethylene tetramine + sulphuric acid	4.38 pM/L Pt(II), 2.80 pM/L for Rh(III)	Dalvi *et al*., 2008
Pd(II)	Dimethylglyoxime in acetate buffer (pH = 4.4)	0.15 μg/L Pd(II)	Bobrowski *et al*., 2009
Pd(II), Pt(II), Rh(III)	Hydroxylamine + formaldehyde + hydrochloric acid	0.021 μg/L Pd(II), 0.035 μg/L Pt(II), 0.031 μg/L Rh(III)	Locatelli, 2006
Pd(II	α-(2-benzimidazolyl)-α',α''-(*N*-5-nitro-2-pyridiylhydrazone)-toluene	5 *ng*/ml	Kim and Cha, 2002
Pd(II)	DMG in acetic/acetate buffer (pH = 4.85)	–	Ramirez & Gordillo, 2009
Pd(II)	Dimethylglyoxime in hydrochloric acid	0.019 μg/L Pd(II)	Locatelli, 2006
Pt(II), Rh(III)	Hydroxylamine + formaldehyde + hydrochloric acid	0.021 μg/L Pt(II), 0.027 μg/L Rh(III)	Locatelli, 2006
Pt(II)	Thiosemicarbazide + formaldehyde + sulfuric acid	0.03 *ng*/L	Huszal, *et al*., 2005

Pt−platinum; Rh−rhodium; Pd−palladium

2.4. Non electroanalytical methods

A wide variety of PGMs determination techniques has been developed. The majority of these techniques are based on analytical instrumentation methods. The most popular techniques for the determination of PGMs are inductive coupled plasma atomic emission spectrometry (ICP-AES), inductive coupled plasma mass spectrometry (ICP-MS), instrumental neutron activation analysis (INAA), graphite furnace atomic absorption spectrometry (GFAAS), electrothermal atomization-atomic absorption spectrometry (ETA-AAS), electrothermal atomization laser-excited fluorescence spectrometry (ETA-LEAFS), high performance liquid chromatography-inductive coupled plasma mass spectrometry (HPLC-ICP-MS), high resolution inductive coupled plasma mass spectrometry (HR-ICP-MS) and total reflection X-ray fluorescence spectrometry (TXRF). These methods can determine PGMs with very high sensitivity, selectivity and has control over the interference effects, but imply prior pre-concentration or matrix separation steps to assess PGM concentrations at the required ultra trace levels (Begerow *et al*., 1997; Heinrich *et al*., 1996; Lustig *et al*., 1997; Aucelio *et al*., 1998; Kubrakova *et al*., 1996).

Other techniques used for the determination of PGMs in various types of samples are particle induced X-ray excitation (PIXE), secondary ion mass spectrometry (SIMS), accelerator mass spectrometry (AMS) and auger electron spectrometry (Qu, 1996; Barefoot and Van Loon, 1999). In Table 6 the most important analytical methods with their limits of detection are summarised.

Table 6. **List of LOD values obtained in various analytical methods for PGMs determination (Hees *et al*., 1998).**

Method	Limit of detection	Reference
HR-ICP-MS	Pt = 0.03 *n*g/L Pd = 0.2 *n*g/L Rh = 0.03 *n*g/L	Krachler *et al*., 1998
ICP-MS	Pt = 5 ppb Pd = 2 ppb Rh =1 ppb	Economou-Eliopoulos, 2010
INAA	Pt = 5 ppb Pd = 5 ppb Rh = 0.1 ppb	Hoffman *et al*., 1978
GFAAS	Pt = 1.0 μg/kg Pd = 0.5 μg/kg Rh = 0.7 μg/kg	Zereini, 1997
HPLC-ICP-MS	Pt = 4 μg/L	Klüppel, 1997
ETA-LEAFS	Pt = 50fg	Aucelio *et al*., 1998
TXRF	Pt = < 35 pg/g Pd = < 35 pg/g Rh = < 35 pg/g	Sures *et al*., 2002

HR-ICP-MS−high resolution inductive coupled plasma mass spectrometry; ICP-MS−inductive coupled plasma mass spectrometry; INAA−instrumental neutron activation analysis; GFAAS−graphite furnace atomic absorption spectrometry; HPLC-ICP-MS−high performance liquid chromatography inductive coupled plasma mass spectrometry; ETA-LEAFS−electrothermal atomization laser-excited fluorescence spectrometry; TXRF−total reflection X-ray fluorescence spectrometry.

2.5. Summary

The determination of ultra-traces of platinum group metals in standards and environmental samples is a huge challenge for the analyst. During the past 3 decades electrochemical sensors has satisfy the expanding need for rapid, simple and economic methods of determination of many analytes and has become an accepted part of analytical chemistry. This review has summarised the roles that electrochemical sensors play in the determination of platinum group metals in standards and environmental samples. Most of the research on PGMs in this review was done by using a hanging mercury drop or mercury based electrodes. The bismuth film electrode was also used and shown good results but the major draw-back was the ability to operate only in highly alkaline media. In this study we observed that the application of metallic silver electrodes is not so common in the determination of PGMs in environmental samples. Finally the challenge in this study will focus on the development of an electrochemical sensor which has no practical difficulty of establishing reproducible and reliable results in the determination of PGMs in environmental samples.
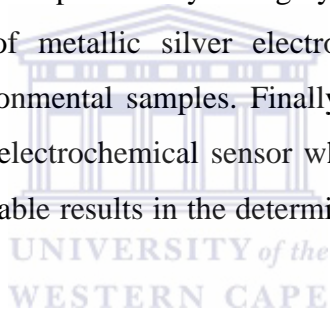
Chapter 3

Experimental Methods and Analytical Techniques

3.1. Introduction

In this study the main focus was to understand the different electroanalytical techniques employed in this study such as differential pulse voltammetry (DPV), cyclic voltammetry (CV) and adsorptive stripping voltammetry (ASV). It further included different type of electron microscopic techniques such as transmission electron microscopy (TEM) and scanning electron microscopy (SEM) and the different types of spectroscopic techniques such as ultraviolet visible (UV-Vis) and Fourier transform infrared (FT-IR) spectroscopy for the characterisation of all the nanoparticles (NPs) synthesised. Inductive coupled plasma mass spectroscopy (ICP-MS) was used for the detection of platinum group metals (PGMs) in sediment and fresh-water environmental samples in this study.
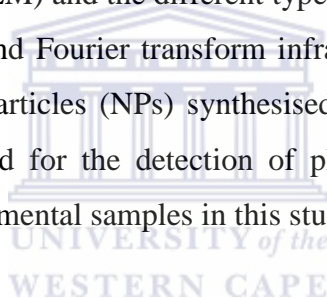
3.2. Electroanalytical Techniques

The most frequently used electroanalytical methods are voltammetry and amperometry. These electroanalytical methods are especially suitable for large scale of environmental monitoring of electrochemically active pollutants in various types of matrices (water, sediment, biota, etc.). They present an independent alternative to popular spectrometric and separation techniques, suitable for speciation, extremely sensitive and inexpensive (Wang, 2006).

Anodic stripping voltammetry (ASV) and adsorptive stripping voltammetry (AdSV) are the two most important voltammetric techniques used in water analysis. Cathodic stripping voltammetry (CSV) and potentiometric stripping analysis (PSA) are the other stripping techniques available. Voltammetric techniques also include linear sweep

voltammetry (LSV), differential pulse voltammetry (DPV), and square wave voltammetry (SWV) that are fast but not very sensitive techniques. Cyclic voltammetry (CV) is not sensitive enough for determination of trace metals in natural waters, but is used to study electrode processes and finding optimum analytical conditions (Buffle *et al*., 2000).

According to Locatelli, (2007) voltammetric techniques with its great versatility (e.g. high sensitivity, multi-component analysis and low instrument cost) has allowed its application in a large number of analytical problems relevant to clinical, environmental, industrial and food matrices.

3.2.1. Cyclic Voltammetry

The technique of cyclic voltammetry (CV) belongs to the category of voltammetric techniques based on linear potential sweep chrono-amperometry. Cyclic voltammetry is a reversal technique that is extremely powerful, and is the potential-scan equivalent of double potential step chronoamperometry. During the initial electrochemical studies of new systems CV has become a very popular electrochemical technique and has proven very useful in obtaining information about fairly complicated electrode reactions. It offers a rapid location of redox potentials of the electroactive species. In order to ensure that the mass transport is purely diffusive the CV experiment is carried out under stationary conditions (the solution is kept unstirred). A disadvantage is the frequently overestimated power of the technique in that simple cyclic voltammetric measurement rarely allows one to gain complete electrochemical information (Skoog *et al*., 2007; Kissinger and Heineman, 1983). Figure 12 illustrates a typical cyclic voltammogram for a redox couple.
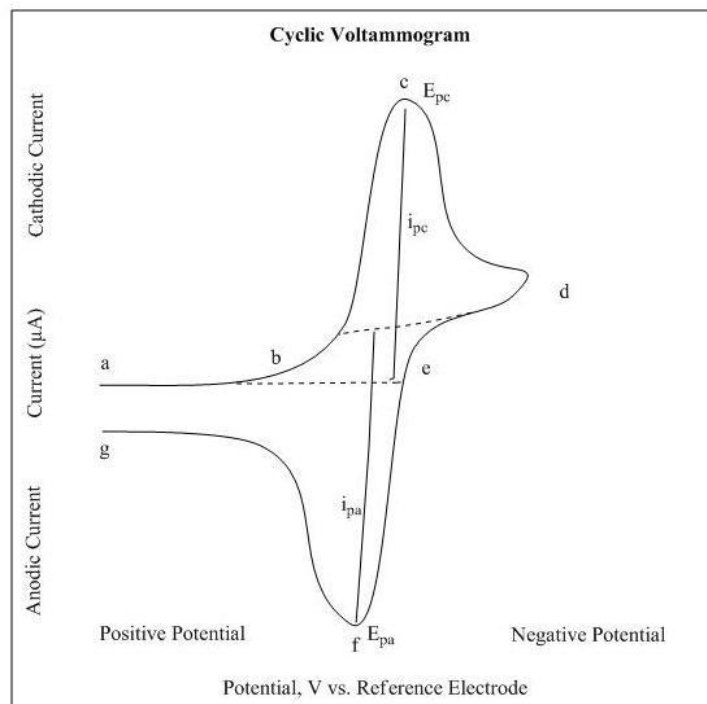
Figure 12. **Typical cyclic voltammogram for a reversible process. E_{pa} = anodic peak potential, E_{pc} = cathodic peak potential, I_{pa} = anodic peak current, I_{pc} = cathodic peak current (Jurgen, 1984; Skoog *et al*., 2007).**
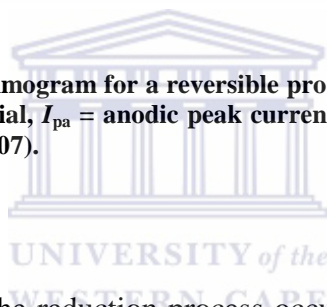
According to Figure 12, the reduction process occurs from the initial potential (a) to the switching potential (d). To cause a reduction reaction in this region, the potential is scanned in a negative direction. The resulting current due to reduction is called cathodic current (I_{pc}) and the corresponding peak potential is called cathodic peak potential (E_{pc}) at (c). The E_{pc} is reached when all of the substrate at the surface of the electrode has been reduced. Before the potential is scan in a positive direction from (d) to (g) the switching potential must be reached. Oxidation occurs and results and is called the anodic peak current (I_{pa}). To obtain I_{pa} all the substrate at the surface of the electrode must be oxidized (Skoog *et al*., 2007; Kissinger and Heineman, 1983).

3.2.3. Differential Pulse Voltammetry

The electro-analytical technique such as differential pulse voltammetry (DPV) is often used to make electrochemical measurements. This method is also known as differential pulse polarography (DPP) and can be considered as a derivative of staircase voltammetry or linear sweep voltammetry with a series of regular voltage pulses superimposed on the potential stair steps or linear sweep. Before each potential change the current is measured and the change in current is plotted as a function of potential. The effect of the charging current can decreased by sampling the current just before the potential is changed. The characteristics of differential pulse voltammetry are the symmetrical peaks obtained by reversible reactions and asymmetrical peaks by irreversible reactions. The peak potential is equal to $E_{1/2}$-ΔE in reversible reactions, and the peak current is proportional to the concentration with a detection limit of about 10^{-8} M (Bard and Faulkner, 2000; Drake *et al*., 1978).

According to Sujaritvanichpong *et al*. (1986), the main disadvantage of the DPV method is the long measurement time. In this method it takes approximately 20 min to obtained well defined peaks in the range of 1 V. Time saving analysis is introduced into the simple method by shorted the pulse interval, which is conventionally as long as a few or several seconds. In DPV the main problem encountered in shortening interval between pulses leads to distortion of the peak shape. This phenomenon is because of the influence of the whole sequence of pulse electrolysis preceding a given pulse.
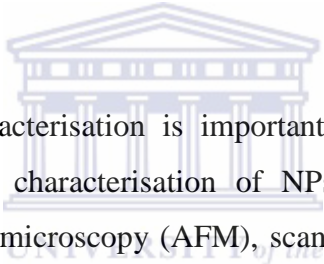
3.2.4. Adsorptive Stripping Voltammetry

Adsorptive stripping voltammetry (AdSV) is the technique that involves the accumulation of the analyte of interest onto the electrode surface by adsorption, generally without electrolysis, followed by differential pulse, square wave or direct current voltammetric determination of the surface adsorbed species. The surface active species is formed during trace metal analysis by either reaction of the metal ion with a suitable reagent giving a complex, which is then adsorbed on the electrode surface or by reaction of the metal ion with the reagent adsorbed on the electrode surface. The reduction of the metal or ligand in

the adsorbed complex or the catalytic evolution of hydrogen produced a current during the cathodic scan. According to the literature the adsorbed layer can be reduced during the cathodic scan giving low limits of detection (Maxwell and Smyth, 1996).

This AdSV results in procedures for measuring more than 25 trace metals, coupled with conventional stripping schemes, and about 45 elements are now measurable by stripping analysis. It also allows the simultaneous determination of 2 or 3 metals, based on the metal chelates peak potentials separations. In the presence of dissolved oxygen adsorptive stripping chronopotentiometry metal analysis are also possible (Wang *et al.*, 1989; Adeloju *et al.*, 1984).

3.3. Microscopy Techniques

Nanoparticles (NPs) characterisation is important to control and understand NPs synthesis and applications. The characterisation of NPs are performed using different techniques such as, atomic force microscopy (AFM), scanning electron microscopy (SEM), transmission electron microscopy (TEM), powder X-ray diffractometry (XRD), X-ray photoelectron spectroscopy (XPS), dynamic light scattering (DLS), ultraviolet-visible spectroscopy (UV-Vis), Fourier transform infrared spectroscopy (FT-IR) and Raman spectroscopy. The use of these techniques is for the determination of different parameters such as particle shape, size, pore size and surface area, crystallinity, fractional dimensions (Abou El-Nour *et al.*, 2010; Choi *et al.*, 2007; Yoosaf *et al.*, 2007; Hutter and Fendler, 2004; Sun *et al.*, 2008; Vilchis-Nestor *et al.*, 2008; Yeo *et al.*, 2003; Zhang *et al.*, 2004, 2006; Chimentao *et al.*, 2004; He *et al.*, 2004; Khomutov and Gubin, 2002).

In the next sections the microscopy techniques used in this study is discussed.

3.3.1. Atomic Force Microscopy

In a broad spectrum of applications such as biology and biomaterials, materials and manufacturing, semi-conductors, polymers and electronics, atomic force microscopy (AFM) analysis has evolved into a useful tool and can be employed for direct measurement of intermolecular forces with atomic-resolution. Additional capabilities and advantages relative to scanning electron microscopy (SEM) and transmission electron microscopy (TEM) are provided by AFM in studies metallic surfaces and micro-structures by providing reliable measurements at the nanometer scale (Goeken and Kempf, 1999; Kempf *et al*., 1998; Nagashima *et al*., 1996; Westra and Thomson, 1995; Yamamoto *et al*., 2000).

Atomic force microscopy measures three dimensional images so that particle height and volume can be calculated and is an advantage over the traditional microscopy techniques such as SEM and TEM (Abou El-Nour *et al*., 2010). Figure 13 illustrates a schematic diagram of a typical AFM system. The AFM system consists of a micro-machined cantilever probe mounted with a sharp tip, a Piezoelectric (PZT) scanner and a position sensitive photo detector. The photo detector receives a laser beam reflected off the end-point of the beam to provide cantilever deflection feedback. In AFM operation, the principal is to scan the tip over the sample surface with feedback mechanisms that enable the PZT scanners to maintain the tip at a constant height above the sample surface. The resulting laser beam deflected from the cantilever provides measurements of the difference in light intensities between the upper and lower photo detectors as the tip scans the surface of the sample, by moving up and down with the contour of the surface. As a result the feedback from the photodiode difference signal, through software control from the computer enables the tip to maintain either a constant height above the sample (Jalili and Laxminarayana, 2004).
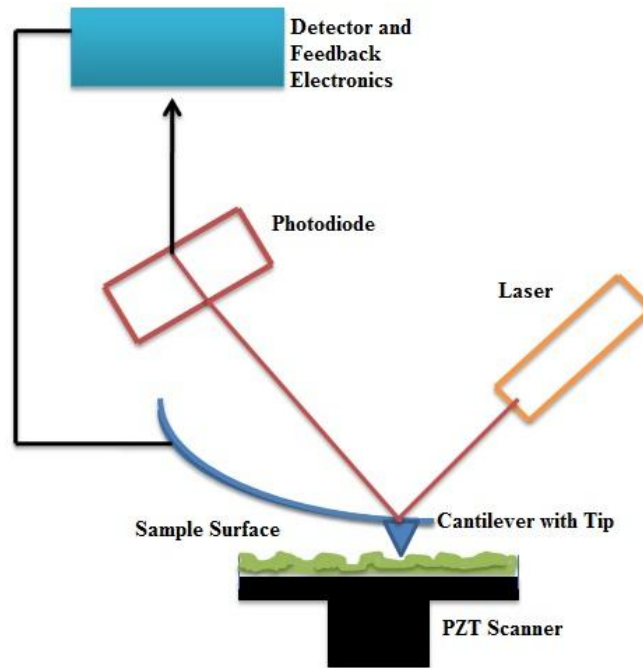
Figure 13. **Schematic diagram of a typical AFM instrument (Santosa and Castanhob, 2004).**
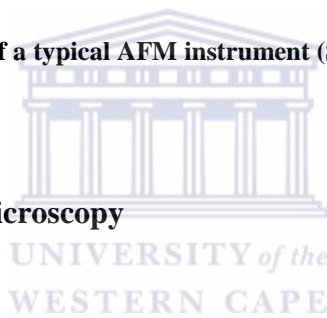
3.3.2. Transmission Electron Microscopy

The electron microscope is a scientific instrument that uses a beam of highly energetic electrons to examine objects on a very fine scale. From this examination, information about the morphology (shape and size of the particles making up the object), topography (surface features of an object), crystallographic (how the atoms are arranged in the abject) and composition (the elements and compounds that the object is composed of and the relative amounts of them) information are obtained. In 1931 Max Knoll and Ernst Ruska developed the first transmission electron microscope (TEM) in Germany. This transmission electron microscope developed was the first type of electron microscope. The construction of this TEM was exactly based on the construction of the Light Transmission Microscope, except that a focused beam of electrons is used instead of light to "see through" the specimen (Ruska and Knoll, 1931).

The technique of TEM is where an electron beam interacts and passes through a specimen. The electrons are emitted by a source and are focused and magnified by a system

of magnetic lenses. Figure 14 illustrates a schematic diagram of a typical TEM system with all the important components of the instrument highlighted. In the TEM system two condenser lenses confined and control the brightness of the electron beam that passes through the condenser aperture and "hits" the sample surface. The transmitted beams consist of electrons that are elastically scattered which pass through the objective lens. The image display and the following apertures are formed by the objective lens and the objective and selected area aperture are used to choose the elastically scattered electrons that will form the image of the microscope. This transmitted beam goes to the magnifying system that consists of three lenses, the first and second intermediate lenses that control the magnification of the image and the projector lens. a fluorescent screen or monitor are used to show the formed image and is printed on a photographic film (Voutou and Stefanaki, 2008).

The initial designs of TEM were able to magnify specimens up to seventeen times greater than that of a light microscope. Nowadays, the modern TEM have a resolution at most of 10 000 times greater. A disadvantage of TEM is that electrons are largely unable to pass through thick specimens and it was largely impossible to utilize this instrument to full capacity. In 1951 the design of the diamond knife and ultra-microtome eliminated these limitations. Many different techniques based on TEM are used in materials science (Voutou and Stefanaki, 2008).
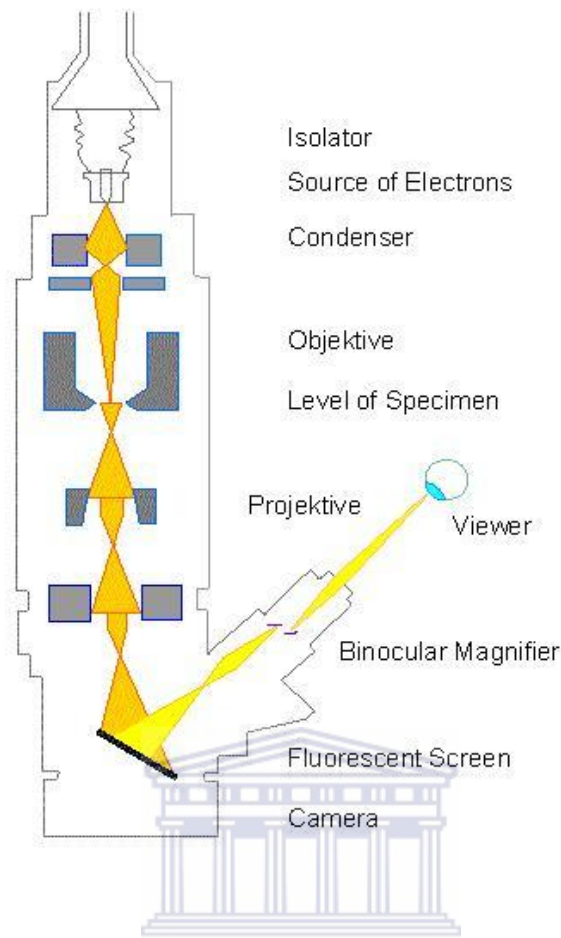
Figure 14. **Schematic diagram of a typical TEM instrument (www4.nau.edu).**

3.3.3. Scanning Electron Microscopy

The introduction of the first scanning electron microscope (SEM) was in 1938 by Von Ardenne with the first commercial instruments available around 1965. Due to the electronics involved in "scanning" the beam of electrons across the sample, some difficulty was experience and this is the reason for the late development. The two main components of the SEM instrument are the electron column and the electronic console. Control knobs and switches provided by the electronic console allow for the instrument adjustments such as accelerating voltage, magnification, filament current, focus, brightness and contrast. A computer system is used by the FEI Quanta 200 and this is a state of the art electron microscope. The use of this computer system in conjunction with electronic console eliminates the bulky console with its control knobs, CRTs and an image capture device. All

of these primary controls are accessed through the computer system and are operated by the mouse and keyboard. In the past the SEM image that is produced was usually viewed on CRTs located on the electronic console. Nowadays with FEI the image can be seen on the computer monitor and the captured images can be saved in digital format or printed directly (Postek *et al*., 1980; Lyman *et al*., 1990). A good illustration of a SEM instrument is shown in Figure 15.
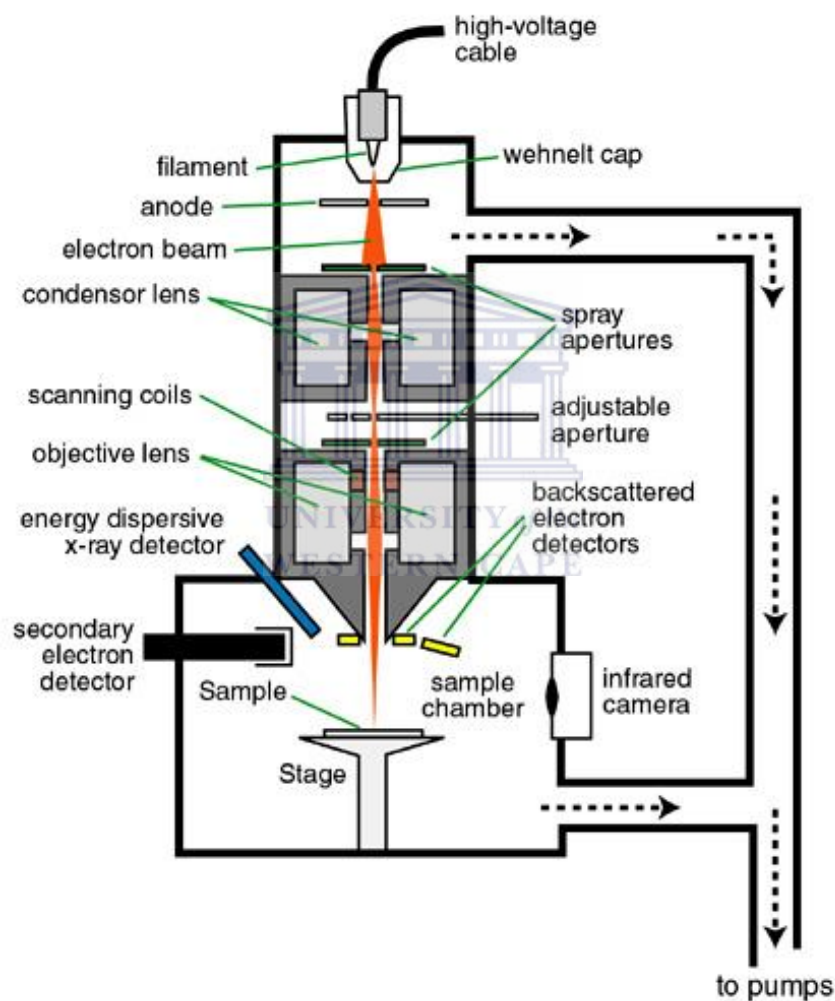
Figure 15. **Schematic diagram of a typical SEM instrument (www4.nau.edu.).**

The SEM system consists of an electron gun located at the top of the column where free electrons are generated by thermionic emission from a tungsten filament at ~2700K. In the electron gun, the Wehnelt consist of a filament that controls the number of electrons leaving the

gun. The condenser lenses focuses the beam after it passes the anode causes the beam to converge and pass through a focal point. In this process, the electron beam is essentially focused down to 1000 times its original size. The column consists of one or more apertures depending on the size of the microscope. The function of these apertures is to reduce and exclude extraneous electrons in the lenses. Images are formed in the scanning system by closely scanning the electron beam across the specimen using deflection coils inside the objective lens. The specimen chamber is located at the lower portion of the column. From the specimen the secondary electrons are attracted to the detector by a positive charge (Postek *et al*., 1980; Goldstein *et al*., 1975; Watt, 1985).

3.4. Spectroscopic Techniques

3.4.1. Inductive Coupled Plasma-Mass Spectroscopy
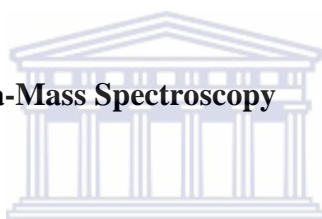
An analytical technique such as inductively coupled plasma mass spectroscopy (ICP-MS) was developed in the late 1980's to perform elemental analysis with excellent sensitivity and high sample throughput. A plasma (ICP) as the ionization source and a mass spectrometer (MS) analyzer to detect the ions produced are employed by the ICP-MS instrument. The advantage of ICP-MS is the simultaneous determination of most elements in the periodic table and determine analyte concentration down to the subnanogram-per-liter or part-per-trillion (ppt) level. Inductive coupled plasma mass spectrometry can perform semi-quantitative, quantitative, qualitative analysis and compute isotopic ratios (Gray, 1989; Jarvis *et al*., 1992).

Over the years ICP-MS has been widely used in a number of different fields including food sciences, medicine, drinking water, natural water systems/hydrogeology, wastewater, mining/metallurgy, soil science and geology. This ICP technology was built upon the same principles used in inductive coupled plasma atomic emission spectrometry (ICP-AES). These principles consist of the decomposition of samples to neutral elements in high temperature argon plasma and analysed based on their mass to charge ratios. Inductive coupled plasma

mass spectrometry method are divided into four main processes, including sample introduction and aerosol generation, ionisation by an argon plasma source, mass discrimination, and the detection system (Kishi, 1997). Figure 16 is a good illustration of the sequence of processes for ICP-MS analysis.
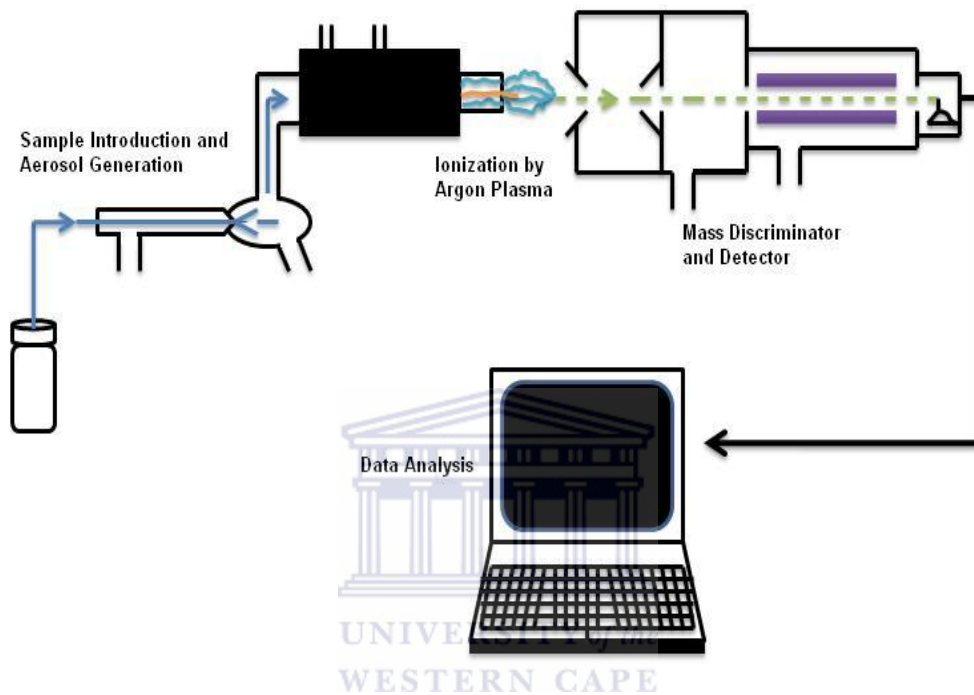
Figure 16.   **Schematic diagram of a typical ICP-MASS spectrophotometer (Jarvis *et al*., 1992).**

3.4.2. Inductive Coupled Plasma-Atomic Emission Spectroscopy

One of the most common analytical techniques for the detection of trace metals is Inductively Coupled Plasma-Atomic Emission Spectrometry (ICP-AES). Inductively coupled plasma atomic emission spectroscopy is also referred to as inductively coupled plasma optical emission spectrometry (ICP-OES). The use of this technique in a large variety of applications is due to its multi-element capability, good detection limits and its high specificity. Analysis is done on all kinds of dissolved samples, varying from solutions containing high salt concentrations to diluted acids. The sample is dissociated into its constituent atoms or ions by a plasma source and exciting them to a higher energy level for detection and analysis.

Photons of a characteristic wavelength depending on the element present are emitted by the exited atoms or ions when they returning to their ground state. An optical spectrometer records this emitting light and when calibrated against standards the technique provides a quantitative analysis of the original sample. Inductive coupled plasma-optical emission spectroscopy is used for example in motor oil analysis, the determination of metals in wine, arsenic in food and trace elements bound to proteins. Inductively coupled plasma atomic emission spectroscopy is often used for analysis of trace elements in soil, and in forensic science to ascertain the origin of soil samples found at crime scenes or on victims, etc. (Stefánsson *et al.*, 2007). Figure 17 is a very good illustration of an ICP-AES spectrophotometer.
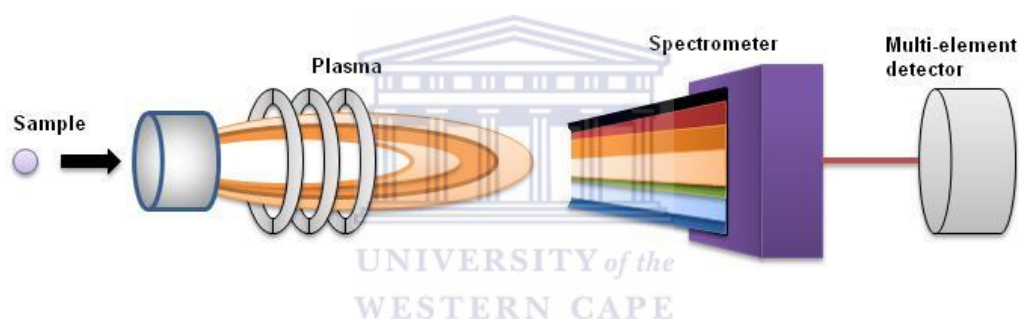
Figure 17.   Schematic diagram of a typical ICP-AES spectrophotometer (Aceto *et al*., 2002).

3.4.3. Electrochemical Impedance Spectroscopy

Information about the chemical and physical processes occurring on electrode surfaces is provided by electrochemical impedance spectroscopy (EIS). In electrochemical impedance spectroscopy it is known that real electrodes deviate from purely capacitive behaviour, as is expected for ideally clean and smooth surfaces. It is known that EIS is a powerful tool in mechanism characterisation and the determination of reaction parameters (Scribner and Taylor, 1990; Sluyters-Rehbach and Sluyters, 1984; Sluyters-Rehbach and Sluyters, 1986; Smith, 1966).
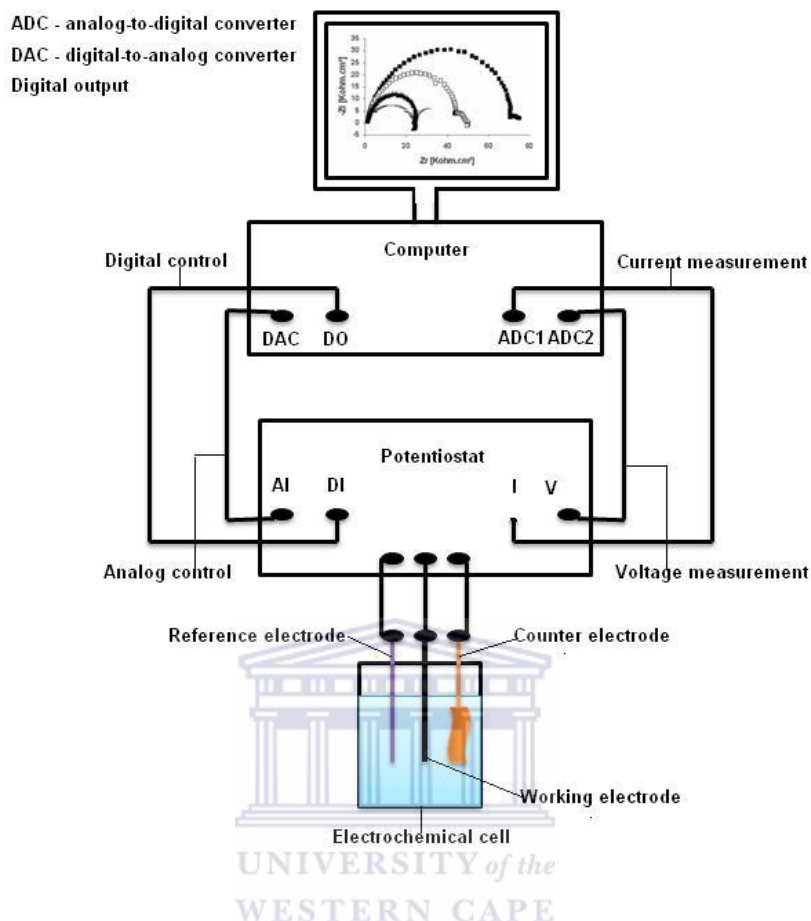
Figure 18. Schematic diagram of a typical electrochemical impedance spectroscopy instrument (Ragoisha and Bondarenko, 2003).

The application of EIS has been relatively infrequent but electrochemical sensor characterisation has increased. In electroanalytical experiments, EIS characterisation was performed in several electrolytes over a wide range of pH values, studying the influence of pretreatment of the electrode surface by potential cycling in perchloric acid on the voltammetric profile. According to Filipe and Brett (2004), the reactivity of the electrode surface depends on the electrolyte and the pre-treatment, altering the magnitude of the impedance and the shape of the impedance spectra. For useful electro-analytical applications, more reactive surfaces are obtained by a pre-treatment in perchloric acids (Hayama *et al*., 2002; Cui and Martin, 2003; Katz and Willner, 2003; Brahim *et al*., 2003; Filipe and Brett, 2004). In Figure 18 a good schematic diagram of EIS is shown.

3.4.4. Ultraviolet Visible Spectroscopy

Analytical techniques based on the interaction of light and matter is called spectroscopy. The measurement of the absorption of light by molecules that are in a gas or vapour state or dissolved molecules/ions is spectrophotometry and forms a branch of spectroscopy. Spectrophotometry investigates the absorption of the different substances between the wavelength limits 190 nm and 780 nm. The absorption of the electromagnetic radiation in this wavelength range is caused by the excitation (*i.e.* transition to a higher energy level) of the bonding and non-bonding electrons of the ions or molecules. The sample's absorption spectrum is given by a graph of absorbance against wavelength and is automatically drawn by modern spectrophotometers. Due to the fact that the different vibration and rotation states of the molecules make the absorption band wider, a resulting continuous spectrum is obtained (Skoog *et al.*, 2007). Figure 19 demonstrates the schematic diagram of a single beam UV-Vis spectrophotometer.
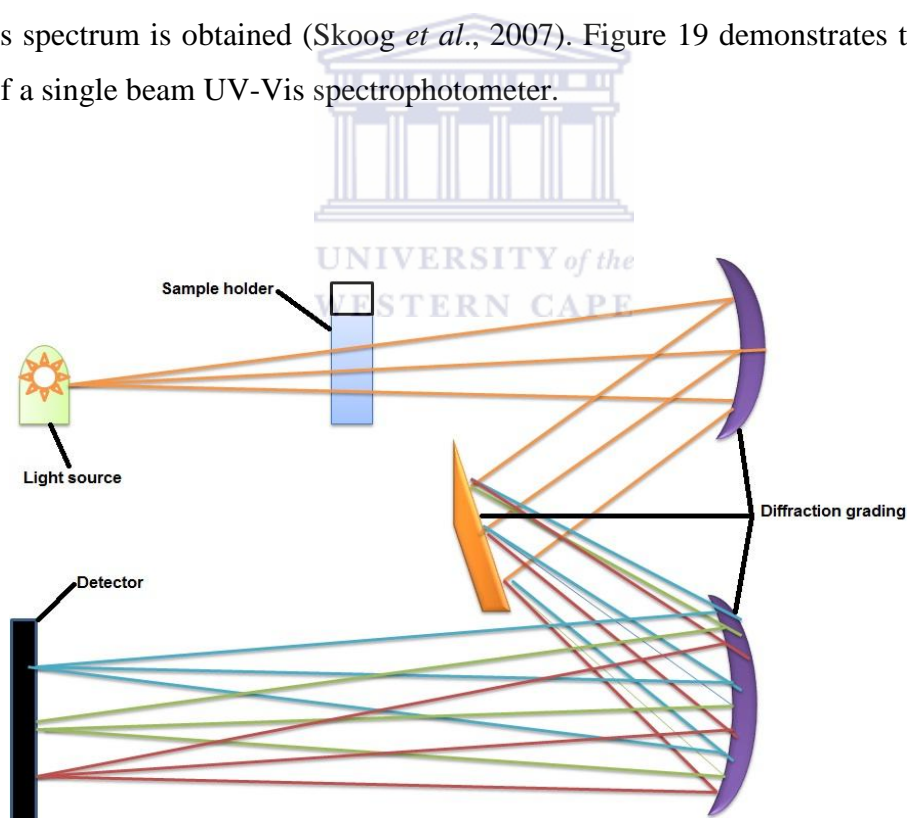
Figure 19.   Schematic diagram of a single-beam UV-Vis spectrophotometer (Skoog *et al*., 2007).

3.4.5. Fourier transform infrared Spectroscopy

The technique whereby spectra are collected based on measurements of the coherence of a radiative source, using time-domain or space-domain measurements of the electromagnetic radiation or other type of radiation is called Fourier transform spectroscopy. This technique can be applied to a variety of types of spectroscopy including infrared spectroscopy (FT-IR), optical spectroscopy, mass spectroscopy (MS), electron spin resonance (ESRS) spectroscopy, nuclear magnetic resonance (NMR) and magnetic resonance spectroscopic imaging (MRSI). The temporal coherence of light can be measured by several methods including the pulsed Fourier transform spectrograph and the continuous wave Michelson or Fourier transform spectrometer. In the technique of Fourier transform spectroscopy a Fourier transform is required to turn the raw data into an actual spectrum and is also based on the Wiener-Khinchin theorem in cases of optics involving interferometers (Griffiths and de Hasseth, 2007). A schematic diagram of a Michelson interferometer is shown in Figure 20.
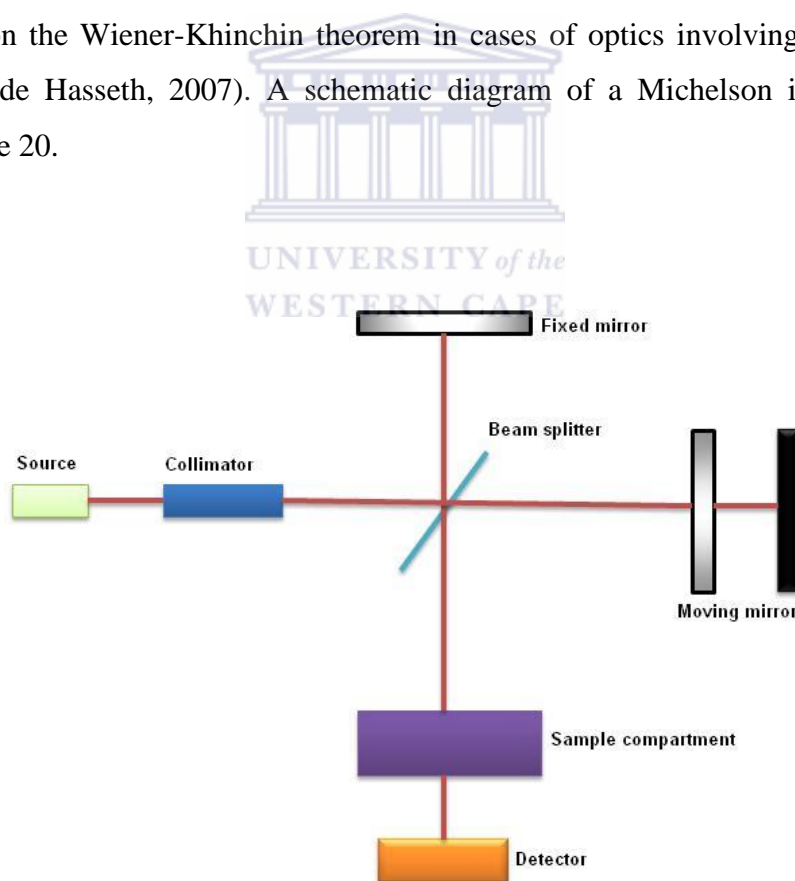
Figure 20.   **Schematic diagram of a Michelson interferometer (Griffiths and de Hasseth, 2007).**

3.4.6. Raman Spectroscopy

The study of vibrational, rotational and other low-frequency modes in a system can be done by a spectroscopic technique such as Raman spectroscopy. Raman spectroscopy relies on monochromatic light from a laser in the visible, near infrared or near ultraviolet ranges. This laser light in Raman spectroscopy interacts with photons, molecular vibrations or other excitations in the system and results in an up and down shift in the energy of the laser photons. The shift in laser photons energy gives information about the vibrational modes in the system and similar information are obtained by Infrared spectroscopy (Gardiner, 1989).

In the chemistry field Raman spectroscopy is commonly used, since vibrational information is specific to the chemical binding and symmetry of molecules. The molecule can be identified by Raman spectroscopy because it provides a fingerprint for a specific molecule. Infrared and Raman spectra are used on the basis of normal coordinate analyses to identify the vibrational frequencies of SiO, Si_2O_2 and Si_3O_3. For organic molecules the fingerprint region is in the wavenumber range of $500 - 2000$ cm^{-1}. The study of changes in chemical bonding is another way where the technique is used, when a substrate is added to an enzyme for example (Khanna, 1981). The setup of a Raman experiment is illustrated in Figure 21.
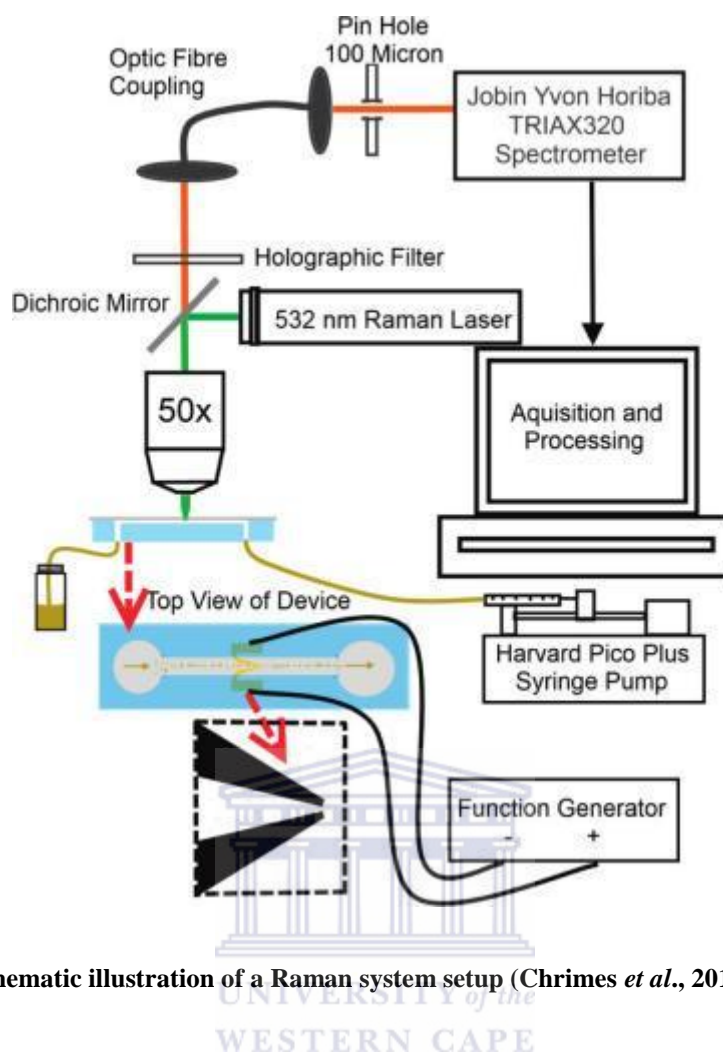
Figure 21.   **Schematic illustration of a Raman system setup (Chrimes *et al*., 2012).**

3.5. Voltammetric Characterisation

Cyclic voltammetric (CV) characterisations were done using classical and modified glassy carbon electrodes (GCEs). For trace metal analysis a glassy carbon bismuth-silver bimetallic film electrode (GCE/Bi-AgFE) were used as the working electrode, Ag/AgCl as the reference electrode and a platinum wire for the auxiliary electrode. Different sample concentrations for the platinum group metals (PGMs) were investigated in various samples. The voltammetric measurements were performed in weak acidic supporting electrolyte solution. The potentials were scanned from -1.0 to +0.4 V vs. (Ag/AgCl). For the platinum group metal analysis a GCE was rinse with deionised water and placed in a sonicator for 8 minutes. The bismuth-silver bimetallic nanoparticles (Bi-Ag NPs) were added by drop wise coating onto the clean GCE and left at room temperature for air drying. A very good Bi-Ag

bimetallic film was coated on the clean GCE surface and the electrode was ready for use. Figure 22 illustrates an Epsilon electrochemical analyser that was used to perform the electrochemical measurements (Willemse, 2009; Van der Horst, 2011).

Figure 22.   Typical Epsilon electrochemical analyser (Willemse, 2009; Van der Horst, 2011).

Chapter 4

Nanoparticles synthesis and characterisation

4.1. Introduction

Heavy metal contamination at trace levels in water resources presents a major current environmental threat, therefore the detection and monitoring of these metal contaminants results in an ever-increasing demand (Heitzmann *et al*., 2005). In electrochemical stripping analysis of heavy metals, and platinum group metals (PGMs), the use of mercury electrodes has gained wide acceptance. Due to the toxicity of mercury, its difficulties in handling, storage, and disposal have restricted its use in electro-analytical techniques (Wang 2005; Economou and Fielden 1998; Wang 1985; Jones and Compton 2008; Daniele *et al*., 2008). Nowadays, many researchers request alternative working electrodes for the determination of heavy metals and PGMs. The search for new electrode materials such as silver (Ag) electrodes, glassy carbon electrodes (GCEs), bismuth film electrodes (BiFEs), carbon nanotubes (CNTs), screen-printed carbon electrodes (SPCEs) or carbon paste electrodes (CPEs), and metal nanoparticles (NPs) (Ag, Bi, and Bi/Ag, etc.) in stripping analysis has increased (Khezri *et al*., 2008; Senthilkumar and Saraswathi 2009; Abdollah and Fatemeh 2009; Li *et al*., 2009; Somerset *et al*., 2010; Maiti *et al*., 2009). The aforementioned metal NPs have received much attention due to their potential application in microelectronics, magnetic devices, electronics, and various sensor applications. For Ag NPs it presents a great interest due to their unique chemical and physical properties such as high electrical and thermal conductivity, optical, and catalytic properties that depend on size and shape of the Ag NPs (Haes and Van Duyne 2003; Magdassi *et al*., 2003; Nie and Emory 1997; Pradhan *et al*., 2002; Ye *et al*., 1999). Due to the high surface area, very small size (< 20 nm), and high dispersion, Ag NPs are applied as antimicrobial and antifungal agent (Gaidau *et al*., 2009). The work done by Shukla *et al*. (2012), the "green" synthesis method was used to synthesise silver NPs. This "green" synthesis is eco-friendly and nontoxic for nanosilver formation, efficient, easy going, fast, and renewable. The characterisation of these NPs was done by X-ray diffraction pattern (XRD), transmission electron microscopy (TEM), ultraviolet-visible

(UV-Vis) spectroscopy and Fourier transformed infrared spectroscopy (FT-IR). In this study, azadirachtin was used as the reducing and stabilizing agent for nanosilver formation with particles size of 8.25 ± 1.37 nm. These silver NPs show potential applications in the field of fuel cells, catalysis, nanodevices and sensors.

In recent years bismuth (Bi) has gained much attention in metallurgical and pharmaceutical additives and has been used to replace mercury in environmental sensor application (Sun *et al*., 1999; Guo *et al*., 2005). The ability of Bi to form alloys with different metals are one of the advantageous analytical properties and its alloys are used as high-temperature heat-transfer agents (Wang *et al*., 2006; Hocevar *et al*., 2002; Kefala *et al*., 2006). Bismuth, which has semi-metal properties, can be converted to a semiconductor by molecular beam epitaxy in thin Bi layer growth. The applications of Bi are also expanded by the magnetoresistance effect observed in single crystals and thin films (Kefala *et al*., 2006; Wang *et al*., 2006). The reduction of mixtures of various metal salts is of the same interest as the manufacturing of metallic Bi for the formation of intermetallic compounds or bismuth-base alloys. The Ag alloy of Bi prepared by electrochemical deposition from alkaline solutions is significant for application and the powders of Ag and Bi are widely used in medicine (Krastev *et al*., 2004; Briand and Burford 1999). The work done by Rico *et al*. (2009), illustrates a simple procedure for the chemical synthesis of bismuth NPs for the quantification of trace zinc, cadmium and lead in non-dearated water samples using anodic stripping square wave voltammetry. Bismuth NPs were subsequently adsorbed onto commercial screen-printed carbon electrodes. In this study the square-wave current signal was linear over the low *n*g/mL range and limit of detection ranging from 0.9 to 4.9 *n*g/mL with good precision.

Dong *et al*. (2012), has synthesized bismuth sulfide nanorods by a simple single source route using bismuth diethyldithiocarbamate as the precursor under hydrothermal conditions. A glassy carbon electrode was modified with these novel bismuth sulfide nanorods were modified for the determination of ascorbic acid. The bismuth sulfide nanorods sensor exhibit good response current with linear relationship for the concentration of ascorbic acid from 1.0×10^{-6} to 1.0×10^{-3} M, correlation coefficient of 0.997 and limit of detection of 8.3×10^{-7} M on signal-to-noise ratio of 3. Good recoveries were obtained with the application of this method for the determination of ascorbic acid in tap water and some real samples. In the case of bismuth-silver (Bi-Ag) NPs it was successfully synthesised according to

Kaowphong, (2012), in a simple biomolecule-assisted hydrothermal method (using L-cysteine) for the preparation of silver bismuth sulphide ($AgBiS_2$) NPs. In the aforementioned study of $AgBiS_2$ NPs, it refers to a pseudo-metallic film prepared while only characterisation of the NPs was done with no electrochemical sensor application.

In this study the focus was on the synthesis and characterisation of a novel true metallic film for stripping analysis and to differentiate between single Ag, Bi, and Bi-Ag bimetallic NPs for electrochemical sensor application. The individual Ag, Bi, and Bi-Ag bimetallic NPs were compared and characterised by cyclic voltammetry (CV), electrochemical impedance spectroscopy (EIS), UV-VIS spectroscopy, FT-IR spectroscopy, Raman spectroscopy, and TEM analysis to interrogate the structural and morphological properties of the synthesized compounds. The results reported in this study demonstrate that the novel synthesised Bi-Ag bimetallic NPs can be used to construct an electrochemical sensor for application in stripping voltammetric analysis for the determination of metal ions in environmental samples.

4.2. Experimental Methods

4.2.1. Materials and reagents

Sodium acetate, nitric acid (55%), sulphuric acid (95%), and ethanol (absolute 99.9%) were purchased from Merck (South Africa). Silver nitrate ($AgNO_3$) and glacial acetic acid (95%) was purchased from Kimix. The reagent *N,N*-dimetylformamide (98%) was also purchased from Merck (South Africa). Bismuth nitrate pentahydrate ($Bi(NO_3)_3$ $5H_2O$), poly(vinyl) alcohol, citric acid and sodium boronhydride ($NaBH_4$) were also obtained from Aldrich (Germany). Platinum standards (1000 mg.L^{-1} AAS), dimethylglyoxime were perchased from Fluka (Germany). A 0.2 M sodium acetate buffer (pH 4.8) was prepared by mixing sodium acetate with acetic acid and deionised water and served as the supporting electrolyte. The 0.01 M dimethylglyoxime (DMG) solution was prepared in 95% ethanol and served as the chelating agent. All solutions were prepared using Milli-Q (Millipore) water.

4.2.2. Instrumentation

The spectral characteristics of the chemically synthesised nanoparticles (NPs) were investigated with the help of a Bruker ALPHA-T, FT-IR (Bruker, South Africa) spectrometer fitted with Bruker Optics aligned Rocksolid^{TM} interferometer over a wavelength interval of 400-4000 cm^{-1} at room temperature. Ultraviolet-visible spectroscopic experiments were performed using a ThermoFisher SpectronicTM Helios$^{(TM)}$ range (Thermo, USA), UV-Vis spectrometer with VISION PC software. Electrochemical measurements were conducted with an Epsilon electrochemical analyzer (BASi Instruments, 2701 Kent Ave., West Lafayette, IN 47906, USA) using cyclic voltammetry (CV) and differential pulse stripping voltammetry (DPSV) modes. A conventional three electrode system was employed, consisting of a 1.6 mm diameter glassy carbon disc working electrode, a 3 M NaCl-type Ag/AgCl reference electrode, and a platinum wire auxiliary electrode, supplied by BASi. All electrochemical experiments were carried out in a single compartment electrochemical cell and at room temperature (21 ± 1 °C). Transmission electron microscopy (TEM) morphology studies were performed by using a Tecnai G2F20 X-Twin Mat 200 kV Field Emission Transmission Electron Microscope (Operated at 200 kV). All electrochemical impedance spectroscopy (EIS) experiments were performed on a VoltaLab instrument (Somerset *et al*., 2010; Silwana *et al*., 2013; Kshirsagar *et al*., 2011; Baleg *et al*., 2011).

4.2.3. Preparation of nanoparticles

4.2.3.1. Chemical synthesis of silver nanoparticles

In the chemical reduction of silver nitrate (AgNO$_3$), 30 mL of 0.002 M sodium borohydride (NaBH$_4$) was added to an Erlenmeyer flask. A magnetic stirrer bar was added, the flask was place in an ice bath on a stirrer plate and stirred, followed by cooling for about 20 minutes. To that solution, 2 mL of AgNO$_3$ (0.001 M) at a rate of approximately 1 drop per

second was added and stirred. Stirring was stopped as soon as all the $AgNO_3$ was added. The presence of a colloidal suspension was detected by the reflection of a laser beam from the particles. Solid polyvinyl alcohol crystals were added to the colloidal suspension to give a 4% solution. Yellow silver nanoparticles (NPs) was obtained, which was filtered, washed with acetone and Milli-Q water, and dried in a fume hood overnight at room temperature (Wang *et al*., 2005; Guzmán *et al*., 2008; Harmami *et al*., 2008).

4.2.3.2. Chemical synthesis of bismuth nanoparticles

Bismuth (Bi) nanoparticles (NPs) was prepared by the chemical reduction method using bismuth nitrate $(Bi(NO_3)_3)$ and sodium borohydride $(NaBH_4)$. This reduction method was performed in aerobic conditions, ambient pressure and room temperature. Approximately 0.01 M Bi solution (3.956 g) and 0.015 M $NaBH_4$ (0.567 g) was prepared separately. The process was started by the addition of the $NaBH_4$ to the Bi solution at once in order to avoid the nucleation effect and the growth of particles. The solution acquires a dark color due to the precipitation of Bi NPs and the products of the reaction were filtered several times using a Buchner funnel and deionized water to remove the undesired ions. It was subsequently washed with acetone to eliminate water and dried overnight in a fume hood at room temperature. The dried Bi NPs were transferred to a dry polyethylene container for storage and further characterisation (Hernandez-Delgadillo *et al*., 2012).

4.2.3.3. Chemical synthesis of bismuth-silver bimetallic nanoparticles

The low temperature synthesis of nanosized bismuth-silver bimetallic (Bi-Ag) particles was done by adding 0.01 M $Bi(NO_3)_3$ (4.85 g) and 0.01 M $AgNO_3$ (1.70 g) to a 2 M HNO_3 solution in an Erlenmeyer flask. Citric acid (3.84 g) was added to the solution and the solution heated while stirring on a hot plate until all the liquids evaporated from the solution. The temperature of the hot plate was kept at 160 ºC for 1 hour. A fluffy gray powder was obtained, collected and calcined at 400 °C for 2 hours and the yield was 95%.

4.2.4. Preparation of bismuth-silver bimetallic modified electrode

The glassy carbon disk electrode (GCE) that was used as working electrode was thoroughly cleaned and polished on a polish pad with 1.0, 0.3 and 0.05 µm alumina (Al_2O_3) powders. The well-polished GCE was first rinse with deionised water and then sonicated in ethanol and doubly distilled H_2O in turn. The GCE was transferred to the electrochemical cell for further cleaning by using cyclic voltammetry between -0.5 and +1.5 V at a scan rate of 100 mVs^{-1} in freshly prepared deoxygenated 0.5 M H_2SO_4 until a stable cyclic voltammetric profile was obtained. The cleaned GCE was gently blown under a nitrogen stream. A 2.5 mg of Bi-Ag bimetallic nanoparticles (NPs) were dispersed through ultrasonic vibration in 50 mL solution of deionised water to form a suspension. A defined quantity of the suspension was applied to a clean surface of glassy carbon (GC) substrate and dried at room temperature to get a thin film on the clean GCE (Noroozifar *et al*., 2011; Cui and Zhang, 2012; Prakash *et al*., 2012).
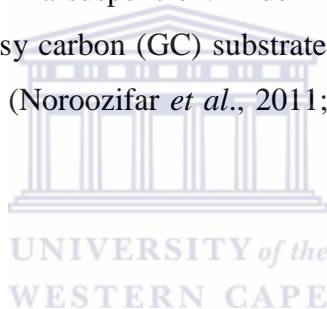
4.3. Results and Discussion

4.3.1. Microscopy characterisation

4.3.1.1. Scanning electron microscopy characterisation of nanoparticles

Figure 23 to 25 shows the high resolution scanning electron microscope (SEM) images of Ag, Bi and the Bi-Ag bimetallic nanoparticles (NPs). The results obtained in Figure 23 for Ag NPs shown an average particle size of 500 nm. The morphology available for the chemical reduction of Ag NPs is truncated octahedron with multiple twinned particles (Corr, 2011). Analysis of the SEM images for the Bi NPs in Figure 24 shows the average particle size is 0.5 to 1 µm. The identification of the morphology of these nanoparticles was

difficult due to the multiple shapes the Bi NPs exhibited. However, the results showed evidence of rod-like structures with small spherical particles in between (Carotenuto *et al*., 2009).

Figure 23. **Scanning electron microscopic (SEM) photographs of chemical synthesised silver nanoparticles.**

| 1 µm | EHT = 10.00 kV | Signal A = SE2 | Date :6 Nov 2012 | ZEISS |
| | WD = 10.8 mm | Mag = 25.00 K X | Time :10:06:11 | |
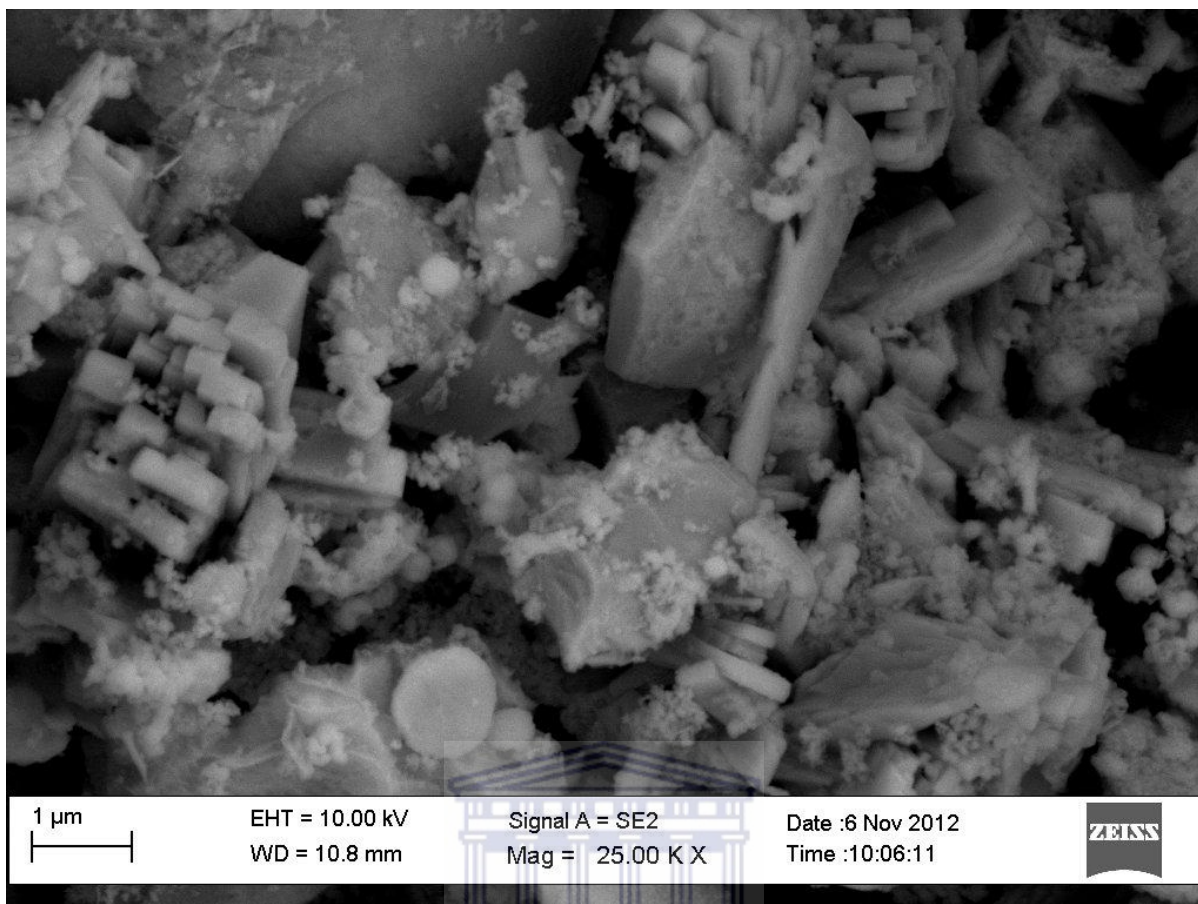
Figure 24.   **Scanning electron microscopic (SEM) photographs of chemical synthesised bismuth nanoparticles.**

Figure 25 illustrates the morphology of the Bi-Ag bimetallic NPs. In this SEM image the NPs have a spherical profile, but with a highly roughened surface. These particles consist of many irregular and randomly arranged protrusions. The average size observed for these NPs were 1-2 nm (Noel and Vasu, 1990; Liang *et al*., 2009).
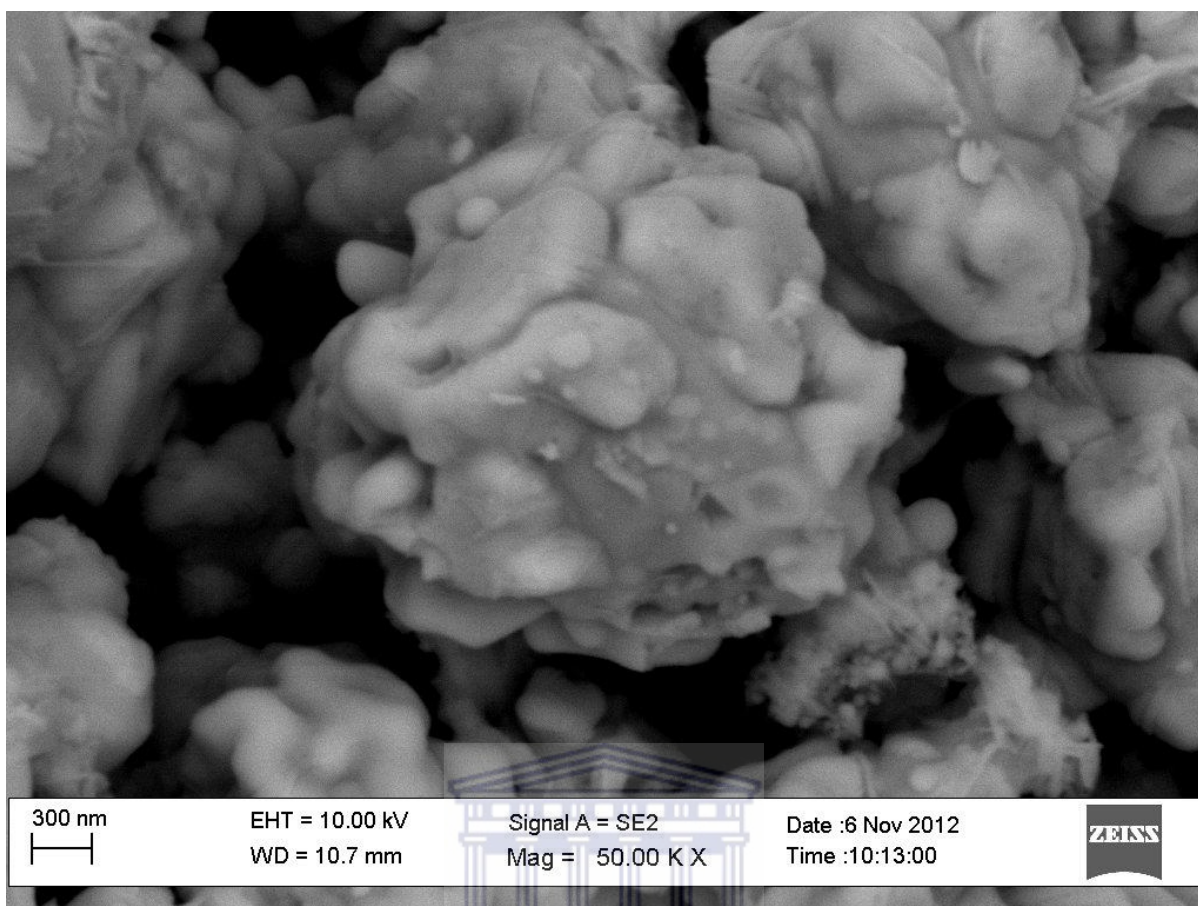
Figure 25. **Scanning electron microscopic (SEM) photographs of chemical synthesised bismuth-silver bimetallic nanoparticles.**

4.3.1.2. Transmission electron microscopy characterisation of nanoparticles

Figures 26 to 31 illustrates the high resolution transmission electron microscopy (HRTEM) images and the electron diffraction x-ray spectra of the chemically synthesised nanoparticles (NPs). In Figure 26 the average particle sizes of the Ag NPs are between 10-20 nm with spherical shapes and accompanied with some aggregates that are several times larger than the average particle size. The poly(vinyl) alcohol co-polymer can also be seen in the background (Shiraishi and Toshima, 1999). According to Meguro *et al*. (1988) the preparation of Ag NPs in the presence of co-polymers of vinyl alcohol and *N*-vinylpyrrolidone are very important and stable Ag nanoparticle clusters were obtained only in the presence of these co-polymers. The electron diffraction x-ray spectrum (Figure 27) of the Ag NPs exhibited the presence of carbon (C), oxygen (O), silicon (Si), silver (Ag) and copper

(Cu) elements. A very high amount of Cu element is observed in the spectrum and comes from the supporting copper grid.
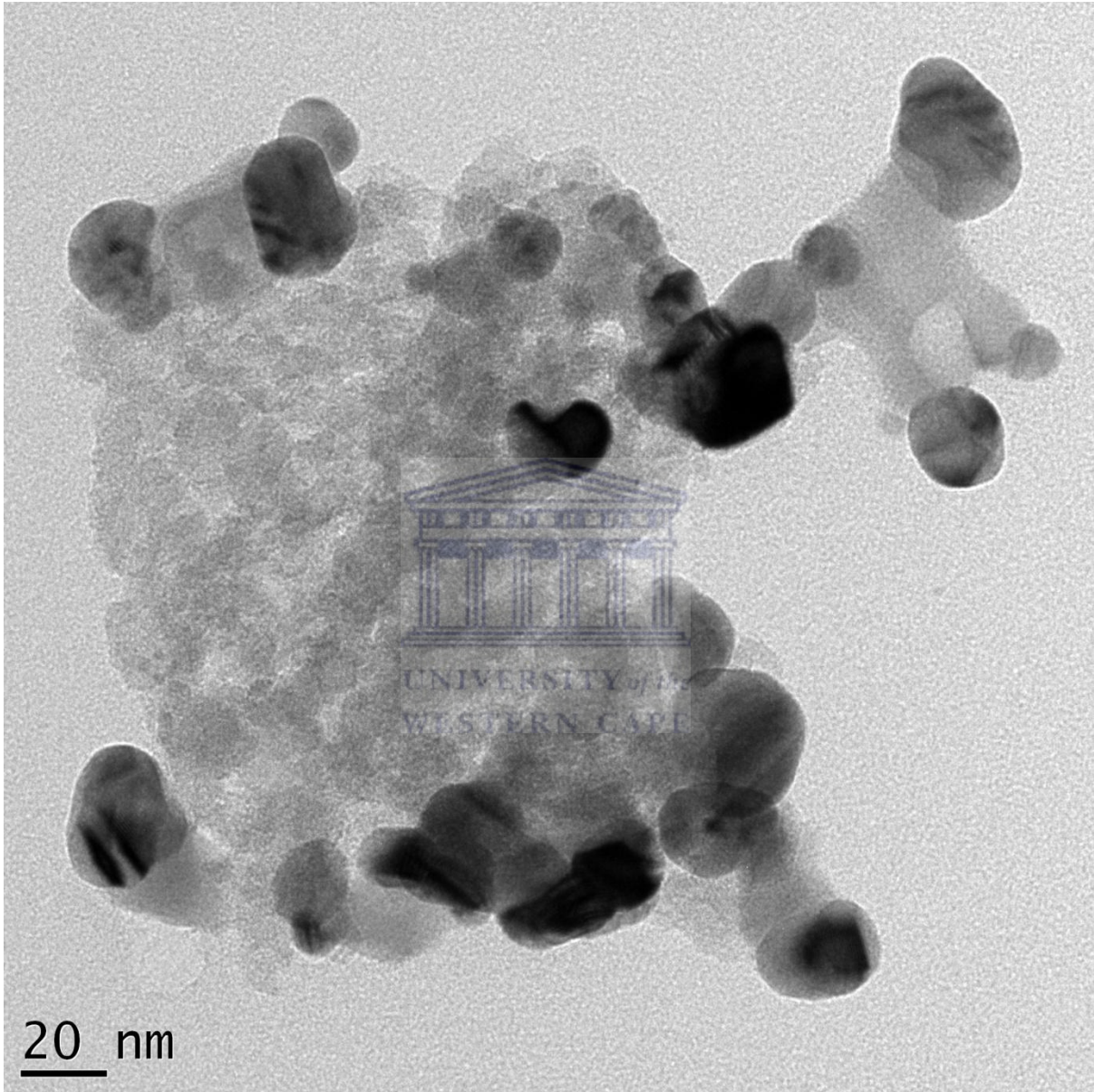
Figure 26. **High resolution transmission electron microscopy results of silver nanoparticles.**
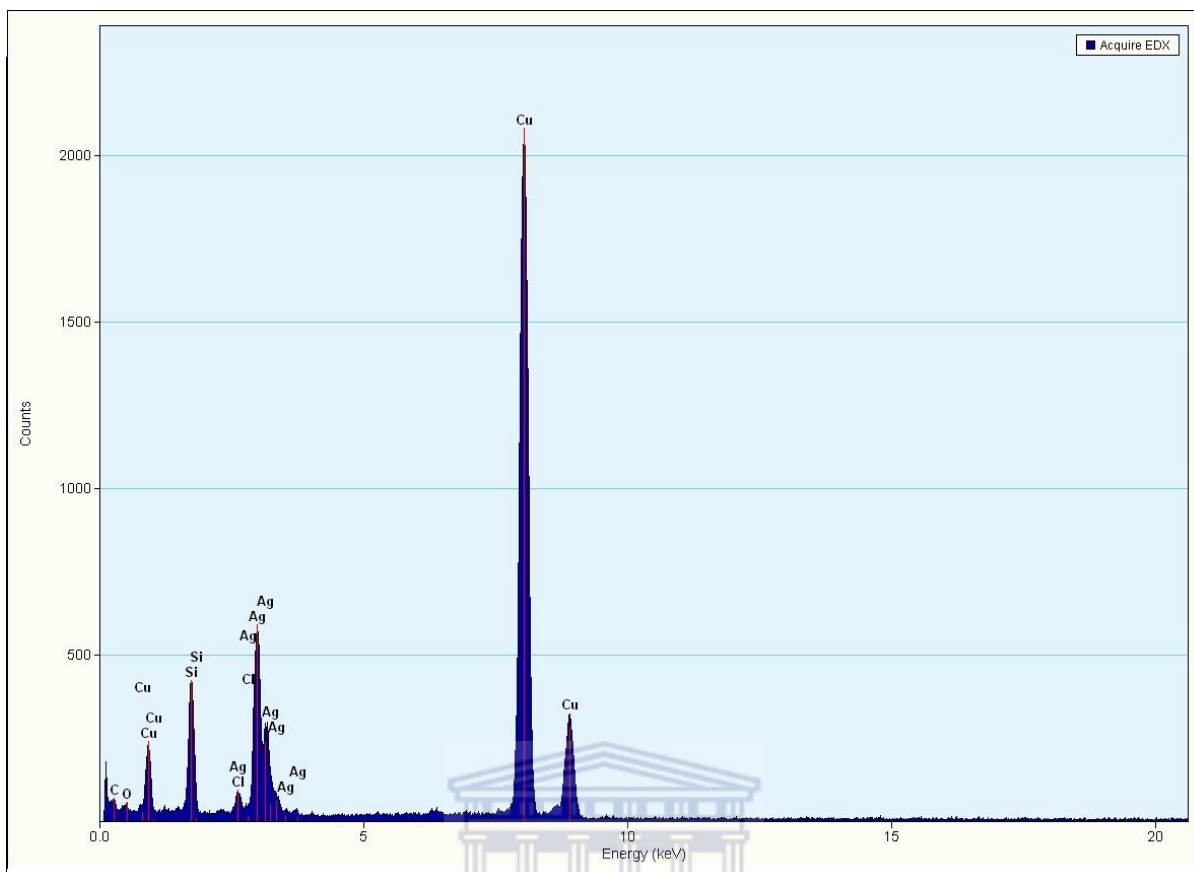
Figure 27. **Electron diffraction x-ray spectra of silver nanoparticles.**

Figure 28 illustrates the HRTEM image and the electron diffraction x-ray spectrum of the black Bi NPs. In the HRTEM image it is seen that the Bi NPs are spherical in shape. The average particle sizes of these NPs are between 10-30 nm. The electron diffraction x-ray spectrum of the Bi NPs confirmed the presence of C, O, Bi and Cu elements. The electron diffraction x-ray spectrum (Figure 29) also showed a very high amount of Bi element in the prepared NPs. It is noted that the Cu element comes from the supporting copper grid (Balan and Burget, 2006).
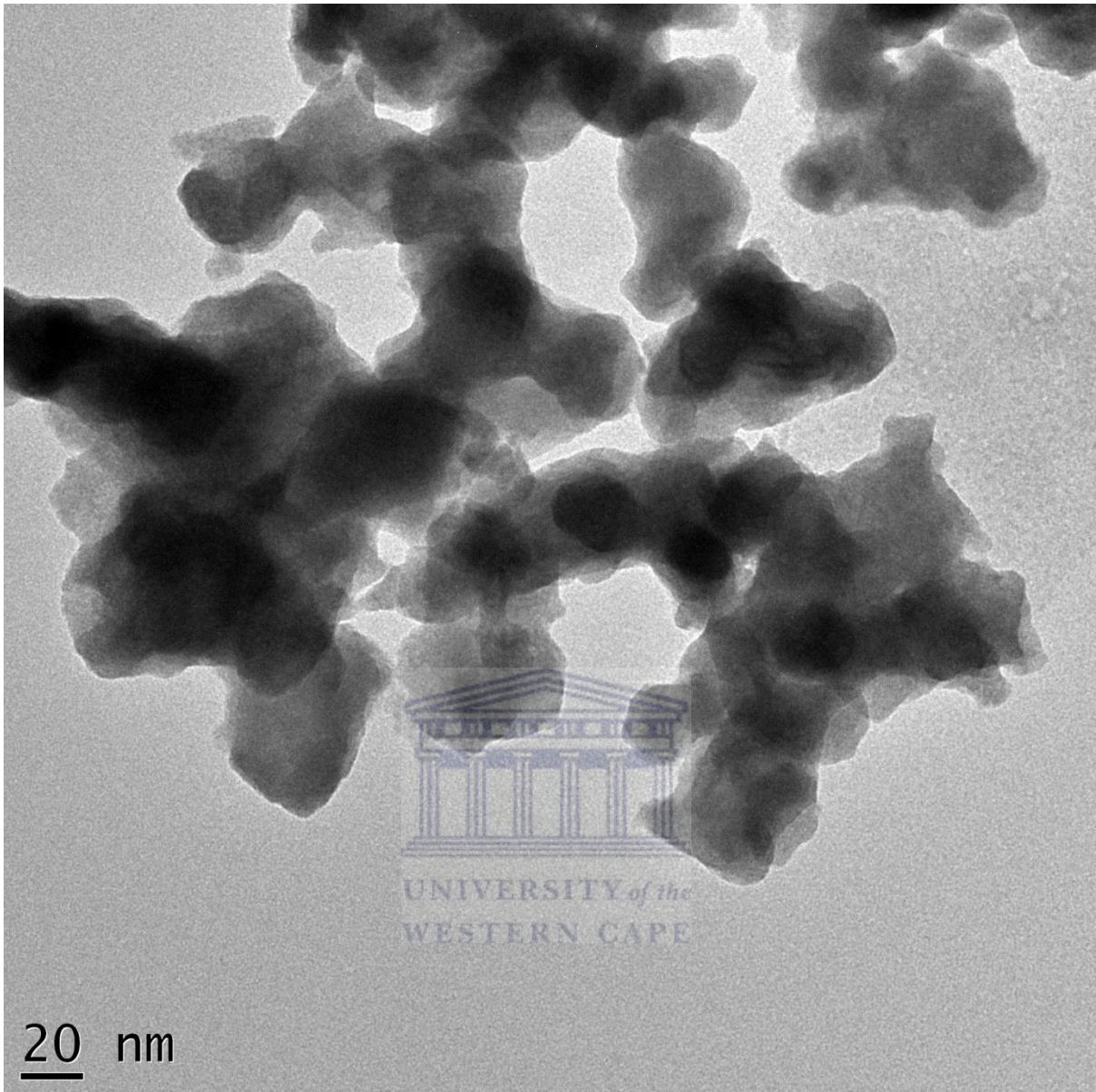
Figure 28.   **High resolution transmission electron microscopy results of bismuth nanoparticles.**
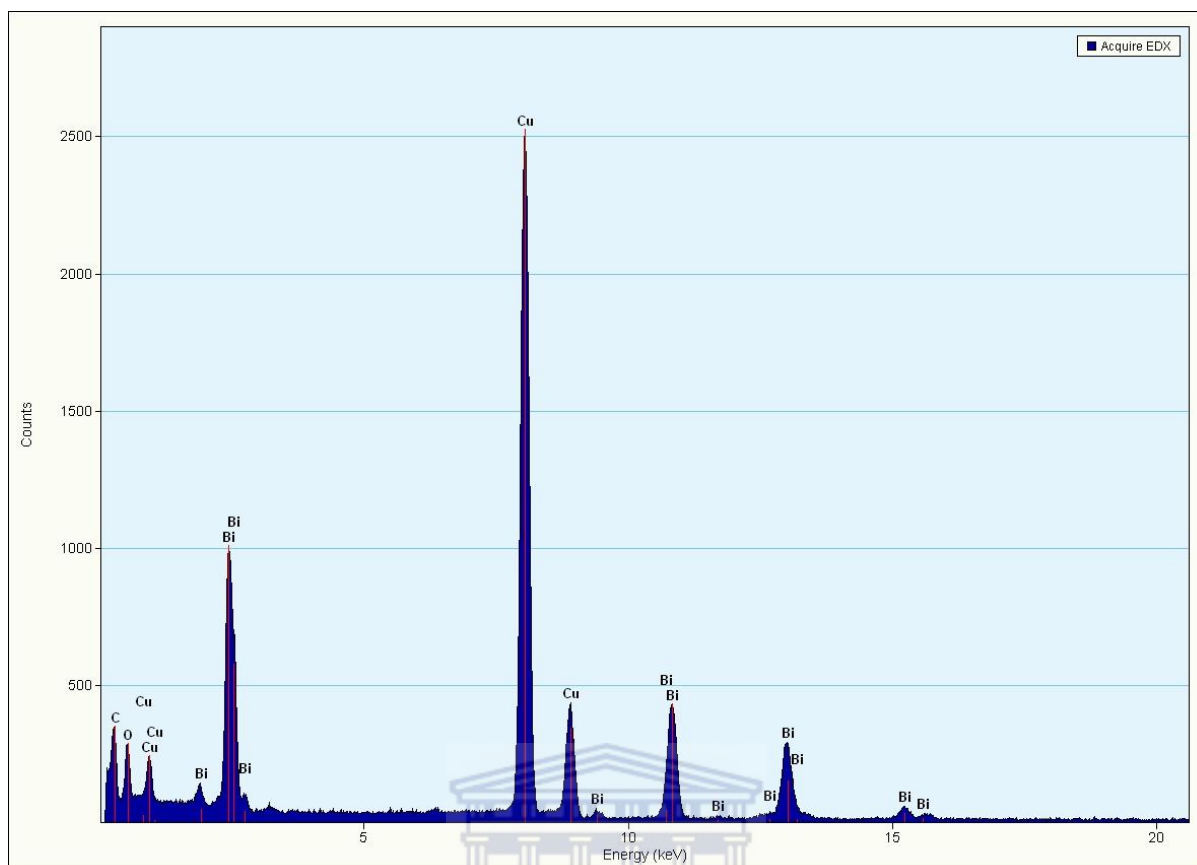
Figure 29. **Electron diffraction x-ray spectra of bismuth nanoparticles.**

Figure 30 show the TEM images of the spherical Bi-Ag bimetallic NPs with a diameter range of between 10-25 nm. The particle size distribution in Figure 32 showed that the majority of NPs measured 10-15 nm, with small quantity of larger particles in the 20-30 nm range. In the electron diffraction x-ray spectrum of the Bi-Ag bimetallic NPs the presence of Bi, C, O, Ag and Cu elements were confirmed. The electron diffraction x-ray spectrum in Figure 31 showed a very high amount of Bi element in the prepared NPs. It is noted that the Cu element comes from the supporting copper grid.
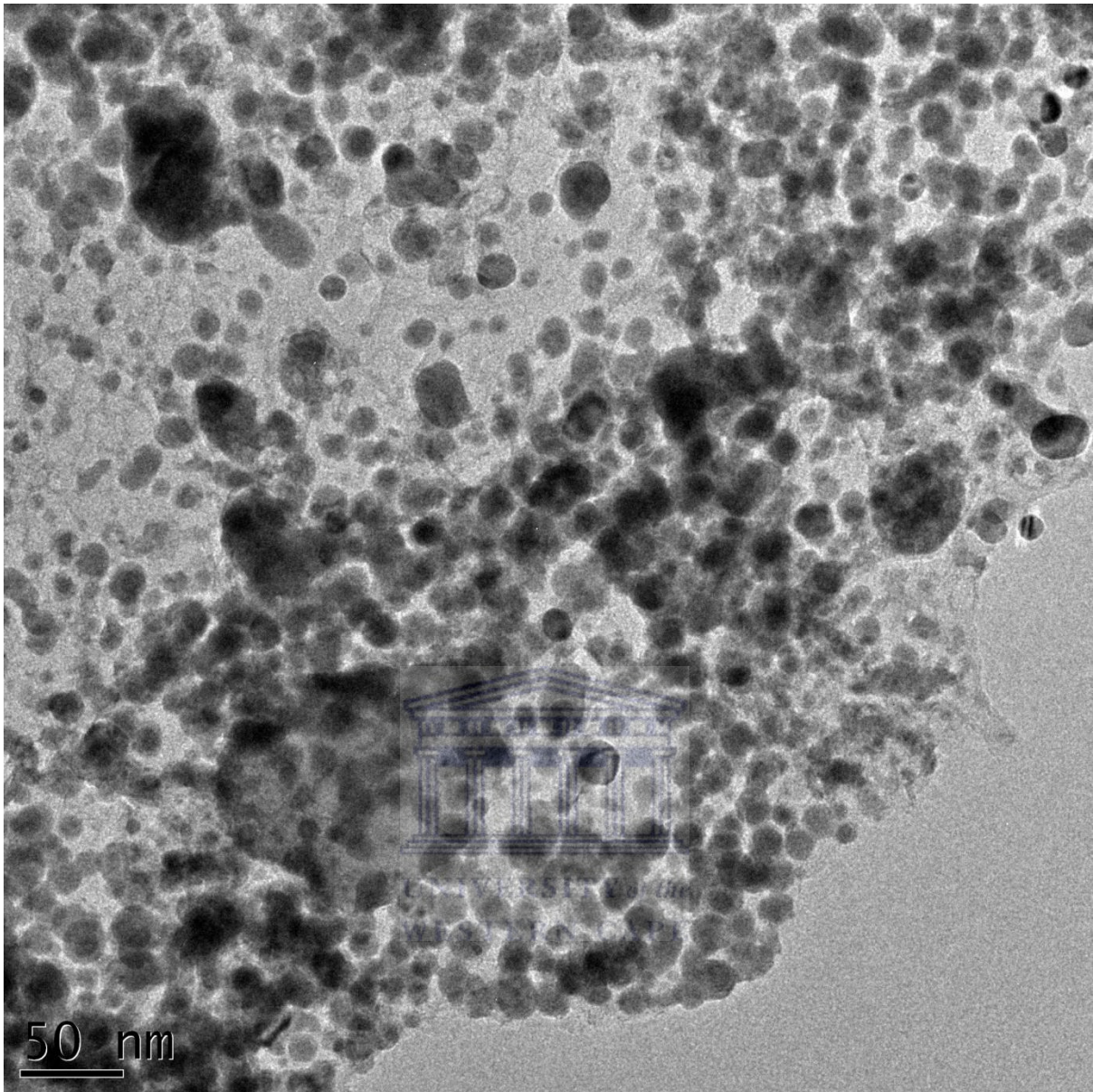
Figure 30. High resolution transmission electron microscopy results of bismuth-silver bimetallic nanoparticles.
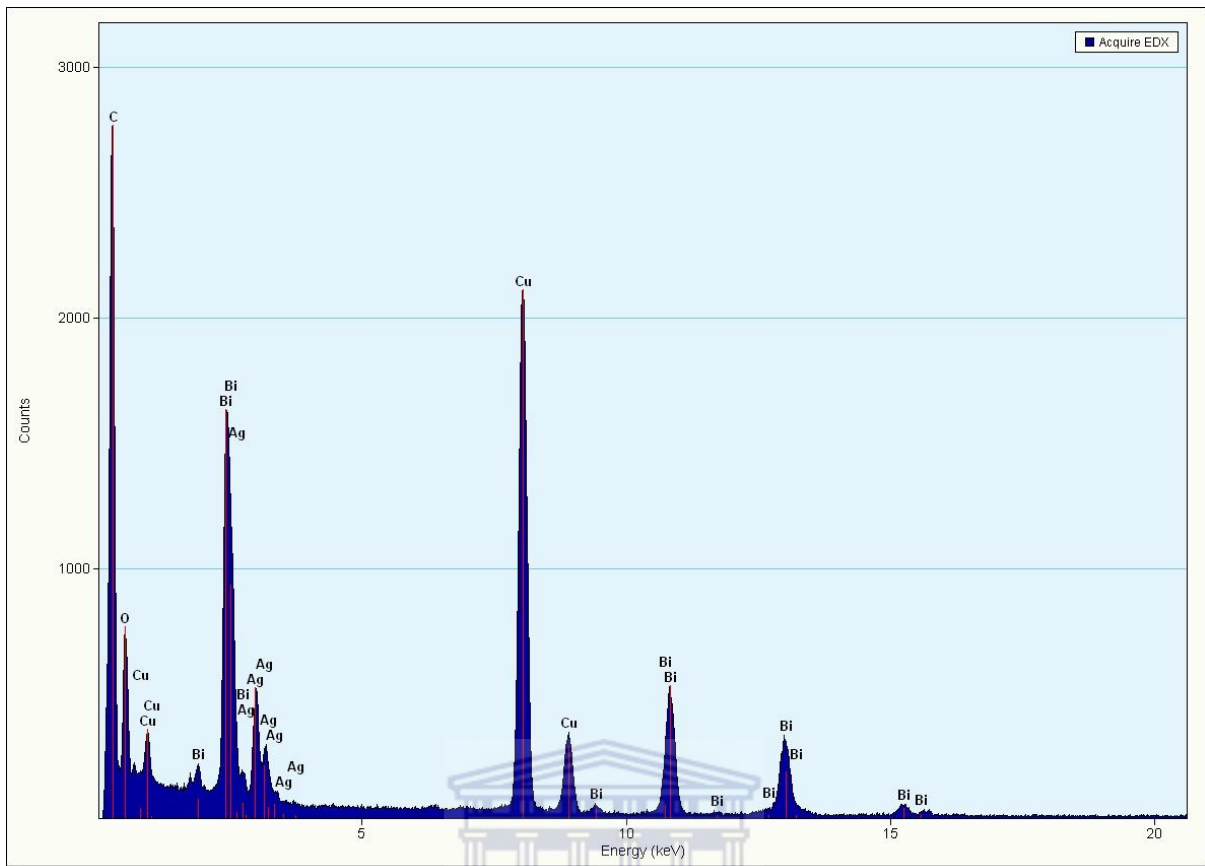
Figure 31. Electron diffraction x-ray spectra of bismuth-silver bimetallic nanoparticles.
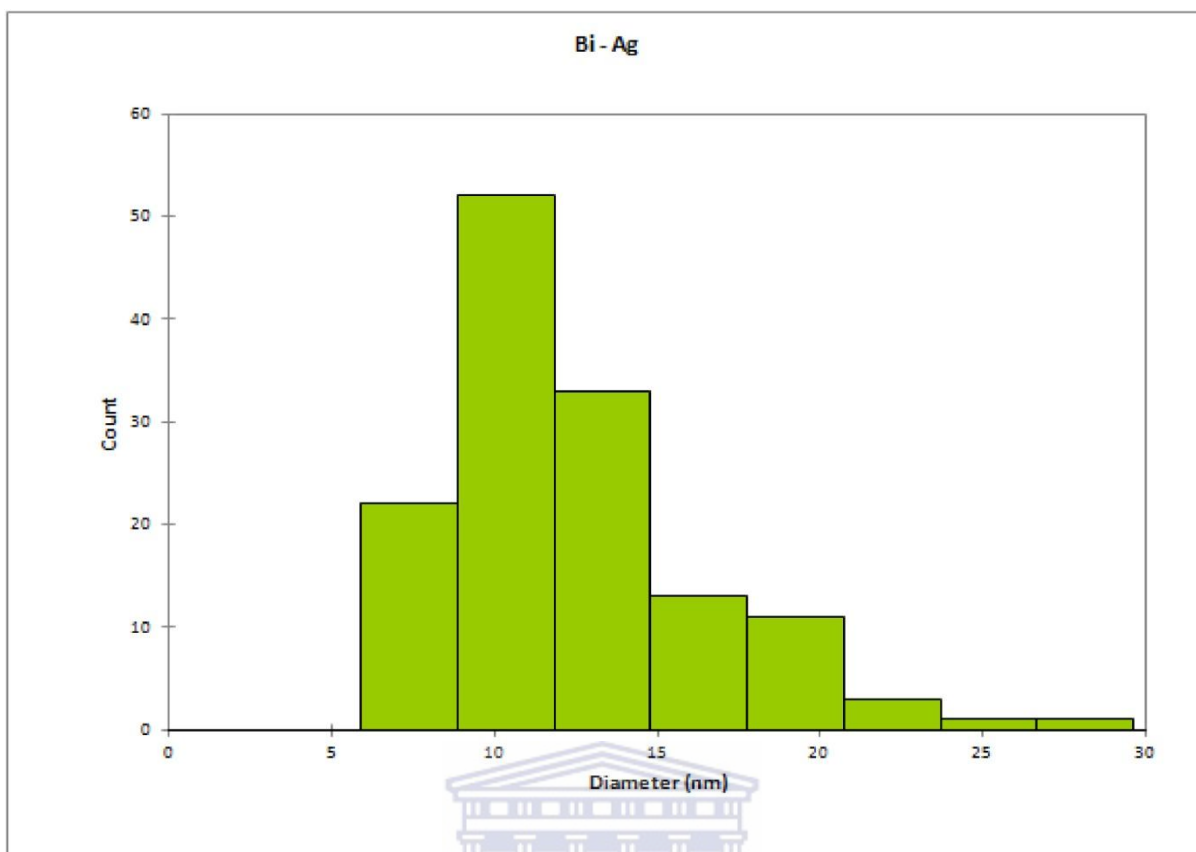
Figure 32.   **Results for the particle size distribution of the synthesised bismuth-silver bimetallic nanoparticles.**
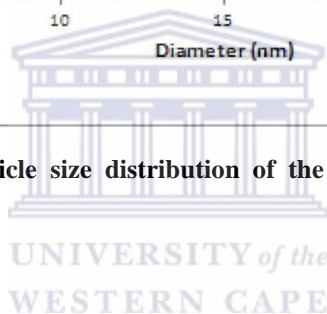
The selected area diffraction patterns of the Bi-Ag bimetallic NPs were also investigated (Figure 33). The results obtained for the selected area diffraction of the Bi-Ag bimetallic NPs showed a pattern that is well defined and intense rings was observed to indicate poly crystallization of the Bi-Ag bimetallic NPs (Kaowphong, 2012).

Figure 33. **Illustrates the selected area diffraction patterns (SAED) of the Bi-Ag bimetallic nanoparticles.**

4.3.2. Spectroscopy characterisation

4.3.2.1. Ultraviolet-visible spectroscopic characterisation of nanoparticles

In this study ultraviolet-visible (UV-Vis) spectroscopy is used to study the interaction of light and the synthesised nanoparticles (NPs) such as silver (Ag), bismuth (Bi) and the

bismuth-silver (Bi-Ag) composite. The investigation of the synthesised nanomaterials is done between the wavelength limits 190 to 870 nm. UV-Vis absorption results confirmed formation of Ag NPs prepared by chemical reduction of silver nitrate using sodium borohydrate as reducing agent.

Figure 34 displays the UV-Vis absorption spectra obtained for the chemically synthesised Bi-Ag bimetallic NPs. In Figure 34a three characteristic absorption peaks were observed at 280 nm, 410 nm and a broad peak between 570 and 750 nm. The peak at 280 nm is assigned to the Bi NPs, the second peak at 410 nm is assigned for Ag nanoparticles and the broad peak is assigned to the Bi-Ag bimetallic NPs.
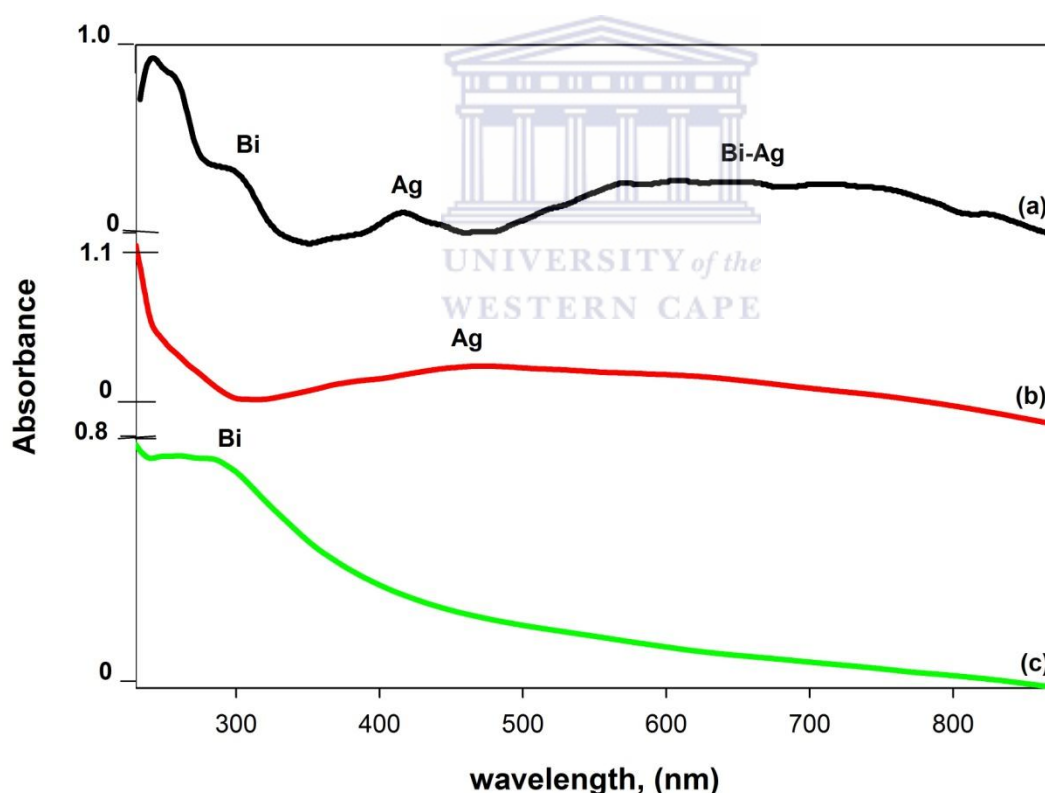
Figure 34.   **Ultraviolet-visible absorption spectra of chemically synthesised (a) bismuth-silver bimetallic, (b) silver and (c) bismuth nanoparticles dissolved in *N,N*-dimetylformamide solution (Ag−Silver; Bi−Bismuth; Bi-Ag−Bismuth-silver).**

The UV-Vis absorption spectra of the chemically synthesised Ag NPs (Figure 34b), showed an absorption maximum at 400 nm. These UV-Vis absorption spectra have proved to

be quite sensitive because the Ag NPs exhibit an intense absorption peak due to surface plasmon excitation. Silver NPs display plasmon adsorption in the visible region and have an absorption maximum at 404 nm. UV‑Vis absorption spectra have proved to be quite sensitive to the presence of Ag colloids because these NPs exhibit an intense absorption peak due to the surface plasmon excitation (Wang *et al*., 2005; Solomon *et al*., 2007). The UV-Vis results obtained for the Bi NPs (Figure 34c) showed a characteristic absorption peak of nano-sized Bi at approximately 280 nm (Gutiérrez and Henglein, 1996; Creighton and Desmond, 1991).

4.3.2.2. Fourier-transformed infrared spectroscopic characterisation of nanoparticles

Fourier-transformed infrared (FT-IR) analysis of the nanoparticles (NPs) was also employed, since it is the most common vibrational spectroscopic technique for assessing molecular motion and fingerprinting in synthesized materials. Figure 35 shows the FT-IR spectra obtained for the chemically synthesised silver (Ag), bismuth (Bi), and bismuth-silver bimetallic (Bi-Ag) NPs. The FT-IR spectra obtained for the Ag NPs (Figure 35a) showed stretching frequencies for the carbonyl group C=O around 1651 cm^{-1} and for the methyl group CH_2 bending around 1450 cm^{-1}. The characteristic NO_3^- groups were the peaks obtained at 1385, 1024, and 731 cm^{-1}. Figure 35b shows the FT-IR spectra obtained for the crystalline Bi-Ag bimetallic NPs derived from the low temperature synthesis described earlier. The results obtained for the antisymmetric and symmetric stretching of H_2O and OH^- bonds were observed by the broad bands between 3000 and 3600 cm^{-1}, while the bending vibrations of H_2O was observed at 1719 cm^{-1}. The presence of trapped nitrates is confirmed by the band around 1384 cm^{-1}. The FT-IR spectra of the Bi NPs (Figure 35c) showed stretching frequencies located at 2930 cm^{-1} for the C-H group and the C=O stretch vibration was observed around 1750 cm^{-1}. The characteristic NO_3^- groups were the peaks obtained at 1385, 1024, and 731 cm^{-1}, while metal-oxygen (M-O) vibrations were observed around 400-700 cm^{-1} (Simões *et al*., 2008; Gabbasova *et al*., 1991).
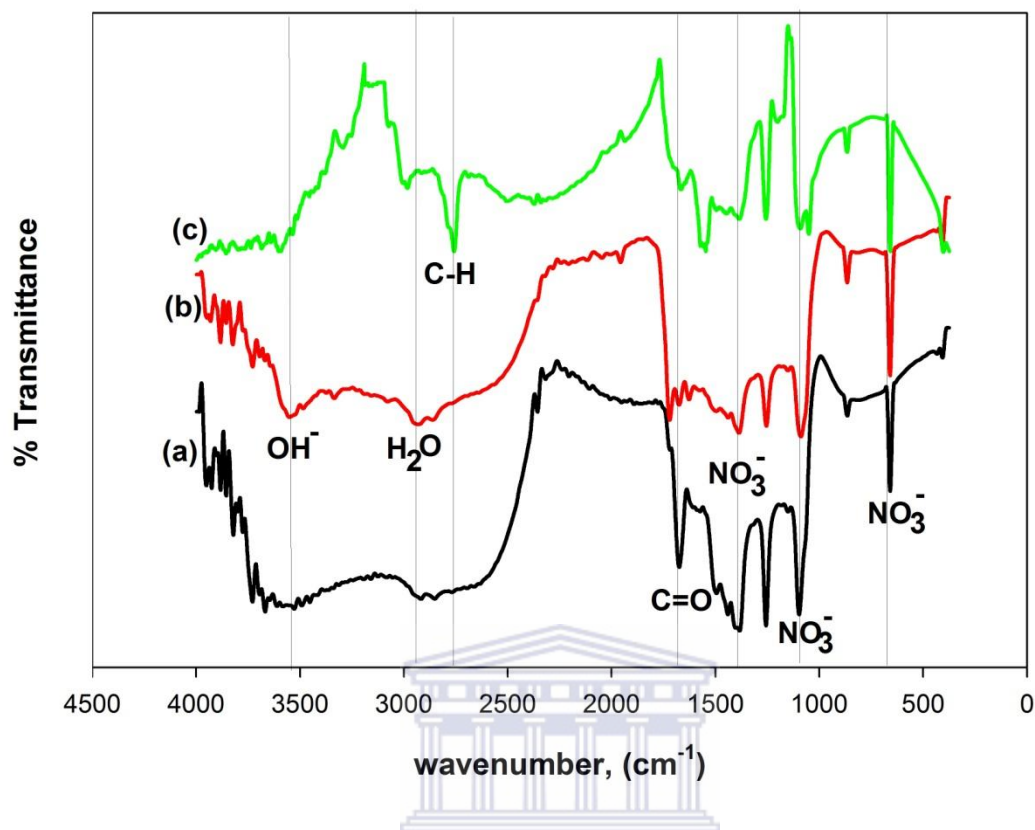
Figure 35. **Fourier-transformed infrared absorption spectra of chemically synthesised (a) silver, (b) bismuth-silver bimetallic and (c) bismuth nanoparticles prepared in *N,N*-dimetylformamide (C-H− methyl group; C=O− Carbonyl group; H_2O− Water; NO_3^- − Nitrate group; OH^-−hydroxy group).**

4.3.2.3. Raman spectroscopic characterisation of nanoparticles

The Raman spectra of the chemically synthesised silver (Ag), bismuth (Bi) and bismuth-silver bimetallic nanoparticles (Bi-Ag NPs) were also collected for chemical structure elucidation. Raman scattering has proven to be an important technique to obtain information about local structures within the different NPs. Due to the high sensitivity of detection for Raman active species, the detection of impurities cannot be completely ignored, especially since exhibited features in the CH- stretching region are difficult to interpret.

The results obtained for the Raman spectra of the Ag NPs (Figure 36a), showed a vibration band at 250 cm^{-1} that can be assigned to an Ag-O mode and a vibration band at

106

1050 cm^{-1} for Ag mode (Débarre *et al.*, 2004). The Raman spectra obtained for the Bi NPs in Figure 36b were collected in the range between 50 to 150 cm^{-1}, which is the region where Bi has Raman activity. The Raman spectra showed 2 peaks at 58 and 90 cm^{-1} that confirmed the rhombohedral Bi structure for the synthesised NPs (Salazar-Pérez *et al.*, 2005).
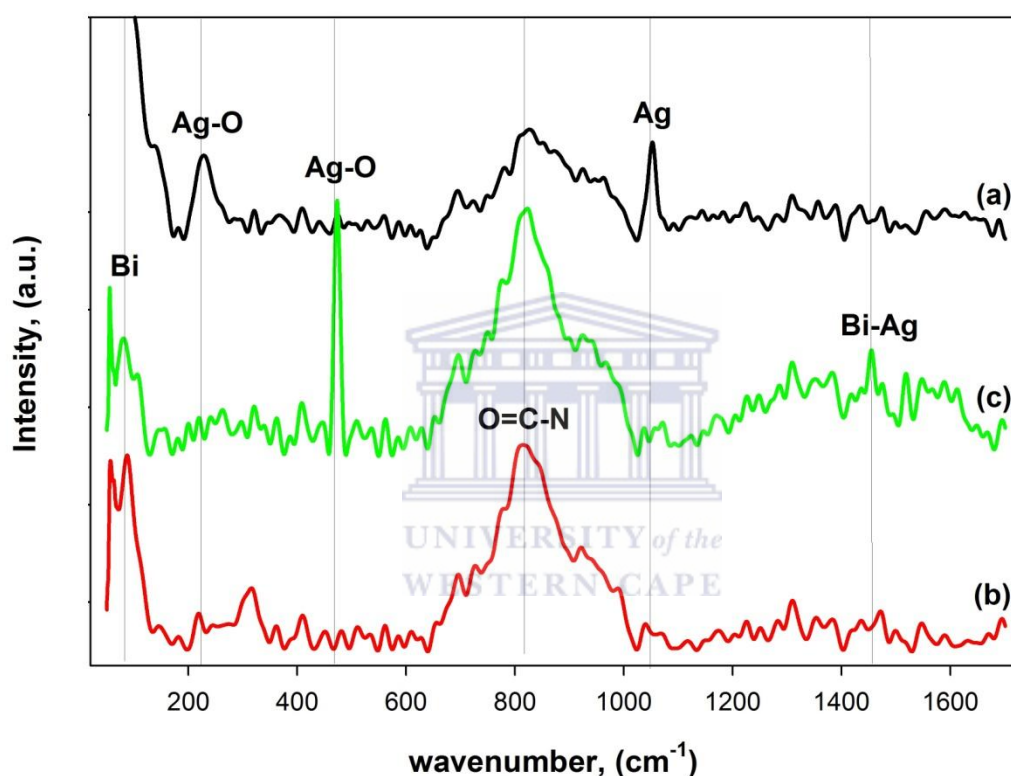
Figure 36. **Raman absorption spectra of chemically synthesized (a) silver, (b) bismuth and (c) bismuth-silver bimetallic nanoparticles dissolved in *N,N*-dimetylformamide for Raman analysis (Ag− Silver; Ag-O− Silver oxide; Bi− Bismuth; Bi-Ag− Bismuth-silver; O=C-N− carboxamide group).**

In Figure 36c the Raman absorption spectra for the Bi-Ag bimetallic NPs are shown, which were compared to that of the results for the individual Ag NPs and Bi NPs. The spectrum in Figure 36c showed sharp peaks around 90 and 490 cm^{-1} that is followed by a broad peak between 650 to 1000 cm^{-1}, followed by minor peaks between 1310 to 1650 cm^{-1}. Although some shifts occurred in the spectrum of the Bi-Ag bimetallic NPs, the peaks obtained confirmed both the presence of individual Ag and Bi NPs and that of the Bi-Ag

bimetallic NPs. The broad band at 820 cm^{-1} can be assigned to O=C-N vibrations originating from *N,N*-dimetylformamide (Fujii *et al*., 2006).

4.3.3. Cyclic voltammetric characterisation

Complex chemical systems such as particulate deposits and electrodes modified with films may be studied quantitatively by cyclic voltammetry (CV) due to the significant advances in the theoretical understanding of the technique (Oldham and Myland, 1994; Noel and Vasu, 1990). In the CV characterisation of the synthesised nanoparticles (NPs), the individual silver (Ag) and bismuth (Bi) NPs were characterised and compared to the results obtained for the bismuth-silver bimetallic nanoparticles (Bi-Ag NPs). Figures 37-39 show the typical CVs of the different nanoparticles evaluated in 0.1 M HCl solution, compared to the CV of the bare GCE also collected in 0.1 M HCl solution. In Figure 37 the CV results show the well-defined redox couple of A/A´ (+0.18, -0.24 V vs. Ag/AgCl) obtained for the Ag NPs. The CV results show clearly how the Ag NPs show a different redox response, compared to the bare GCE surface in 0.1 M HCl solution.
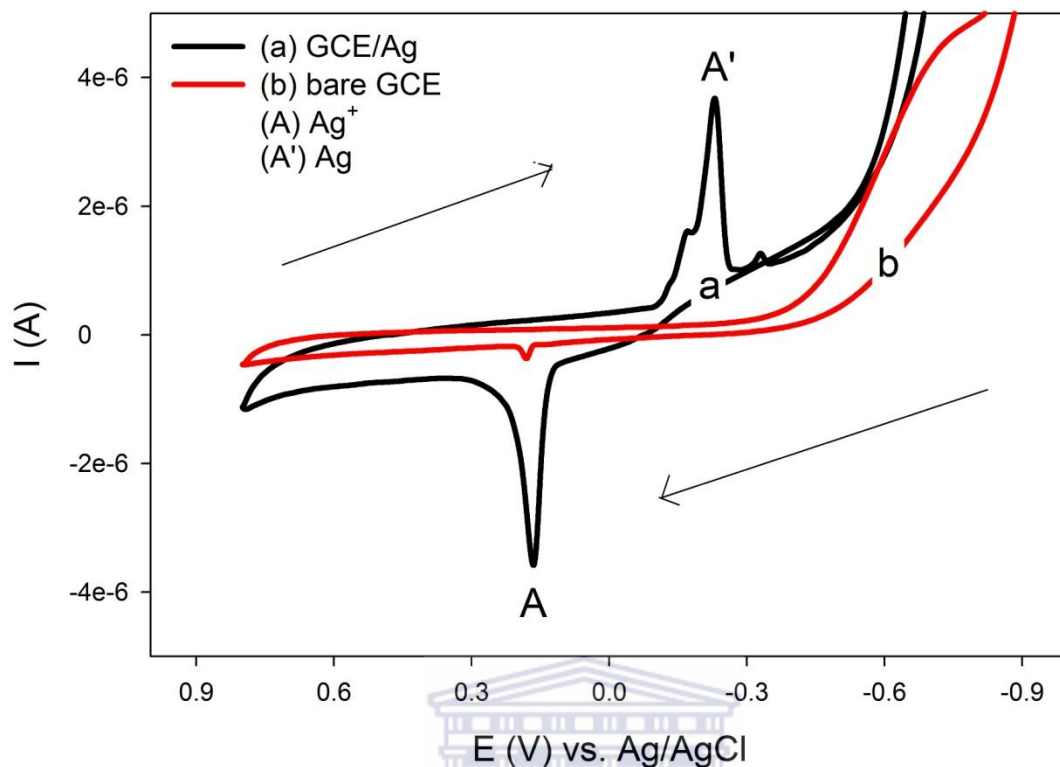
Figure 37. **Cyclic voltammetric results of chemically synthesised silver nanoparticles, in 0.1 M HCl solution at a glassy carbon electrode at 40 mV/s scan rate. The potential window was between -1.3 V and +0.8 V.**

The CV results for the Bi nanoparticles compared to the bare GCE in 0.1 M HCl solution are shown in Figure 38. The CV results for the Bi NPs have shown two anodic peaks at +0.19 and +0.25 V (vs. Ag/AgCl), while the cathodic peaks were obtained around -0.7 and -1.1 V (vs. Ag/AgCl). In Figure 38 the two main redox couples are denoted as (C/C´) and (B/B´) for the chemical synthesised Bi nanoparticles, representing the conversion of Bi^{2+}/Bi^{+} and Bi^{3+}/Bi^{2+}, respectively. These CV peaks for the Bi nanoparticles were just as well defined as that obtained for the Ag NPs.
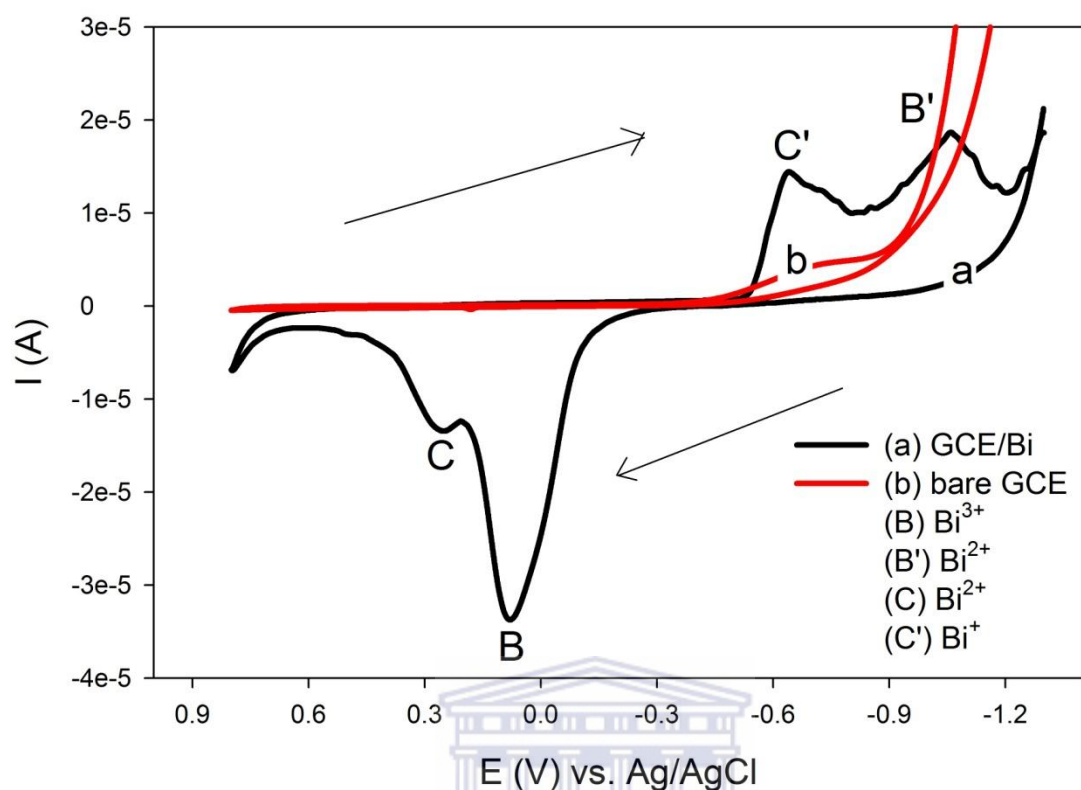
Figure 38. **Cyclic voltammetric results of chemically synthesised bismuth nanoparticles, in 0.1 M HCl solution at a glassy carbon electrode at 40 mV/s scan rate. The potential window was between -1.3 V and +0.8 V.**

Similarly as for the individual Ag and Bi NPs, the CV results for the Bi-Ag bimetallic NPs were collected and compared to that of the bare GCE surface in 0.1 M HCl solution. In the case of the Bi-Ag bimetallic NPs, the CV results in Figure 39 showed two redox couples around anodic peaks at +0.23 and -0.39 V (vs. Ag/AgCl) (redox couple E/E´) and corresponding cathodic peaks at 0.02 and -0.65 V (vs. Ag/AgCl) (redox couple D/D´), respectively. In the Bi-Ag bimetallic NPs the two redox processes observed represents the conversion of Bi^{2+}/Bi^{3+} (D/D´) and Ag/Ag^+ (E/E´), respectively. The CV results were informative of the electroactivity of the different nanoparticles synthesised and further structural elucidation was done using other analytical techniques.
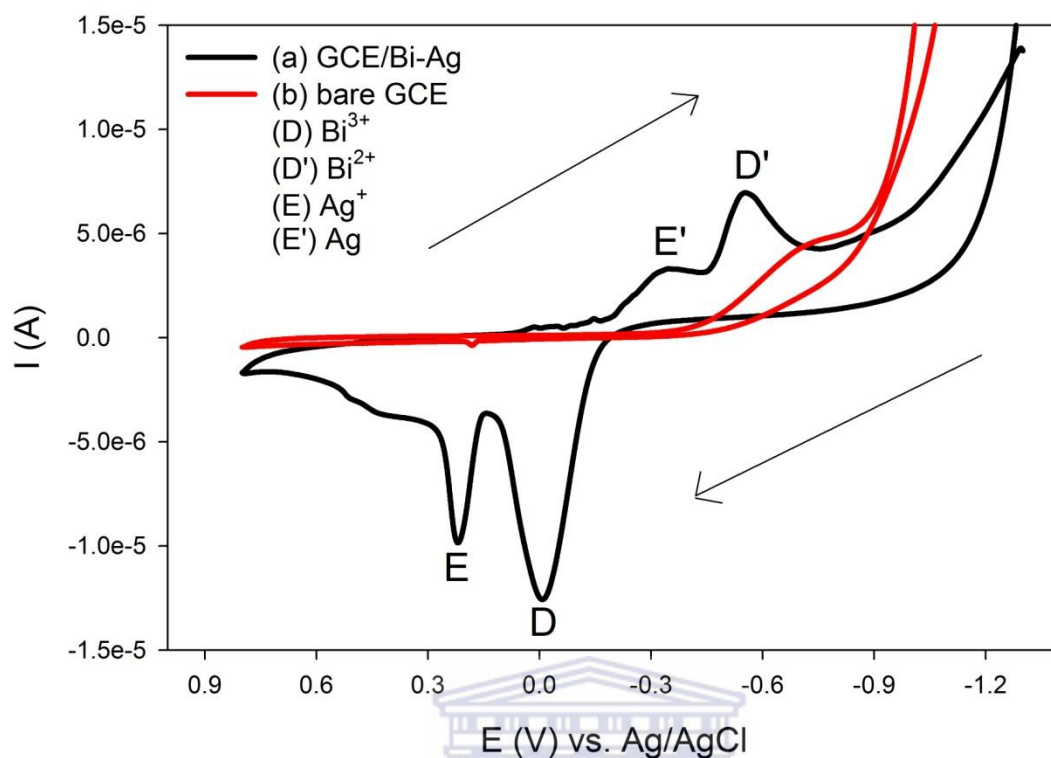
Figure 39. **Cyclic voltammetric results of chemically synthesised bismuth-silver bimetallic nanoparticles, in 0.1 M HCl solution at a glassy carbon electrode at 40 mV/s scan rate. The potential window was between -1.3 V and +0.8 V.**

According to the Laviron equation (1) the surface concentration of electroactive Bi-Ag (Γ) in GCE/Bi-Ag surface can be estimated. Equation 1, Laviron's equation (Laviron, 1979) and equation 2 were re-expressed to give equation 3.

$$I_{\mathrm{p}} = \frac{n^2 F^2 v A \Gamma}{4RT} \tag{1}$$

$$Q = nFA\Gamma \tag{2}$$

$$I_p = \frac{nFQv}{4RT} \qquad\qquad (3)$$

where A was the electrode area (cm^2), Γ was the surface concentration of the electrode material (Bi-Ag, mol cm^{-2}) and Q was the quantity of charge (C) calculated from the reduction peak area of the voltammogram, n was the number of electrons, F was the Faraday constant, I_p was the peak current, R was the gas constant and T was the absolute temperature. From the slopes of I_p versus v plots in Figure 40, n was calculated to be (1.04 and 1.2) for the cathodic and anodic processes, respectively, showing that Bi-Ag bimetallic NPs undergo a one electron redox reaction at the GCE in 01 M HCl buffer solution. From equation 2, the surface concentration of Bi-Ag was calculated to be 1.59×10^{-2} mol cm^{-2}. The ΔE_p values were found to be linear with I_p vs scan rate ($R^2 = 0.971$), which is as expected for a reversible process (Laviron, 1979). The relationships of E_{pa} and E_{pc} with log v were constructed with the linear regression equations as:
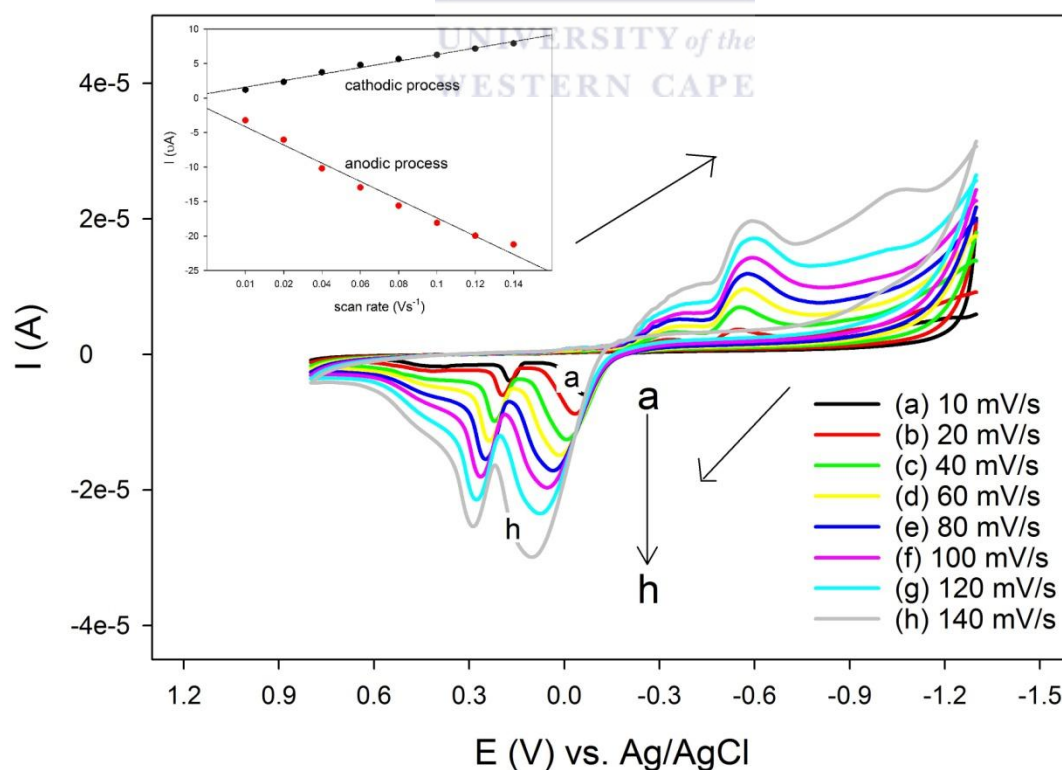
Figure 40.   **Cyclic voltammograms of glassy carbon/bismuth-silver bimetallic electrode in 0.1 M HCl buffer solution: Inset; anodic and cathodic plots of peak current versus scan rate.**

$$E_{pc} \text{ (V)} = 0.0488 \log \nu - 1.3941 \ (n = 8, \ R^2 = 0.9716) \tag{4}$$

$$E_{pa} \text{ (V)} = -0.1367 \log \nu - 3.6742 \ (n = 8, \ R^2 = 0.9675). \tag{5}$$

According to the Equations 6-8 (Laviron, 1979): the electron transfer coefficient (α) was calculated as 0.66 and the electron transfer rate constant (k_s) was further estimated to be 2.52 s^{-1}.

$$E_{pc} = E^{0'} - \frac{RT}{\alpha n F} \log \nu \tag{6}$$

$$E_{pa} = E^{0'} + \frac{RT}{(1-\alpha)nF} \log \nu \tag{7}$$

$$\log k_s = \alpha \log(1 - \alpha) + (1 - \alpha)\log \alpha - \log(\frac{RT}{nF\nu}) - (1 - \alpha)\frac{\alpha n F \Delta E_p}{2.3RT} \tag{8}$$

4.3.4. Electrochemical impedance spectroscopy characterisation of nanoparticles

Electrochemical impedance spectroscopy (EIS) was also employed to study the information of physical and chemical processes occurring at the modified electrode surfaces containing the nanomaterials synthesised in this study. The semicircle diameter of EIS equals the electron transfer resistance (R_{ct}), which controls the electron-transfer kinetics through the electrode interface in EIS. Figure 41 shows the impedance spectra presented as Nyquist plots

for the bare glassy carbon electrode (GCE), the silver (Ag) nanoparticle film, the bismuth (Bi) film and the bismuth-silver bimetallic nanoparticle (Bi-Ag) film. A simplified electrical equivalent circuit (not shown) consisting of a solution resistance (R_s), charge transfer resistance (R_{ct}) and constant phase element (CPE_{dl}). The resistance to the charge transfer between the electrolyte and the electrode are represented by R_{ct} and contains information on the electron transfer kinetics of the redox probe at the electrode interface. The R_{ct} values of bare GCE and GCE/Bi-Ag electrodes were 4844 and 317.3 Ω, respectively. This represents sharp decrease in R_{ct} value when the bare GCE was modified with Bi-Ag NPs. This 93 percent decrease in R_{ct} value clearly indicates the excellent conductivity and catalytic effect of the Bi-Ag nanoparticle film on HCl electrochemistry. The decrease in resistance is due to the electrostatic attraction between Bi-Ag (cationic) and HCl (anionic) of the buffer solution. A comparative analysis of the interfacial heterogeneous electron transfer rate of the bare GCE and the GCE/Bi-Ag electrodes was done using equations 9 and 10 (Bard, A. J. and L. R. Faulkner, 2000):
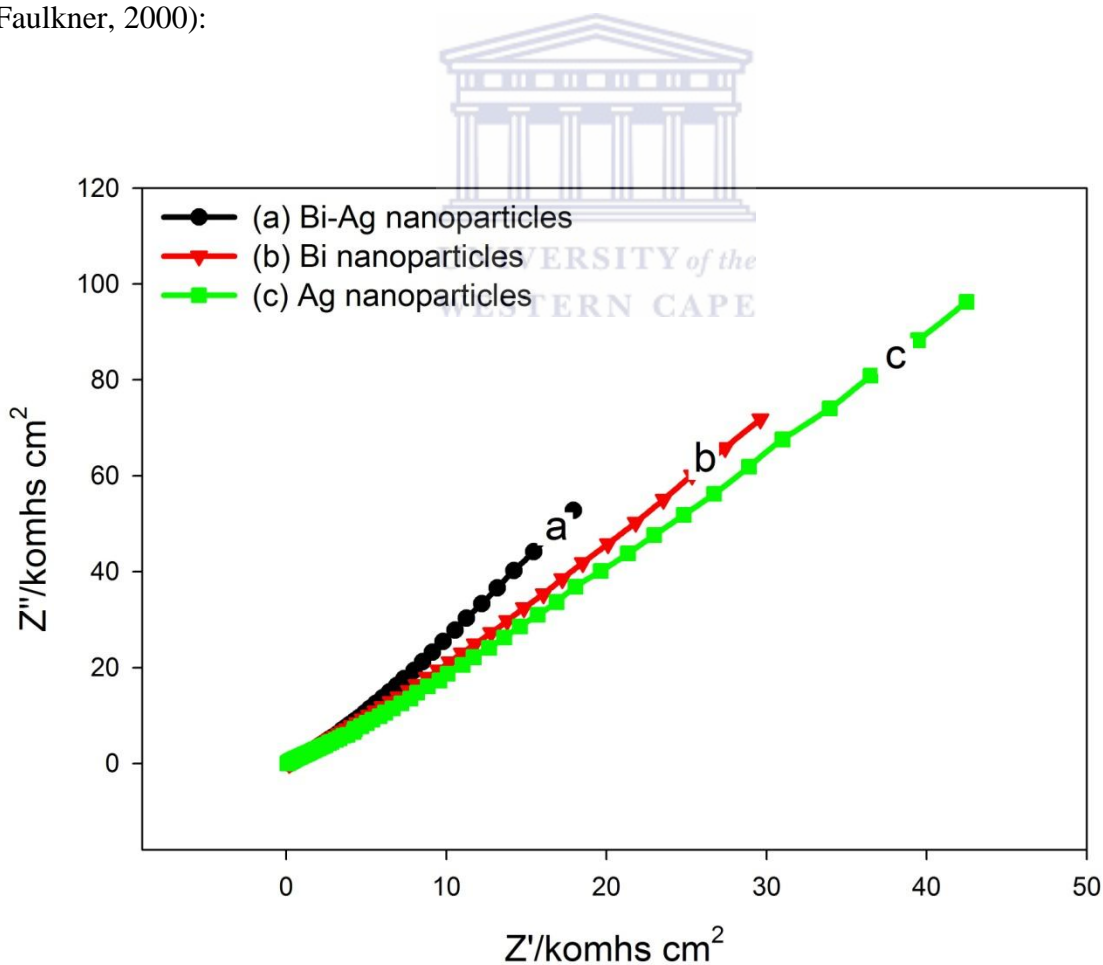
Figure 41. Nyquist plots for bare glassy carbon electrode, silver nanoparticles, bismuth nanoparticles and bismuth-silver bimetallic nanoparticles in 0.1 M HCl solution (Ag−Silver; Bi−Bismuth; Bi-Ag−Bismuth-silver).

$$R_{ct} = \frac{RT}{nFi_0} \tag{9}$$

$$i_0 = nFAk^0C* \tag{10}$$

where n is the number of electrons transferred, F is the Faraday constant (96,584 C mol^{-1}), R is the gas constant (8.314 J mol^{-1} K^{-1}), T is the reaction temperature (298 K), i_0 is the standard exchange current (A), A is the geometric area of the electrode (0.0707 cm^2), k^0 is the heterogeneous rate transfer constant (cm s^{-1}) and $C*$ is the concentration of HCl (0.1 M).

Table 7 illustrates the summary of the results obtained for the chemically synthesized NPs. The values of i_0 for the bare GCE and GCE/Bi-Ag electrodes were 5.5×10^{-6} A and 8.4×10^{-5} A, respectively and the corresponding k^0 values were 8.48×10^{-6} cm s^{-1} and 1.29×10^{-4} cm s^{-1}. The larger value of k^0 for GCE/Bi-Ag electrode supports the theory that the conducting Bi-Ag NPs increase the charge transfer of the HCl redox probe.

Table 7.   **Diagnostics electrochemical parameters of silver, bismuth and bismuth-silver bimetallic nanoparticle films.**

Nanoparicles	n	Q (A)	Γ (mol cm^{-2})	α	k_s (s^{-1})
Ag	1.30	1.94×10^{-4}	2.83×10^{-5}	0.21	0.05
Bi	1.12	3.20×10^{-2}	4.69×10^{-3}	0.51	5×10^{-4}
Bi-Ag	1.02	1.59×10^{-2}	2.32×10^{-3}	0.66	1.06

Ag − Silver; Bi − Bismuth; Bi-Ag − Bismuth-silver; n − Number of electrons; Q − Quantity of charge; Γ − Surface concentration; α − Electron transfer coefficient; k_s − Electron transfer rate constant

In Table 8 it was observed that the Bi-Ag NPs had the lowest R_{ct} value as compared to the other two films, while the bare GCE had the highest R_{ct} value. These values indicate a fast electron transfer process on the Bi-Ag bimetallic film modified GCE and slow electron

transfer process at the bare GCE. The results in Table 8 showed that no substantial difference in R_s for the different films was observed, with all values only differing slightly. These values obtained for CPE_{dl} were the same order of magnitude for the Ag nanoparticle film, Bi nanoparticle film and the Bi-Ag nanoparticle film, compared to the bare GCE that was one order of magnitude lower. Compared to the bare GCE, the above results indicated that the Bi-Ag nanoparticle film compares favourably as a transducer surface for stripping analysis.

Table 8.   **Diagnostics impedance parameters of silver, bismuth, and bismuth-silver bimetallic nanoparticle films.**

Element	Ag nanoparticles	Bi nanoparticles	Bi-Ag bimetallic nanoparticles	Bare GCE
R_s (Ω)	86.49	168.2	223.3	69.58
CPE (F)	1.129×10^{-6}	1.629×10^{-6}	1.526×10^{-6}	2.114×10^{-7}
R_{ct} (Ω)	630.7	534.6	317.3	4844
i_o (A)	$4.07 \times 10^{-5-}$	$4.8 \times 10^{-5-}$	$8.4 \times 10^{-5-}$	$5.5 \times 10^{-6-}$
k^0 (cm.s^{-1})	5.96×10^{-5}	7.04×10^{-6}	1.29×10^{-4}	8.48×10^{-6}

Ag − silver; Bi − bismuth; Bi-Ag − bismuth-silver; GCE − Glassy carbon electrode; R_s − Solution resistance; CPE − Constant phase element; R_{ct} − Electron transfer resistance; i_o − Standard exchange current; k^0 − Heterogeneous rate transfer constant
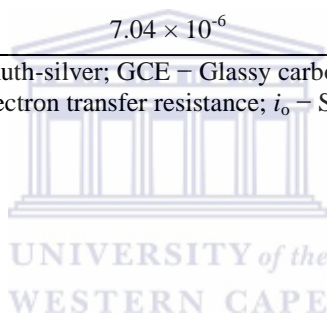
4.4. Summary

In this study, chemical synthesis of Ag, Bi, and Bi-Ag bimetallic NPs was successfully performed. The novel Bi-Ag bimetallic NPs was chemically synthesised by using AgNO$_3$, Bi(NO$_3$)$_3$ 5H$_2$O and the addition citric acid as reducing agent. Electrochemical characterisation in addition to spectroscopy and microscopy analysis was employed to study the properties of each of the Ag, Bi, and Bi-Ag bimetallic NPs. The UV-Vis, FT-IR and Raman spectroscopy results confirmed the structural properties of the Bi-Ag bimetallic NPs. In addition the TEM and selected area diffraction morphological characterisation confirmed the nanoscale nature of the Bi-Ag NPs. The electrochemical results obtained have shown that the Bi-Ag bimetallic NPs exhibit good electro-catalytic activity that can be harnessed for sensor construction and related applications. The developed procedure presented in this study includes advantages of simplicity, high sensitivity, high selectivity, speed, and low cost. Chemically synthesized bismuth-silver bimetallic NPs for sensor development have shown

better DPAdSV results compare to the individual silver and bismuth NPs and very sensitive detection towards the determination of Pt(II) in environmental samples. The novelty of this sensor lies in the fact that this type of nanofilm sensor has not been applied for the determination of Pt(II) in environmental samples before.

Chapter 5

Optimisation and Application of a Bi-Ag bimetallic nanosensor

5.1. Introduction

In the development of the latest electrochemical sensors, nanotechnology is playing an increasingly important role. The design of new and improved sensing devices makes nanoparticles (NPs) very suitable for chemical and biosensors due to their unique chemical and physical properties. It has been found that NPs are not merely small crystals but an intermediate state of matter somewhere between bulk and molecular materials. In the study of NPs several parameters play an important role leading to their enhanced optical, magnetic, electrical, structural and mechanical properties. One of the main benefits of these microscopic NPs is their relatively large surface area causing a high reactivity to weight ratio. In the development of the latest electrochemical sensors, nanotechnology plays an increasingly important role. This study focuses on investigating new electrode materials, such as metal NPs (silver, bismuth and bismuth-silver, etc.), for heavy metal analysis (Abdollah and Fatemeh, 2009; Senthilkumar and Saraswathi, 2009; Penn *et al*., 2003).

The most important problem for the analytical chemist is the quantification of the increasing number of substances in the environment. Heavy metals are always a matter of concern for the analytical chemist as new substances are reported as toxic. In the environment heavy metals accumulate and are distributed between air, water, soil and the biota. Platinum group metals (PGMs) form an important group of elements of increasing usage in the technologically developing world. This group of metals consists of six metals, palladium, rhodium, platinum, osmium, ruthenium and iridium and can be divided into light triad (rhodium, ruthenium and palladium) and the heavy triad (platinum, osmium and iridium) (Zimmermann and Sures, 2004; Rao and Reddi, 2000).

Platinum group metals (PGMs) have a permanent lustre and have aesthetic qualities. Like gold, PGMs is used in the manufacture of jewellery and has also an investment role. The applications of PGMs are very important and are used as a catalyst, in the enabling of

petroleum, other fuels and chemicals from crude oil. It is difficult to substitute PGMs with other metals in this important application and platinum compounds are also used in cancer treatment drugs. Adsorptive striping voltammetry (AdSV) is a very sensitive technique for the analysis of several metals including PGMs. A disadvantage of this method is that it suffers from surface active organic matrices. In adsorptive stripping analysis its best to destroy the organic matrix to limit the carbon content of the solutions. To obtain very good results it's better to avoid nitric acid in the analysis. This electro-analytical method is used for the determination of PGMs in airborne particulate matter, road dust, human body fluids, sediments and surface water (Alvarez *et al*., 1980; Rao and Reddi, 2000; Ulakhowich *et al*., 1992; Barefoot and Van Loon, 1999).

According to the literature palladium, cobalt and nickel react with dimethylglyoxime (DMG) to form 1:2 complexes, e.g. $M(HDMG)_2$ and can be adsorb on the hanging mercury drop electrode (HMDE), mercury film electrode (MFE) and bismuth film electrode (BiFE). In the work done by Van der Horst *et al*. (2012) glassy carbon bismuth film electrode (GC/BiFE) was constructed for the differential pulse adsorptive stripping voltammetric (DPAdSV) measurements of PGMs in the presence DMG as the complexing agent. It was found that this GC/BiFE sensor exhibited well-defined peaks and highly linear behaviour for the stripping analysis of the PGMs in the concentration range between 0 and 3.5 μg/L, which exhibited good and reproducible sensor characteristics. In the work done by Van der Horst *et al*. (2012) we observed only the simultaneous determination of Pd-Rh and Pt-Rh complexes and the limit of detection of Pt, Pd and Rh was found to be 0.04 μg/L, 0.12 μg/L, and 0.23 μg/L (Ramirez *et al*., 1996; Cordon *et al*., 2002; Georgieva and Pihlar, 1996; Abiman *et al*., 2008; Wang *et al*., 2005; Krolicka and Bobrowski, 2004; Hutton *et al*., 2003).

In this chapter the focus was to construct a bismuth-silver bimetallic nanosensor for PGMs determination in standards and environmental samples using DPAdSV as technique. Furher, to optimise the chelating agent concentration, ionic strength of supporting electrolytes, accumulation potential, accumulation time, transport rate to the electrode surface and stability of the sensor because this parameters are very important in DPAdSV analysis.

5.2. Materials and methods

5.2.1. Reagents

Sodium acetate (NaOAc), ammonia (NH$_3$) (25%), ammonium chloride (NH$_4$Cl), hydrochloric acid and nitric acid were supplied by Merck (South Africa). All precious and heavy metal standards (1000 mg/L AAS), dimethylglyoxime (DMG) were purchased from Sigma-Aldrich (South Africa). Glacial acetic acid (95%), ethanol (95%) were supplied by Kimix (South Africa).

A 0.2 M sodium acetate buffer (pH = 4.7) was prepared by mixing sodium acetate with acetic acid and deionised water and served as the supporting electrolyte. The 0.01 M DMG solution was prepared in 95% ethanol and served as the chelating agent. All solutions were prepared by Milli-Q (Millipore 18 M Ohm cm) water.
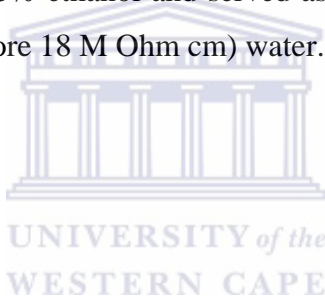
5.2.2. Instrumentation

In this chapter electrochemical measurements were conducted with an Epsilon electrochemical analyzer (BASi Instruments, 2701 Kent Ave., Westr Lafayette, IN 47906, USA) using cyclic voltammetry (CV), or differential pulse adsorptive stripping voltammetry amperometric (DPAdSV) modes. A conventional three electrode system was employed, consisting of bismuth-silver nano film prepared by drop coating the nanoparticles on a BASi 1.6 mm diameter glassy carbon disc working electrode. A BASi 3 M NaCl-type Ag/AgCl reference electrode was used, and a platinum wire as auxiliary electrode. An Agilent 7500 series inductive coupled plasma mass spectroscopy (ICP-MS) was used for the trace PGMs determination in roadside dust and soil samples. All experiments were performed in a 20 mL electrochemical cell at conditioned room temperature (Van der Horst *et al*., 2012; Somerset *et al*., 2015; Somerset *et al*., 2011; Somerset *et al*., 2012).

5.2.3. Preparation of the bismuth-silver nano-film electrode (Ag/BiFE)

A disk glassy carbon electrode (GCE) was used as the working electrode and was thoroughly cleaned and polished on a polish pad with 1.0, 0.3 and 0.05 μm alumina (Al_2O_3) powders. The clean GCE was first rinse with deionised water and then sonicated in ethanol and doubly distilled H_2O in turn. The GCE was transferred to the electrochemical cell for further cleaning by using cyclic voltammetry (CV) between -1.0 and +1.0V at a scan rate of 50 mV/s in freshly prepared deoxygenated 0.5 M aqueous H_2SO_4 until a stable CV profile was obtained. A 2.5 mg of bismuth-silver (Bi-Ag) bimetallic nanoparticles were dispersed through ultrasonic vibration in 50 mL solution of deionised water to form a suspension. A defined quantity of the suspension was applied to a clean surface of GCE and dried at room temperature to get a thin film on GCE surface (Noroozifar *et al.*, 2011; Cui and Zhang, 2012; Prakash *et al.*, 2012). After each voltammetric cycle the cleaning of the Bi-Ag bimetallic nanofilm was carried out by holding the potential of the electrode at +1.0 V. Traces of the remaining DMG complexes on the electrode surface were reduced and quickly desorbed at this potential. A short cleaning period of 30 s was required to refresh the electrode surface completely (Morfobos *et al.*, 2004).
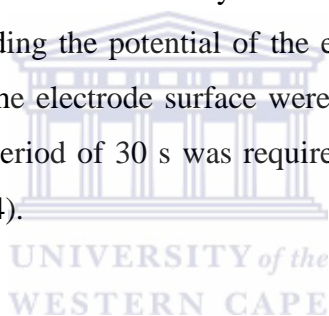
5.2.4. Procedure for the determination of PGMs

A 10 mL 0.2 M acetate buffer solution (pH = 4.7) containing 1×10^{-5} M DMG was used as electrolyte in the cyclic and stripping voltammetric procedures. The nanofilm electrode was immersed into the solution and an accumulation potential of -0.7 V (vs. Ag/AgCl) for Pd(II) and -0.6 V for Pt(II), and -0.7 V (vs. Ag/AgCl) for Rh(III) were applied while the solution was stirred. A 30 s quiet time was used and the voltammogram was scanned from +0.8 to -1.4 V (vs. Ag/AgCl) at a scan rate of 60 mV/s for cyclic voltammetry measurements, while scanning was performed from -0.8 to -0.1 V (vs. Ag/AgCl) for adsorptive differential pulse stripping voltammetry (AdSV) measurements. The PGMs were introduced into the solution after the background voltammogram was recorded. All the experiments were performed in the presence of oxygen and at room temperature (Van der Horst *et al.*, 2015; Van der Horst *et al.*, 2012). According to Zhang *et al.* (2010) the analysis of heavy metal ions using AdSV method consists of three steps such as accumulation,

121

electrochemical reduction and stripping out. In this method both the sensitivity and the selectivity of the analysis can be enhance by the combination of accumulation and reduction prior to the stripping detection process. The efficiency of accumulation and electrochemical reduction steps plays a great role in the entire analysis. Figure 42 is a schematic illustration of the AdSV method consists of the three steps mentioned previously.
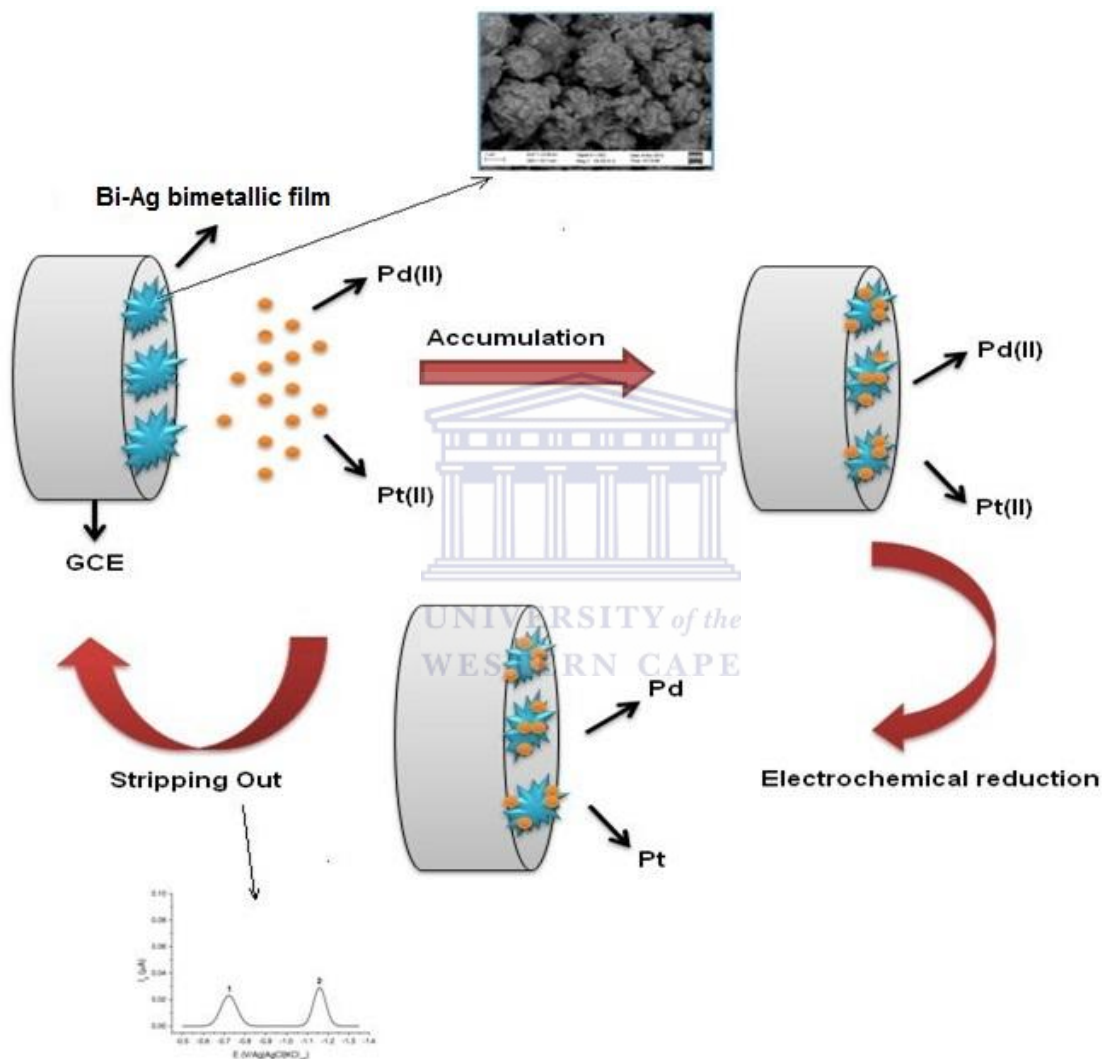
Figure 42. **Schematic diagram for differential pulse adsorptive stripping analysis of PGMs and including accumulation, electrochemical reduction and stripping out steps (Zhang *et al*., 2010).**

5.3. Results and discussion

5.3.1. Modified sensor electrode surfaces

In voltammetric measurements platinum group metals (PGMs) have different electrochemical behaviours in different electrolytes with different pH ranges. Supporting electrolytes such as 0.1 M phosphate buffer (pH = 9.0), 0.2 M acetate buffer (pH = 4.7), and 0.1 M phosphate buffer solutions (pH = 7.1) were investigate. The purpose of this investigation is to determine which of these electrolytes will give the largest peak current, the best shape of peak and the lowest background current (Hu *et al*., 2003). In the work done by Georgieva and Pihlar (1996) the effect of pH and deposition potential on the stripping response of a Pd(HDMG)$_2$ complex were studied. In weak acidic medium like sodium acetate buffer the following equalibria exist:

$$Pd(H_2O)_n^{2+} \leftrightarrow Pd(OH)^+ \leftrightarrow Pd(OH)_2 \, (aq) \leftrightarrow Pd(OH)_2 \, (s)$$
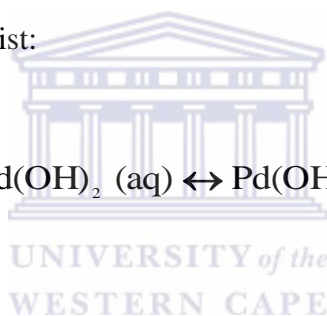
They developed a global equation for the accumulation of Pd(II) in the presence of DMG complexes on a HMDE (Ramírez and Gordillo, 2009). In that equation they consider the protolytic reactions of DMG and the equilibrium concentration of complex forming ions of HDMG$^-$ is dependent on the pH. The possible bismuth-silver bimetallic electrode process for Pd(II) and Pt(II) can be viewed as follows:

Accumulation: $M(HDMG)_2 \, (ads) + 2H^+ + 2e^- \leftrightarrow M + 2H_2DMG(aq)$

Reduction: $M(HDMG)_2 \, (ads) + (Bi - Ag) + 2H^+ + 2e^- \leftrightarrow M(Bi - Ag) + 2H_2DMG(des)$

Stripping: $M(Bi - Ag) \, (surf) \leftrightarrow (Bi - Ag) + M^{2+}(aq) + 2e^-$
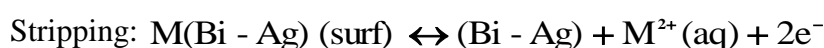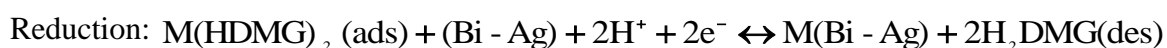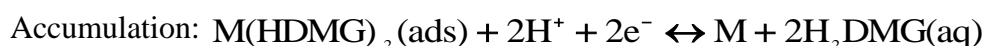
The electrode process for Rh(III) can be observed by the following equations:

Accumulation: $Rh(HDMG)_3 (ads) + 3H^+ + 3e^- \leftrightarrow Rh^{3+} + 3H_2DMG(aq)$

Reduction: $Rh(HDMG)_3 (ads) + (Bi\text{-}Ag) + 3H^+ + 3e^- \leftrightarrow Rh(Bi\text{-}Ag) + 3H_2DMG(des)$

Stripping: $Rh(Bi\text{-}Ag)(surf) \leftrightarrow (Bi\text{-}Ag) + Rh^{3+}(aq) + 3e^-$
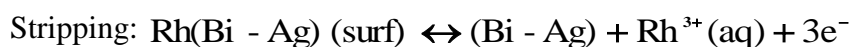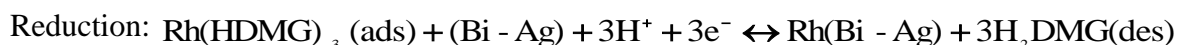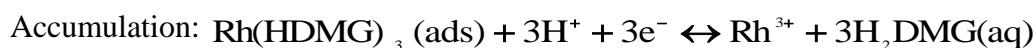
The present study illustrates the characterisation of a bare and modified glassy carbon electrode in different supporting electrolytes. In this work a bismuth-silver bimetallic nanofilm electrode (Bi-AgFE) was used and the redox activity of the Bi-AgFE was studied in different supporting electrolytes with different pH values. The results obtained are shown in Figure 43 with cyclic voltammetry (CV) results that illustrate the combined evaluation of the bare glassy carbon electrode versus the GC/Bi-AgFE sensor in various buffer solutions of (a) 0.2 M NaOAc (pH = 4.7), (b) 0.1 M phosphate buffer solution (pH = 9), (c) 0.1 M phosphate buffer solution (pH = 7.1) and (d) bare GCE in 0.2 M NaOAc (pH = 4.7) with potential window of -1.4 V to +0.8 V (vs. Ag/AgCl) at a scan rate of 60 mV/s (Van der Horst *et al.*, 2012; Silwana *et al.*, 2014).

The results obtained in Figure 43 have shown that weak redox activity is observed at the bare glassy carbon electrode. In the forward anodic scan sharp peaks for the oxidation of Bi and Ag was observed and on the reverse cathodic scan smaller peaks for the reduction of Bi and Ag were obtained.
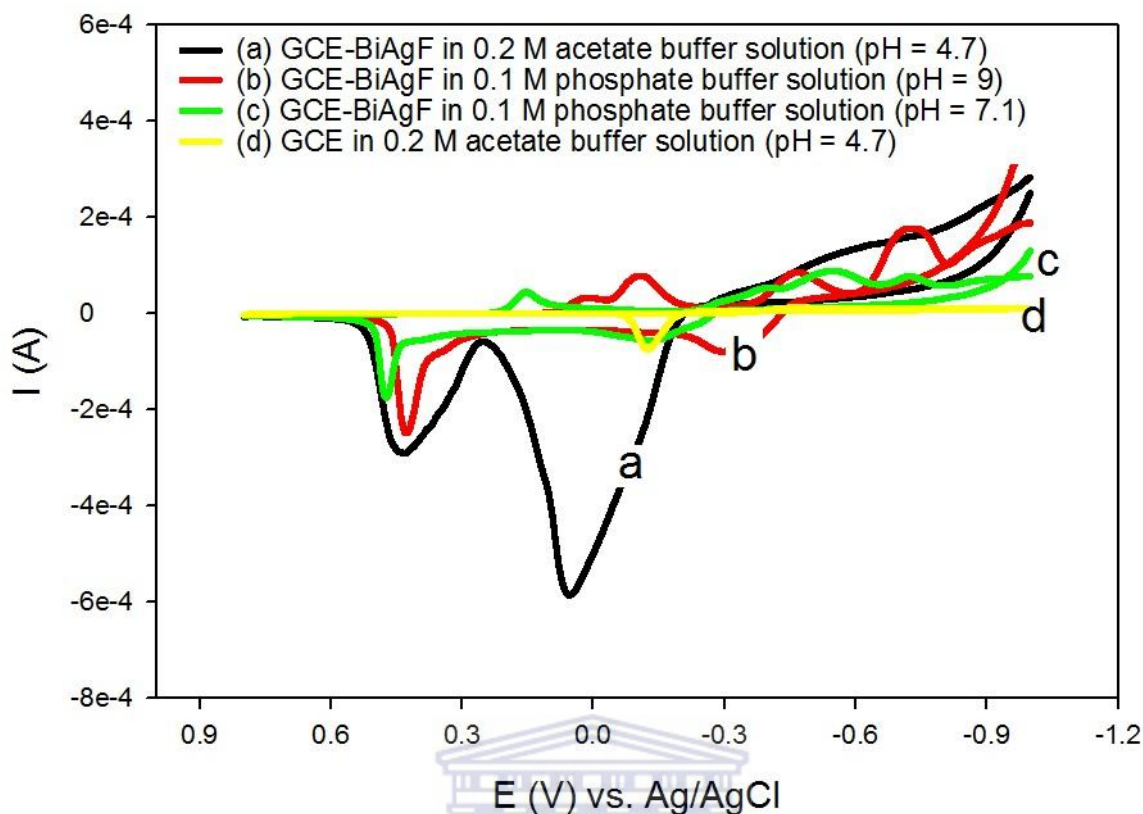
Figure 43. Cyclic voltammetry (CV) results for the combined evaluation of the clean GCE versus the GCE/Bi-AgF sensor electrode in various buffer solutions of (a) 0.2 M NaOAc (pH = 4.7), (b) 0.1 M PBS (pH = 9), (c) 0.1 M PBS (pH = 7.1) and (d) GCE in 0.2 M NaOAc (pH = 4.7). The potential was scan between -1.0 and +0.8 V (vs. Ag/AgCl) at a scan rate of 60 mV/s.

It was observed that in 0.2 M NaOAc (pH = 4.7) solution, the best peak current response was obtained and this buffer solution was used for further analysis in this investigation.

5.3.2. Effect of reagent concentration

The use of a complexing agent with a GC/Bi-AgFE sensor can greatly increase the sensitivity of determination, which is due to complexation of the platinum group metals (PGMs) with dimethylglyoxime (DMG). Dimethylglyoxime forms stable complexes with Pd(II), Pt(II) and Rh(III) ions in acidic and alkaline buffer solutions. In the determination of these PGMs the amount of DMG can affect the electrochemical behaviours of PGM ions at

the bismuth-silver bimetallic sensor. The following set of results revealed the optimisation studies of DMG concentrations using 1 ppt of these PGMs in 0.2 M acetate buffer (pH = 4.7).

In this study three different concentrations of DMG was used to determined the effect of complexing agent on the peak current of these PGMs. Differential pulse adsorptive stripping voltammetry (DPAdV) mode were used with different deposition times and a deposition potential of -0.7 V (vs. Ag/AgCl). In Figure 44 a plot of peak current as a function of time is illustrated. The results obtained in Figure 44 reveals the concentration of dimethylglyoxime was optimised at 1×10^{-5} M for Pd(II) in further analytical measurements.
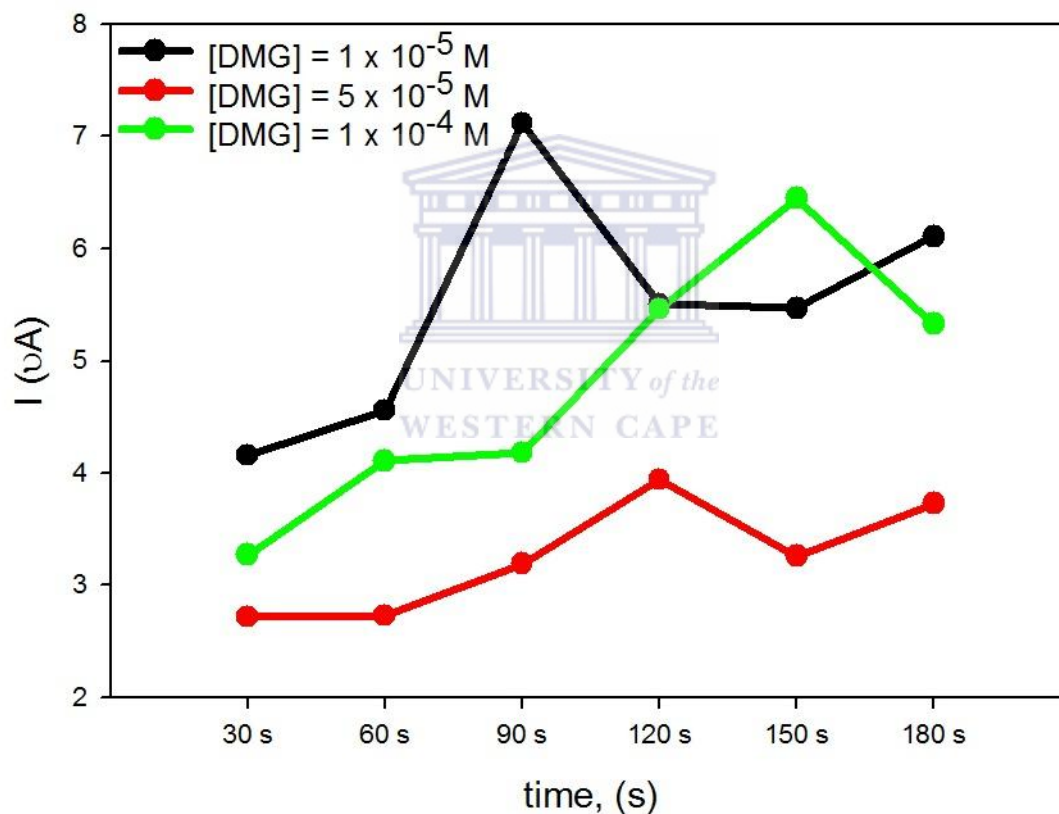
Figure 44.   **Effect of varying dimethylglyoxime (DMG) concentrations on the peak current for 1 ppt Pd(II) in the presence of 0.2 M acetate buffer, (pH = 4.7) solution.**

The plot for peak current as a function of time for Pt(II) using DMG as the complexing agent in 0.2 M acetate buffer (pH = 4.7) solution is illustrated in Figure 45. Only two concentrations of DMG were close to each other at 120 and 180 s with the highest peak current obtained for 1×10^{-5} M DMG. The results obtained in Figure 45 reveals the

concentration of dimethylglyoxime was optimised at 1×10^{-5} M for Pt(II) analytical measurements.
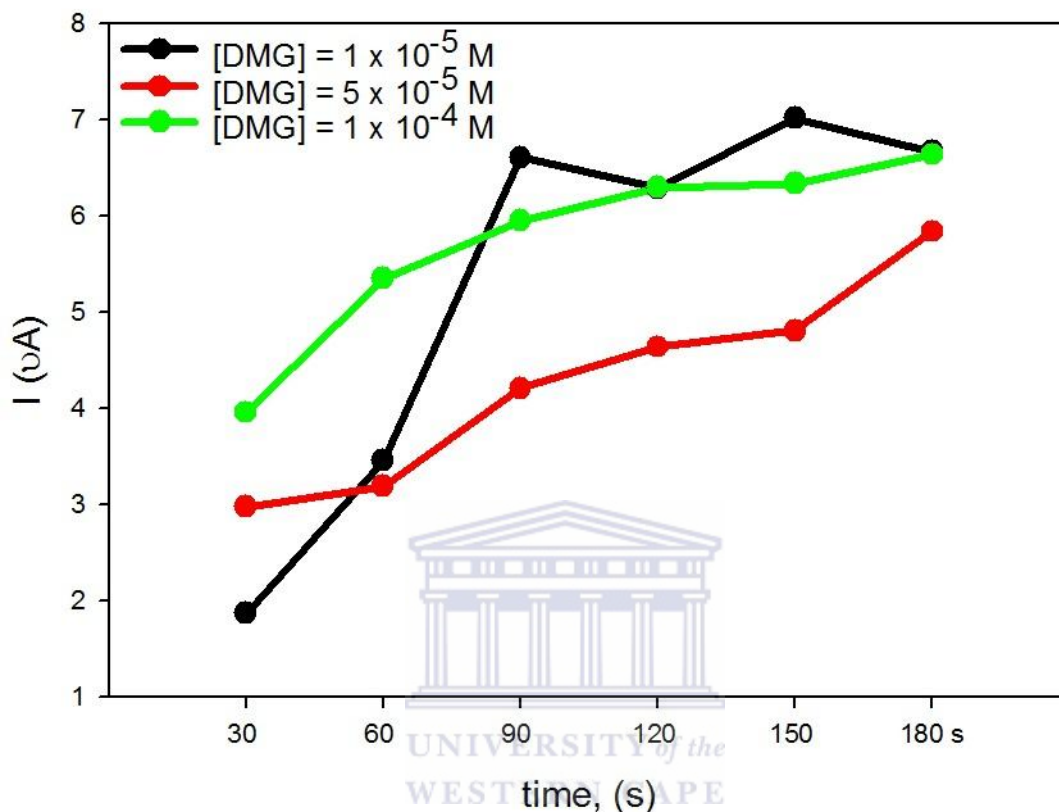
Figure 45. **Effect of varying dimethylglyoxime (DMG) concentrations on the peak current for 1 ppt Pt(II) in the presence of 0.2 M acetate buffer, (pH = 4.7) solution.**

The effect of varying DMG concentration on peak height for Rh(III) in 0.2 M acetate buffer (pH = 4.7) solution was also studied. Figure 46 illustrates a plot of peak current as a function of time for the Rh(III) complex. The effect of DMG concentration upon reduction peak current shown for 5×10^{-5} M DMG a sharp decrease in peak height between 30 s and 60 s, and the peak current increase linearly between 60 s and180s. For DMG concentration 1×10^{-4} M, the reduction peak current increased from 30 till 90 s linearly, decreased from 90 till 120 s and increased again linearly till 180 s. The 1×10^{-5} M DMG increased linearly from 30 till 180 s and at 120 s it reached 1×10^{-4} M DMG. The results showed that 1×10^{-5} M DMG was used as the optimum concentration due to increasing of peak current with an increase in deposition time.

127
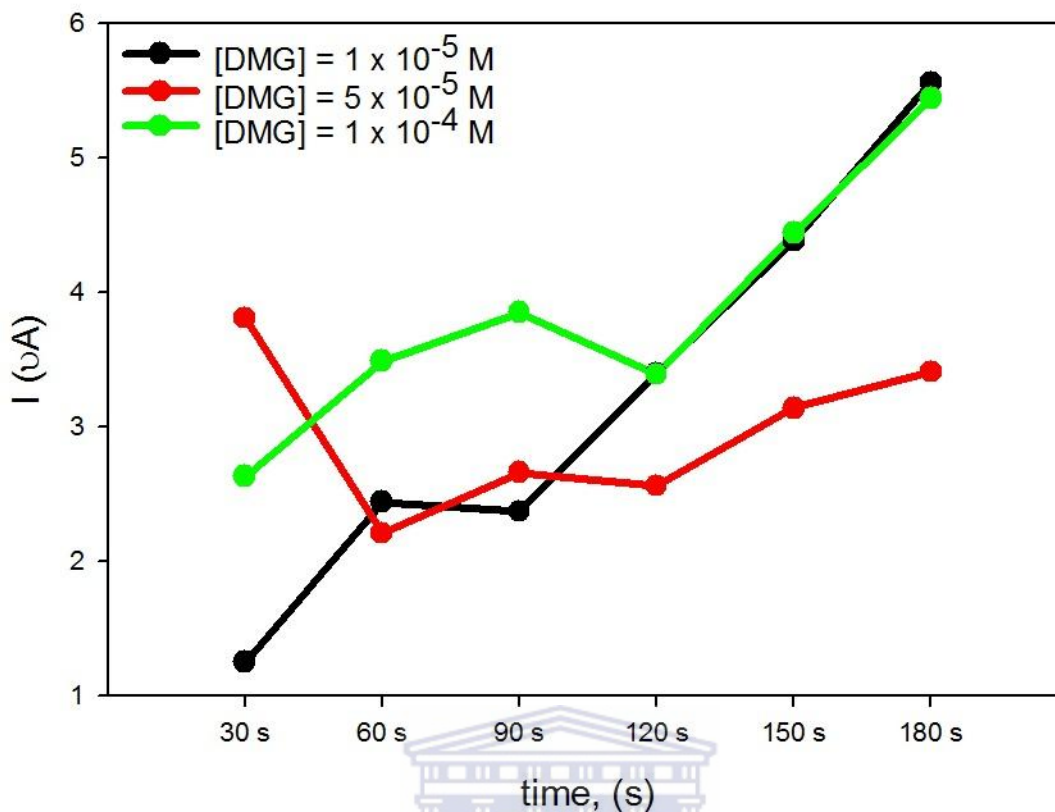
Figure 46. **Effect of varying dimethylglyoxime (DMG) concentrations on the peak current for 1 ppt Rh(III) in the presence of 0.2 M acetate buffer, (pH = 4.7) solution.**

5.3.3. Cyclic voltammetric studies of PGMs

Cyclic voltammetry was used for the preliminary investigation of the electro-activity of the PGMs with DMG on the GC/Bi-AgFE sensor. In Figure 47 three cyclic voltammograms (in the range of +0.8 to +1.0 V) of 0.2 M acetate buffer solutions (pH = 4.7) containing 0.2 to 1.0 ppt Pd(II) in the presence of 1×10^{-5} M DMG after deposition are shown. The three CVs revealed two cathodic peaks at -0.1 and -0.3 V (vs. Ag/AgCl) with two anodic peaks at 0.0 V and +1.5 V (vs. Ag/AgCl) arising from the reduction of Pd(II) in complex with DMG, which was adsorbed on the bismuth-silver bimetallic sensor. This phenomenon suggesting that the reduction of the Pd(II) complex was an reversible process. The decrease in peak current in the cathodic peak at -0.1 V (vs. Ag/AgCl) is due to fast desorption of the complex at the electrode surface. The bimuth-silver bimallic nanosensor shown a big peak observed at +0.55 V (vs. Ag/AgCl) in 0.2 M acetate buffer (pH = 4.7) solution and can be assigned to the stripping of bismuth.
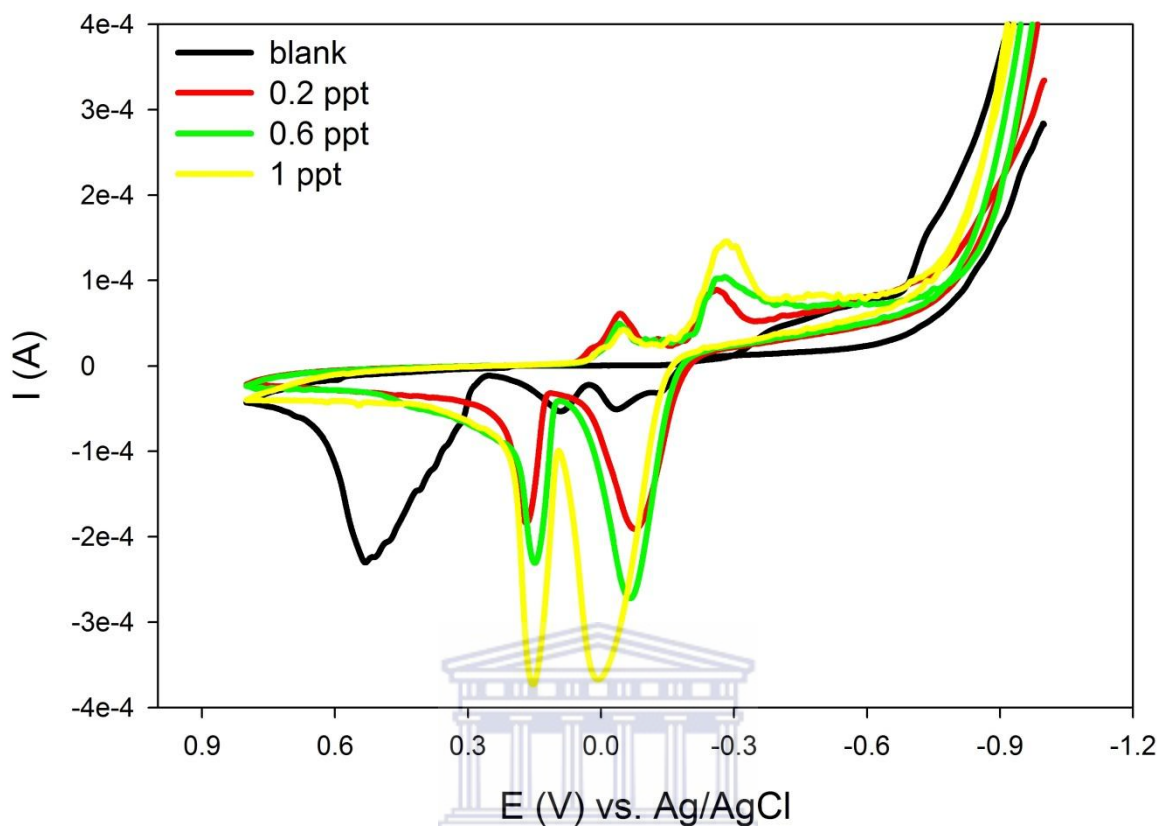
Figure 47. **Cyclic voltammograms for Pd(II) in 0.2 M acetate buffer (pH = 4.7) solution containing 1 × 10⁻⁵ M DMG solution. The scan rate is 50 mV/s and the potential was scanned from +0.8 to -1.0 V (vs. Ag/AgCl).**

Figure 48 shows the CVs obtained for the GC/Bi-AgFE sensor in 0.2 M acetate buffer solution (pH = 4.7) containing 1×10^{-5} M DMG in the present of 0.2 to 1.0 ppt Pt(II) ions. As shown in Figure 48 we observed two cathodic peaks (-0.1 and -0.4 V vs. Ag/AgCl) with two anodic peaks (+0.1 and -0.1 V vs. Ag/AgCl) arising from the reduction of Pt(II) in complex with DMG, which was adsorbed on the bismuth-silver bimetallic sensor. This phenomenon suggesting that the reduction of the Pt(II) complex was a reversible process. The decrease in peak current in the cathodic peak at -0.1 V (vs. Ag/AgCl) is also due to fast desorption of the complex at the electrode surface. The bimuth-silver bimallic nanosensor shown a big peak observed at +0.55 V (vs. Ag/AgCl) in 0.2 M acetate buffer (pH = 4.7) solution and can be assigned to the stripping of bismuth.
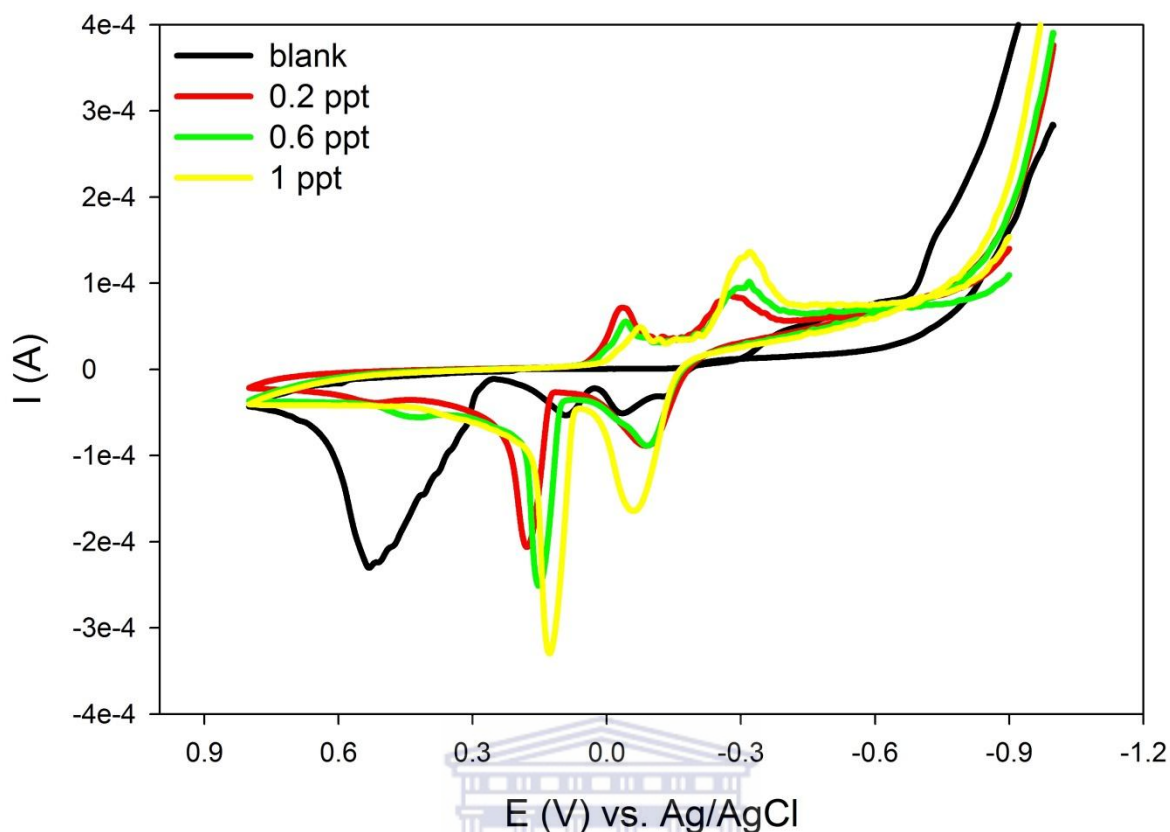
Figure 48. Cyclic voltammograms for Pt(II) in 0.2 M acetate buffer (pH = 4.7) solution containing 1 × 10^{-5} M DMG solution. The scan rate is 50 mV/s and the potential was scanned from +0.8 to -1.0 V (vs. Ag/AgCl).

In Figure 49 a cyclic voltammogram for a solution of acetate buffer containing 1 × 10^{-5} M DMG with increasing concentration of Rh(III) (0.2 to 1.0 ppt) was presented. The three CVs revealed no cathodic peaks with two anodic peaks at +0.1 and -0.1 V (vs. Ag/AgCl) arising from the reduction of Rh(III) in complex with DMG which was adsorbed on the GC/Bi-AgFE sensor. This phenomenon suggesting that the reduction of the Pd(II) complex was an irreversible process. The bimuth-silver bimallic nanosensor shown a big peak observed at +0.55 V (vs. Ag/AgCl) in 0.2 M acetate buffer (pH = 4.7) solution and can be assigned to the stripping of bismuth.

130
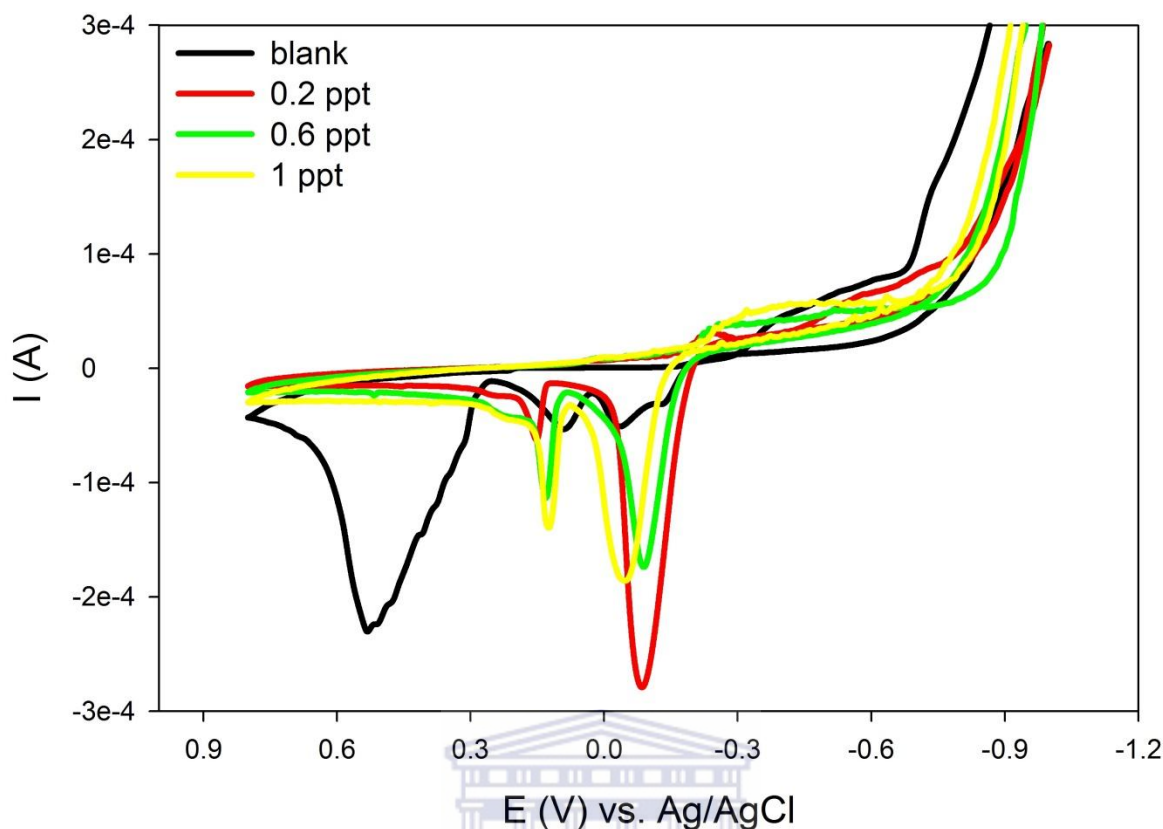
Figure 49.　　Cyclic voltammograms for Rh(III) in 0.2 M acetate buffer (pH = 4.7) solution containing 1×10^{-5} M DMG solution. The scan rate is 50 mV/s and the potential was scanned from +0.8 to -1.0 V (vs. Ag/AgCl).

5.3.4. Stability test of the bismuth-silver bimetallic sensor

Figure 50 illustrates the stability test results obtained for bismuth-silver bimetallic nanoparticles drop-coated in the construction of a GC/Bi-AgFE sensor. This GC/Bi-AgFE sensor was tested in model solutions of 0.2 M acetate buffer (pH = 4.7) solution containing 5 $\times 10^{-5}$ M DMG and 1.0 ppt Pd(II), Pt(II) and Rh(III) ions, respectively. A sharp decrease in reduction peak current for Pd(HDMG)$_2$ was observed from 0 to 7 hours, but after 7 hours it slightly increase till 28 hours. For Pt(HDMG)$_2$ a sharp decrease in peak current was observed from 7 to 14 hours and the reduction peak current reached a plateau from 14 hours onwards. In the case of Rh(HDMG)$_3$, a samll decrease in peak current from 7 to 14 hours was observed with a slightly linear increase in reduction peak current until 28 hours. The results obtained in Figure 50 for the stability testing have shown that the GCE/Bi-AgF sensor are stable for 14 hours and should be used within 24 h after construction.
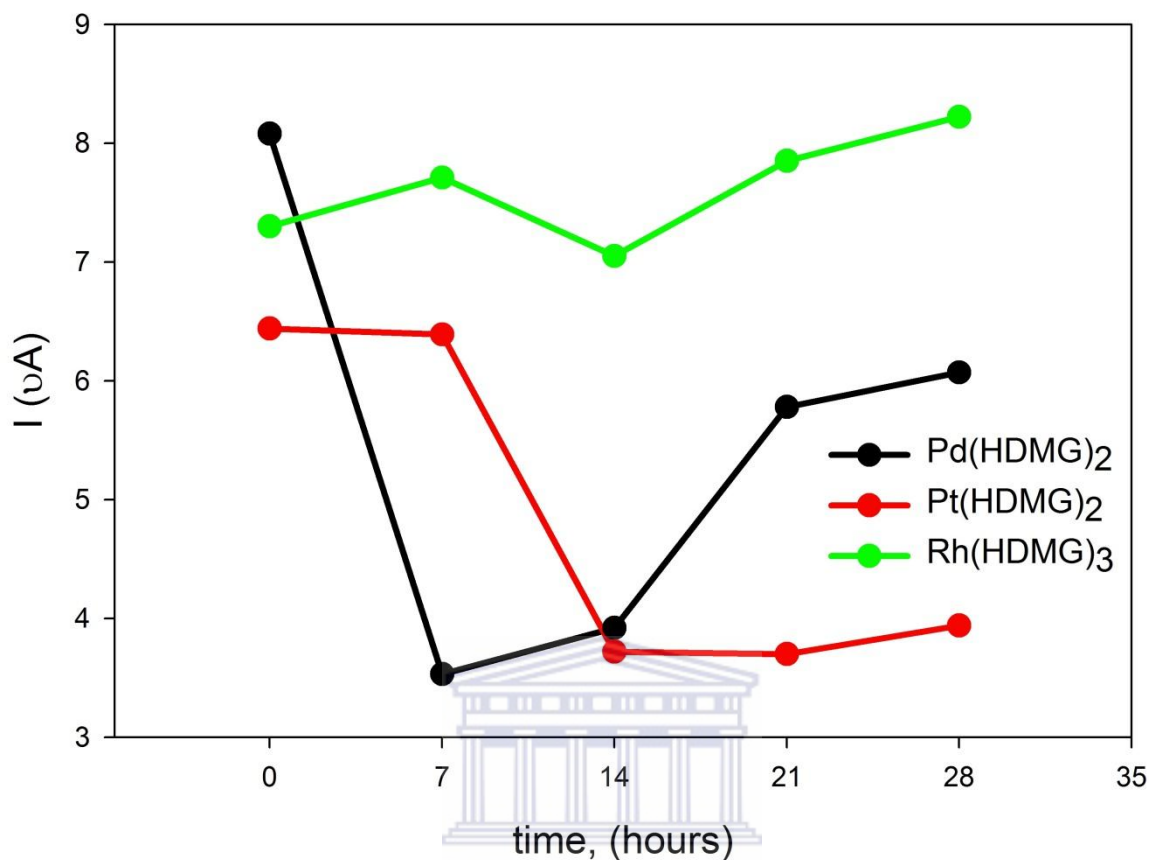
Figure 50. The stability test results obtained for the GC/Bi-AgFE. A 0.2 M acetate buffer (pH = 4.7) solution containing 1 ppt Pd(II), Pt(II), Rh(III) with 1×10^{-5} M of DMG; deposition potential was -0.7 V (vs. Ag/AgCl) and deposition time 30 s.

5.3.5. Deposition potential studies

The analytical performance of the bismuth-silver bimetallic sensor was improved by the optimisation of some operational parameters. Deposition potential is a very important parameter for adsorptive stripping voltammetry and has no negative influence on the sensitivity of determination. In Figure 51 the effect of deposition potential on the stripping peak current for 1.0 ppt Pd(II) ions in 0.2 M acetate buffer solution with pH = 4.7, containing 1×10^{-5} M DMG is illustrated. The deposition potential study was done by varying the potential from -1.0 to -0.1 V (vs. Ag/AgCl). Initially, the peak current increased and flattens at -0.2 V (vs. Ag/AgCl), decline at -0.4 V (vs. Ag/AgCl). After -0.6 V (vs. Ag/AgCl) the peak current sharply increased to the potential of -0.9 V (vs. Ag/AgCl) evaluated.
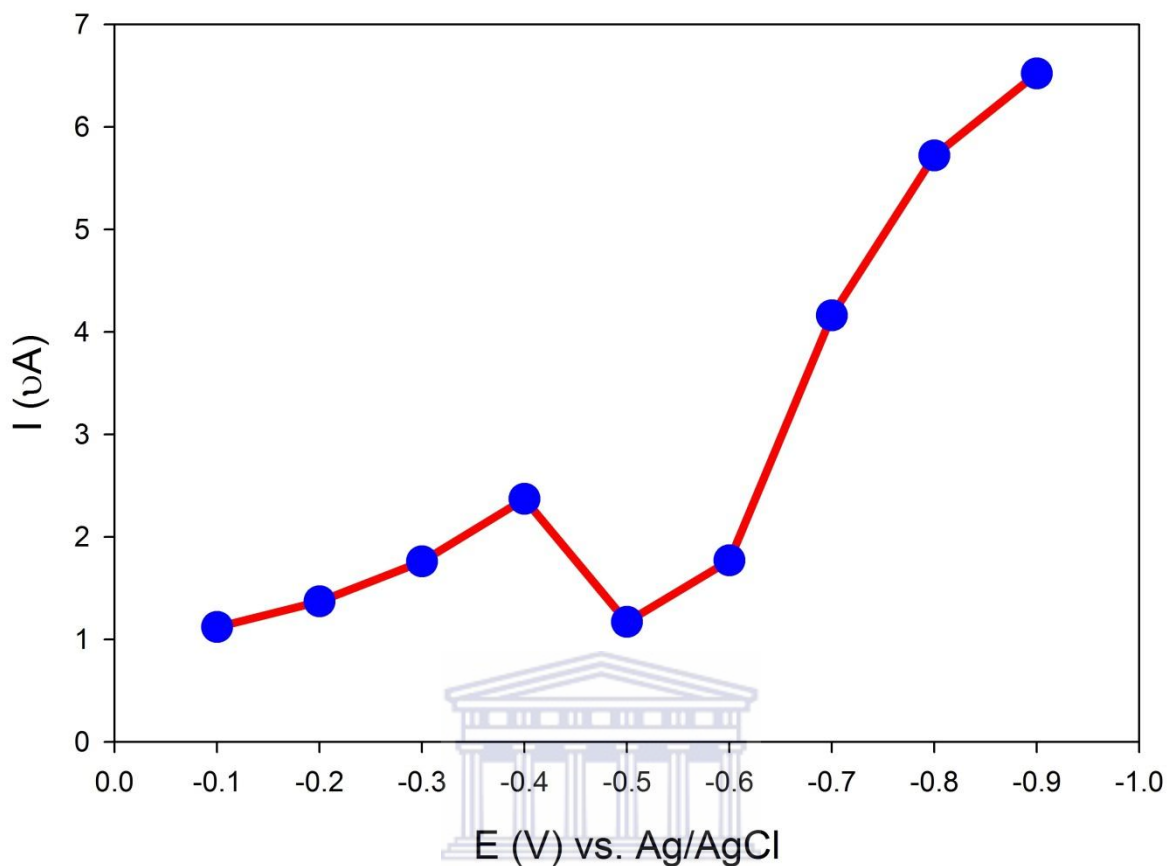
Figure 51.   **Effect of deposition potential upon adsorptive stripping response at a GC/Bi-AgFE. The solution consisted of 0.2 M acetate buffer, (pH = 4.7) containing 1.0 ppt Pd(II) with 1×10^{-5} M DMG, deposition time was 30 s.**

Figure 52 illustrates the effect of deposition potential on the stripping peak current for 1.0 ppt Pt(II) ions in 0.2 M acetate buffer solution with pH = 4.7, containing 1×10^{-5} M DMG. The deposition potentials increased steadily till -0.6 V (vs. Ag/AgCl), decreased at -0.7 V (vs. Ag/AgCl) and increased linearly to 1.0 V (vs. Ag/AgCl). Well-defined stripping peak result was obtained at -0.9 V (vs. Ag/AgCl) and was used as the optimum potenti al for Pt(II) studies.
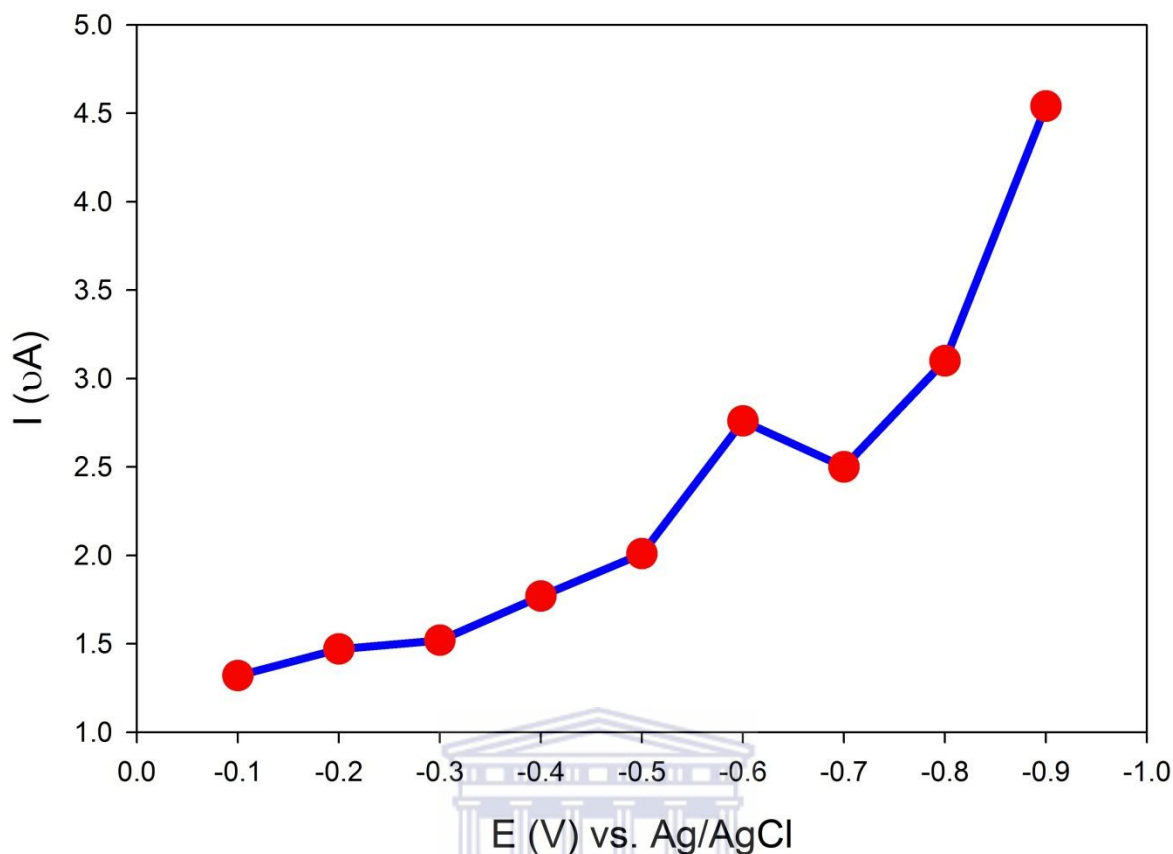
Figure 52. Effect of deposition potential upon adsorptive stripping response for at a GC/Bi-AgFE. The solution consisted of 0.2 M acetate buffer, (pH = 4.7) containing 1.0 ppt Pt(II) with 1 × 10^{-5} M DMG, deposition time was 30 s.

We also studied the effect of deposition potential on the stripping peak current for 1.0 ppt Rh(III) ions in 0.2 M acetate buffer (pH = 4.7) solution , containing 1 × 10^{-5} M DMG. This deposition potential study was done by varying the potential from -1.0 to -0.1 V (vs. Ag/AgCl) as illustrated in Figure 53. The peak current decreased from -0.1 to -0.2 V (vs. Ag/AgCl) and then increased linearly till -0.7 V (vs. Ag/AgCl). At a deposition potential of -0.7 V (vs. Ag/AgCl) the peak current decreased to -0.8 V (vs. Ag/AgCl) and increased again until -0.9 V (vs. Ag/AgCl). A well-defined stripping peak result was obtained at -0.9 V (vs. Ag/AgCl) and was used as the optimum potential for Rh(III) studies.
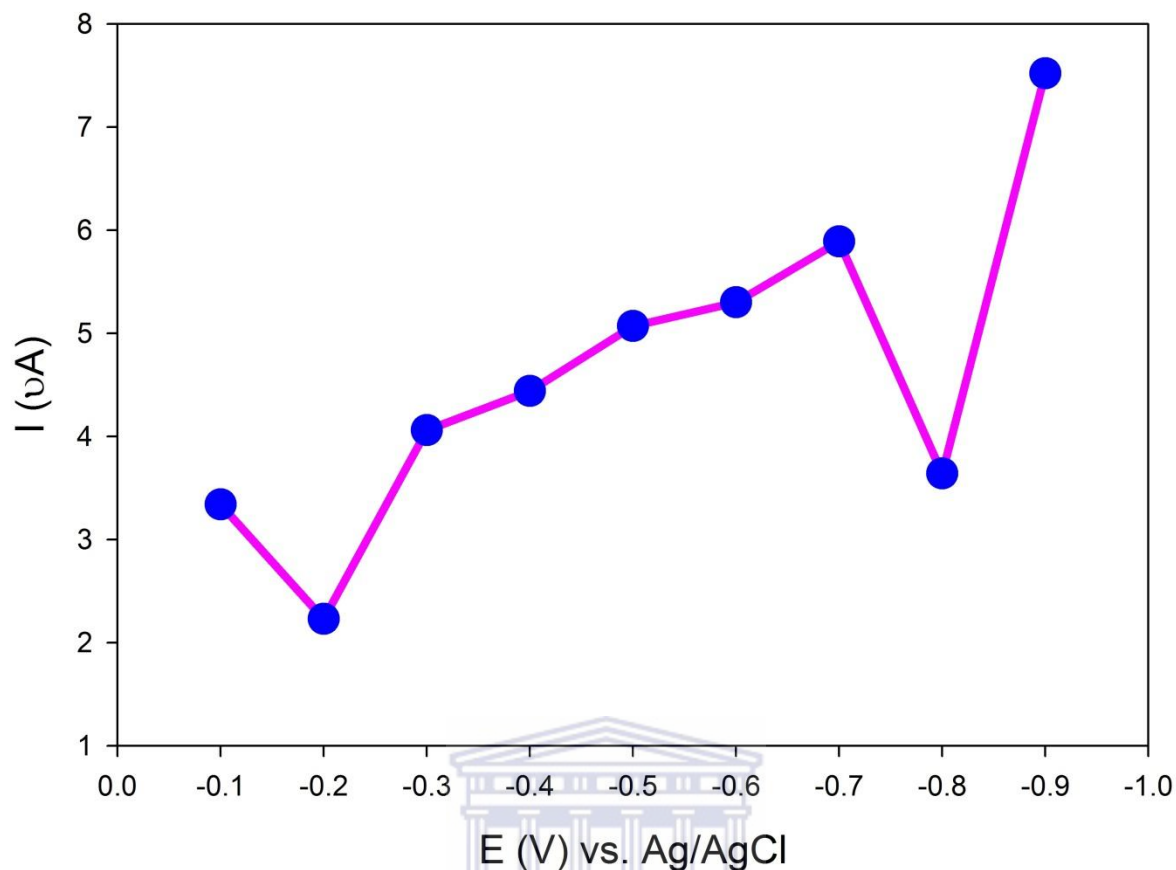
Figure 53. Effect of deposition potential upon adsorptive stripping response at a GC/Bi-AgFE. The solution consisted of 0.2 M acetate buffer, (pH = 4.7) containing 1.0 ppt Rh(III) with 1×10^{-5} M DMG, deposition time was 30 s.

5.3.6. Deposition time studies

In differential pulse adsorptive stripping voltammetry deposition time can apparently influence the determination of PGMs. Figure 54 illustrate the results obtained for optimisation of deposition time for Pd(II) ions with a concentration of 1.0 ppt in a model solution containing 1×10^{-5} M DMG and 0.2 M acetate buffer (pH = 4.7). In the present study the deposition time used range from 30 to 180 s with a deposition potential of -0.9 V (vs. Ag/AgCl) for Pd(II). Initially, the peak currents increase linearly and at a deposition time 90 s it started to decline at a deposition time of 150 s and increased again at 180 s. This observation are due to the saturation of electrode surface with the Pd-(HDMG)$_2$ chelate.
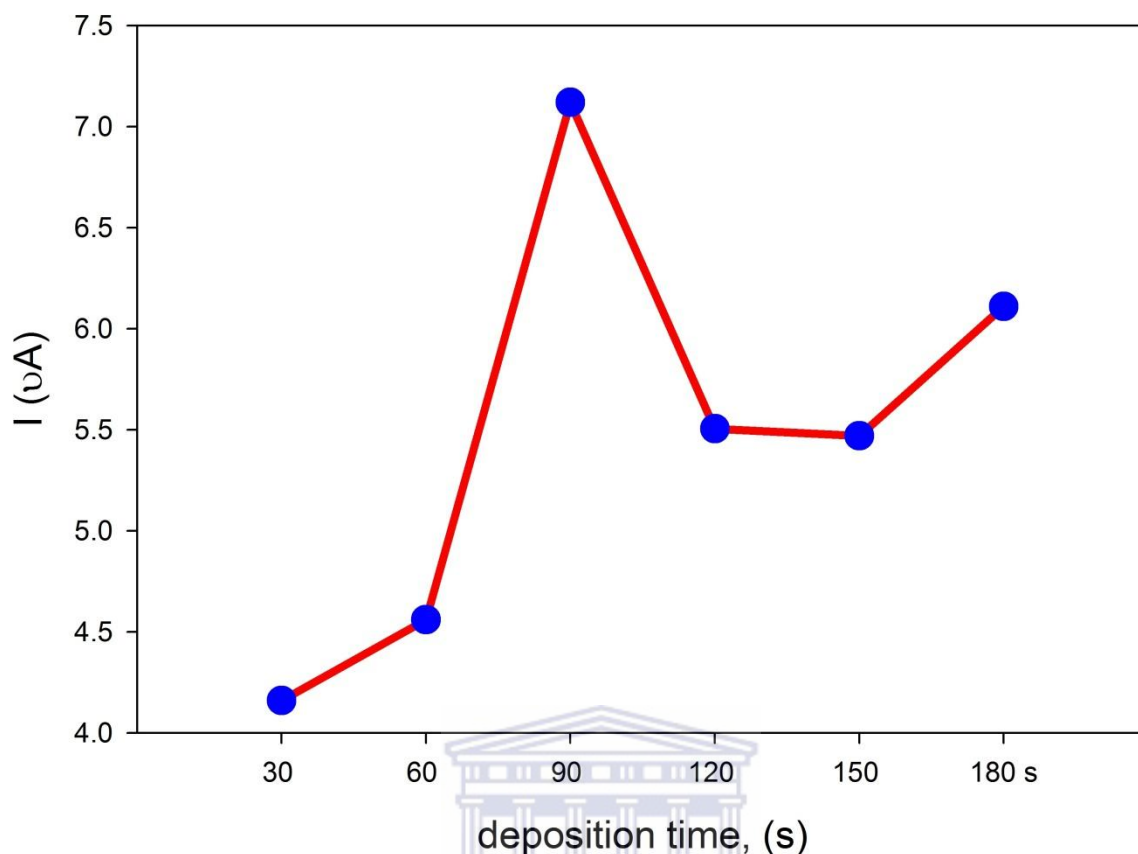
Figure 54. **Effect of deposition time upon adsorptive stripping response at a GC/Bi-AgFE. The solution consisted of 0.2 M acetate buffer, (pH = 4.7) containing 1.0 ppt Pd(II) with 1 × 10^{-5} M DMG, deposition potential was -0.9 V (vs. Ag/AgCl).**

The effect of deposition time upon reduction peak current for 1.0 ppt Pt(II) ions was investigated in a model solution containing 1×10^{-5} M DMG and 0.2 M acetate buffer (pH = 4.7). Figure 55 illustrate the results obtained for deposition time upon the reduction peak current. The reduction peak current increased with increasing deposition time between 30 s and 90 s. The deposition time results flattened above 90 s to 180 s due to surface saturation of the bismuth-silver bimetallic nanosensor.
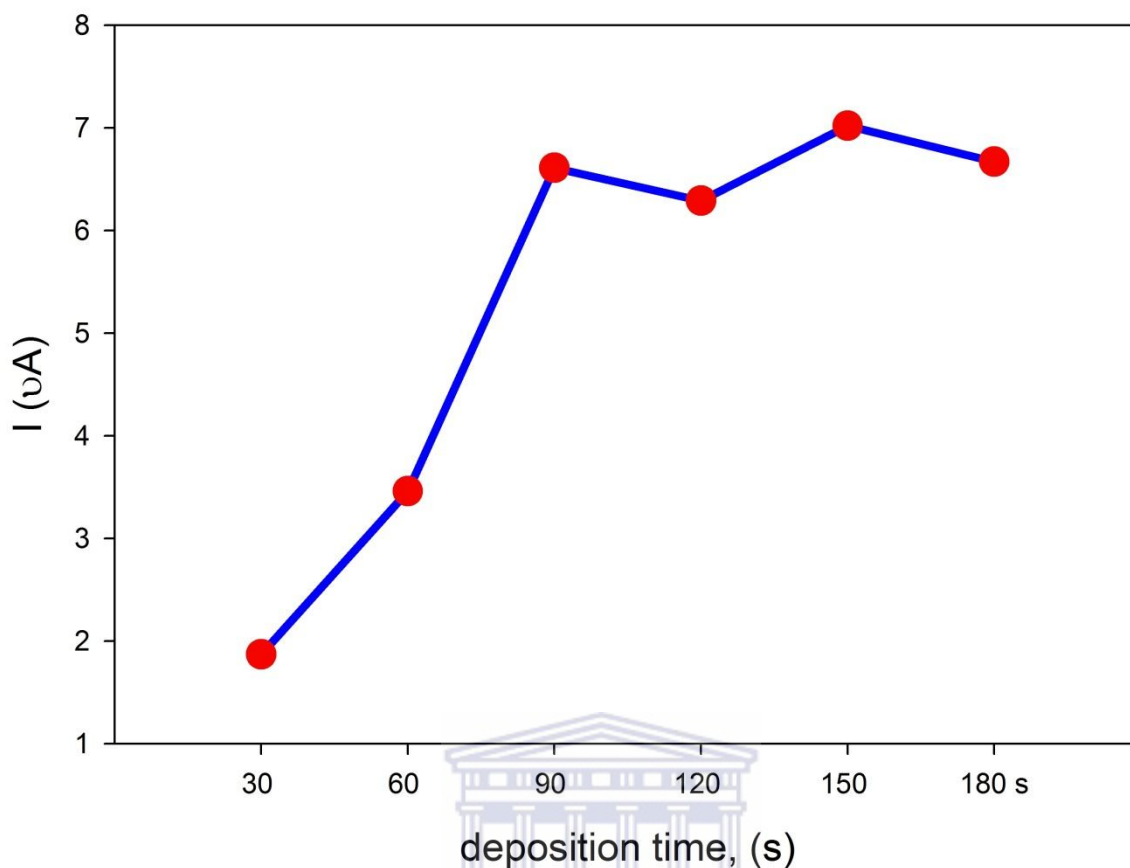
Figure 55. **Effect of deposition time upon adsorptive stripping response at a GC/Bi-AgFE. The solution consisted of 0.2 M acetate buffer, (pH = 4.7) containing 1.0 ppt Pt(II) with 1 × 10^{-5} M DMG, deposition potential was -0.9 V (vs. Ag/AgCl).**

In Figure 56 the effect of deposition time on the reduction peak current for Rh(III) in the solution containing 1.0 ppt Rh(III) ions, 1 × 10^{-5} M DMG and 0.2 M acetate buffer (pH = 4.2) is illustrated. Initially the reduction peak current increased till 60 s, decreased till 90 s and linearly increases till 180 s. In further experiments, 60 s was used as the deposition time and ensures high sensitivity of Rh(III) ions and short time of analysis due to over saturation of the bismuth-silver bimetallic sensor.
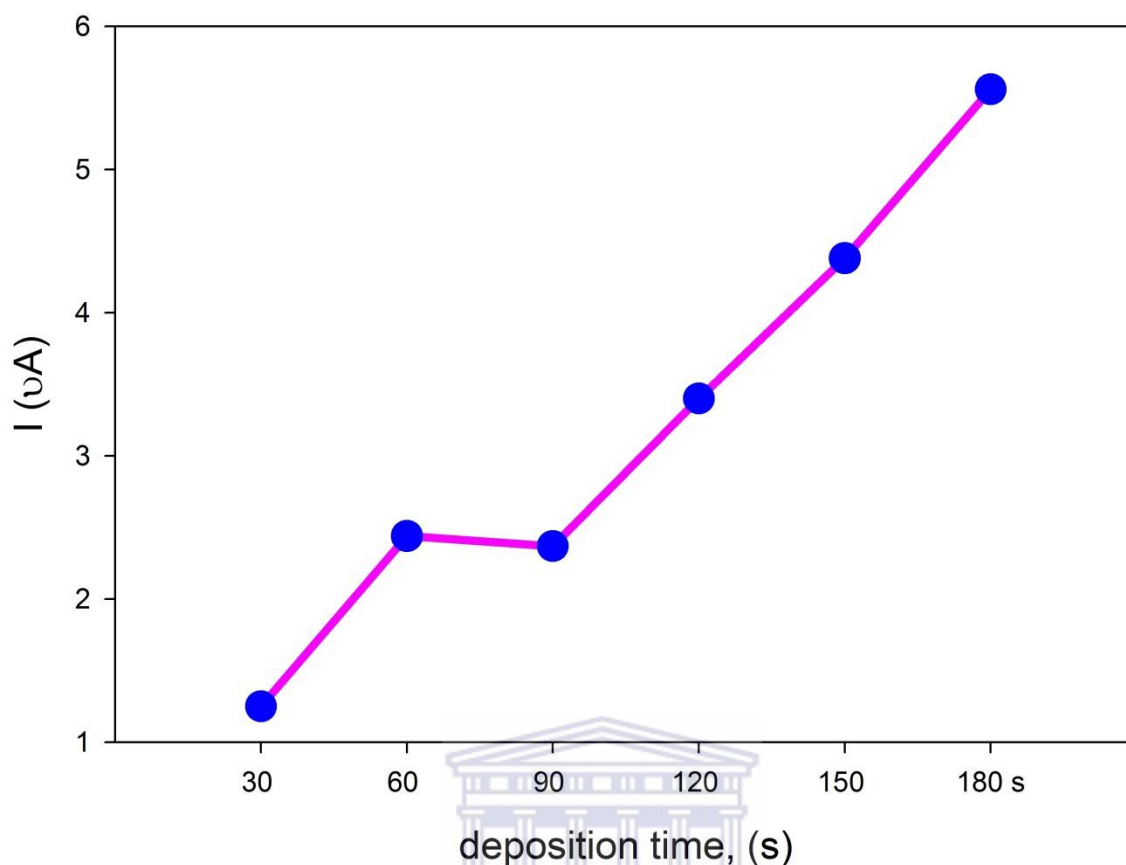
Figure 56. **Effect of deposition time upon adsorptive stripping response at a GC/Bi-AgFE. The solution consisted of 0.2 M acetate buffer, (pH = 4.7) containing 1.0 ppt Rh(III) with 1×10^{-5} M DMG, deposition potential was -0.7 V (vs. Ag/AgCl).**

In Table 9, only similarities in the optimum working conditions for the voltammetric determination of PGMs in model standard solutions were tabulated. It was found that Pd(II) Pt(II) and Rh(III) have the same deposition potential with the same deposition times. Other working conditions such as DMG concentration, pH and potential window obtained was similar for Pd(II), Pt(II) and Rh(III) throughout the investigation.

Table 9. **Summary of optimum stripping voltammetry conditions for the determination of Pd(II), Pt(II) and Rh(III) with the constructed GC/Bi-AgFE bimetallic nanosensor (Somerset *et al.*, 2011; Van der Horst *et al.*, 2012).**

Step	Condition		
	Pd(II)	Pt(II)	Rh(III)
Reduction step			
pH		4.7	
Reduction potential	-0.9 V	-0.9 V	-0.9 V
Reduction time	90 s	90 s	90 s
Supporting electrolyte		0.2 M NaOAc	
Measurement step			
Supporting electrolyte		0.2 M NaOAc	
Measurement technique		differential pulse voltammetry	
Potential window		Stripping from +300 to -100 mV	
DMG concentration		5×10^{-5} M	

5.3.7. Stripping voltammetric analysis of PGMs

The prime objective of the present study is the determination of PGMs using the bismuth-silver bimetallic modified electrode. The adsorptive stripping analysis of PGMs with DMG resulted in well-shaped stripping peaks at specific and defined potentials. Acetate buffer (pH = 4.7) solution was used as the supporting electrolyte. Figure 57 (a) shows the set of adsorptive stripping voltammograms obtained upon increasing the Pd(II) concentration from 0.2 to 1.0 ppt. The electrochemical scan in the cathodic direction shown reduction peaks at approximately +0.05 V (vs. Ag/AgCl) for Pd(II). The potential was scanned between 0.4 V and -0.1 V (vs. Ag/AgCl) with accumulation time of 90 s and accumulation potential of -0.9 V (vs. Ag/AgCl) with a quiet time of 30 s respectively. In this study deposition of PGMs was usually performed for 90 s, longer periods has not been used due to possible problems with surface saturation effects of the GC/Bi-AgFE sensor. Well defined peaks were observed with a flat baseline for the blank solution. The calibration plot peak current upon increasing concentration for Pd(II) are illustrated in Figure 57 (b). The six concentrations used yielded a linear response and the equation of the linear calibration curve is $y = 5.236x + 1.876$ ($R^2 = 0.984$).

Figure 58 (a) reveals the differential pulse adsorptive stripping voltammograms obtained for Pt(II) ions with a GC/Bi-AgFE sensor in 0.2 M acetate buffer solution (pH = 4.7). The model solution for the investigation contains 0.2 to 1.0 ppt Pd(II) ions with 1×10^{-5}

M DMG. Figure 58 (a) exhibited well-defined reduction peaks with a flat baseline for the blank solution at ~ +0.025 V (vs. Ag/AgCl). These voltammograms were obtained by keeping the sensor in contact with a stirred model solution for 90 s at -0.9 V (vs. Ag/AgCl). The calibration plot peak current upon increasing concentration for Pd(II) is illustrated in Figure 58 (b). The six concentrations used yielded a linear response and the equation of the linear calibration curve is $y = 5.907x + 1.048$ ($R^2 = 0.970$).

The electrochemical characteristics of Rh(III) ions was investigated on the bismuth-silver bimetallic film electrode (Bi-AgFE). Differential pulse adsorptive striping voltammetry was used to demonstrate the adsorption of Rh(III) onto the surface of the GC/Bi-AgFE sensor. The GC/Bi-AgFE was used as a working electrode and kept in contact with a stirred model solution for 60 s at -0.7 V (vs. Ag/AgCl). This model solution contains Rh(III) ions with 1×10^{-5} M DMG in 0.2 M acetate buffer (pH = 4.7) solution. Subsequently recorded voltammograms exhibited well-defined reduction peaks at ~ +0.025 V (vs. Ag/AgCl), including that of a sample blank and is illustrated in Figure 59 (a). The calibration plot peak current upon increasing concentration for Rh(III) are illustrated in Figure 59 (b). The six concentrations used yielded a linear response and the equation of the linear calibration curve is $y = 2.0731x + 1.3835$ ($R^2 = 0.9933$).
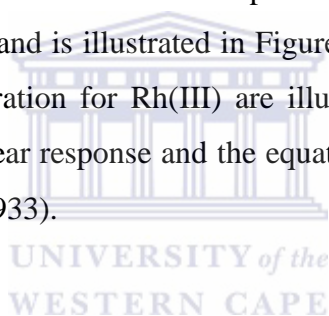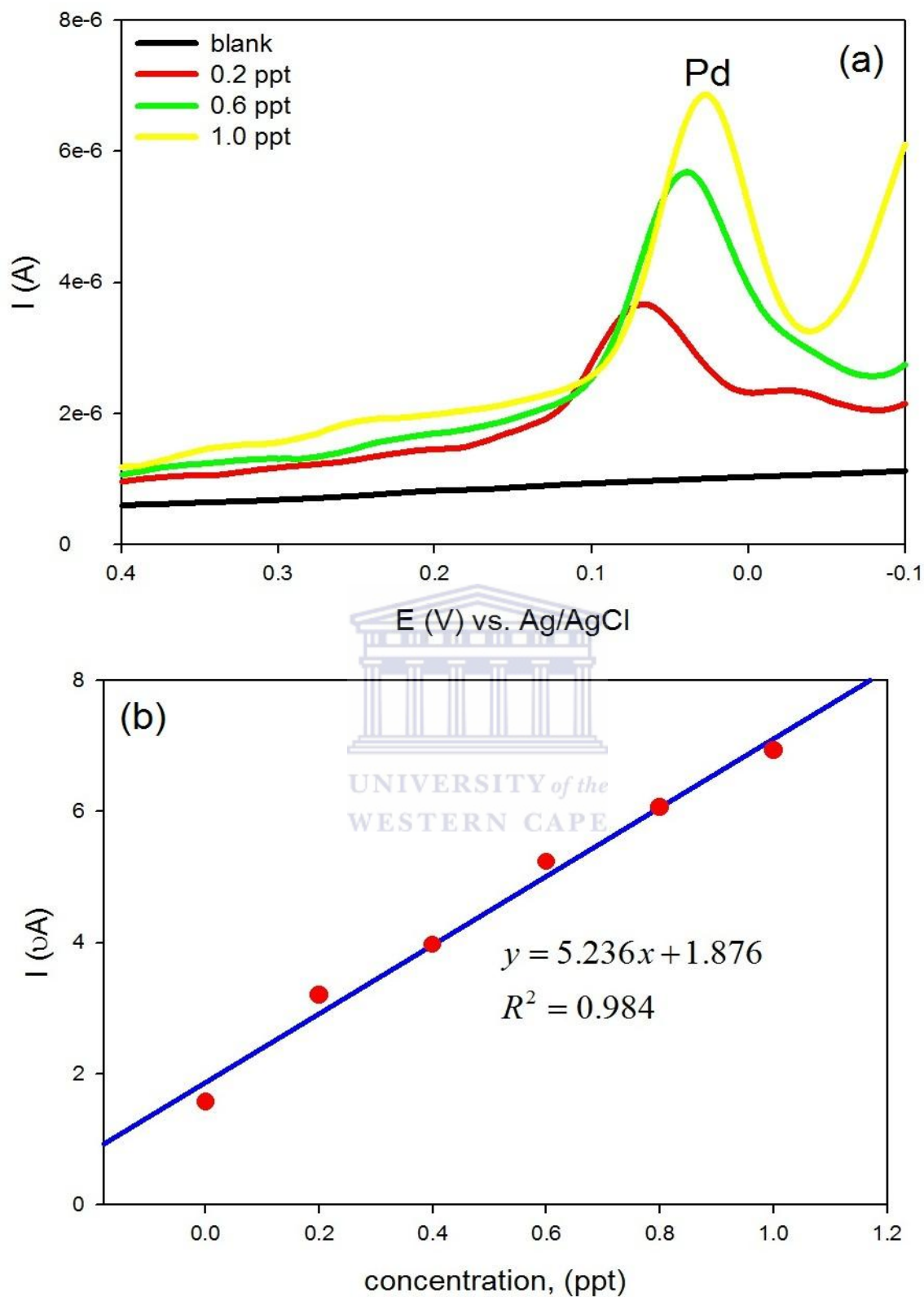
Figure 57. Differential pulse adsorptive stripping voltammetry for increasing concentrations of Pd(II) at a GC/Bi-AgFE in (a). Corresponding calibration curve obtained for the Pd(II) in (b). The solution consisted of 0.2 M acetate buffer (pH = 4.7) containing 0.2 to 1.0 ppt Pd(II) with 1×10^{-5} M DMG; deposition potential was -0.7 V (vs. Ag/AgCl) and deposition time 90 s.
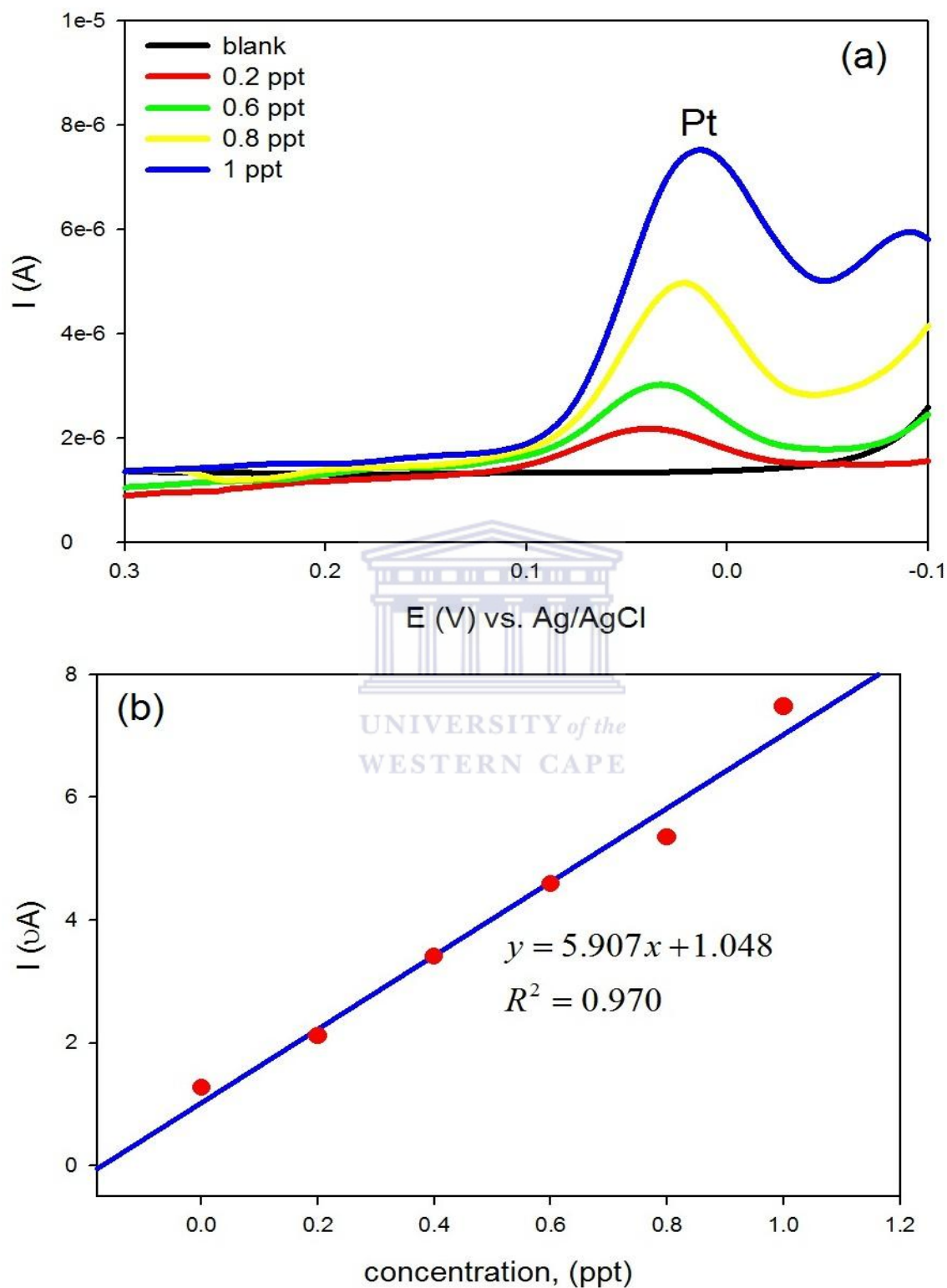
Figure 58. Differential pulse adsorptive stripping voltammetry for increasing concentrations of Pt(II) at a GC/Bi-AgFE in (a). Corresponding calibration curve obtained for the Pt(II) in (b). The solution consisted of 0.2 M acetate buffer (pH = 4.7) containing 0.2 to 1 ppt Pt(II) with 1×10^{-5} M DMG; deposition potential was -0.9 V (vs. Ag/AgCl) and deposition time 90 s.
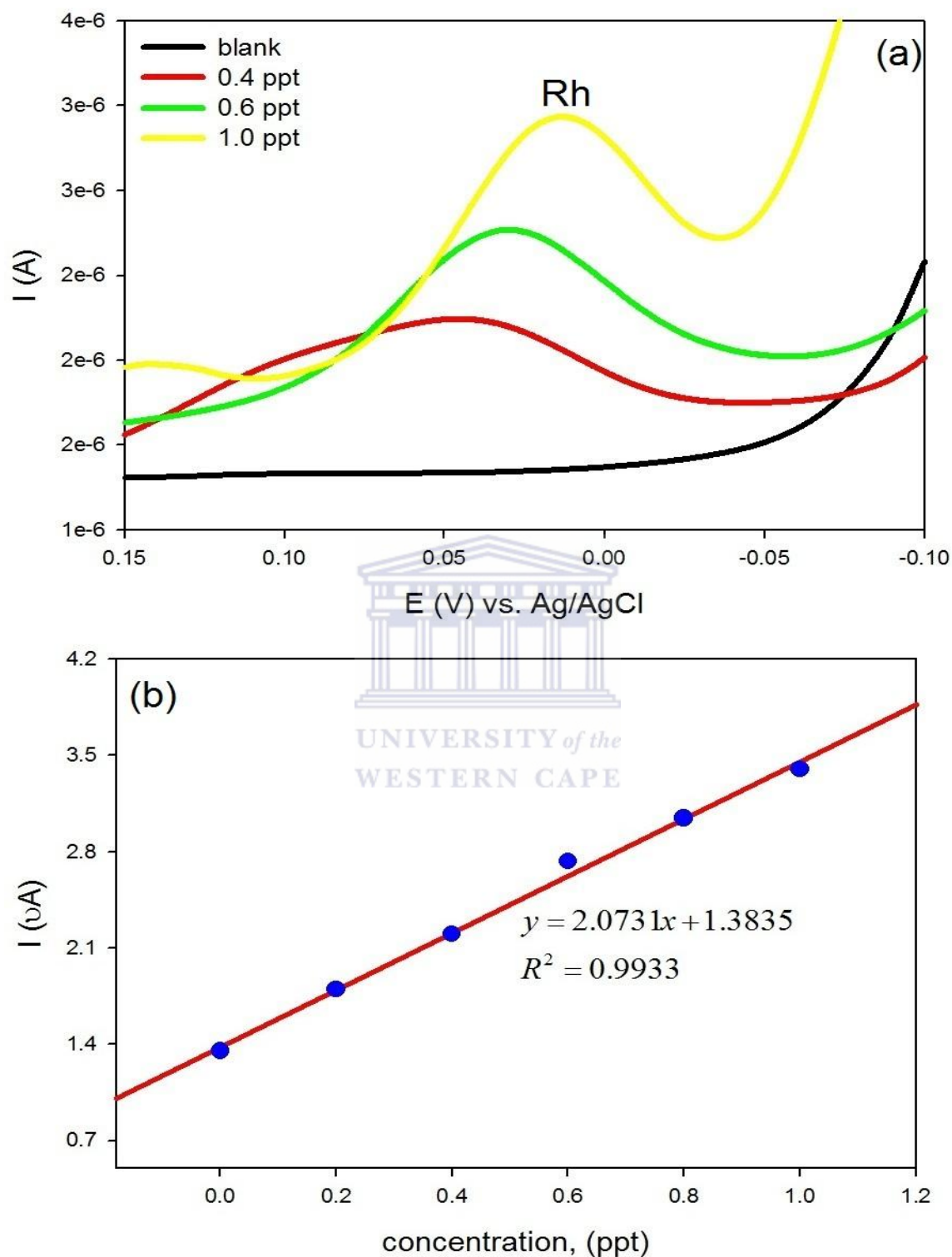
Figure 59. Differential pulse adsorptive stripping voltammetry for increasing concentrations of Rh(III) at a GC/Bi-AgFE in (a). Corresponding calibration curve obtained for the Rh(III) in (b). The solution consisted of 0.2 M acetate buffer (pH = 4.7) containing 0.4 to 1.0 ppt Rh(III) with 1×10^{-5} M DMG; deposition potential was -0.7 V (vs. Ag/AgCl) and deposition time 60 s.

Simultaneous determination of palladium, platinum and rhodium in slightly acidic acetate buffer solution (pH = 4.7) was not possible due to interference of the platinum complex with the palladium complex using DPAdSV mode. According to the literature, simultaneous determination of Pd and Rh or Pt and Rh were done at HMDE and BiFEs surfaces and was also possible in this study (Dalvi *et al*., 2008; Locatelli, 2006; Van der Horst *et al*., 2012; Silwana *et al*., 2014).

Figure 60 illustrates the simultaneous determination of Pd and Rh with the GC/Bi-AgFE sensor in a 0.2 M acetate buffer (pH = 4.7) solution. In this study the DPAdSV peak potentials were obtained at approximately -0.06 V (vs. Ag/AgCl) for Pd(II) and at -0.1 V (vs. Ag/AgCl) for Rh(III). The obtained results in Figure 60 at the GC/Bi-AgFE sensor shown linear response with linear calibration equation $y = 0.708x - 0.0434$ and $y = 0.222x + 0.0282$ for Pd(HDMG)$_2$ and Rh(HDMG)$_3$, respectively. These results obtained for the simultaneous determination of Pd and Rh complexes were compared with results obtained by other researchers (Van der Horst *et al*., 2012; Silwana *et al*., 2014; Locatelli, 2006). In comparison with the work done by Van der Horst *et al*. (2012) and Silwana *et al*. (2014), better defined peaks were observed for Pd-Rh complexes in this presented study with lower detection limits.

Figure 61 indicate the stripping voltammograms for Pt(HDMG)$_2$ and Rh(HDMG)$_3$ at the GC/Bi-AgFE sensor in a 0.2 M acetate buffer (pH = 4.7) solution. The results shown that the stripping peak potentials were obtained at approximately -0.04 V (vs. Ag/AgCl) for Pt(II) and at -0.14 V (vs. Ag/AgCl) for Rh(III), respectively. The GC/Bi-AgFE sensor showed linear response with linear calibration equation $y = 0.708x - 0.0434$ and $y = 0.222x + 0.0282$ for Pt(HDMG)$_2$ and Rh(HDMG)$_3$, respectively. The results in both analysis have shown that well defined stripping peaks were obtained for both Pd(II) and Pt(II) results, while that of the Rh(III) stripping peaks were less defined and not always consecutive. This observation is an indication that the sensor is more favorable for Pd(II) and Pt(II) studies. The results obtained for the simultaneous determination of Pt(II) and Rh(III) complexes were compared with results obtained by Dalvi *et al*. (2008). The work done by Dalvi *et al*. (2008) showed better defined peaks and with better detection limits for the Pt-Rh complexes as in the present study.
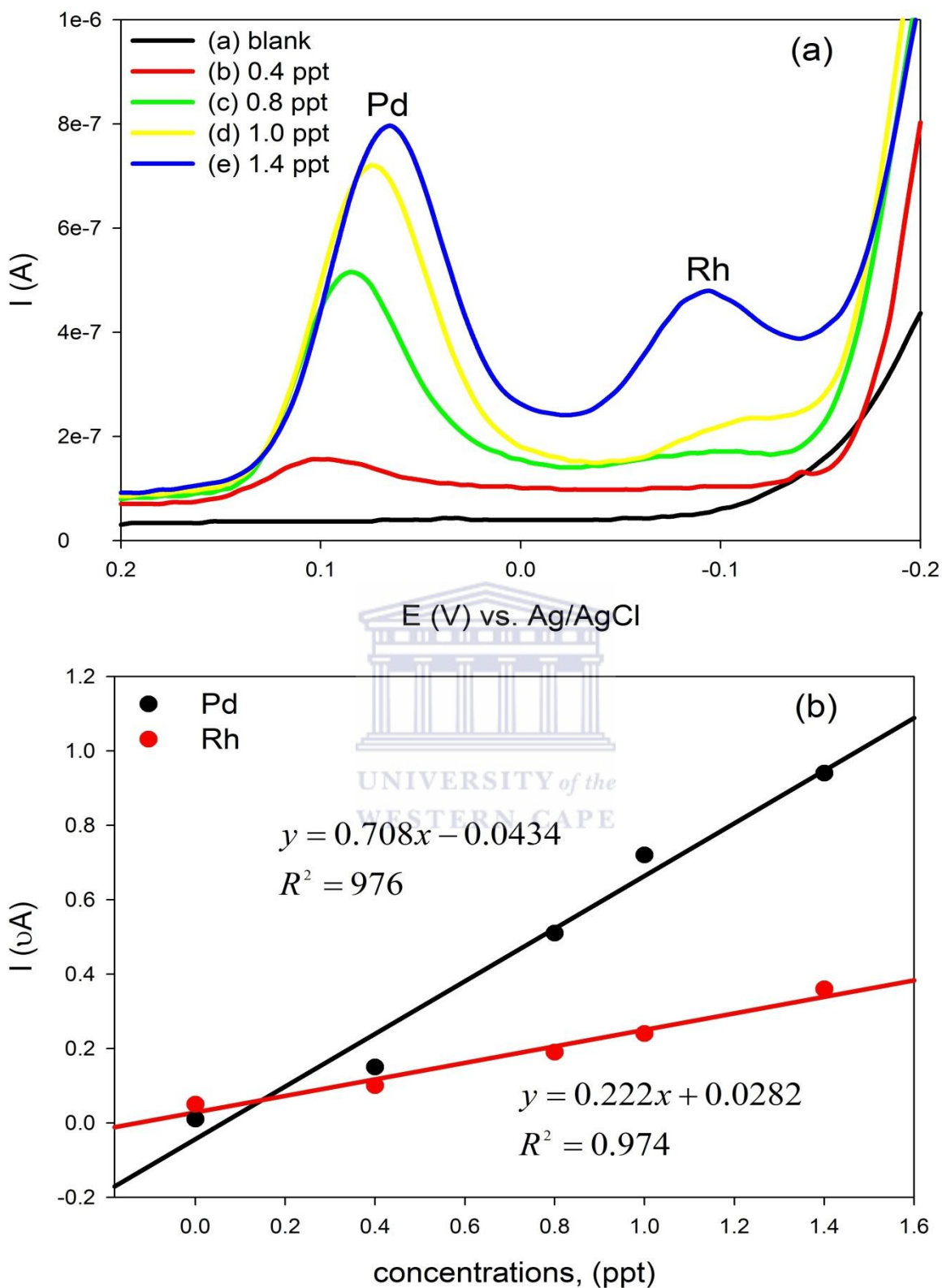
Figure 60. Differential pulse adsorptive stripping voltammetry for increasing concentrations of Pd(II) and Rh(III) at a GC/Bi-AgFE in (a). Corresponding calibration curve obtained for Pd(II) and Rh(III) in (b). The solution consisted of 0.2 M acetate buffer (pH = 4.7) containing 0.4 to 1.4 ppt Pd(II) and Rh(III) with 1×10^{-5} M DMG; deposition potential was -0.7 V (vs. Ag/AgCl) and deposition time 30 s.
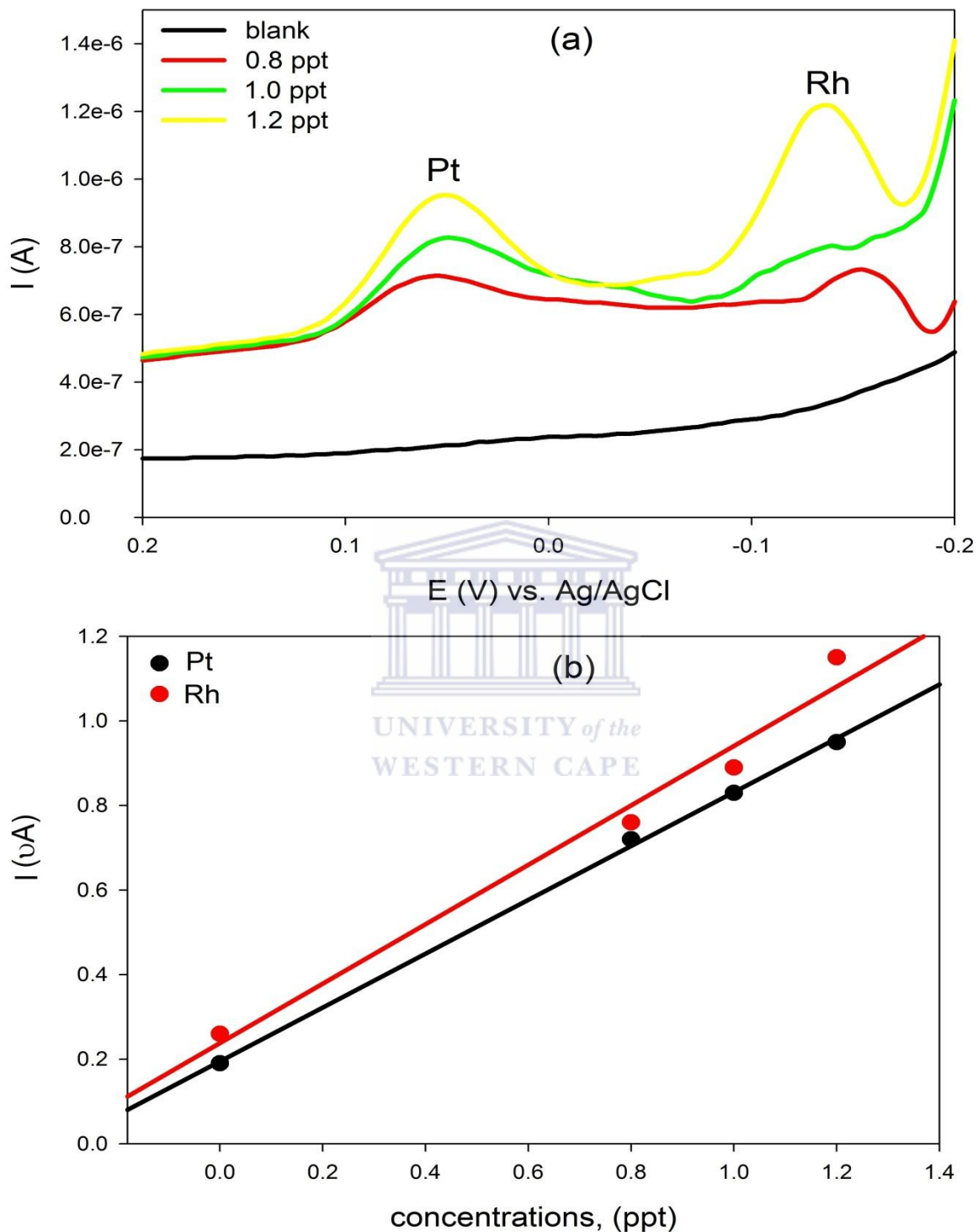
Figure 61.   Differential pulse adsorptive stripping voltammetry for increasing concentrations of Pt(II) and Rh(III) at a GC/Bi-AgFE in (a). Corresponding calibration curve obtained for Pt(II) and Rh(III) in (b). The solution consisted of 0.2 M acetate buffer (pH = 4.7) containing 0.8 to 1.2 ppt Pd(II) and Rh(III) with 1×10^{-5} M DMG; deposition potential was -0.8 V (vs. Ag/AgCl) and deposition time 60 s.

5.3.8. Interference studies

In the determination of PGMs in environmental samples metal ions can also interfere with the measurement of these metal ions by complexing competitively with DMG or by producing reduction peaks that also overlap with, or even completely suppress the Pd(II), Pt(II) and Rh(III) peaks, respectively. Metal ions that could potentially interfere were examined at concentrations of 0.5 to 1.5 ppt for Pd(II), Pt(II) and Rh(III) in the presence of Co(II), Cd(II), Ni(II), Pb(II), Fe(III), Na^+ and Cu(II).

In this study Figure 62 (A) reveals the effect of Ni(II) and Co(II) interfering with Pd(II) ions in a solution containing Ni(II) (1.0 ppt), Co(II) (1.0 ppt) and it seems like Ni(II) and Co(II) only interfere with Pd(II) at the two higher concentrations due to the decrease of peak current at these concentrations.

Figure 62 (B) illustrates the interfering effect of Ni(II) and Co(II) with Pt(II) in model solutions. For the results obtained it was observed that Co(II) and Ni(II) does not interfere with Pt(II) at low concentrations. Nickel(II) and Cobalt(II) does interfere with Pt(II) at the two higher concentrations investigated. It was also observed that at high concentrations of Pt(II), weak reduction peak currents were obtained. In the work done by Melucci and Locatelli, (2007) it was indicated that cobalt and nickel are present at very low concentrations in environmental matrices of PGMs and should be considered as potential interferents.

The interfering effect of Ni(II) and Co(II) upon Rh(III) are presented in Figure 62 (C). In the obtained results in Figure 19 (C) only two peaks were observed for the three metal ions respectively. At a Rh(III) concentration of 0.5 ppt, it was observed that no interferences takes place with a well-defined peak. Nickel(II) and cobalt does interfere with Rh(III) at the two higher concentrations investigated, with a shift in peak potential at the 1.0 ppt concentration
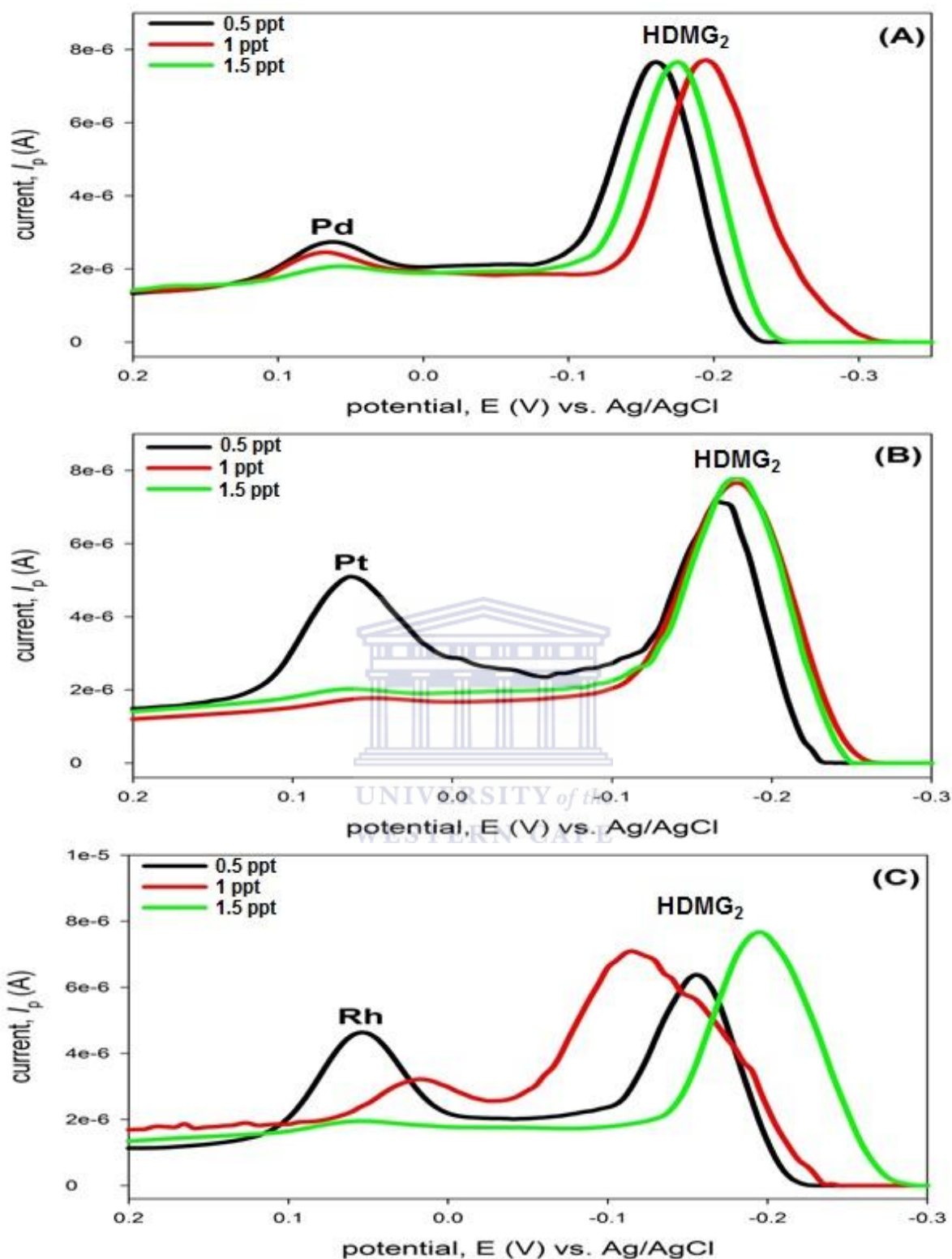
Figure 62. Effect of interfering ions on the peak current responses for Pd(II) in (A), Pt(II) in (B), and Rh(III) in (C) using the GC/Bi-AgFE sensor. The concentrations of Pd(II), Pt(II), and Rh(III) used were (0.5 ppt) in (a), 1 ppt in (b), and 1.5 ppt in (c), respectively. For Ni and Co the concentrations used were 1.0 ppt, with 0.2 M acetate buffer (pH = 4.7) solution containing 1×10^{-5} M DMG solution

In the following investigation the main attention was paid to those metal ions species that could also affect the reduction peak current of Pd(II), Pt(II) and Rh(III).

It has been observed in Figures 63 (A) and 63 (B) that Cd(II), Pb(II), Cu(II) and Fe(III) interfere with Pd(II) and Pt(II) in the acidic acetate buffer solution. It seems that the DMG complexing agent could not be use in the presence of these four metal ions. From Figure 63 (C) good peaks are observed for Rh(III) with Cd(II), Pb(II), Cu(II) and Fe(III) and indicates that DMG can be used as a complexing agent in the present of these metal ions in acidic buffer solutions.

The effect of sulphate (SO_4^{2-}) and phosphates (PO_4^{3-}) present upon Pd(II), Pt(II) and Rh(II) were also studied as shown in Figure 64 by using the salt of sodium sulphate (Na_2SO_4) and sodium phosphate (H_2NaPO_4). Figure 64 (A) illustrates that SO_4^{2-} and PO_4^{3-} does not interfere with Pd(II) ions. From the observed results DMG could be used in the presence of these two ions and with acetate buffer solution as the supporting electrolyte for the determination of Pd(II). In Figures 64 (B) and 64 (C) it was observed that SO_4^{2-} and PO_4^{3-} interferes with Pt(II) and Rh(III) in the presence of DMG. The observed results show that DMG cannot be used as a complexing agent in the presence of these two ions with acetate buffer as the supporting electrolyte.
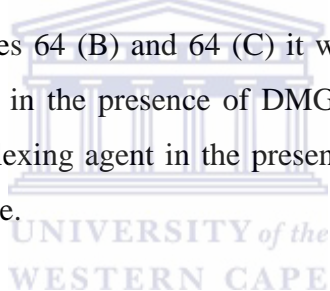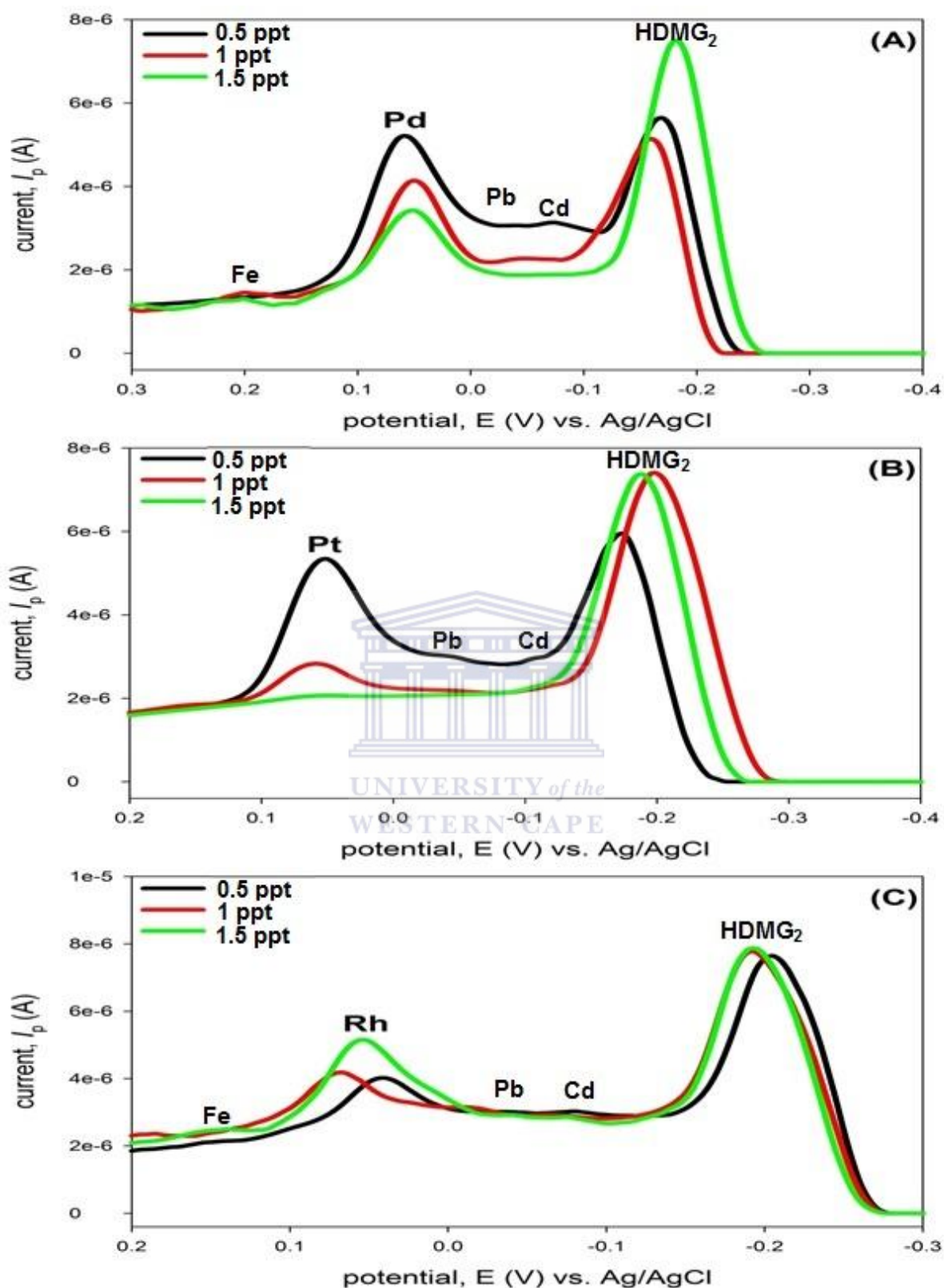
Figure 63.   Effect of interfering ions on the peak current responses for Pd(II) in (A), Pt(II) in (B), and Rh(III) in (C) using the GC/Bi-AgFE sensor. The concentrations of Pd(II), Pt(II), and Rh(III) used were (0.5 ppt) in (a), 1 ppt in (b), and 1.5 ppt in (c), respectively. For Fe, Pb, and Cd the concentrations used were 1.0 ppt, with 0.2 M acetate buffer (pH = 4.7) solution containing 1×10^{-5} M DMG solution.
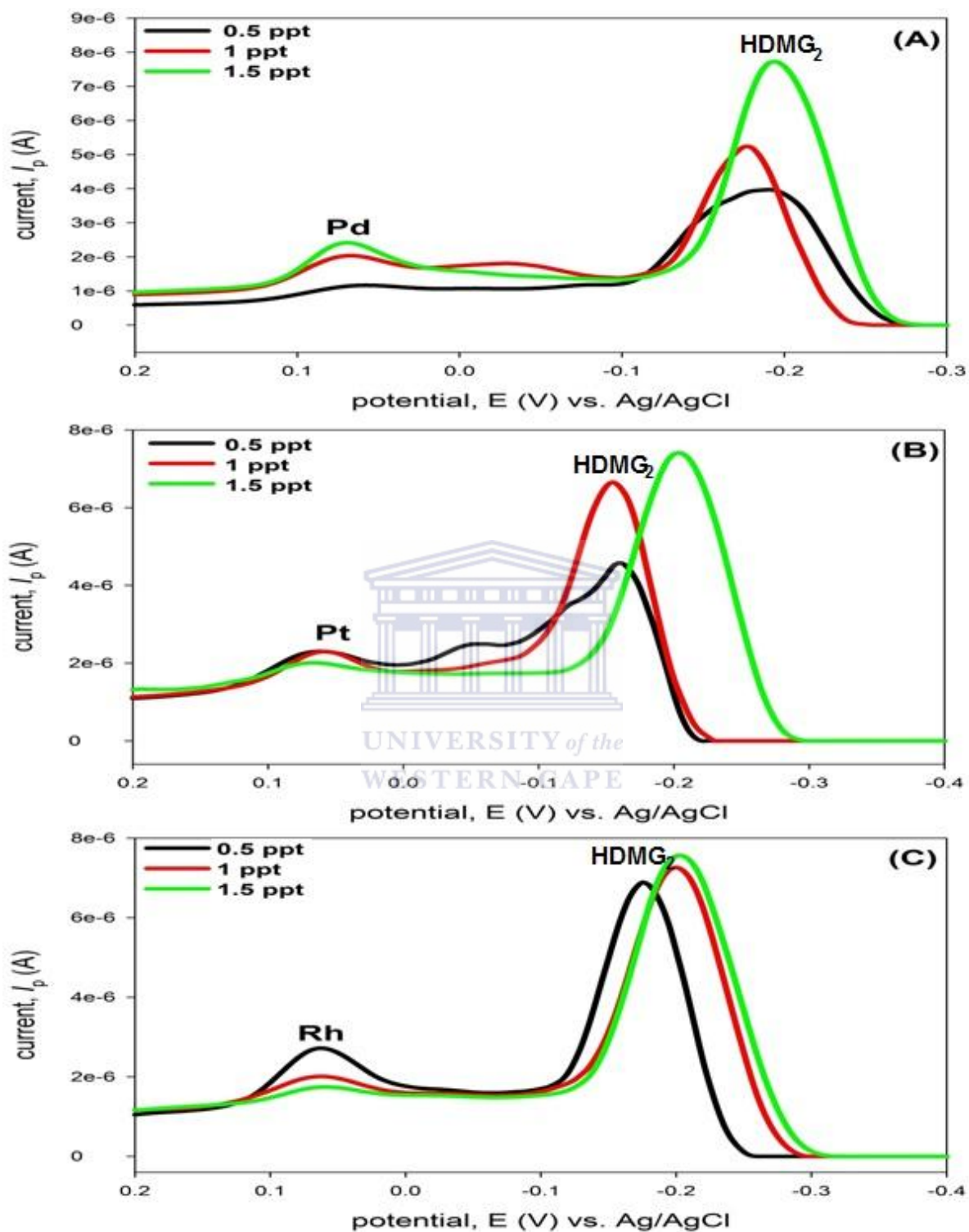
Figure 64. Effect of interfering ions on the peak current responses for Pd(II) in (A), Pt(II) in (B), and Rh(III) in (C) using the GC/Bi-AgFE sensor. The concentrations of Pd(II), Pt(II), and Rh(III) used were (0.5 ppt) in (a), 1 ppt in (b), and 1.5 ppt in (c), respectively. For SO_4^{2-}, and PO_4^{3-} the concentrations used were 1.0 ppt, with 0.2 M acetate buffer (pH = 4.7) solution containing 1×10^{-5} M DMG solution.

5.3.9. Stripping voltammetric analysis of PGMs

The limit of detection and sensitivity are important considerations when the analytical application of any process is assessed (Welch *et al*., 2005). The results obtained in this study were also compared to the work done by other investigations. These comparisons of the analytical features with limits of detection (LODs) of various techniques used are listed in Table 10. The LOD values in Table 10 confirmed good sensitivity of the constructed GC/Bi-AgFE nanosensor for the determination of PGMs in environmental samples. The very low LOD values in this study compared with other studies indicate that the proposed method for the construction of a chemical nanosensor for PGMs determination in environmental samples are very sensitive and can be used as a alternative for the HMDE and other platforms.

Table 10. Comparison of results obtained in present work with other modified stripping voltammetric procedures for the determination of PGMs in model standard solutions and environmental samples are listed.

Electrode	Modifier	Method	Linear range	Limit of detection (LOD)	Ref.
GCE	Bi-Ag	AdDPSV	Pd(II): 0.2 – 1.0 ng/L	Pd(II) – 0.19 ng/L	This work
			Pt(II): 0.2 – 1.0 ng/L	Pt(II) – 0.2 ng/L	
			Rh(III): 0.4 – 1.0 ng/L	Rh(III) – 0.22 ng/L	
GCE	Bismuth	AdDPSV	Pd(II): 0 – 2.5 μg/L	Pd(II) – 0.12 μg/L	Van der Horst *et al*., 2012
			Pt(II): 0 – 3.5 μg/L	Pt(II) – 0.04 μg/L	
			Rh(III): 0 – 3.0 μg/L	Rh(III) – 0.23 μg/L	
SPCE	Bismuth	AdDPSV	Pd(II): 0 – 0.1 μg/L	Pd(II) – 0.008 μg/L	Silwana *et al*., 2014
			Pt(II): 0.2 – 0.1 μg/L	Pt(II) – 0.006 μg/L	
			Rh(III): 0 – 0.08 μg/L	Rh(III) – 0.005 μg/L	
HMDE	ND	AdCSV	Pd(II): 20 – 100 ng/mL	Pd(II) – 2 ng/mL	Kim and Cha, 2002
Ag-based	Hg amalgam	CSV	Pd(II): 1 – 50 μg/L	Pd(II) - 0.15 μg/L	Bobrowski *et al*., 2009

5.3.10. Analysis of environmental samples

The developed voltammetric method was further applied to the determination of PGMs in roadside dust and roadside soil samples collected in the Western Cape Province at Bottelary Road close to Stellenbosch and Old Paarl Road close to Klapmuts, outside Stellenbosch. Four sampling points were identified and at each section of the road leading to a busy traffic light and intersection, where roadside dust and soil samples were collected. In both dust and soil samples PGMs bioavailability was determined by subjecting the samples to a chemical extraction procedure. The extraction of the metals from the roadside dust and soil samples was done by a three-step sequential extraction procedure (Li *et al.*, 2010; Morera *et al.*, 2001).

5.3.10.1. Dust samples

The preparation of the dust samples was done by pipetting 9 mL of 0.2 M acetate buffer (pH = 4.7) solution, containing 1×10^{-5} M DMG and 0.5 *n*g/L PGMs. A 1 mL of roadside dust sample was added to the solution and the determination of PGMs was performed by DPAdSV procedure (Locatelli, 2006). The results obtained are shown in Table 11 for the detection of PGMs in dust samples using a GC/Bi-AgFE sensor and ICP-MS, respectively. The accuracy and sensitivity of the constructed electrochemical sensor were determined by single PGM analysis in all experiments and no simultaneous determination of PGMs was investigated. From the results in Table 11 it was observed that the DPAdSV results are lower than the ICP-MS results. These results indicate that the constructed bimuth-silver bimetallic sensor is more sensitive towards the determination of Pd(II), Pt(II) and Rh(III) in environmental samples.

Table 11. Results obtained for the determination of PGMs concentrations using a GC/Bi-AgFE nanosensor and ICP-MS analysis in dust samples collected from roads near Stellenbosch, Western Cape Province.

	DPAdSV			ICP-MS		
	Carbonate-bound	Organic-bound	Fe-Mn bound	Carbonate-bound	Organic-bound	Fe-Mn bound
Sample	Pd(II) (*ng*/L)	Rh(III) (*ng*/L)	Pt(II) (*ng*/L)	Pd (*µ*g/L)	Rh (*µ*g/L)	Pt (*µ*g/L)
BOT1	1.18 ± 0.06	4.44 ± 0.14	3.58 ± 0.09	0.06	0.01	0.01
BOT2	1.13 ± 0.08	3.32 ± 0.20	3.69 ± 0.37	0.08	0.03	0.03
BOT3	0.94 ± 0.16	3.38 ± 0.15	3.17 ± 0.12	0.09	0.04	0.06
BOT4	1.37 ± 0.16	5.63 ± 0.81	3.35 ± 0.57	0.10	0.05	0.08
OP1	3.62 ± 0.88	8.52 ± 0.57	5.46 ± 0.14	0.04	0.004	0.02
OP2	1.28 ± 0.19	6.07 ± 0.68	3.67 ± 0.44	0.07	0.01	0.04
OP3	1.27 ± 0.20	8.70 ± 0.52	1.41 ± 0.22	0.09	0.03	0.06
OP4	1.30 ± 0.09	8.24 ± 0.32	3.94 ± 0.44	0.11	0.03	0.08

5.3.10.2. Soil samples

The described voltammetric procedure was further applied for PGMs determination in roadside soil samples to evaluate its effectiveness using the GC/Bi-AgFE sensor. A 1 mL of extracted soil sample solution was added to 9 mL of 0.01 M acetate buffer (pH = 4.7) solution, containing 1×10^{-5} M DMG and 0.5 *n*g/L PGMs and the determination was done by DPAdSV analysis. Table 12 shows the results for the comparison between DPAdSV and ICP-MS analysis, and according to the results in Table 12, good recoveries were obtained for all three fractions of the soil samples analysed. In the analysis of Rh(III) in the organic-bound fraction, good results were obtained while weak results were obtained for Pd(II) in the carbonate-bound fraction. The obtained results in this study indicate that the adsorptive differential pulse stripping voltammetric method showed good recovery and accuracy, using the developed GC/Bi-AgFE nanosensor.

Table 12. Results obtained for the determination of PGMs concentrations using a GC/Bi-AgFE nanosensor and ICP-MS analysis on digested and extracted soil samples collected from roads near Stellenbosch, Western Cape Province.

	DPAdSV			ICP-MS		
	Carbonate-bound	Organic-bound	Fe-Mn bound	Carbonate-bound	Organic-bound	Fe-Mn bound
Sample	Pd(II) (ng/L)	Rh(III) (ng/L)	Pt(II) (ng/L)	Pd (μg/L)	Rh (μg/L)	Pt (μg/L)
BOT1	0.94 ± 0.02	3.89 ± 0.22	3.96 ± 0.29	0.03	0.005	0.004
BOT2	1.24 ± 0.10	3.65 ± 0.48	3.93 ± 0.36	0.06	0.01	0.02
BOT3	1.17 ± 0.42	3.78 ± 0.16	3.57 ± 0.04	0.34	0.02	0.05
BOT4	2.5 ± 0.25	4.31 ± 0.22	3.06 ± 0.72	0.08	0.04	0.07
OP1	1.75 ± 0.55	7.10 ± 0.99	2.80 ± 0.61	0.02	0.002	0.01
OP2	1.35 ± 0.22	5.88 ± 0.51	4.09 ± 0.30	0.03	0.01	0.03
OP3	1.61 ± 0.66	7.02 ± 0.63	4.15 ± 0.19	0.04	0.02	0.04
OP4	1.48 ± 0.19	7.04 ± 0.18	3.56 ± 0.42	0.06	0.02	0.06

5.4. Summary

The present study demonstrated that DPAdSV analysis is an excellent method for the determination of PGMs in environmental samples. In conclusion, the above method combined with a bismuth-silver bimetallic nanofilm electrode offers a more sensitive and practical approach for the determination of trace amounts of Pt(II), Pd(II) and Rh(III) in environmental samples. The developed procedure presented in this study includes advantages of simplicity, high sensitivity, high selectivity, speed and low cost. The novelty of this method lies in the fact that this type of nanosensor has not been applied for the determination of PGMs in environmental samples before. Furthermore, the LODs obtained in this study are in the ng/L concentration range, making this method a more sensitive and attractive analytical approach. The demonstrated capability of the GC/Bi-AgFE nanosensor to determine all three PGM-dimethylglyoxime complexes in both fresh water and sediment samples, further demonstrates the advantages of the approach developed in this study. The ability to detect PGMs in environmental samples makes this bismuth-silver bimetallic nanosensor an

alternative replacement for bismuth films, toxic hanging mercury electrode and carbon paste electrodes.

Chapter 6

PGMs analysis using screen-printed carbon electrodes

6.1. Introduction

Nowadays, the pollution of surface waters with chemical contaminants is one of the most crucial environmental problems. These chemical contaminants enter rivers and streams resulting in tremendous amount of destruction to the aquatic ecosystem (Sonune and Ghate, 2004). Heavy and platinum group metal (PGM) contaminations at trace levels in water resources presents a major current environmental threat, so the detection and monitoring of these metal contaminants results in an ever-increasing demand (Liu *et al*., 2008; Hildebrandt *et al*., 2008). Spectroscopy techniques were used for the simultaneous analysis of metal ions in water and, sediment biota samples. In electroanalysis much attention has been dedicated to the development of mercury-free sensors the last decade (Hwang *et al*., 2008; Sonthalia *et al*., 2004).

The work done by Silwana *et al*. (2014) describes the development of a differential pulse adsorptive stripping voltammetric (DPAdSV) procedure for the determination of palladium, platinum and rhodium in environmental samples. In this procedure a screen-printed carbon electrode modified with a bismuth film, SPCE/BiF was constructed. The optimisation of several stripping voltammetric parameters such as DMG concentration, composition of supporting electrolyte, pH, deposition potential and deposition time were perform. In this study, the results obtained for investigation shown low detection limits of 0.008 *u*g/L, 0.006 *u*g/L and 0.005 *u*g/L for Pd(II), Pt(II) and Rh(III), respectively.

The main aim of this chapter was to investigate the construction and application of chemical sensors that utilise nanomaterials (e.g. silver, bismuth, etc.) for platinum group metals (PGMs) determination. The possibility of developing a stripping voltammetric procedure for PGMs in aqueous solutions using a disposable screen-printed carbon electrode (SPCE) was explored. The electrochemical behaviour of PGMs in solution was investigated

by voltammetry and the optimum instrumental conditions were defined by DPAdSV measurements.

6.2. Experimental

6.2.1. Reagents

Sodium acetate (NaOAc), ammonia (NH_3) (25%), ammonium chloride (NH_4Cl), hydrochloric acid and nitric acid were supplied by Merck (South Africa). All precious and heavy metal standards (1000 mg/L AAS), dimethylglyoxime (DMG) were perchased from Sigma-Aldrich (South Africa). Glacial acetic acid (95%), ethanol (95%), hexamethylene tetramine (HMTA), dichloromethane, hydrazine sulphate, formaldehyde solution were supplied by Kimix (South Africa). Poly(vinyl) alcohol (PVA) was also obtained from Sigma-Aldrich (South Africa). Next, 0.5 to 20 μg/L solutions of platinum group elements were prepared by diluting the corresponding standard stock solutions. A 0.01 M ammonia buffer solution (pH = 9.0) was prepared by mixing ammonium chloride with concentration ammonia and served as the supporting electrolyte. A 0.2 M sodium acetate buffer (pH = 4.7) was prepared by mixing sodium acetate with acetic acid and deionised water. The 0.01 M DMG solution was prepared in 95% ethanol and served as the chelating agent. All solutions were prepared by Milli-Q (Millipore 18 M Ohm cm) water.

6.2.2. Instrumentation

Differential pulse adsorptive stripping voltammetric (DPAdSV) measurements were performed using PalmSens® portable potentiostat/galvanostat, with the PS Trace program and accessories (PalmSens® Instruments BV, 3992 BZ Houten, The Netherlands). The portable potentiostat was connected to a microcomputer controlled by PS 2.1 software for data acquisition and experimental control. All the DPAdSV measurements were performed in a conventional electrochemical cell of 20.0 mL, employing the screen-printed carbon electrode modified with bimuth-silver nanoparticles (SCPE/Bi-Ag) with 4 mm diameter

provided by Dropsens (Oviedo, Spain) as working electrodes. An Agilent 7500 series inductive coupled plasma mass spectroscopy (ICP-MS) was used for the trace PGMs determination roadside dust and soil samples. All experiments were performed at ambient temperatures (Somerset *et al*., 2011; Silwana *et al*., 2013; Silwana *et al*., 2014a, Silwana *et al*., 2014b).

6.2.3. Preparation of the bismuth-silver bimetallic film

A 2.5 mg of Bi-Ag bimetallic NPs were dispersed through ultrasonic vibration in 50 mL solution of deionised water to form a suspension. A defined quantity of the suspension was applied to a clean surface of screen-printed carbon electrode (SPCE) and dried at room temperature to get a thin film on the SPCE surface (Noroozifar *et al*., 2011; Cui and Zhang, 2012; Prakash *et al*., 2012). After each voltammetric cycle the cleaning of the Bi-Ag bimetallic nanofilm was performed by holding the potential of the electrode at 1.0 V. Traces of the remaining DMG complexes on the electrode surface were reduced and quickly desorbed at this potential. A short cleaning period of 10 s was required to refresh the electrode surface completely (Morfobos *et al*., 2004).

6.2.4. Procedure for the determination of PGMs

A 10 mL of 0.2 M acetate buffer (pH = 4.7) solution containing 1×10^{-5} M DMG was used as electrolyte in the cyclic and stripping voltammetric procedures. The SPCE/Bi-Ag nanosensor was immersed into the solution and an accumulation potential of -0.7 V (vs. Ag/AgCl) for Pd(II) and -0.6 V (vs. Ag/AgCl) for Pt(II), and -0.7 V (vs. Ag/AgCl) for Rh(II) were applied while the solution was stirred. A 30 s quiet time was used and the voltammogram was scanned from +0.8 to -1.4 V (vs. Ag/AgCl) at a scan rate of 60 mV/s for cyclic voltammetry measurements, while scanning was performed from -0.8 to -0.1 V (vs. Ag/AgCl) for adsorptive differential pulse stripping voltammetry measurements.

The PGMs were introduced into the solution after the background voltammogram was recorded. All the experiments were performed in the presence of oxygen and at room temperature (Silwana *et al*., 2014; Van der Horst *et al*., 2012). According to Zhang *et al*.

(2010) the analysis of heavy metal ions using ASV method consist of three steps such as accumulation, electrochemical reduction and stripping out. In this method both the sensitivity and the selectivity of the analysis can be enhance by the combination of accumulation and reduction prior to the stripping detection process. The efficiency of accumulation and electrochemical reduction steps plays a great role in the entire analysis.

6.3. Results and discussion

6.3.1. Electrochemical behaviours of Bi-Ag bimetallic modified electrode

The preliminary investigation of the electroactivity of the bismuth-silver bimetallic nanofilm electrode (Bi-AgFE) were done by using cyclic voltammetry (CV) and differential pulse adsorptive stripping voltammetry (DPAdSV) measurements. To obtain optimal conditions it's very important to study the influence of supporting electrolyte, dimethylglyoxime concentration, deposition potential, deposition time and stability test in DPAdSV mode. In this study different electrolytes such as 0.1 M hydrochloric acid, 0.2 M sodium acetate (pH = 4.7), 0.1 M phosphate (pH = 7.0) and 0.1 M phosphate (pH = 9.0) buffers were tested as supporting electrolytes using the bismuth-silver bimetallic nanofilm electrode (Bi-AgFE). Figure 65 (A) illustrates the cyclic voltammograms (CVs) of the resulting electrode obtained in the four different buffer solutions. The results in Figure 65 (A) showed that the redox response peak height was improved in the presence of 0.2 M sodium acetate buffer solution. Thus, for voltammetric measurements a solution of acetic acid and sodium acetate was used as the optimal buffer solutions. Figure 65 (B) showed anodic peaks at -0.2 V and -0.6 V (vs. Ag/AgCl) and cathodic peaks at +0.1 V and +0.4 V (vs. Ag/AgCl).
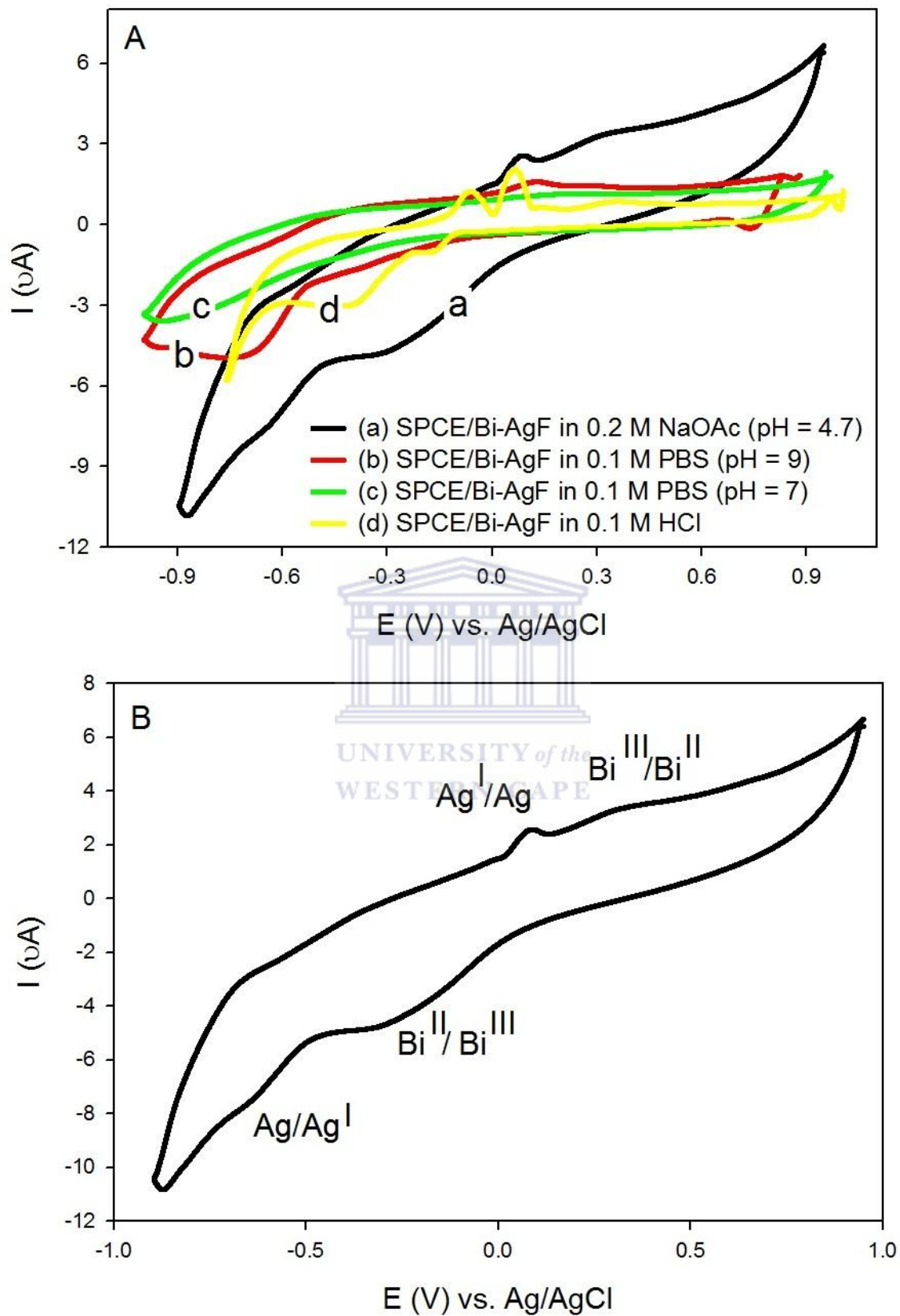
Figure 65. Cyclic voltammetry (CV) results for the combined evaluation of the SPCE/Bi-AgF sensor in various buffer solutions of (a) 0.01 M phosphate (pH = 7), (b) 0.01 M phosphate (pH = 9), (c) 0.2 M NaOAc (pH = 4.7), (d) 0.1 M HCl solution. The potential was scan between -0.9 and +0.9 V (vs. Ag/AgCl) at a scan rate of 50 mV/s.

6.3.2. Effect of reagent concentration

In differential pulse adsorptive stripping voltammetric (DPAdSV) analysis the ligand concentration in solution has a profound effect on the voltammetric peak height. Palladium has a definite adsorption voltammetric peak in acidic medium if dimethylglyoxime (DMG) is used as complexing agent. Dimethylglyoxime is suggested by Georgieva and Pihlar (1997) as the complexing agent if sodium acetate is used as supporting electrolyte. In this investigation the effect of DMG concentrations on the PGMs (Pd, Pt, Rh) peak currents was examined in the range from 5×10^{-6} to 5×10^{-5} M. Figure 66 illustrates the effect of DMG concentration on Pd(II) peak currents in 0.2 M sodium acetate buffer (pH = 4.7) solution. By decreasing the DMG concentration from 5×10^{-5} M to 1×10^{-5} M the voltammetric peak height of Pd(II) increases and shows that the height is strongly dependent upon DMG concentration. For concentrations lower than of 1×10^{-5} M a significant decrease in peak current was observed. From the results observed in Figure 66 the concentration of 1×10^{-5} M DMG were used as the optimum concentration for the determination of Pd(II) in model solutions (Locatelli *et al*., 2005).
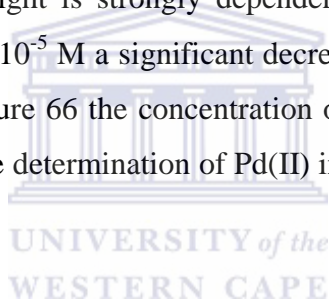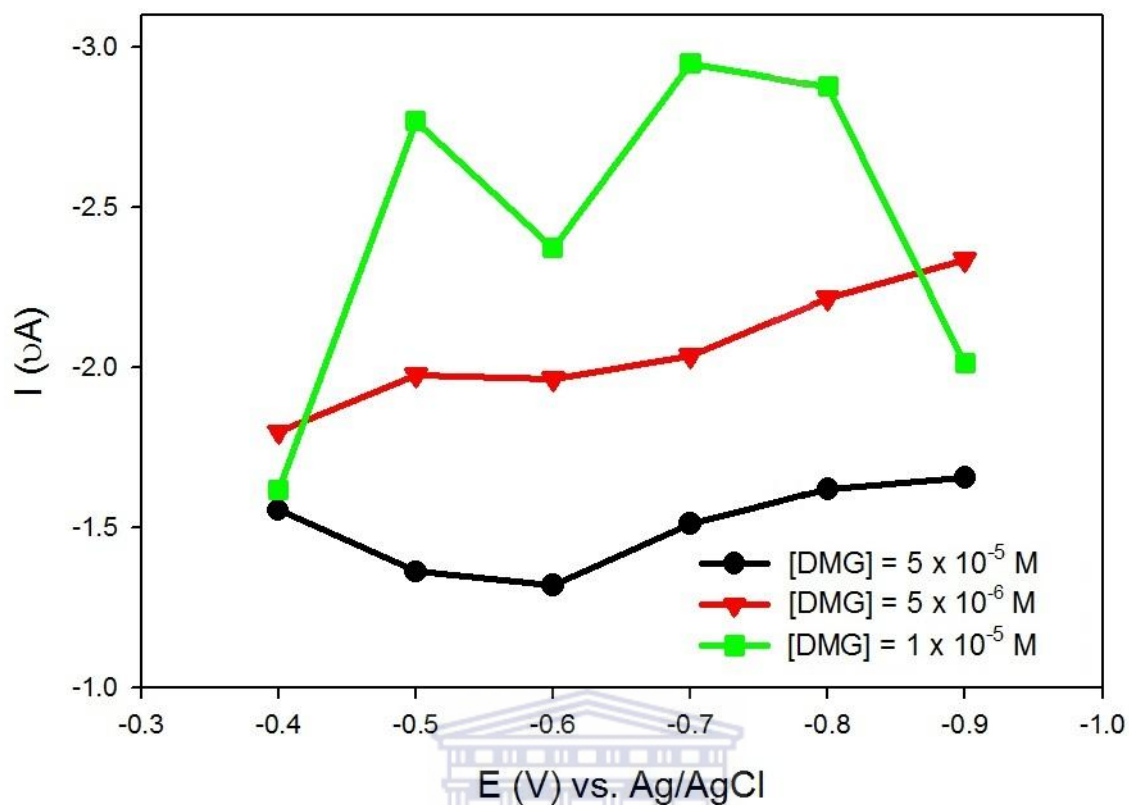
Figure 66. **Effect of varying dimethylglyoxime (DMG) concentrations on the peak current results for 1 ppt Pd(II), in the presence of 0.2 M acetate buffer, (pH = 4.7) solution.**

Figure 67 illustrates the effect of dimethylglyoxime (DMG) concentration on peak currents for Pt(II) in 0.2 M sodium acetate buffer (pH = 4.7) solution. By decreasing the DMG concentration from 5×10^{-5} M to 1×10^{-5} M the voltammetric peak height of Pt(II) increases and shows that the height is strongly dependent upon DMG concentration. At DMG concentration of 1×10^{-6} M, a significant increase in peak current was observed for more negative potentials. The results obtained in Figure 67 revealed that the DMG concentration was optimised at 1×10^{-5} M for Pt(II) analytical measurements.
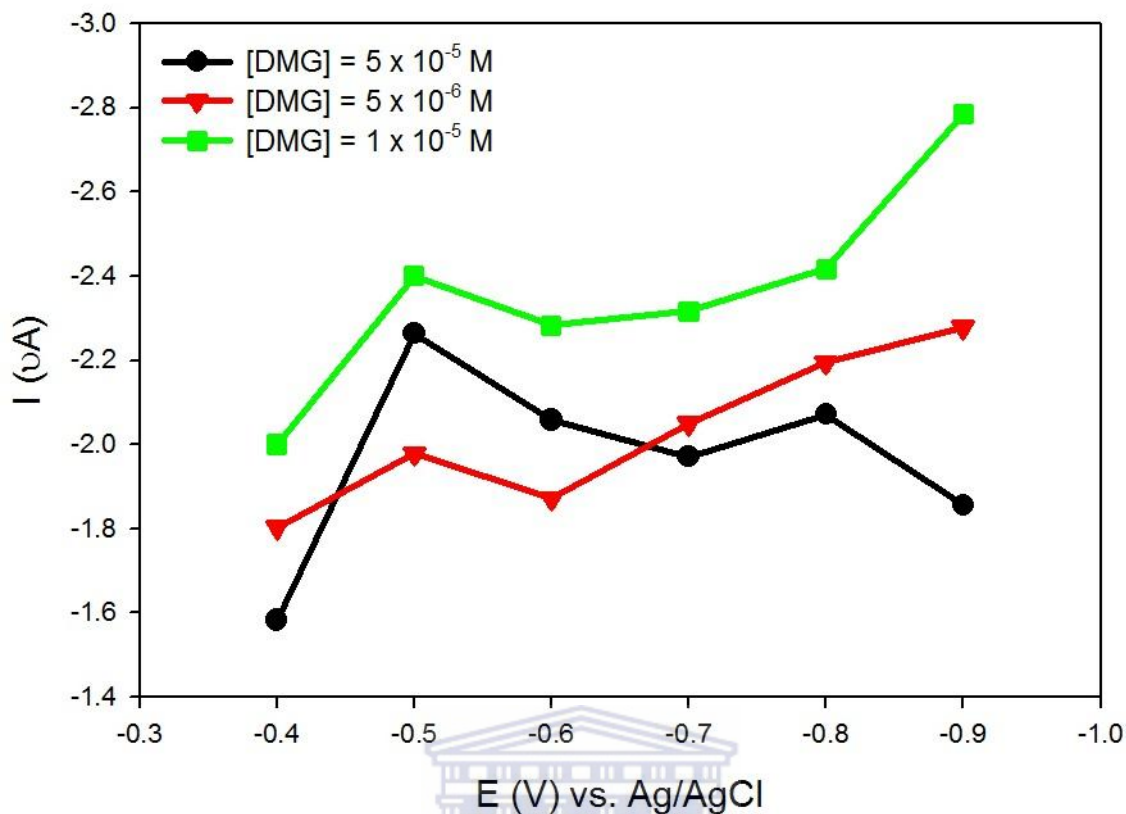
Figure 67. **Effect of varying dimethylglyoxime (DMG) concentrations on the peak current results for 1 ppt Pt(II) in the presence of 0.2 M acetate buffer, (pH = 4.7) solution.**

In Figure 68 the effect of dimethylglyoxime (DMG) concentration on peak current for Rh(III) in 0.2 M sodium acetate buffer (pH = 4.7) solution are also illustrated by plotting the peak current vs. peak potentials. The peak current of 1×10^{-5} M DMG increases at more negative potentials for Rh(III). The same phenomena happened when decreasing the DMG concentration from 5×10^{-5} M to 1×10^{-5} M, the voltammetric peak current of Rh(III) increases and shows that the height is strongly dependent upon DMG concentration and peak potential. At a DMG concentration 1×10^{-6} M a significant increase in peak current was observed for more negative potentials. The results obtained in Figure 68 revealed that the DMG concentration was optimised at 1×10^{-5} M for Rh(III) analytical measurements.
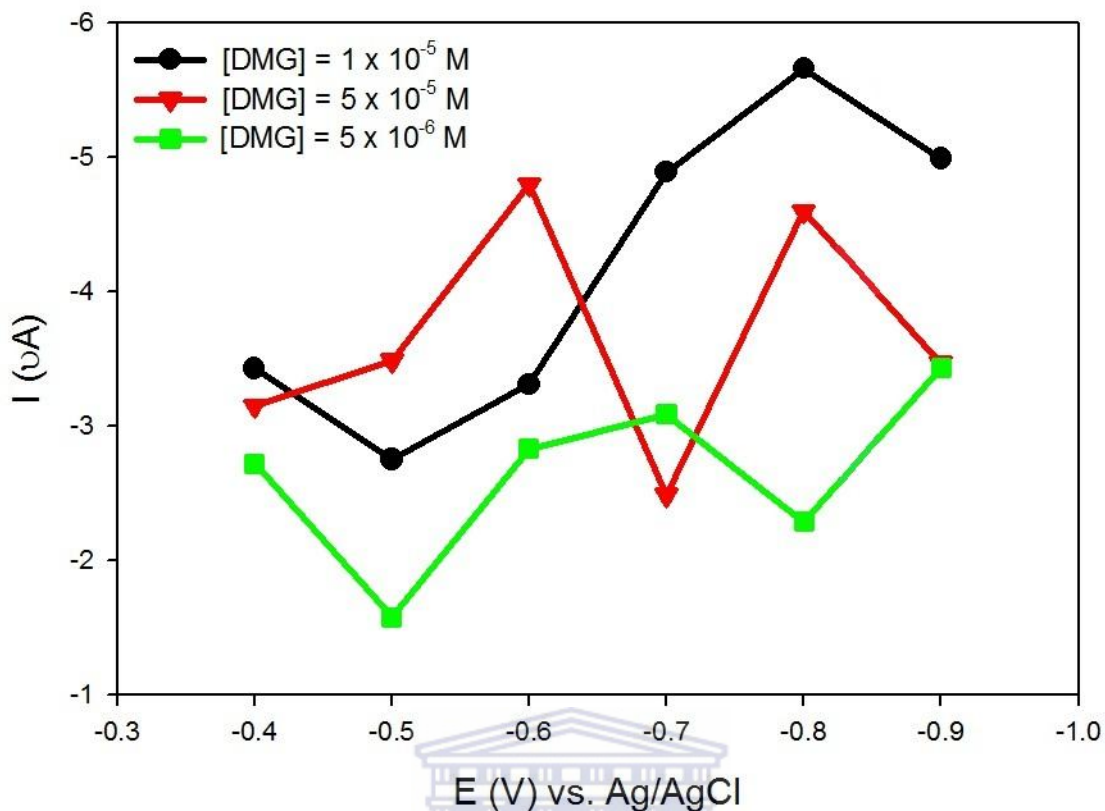
Figure 68. **Effect of varying dimethylglyoxime (DMG) concentrations on the peak current results for 1 ppt Rh(III) in the presence of 0.2 M acetate buffer, (pH = 4.7) solution.**

6.3.3. Stability test of the bismuth-silver bimetallic nanosensor

The reproducibility of the fabricated bismuth-silver bimetallic nanosensor was investigated for the peak current over a defined period of time. Using the optimised conditions for the bimetallic sensor the sensor was utilised for the determination of 1 ppt concentration of the PGMs evaluated. Figure 69 illustrates the results for the stability test of 1 ppt Pd(II), Pt(II) and Rh(III) with 1×10^{-5} M DMG in 0.2 M acetate buffer solutions. The reduction peak current results were plotted versus time and the results obtained showed that the bimetallic sensor is stable for 14 hours and should be used within the 7 to 24 h after construction.
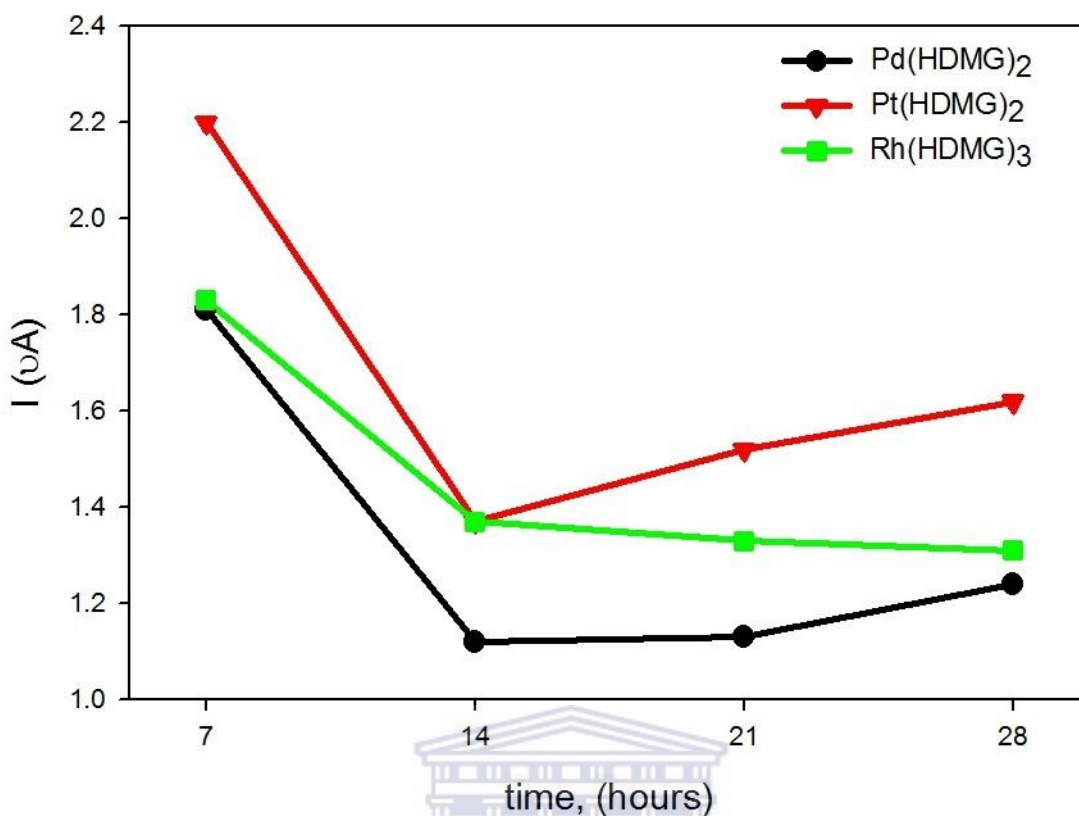
Figure 69. The stability test results for the bismuth-silver bimetallic nanosensor. A 0.2 M acetate buffer (pH = 4.7) solution containing 1 ppt PGMs with 1×10^{-5} M DMG, were employed in the stability optimisation studies.

6.3.6. Deposition potential studies

In electroanalytical chemistry differential pulse voltammetry (DPV) is used as an effective and common technique when the content of analyte is very low due to its sensitivity (Ntsendwana *et al.*, 2012). The influence of deposition potential and time are always important factors on the sensitivity and detection limit in DPV methods. To enhance the electroanalytical performance of the Bi-Ag bimetallic sensor, the deposition potential was optimized. Figure 70 illustrates the dependence of deposition potential on the stripping peak current for 1 ppt Pd(II) at the bismuth-silver nanosensor. Optimum deposition potential for Pd(II) determination in 0.2 M acetate buffer (pH = 4.7) solution is in the range from -0.7 to -0.8 V (vs. Ag/AgCl). For deposition potentials more negative than -0.8 V and more positive than -0.7 V (vs. Ag/AgCl), the Pd(II) stripping peak current decreased significantly. The deposition potential for Pd(II) in this investigation was optimised at -0.7 V (vs. Ag/AgCl) and applied throughout the study.

166
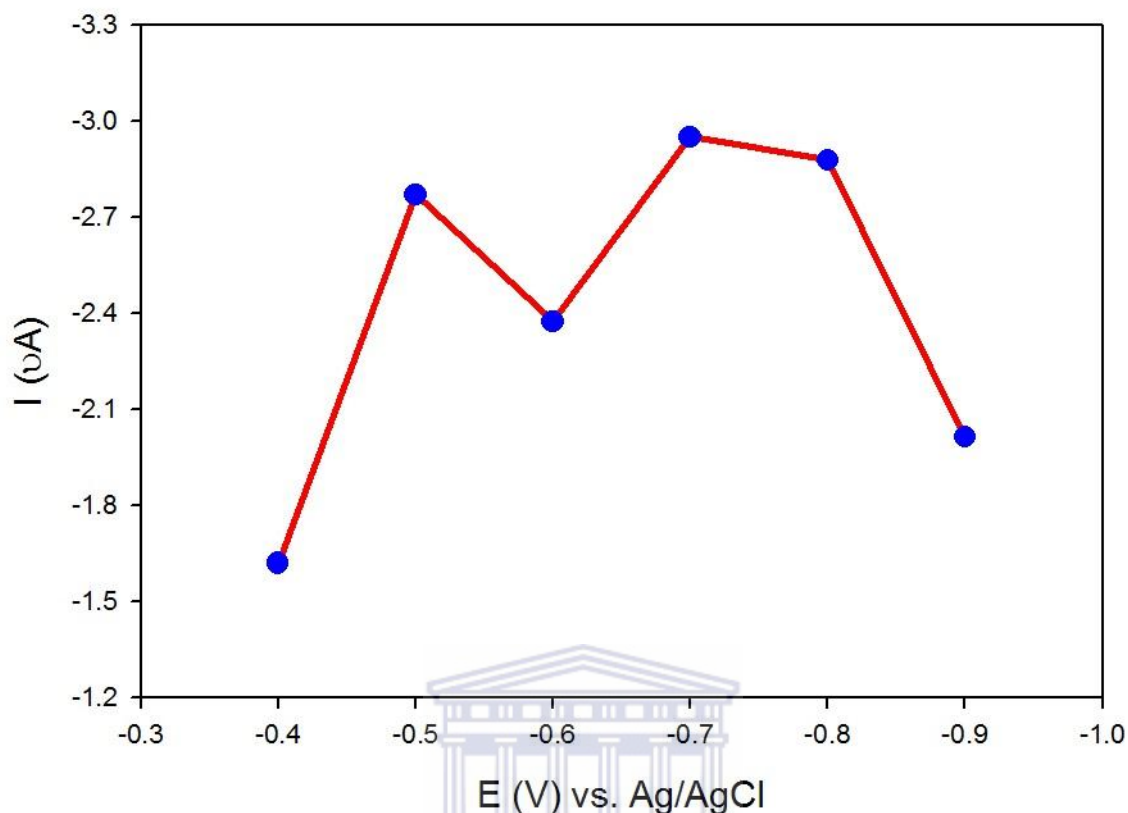
Figure 70. **Effect of deposition potential upon adsorptive stripping redox responses at a bismuth-silver bimetallic nanosensor. The electrolyte consisted of 0.2 M acetate buffer (pH = 4.7) solution containing 1 ppt Pd(II) with 1×10^{-5} M DMG; deposition time was 30 s.**

The dependence of deposition potential on the stripping peak current for 1 ppt Pt(II) at the bismuth-silver nanosensor are illustrated in Figure 71. In this investigation the optimum deposition potential for Pt(II) was at -0.9 V (vs. Ag/AgCl) in 0.2 M acetate buffer (pH = 4.7) solution. At deposition potentials more positive than -0.9 V (vs. Ag/AgCl) the stripping peak current decreased significantly. The deposition potential for Pt(II) in this investigation was optimised at -0.9 V (vs. Ag/AgCl) and applied throughout the study.
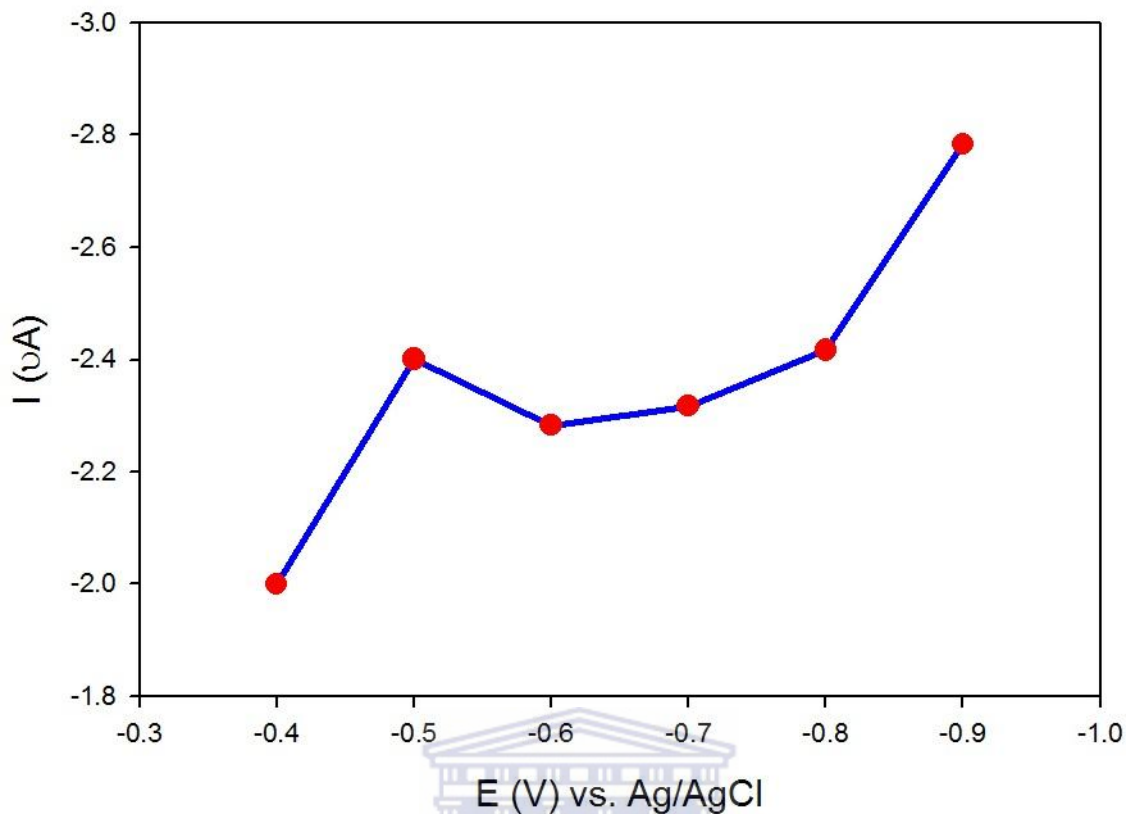
Figure 71. **Effect of deposition potential upon adsorptive stripping redox responses at a bismuth-silver bimetallic nanosensor. The electrolyte consisted of 0.2 M acetate buffer (pH = 4.7) solution containing 1 ppt Pt(II) with 1×10^{-5} M DMG; deposition time was 30 s.**

The effect of deposition potential on the stripping peaks current of 1 ppt Rh(III) complexes with 1×10^{-5} M DMG was investigated over a potential range of -0.4 to -0.9 V (vs. Ag/AgCl). Figure 72 illustrates the plot of stripping peaks current of Rh(III) as a function of deposition potential. In the results obtained the stripping peak currents were independent of deposition potential at potentials more positive than-0.8 and at -0.9 V (vs. Ag/AgCl). The deposition potential for Pt(II) in this investigation was optimised at -0.8 V (vs. Ag/AgCl) and applied throughout the study.
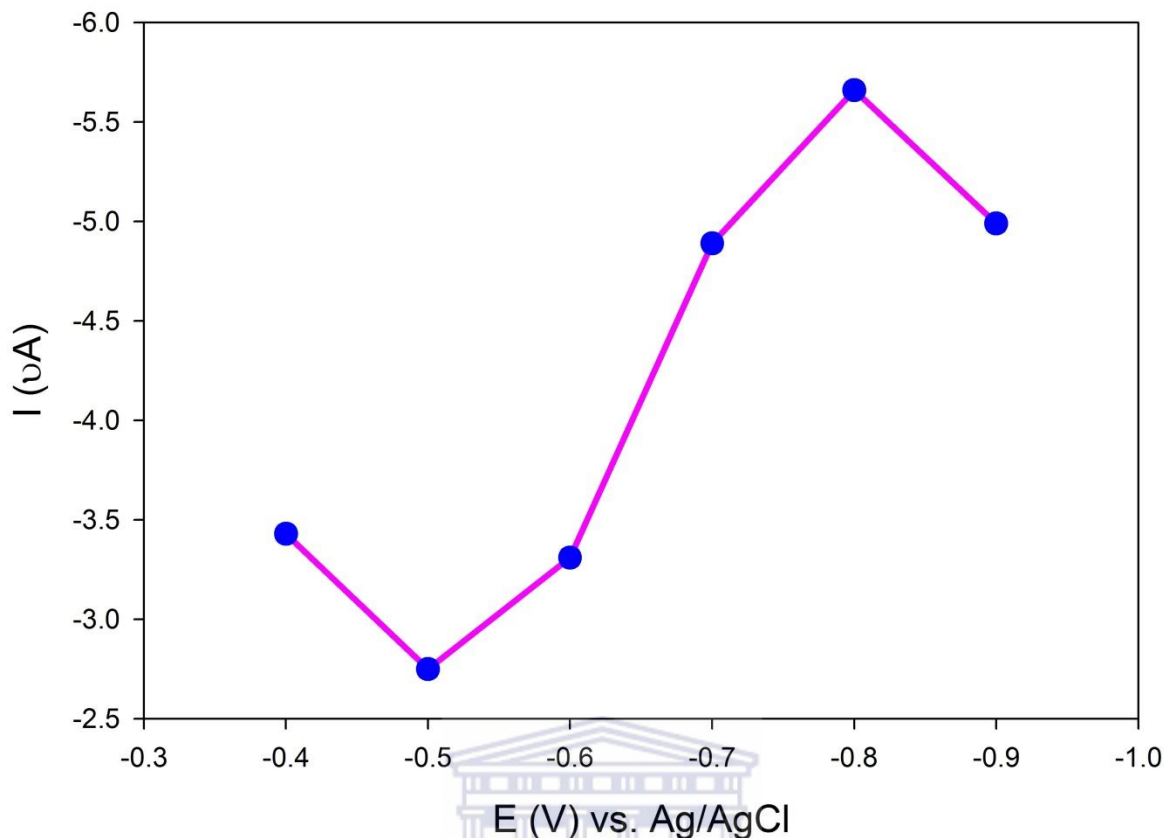
Figure 72. **Effect of deposition potential upon adsorptive stripping redox responses at a bismuth-silver bimetallic nanosensor. The electrolyte consisted of 0.2 M acetate buffer (pH = 4.7) solution containing 1 ppt Rh(III) with 1×10^{-5} M DMG; deposition time was 30 s.**

6.3.7. Deposition time studies

The dependence of deposition time on the stripping peak current of Pd(II), Pt(II) and Rh(III) was investigated using the bismuth-silver bimetallic nanosensor. In Adsorptive stripping voltammetry (ASV) complexing agent in the electrolyte solution, after reaction, form complex ions in the solution and the complex is accumulated onto the sensor surface in the amount proportional to the deposition time (Huszal *et al*., 2005). The dependence of deposition time on the stripping peak current of Pd(II) are shown in Figure 73 and the peak current decrease almost linearly with longer deposition times. A deposition time at 30 s was chosen as the optimum deposition time in this investigation.
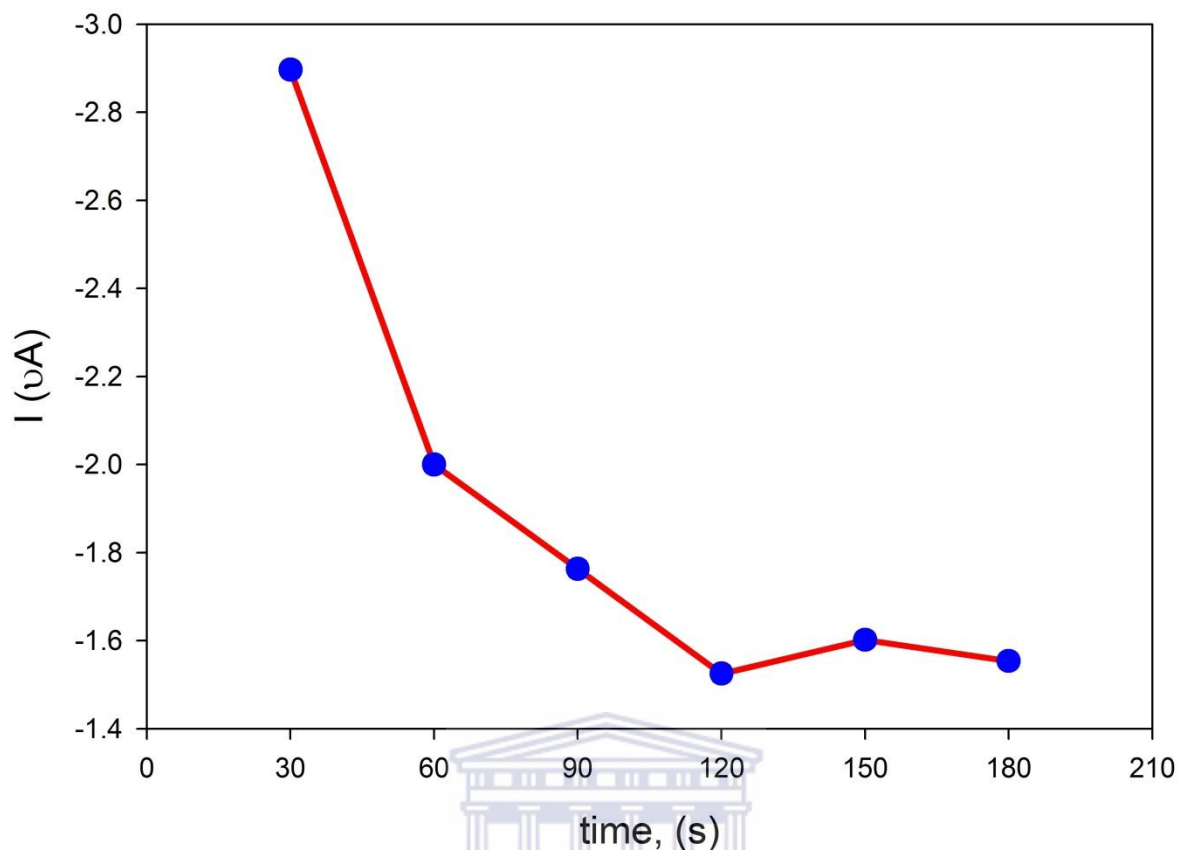
Figure 73. **Effect of deposition time upon adsorptive stripping redox responses at a bismuth-silver bimetallic nanosensor. The electrolyte consisted of 0.2 M acetate buffer (pH = 4.7) solution containing 1 ppt Pd(II) with 1×10^{-5} M DMG; deposition potential was -0.7 V.**

Figure 74 illustrates the dependence of stripping peak current with the deposition time for 1 ppt Pt(II) in 0.2 M sodium acetate buffer (pH = 4.7) solution. The stripping peak current increases with the increasing in the deposition time between 30 and 120 s above which it became nearly constant due to the surface saturation of the bismuth-silver bimetallic nanosensor. In this study for all subsequent Pt(II) measurements deposition time of 90 s was employed due to surface saturation of the bimetallic sensor.
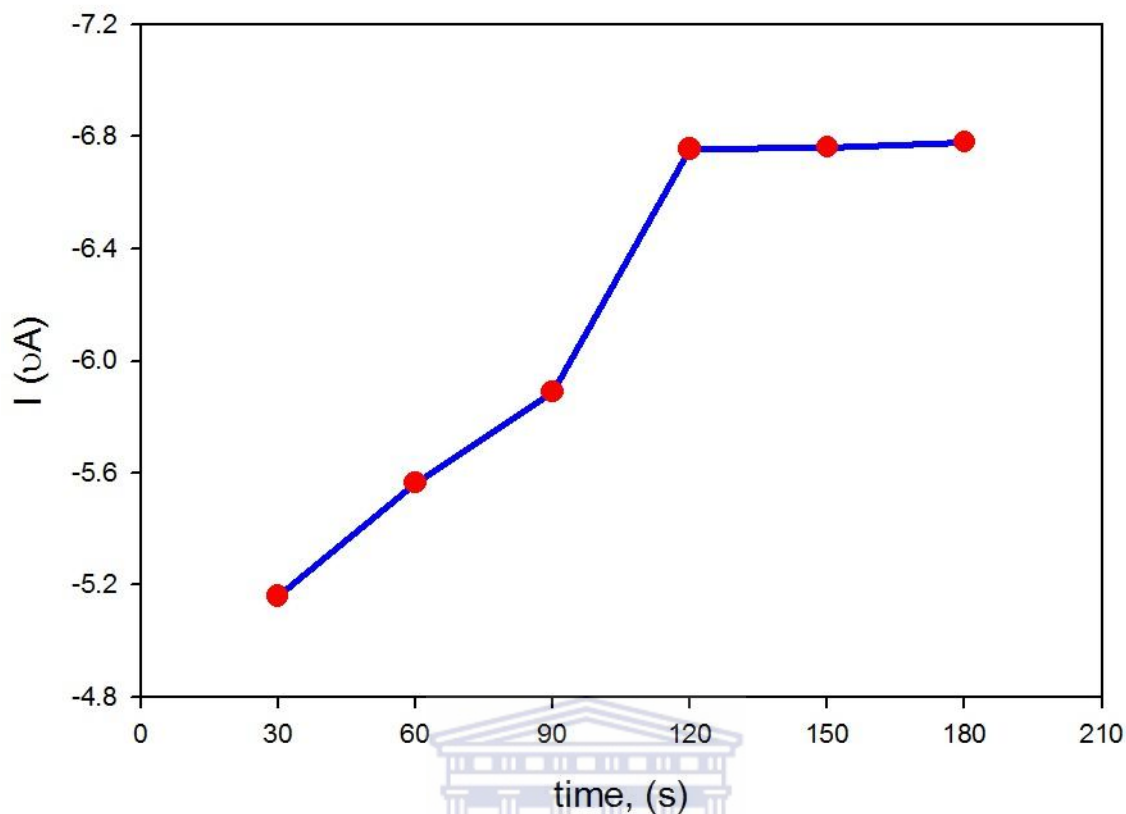
Figure 74. **Effect of deposition time upon adsorptive stripping redox responses at a bismuth-silver bimetallic nanosensor. The electrolyte consisted of 0.2 M acetate buffer (pH = 4.7) solution containing 1 ppt Pt(II) with 1×10^{-5} M DMG; deposition potential was -0.9 V.**

The dependence of deposition time on the stripping peak current for 1 ppt Rh(III) (in Figure 75) was also investigated. The peak current decreases with the increase in deposition time between 30 and 60 s. From 60 to 120 s there is a sharp increase in stripping peak current but decreasing again at 150 s. As expected for adsorption processes the dependence of the peak current on the deposition time is limited by saturation of the electrode. In the deposition times studied for Rh(III) 30 s, seemed the optimum time and was used throughout the investigation as it combines with good sensitivity and very short analysis time.

171
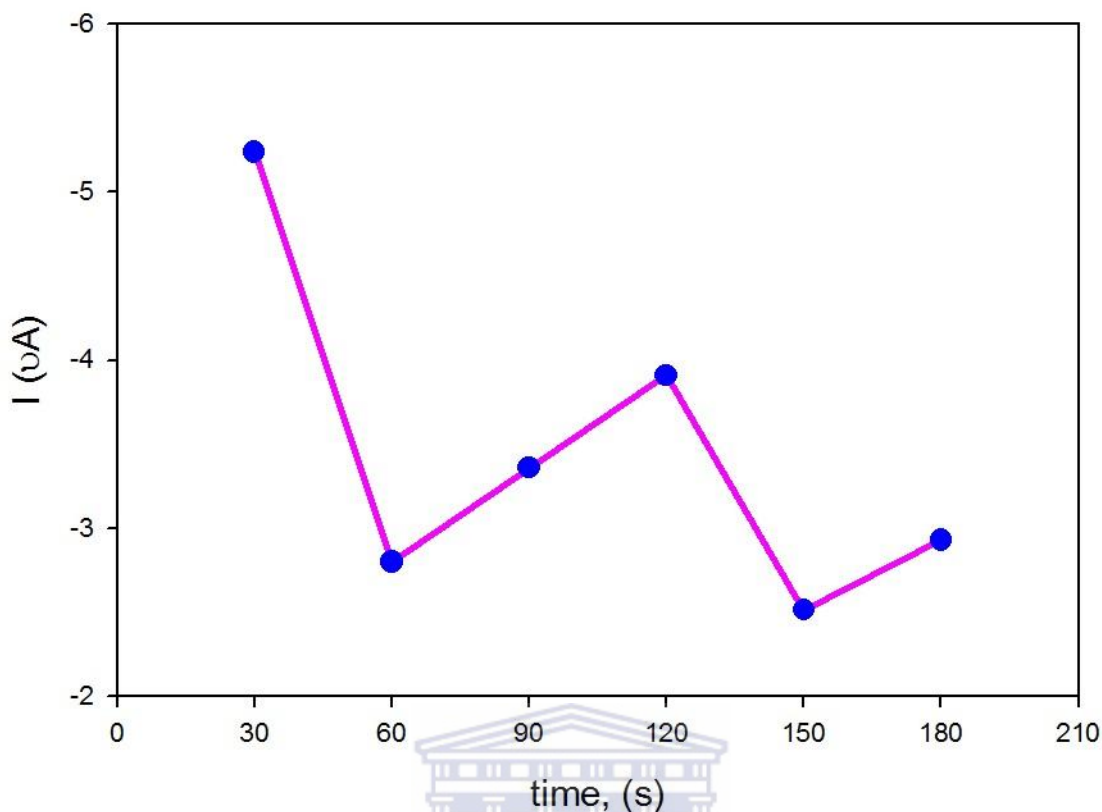
Figure 75.   **Effect of deposition time upon adsorptive stripping redox responses at a bismuth-silver bimetallic nanosensor. The electrolyte consisted of 0.2 M acetate buffer (pH = 4.7) solution containing 1 ppt Rh(III) with 1×10^{-5} M DMG; deposition potential was -0.8 V.**

6.3.8. Analytical features of the adsorptive stripping procedure

In differential pulse adsorptive stripping voltammetry (DPAdSV) nanoparticles play an important role for the determination of heavy metals at trace levels. According to the literature the determination of palladium by DPAdSV at the surface of the hanging mercury drop electrode (HMDE) was first described by Wang and Varughese (1987). Dimethylglyoxime was used as the complexing ligand in slightly acidic media (pH = 5.15) for the deposition of palladium-dimethylglyoxime complex (Pd-(HDMG)$_2$). In the present study the determination of Pd-(HDMG)$_2$ was done in 0.2 M acetate buffer (pH = 4.7) solution at the surface of a bismuth-silver bimetallic nanosensor. The DPAdSV current of the Pd-(HDMG)$_2$ complex at optimal conditions yielded well defined peaks, in the concentration range 0.4 to 1.0 ppt shown in Figure 76(a). The five concentrations used yielded a linear response and the equation of the linear calibration curve is $y = 0.773x + 0.6151$ with a correlation coefficient of 0.991, illustrated in Figure 76(b).

172
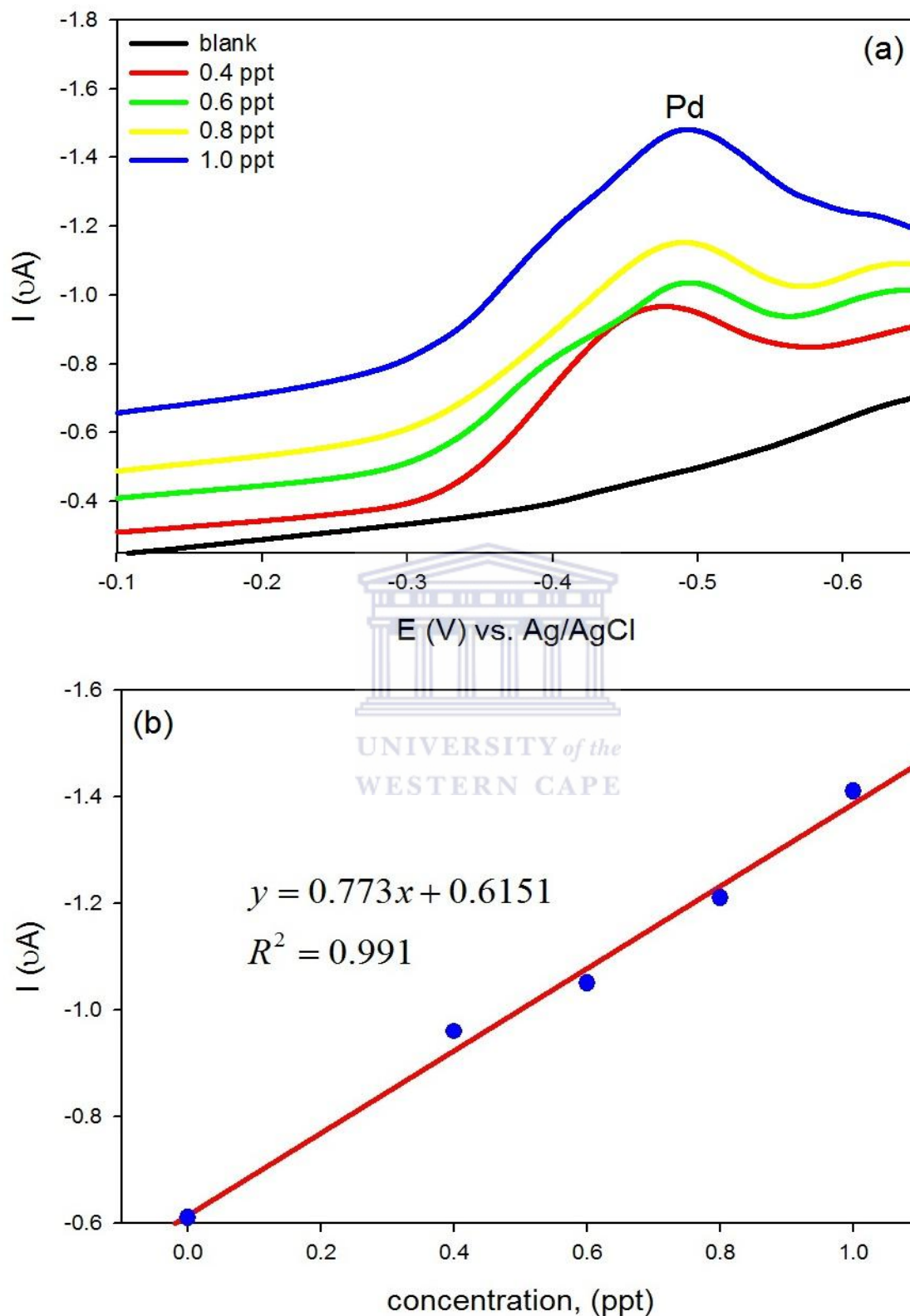
Figure 76. Differential pulse adsorptive stripping voltammetry results for increasing concentrations of Pd(II) at a bismuth-silver bimetallic nanosensor in (a). Corresponding calibration curve obtained for the Pd(II) analysis in (b). The electrolyte consisted of 0.2 M acetate buffer (pH = 4.7) solution containing 0.2 to 1.0 ppt Pd(II) with 1×10^{-5} M DMG; deposition potential was -0.7 V (vs. Ag/AgCl) and deposition time 30 s.

The differential pulse adsorptive stripping voltammetric (DPAdSV) current for the Pt-$(HDMG)_2$ complex were measured at optimal conditions using a bismuth-silver bimetallic nanosensor in Figure 77(a). In these measurements a series of Pt-$(HDMG)_2$ complex concentrations ranging from 0.2 to 0.8 ppt in 0.2 M acetate buffer (pH = 4.7) solution with 30 s deposition time were used. The peaks observed in the differential pulse voltammograms are well-defined and the five concentrations used yielded a linear response and the equation of the linear calibration curve is $y = 0.690x + 0.718$ with a correlation coefficient of 0.988, illustrated in Figure 77(b).
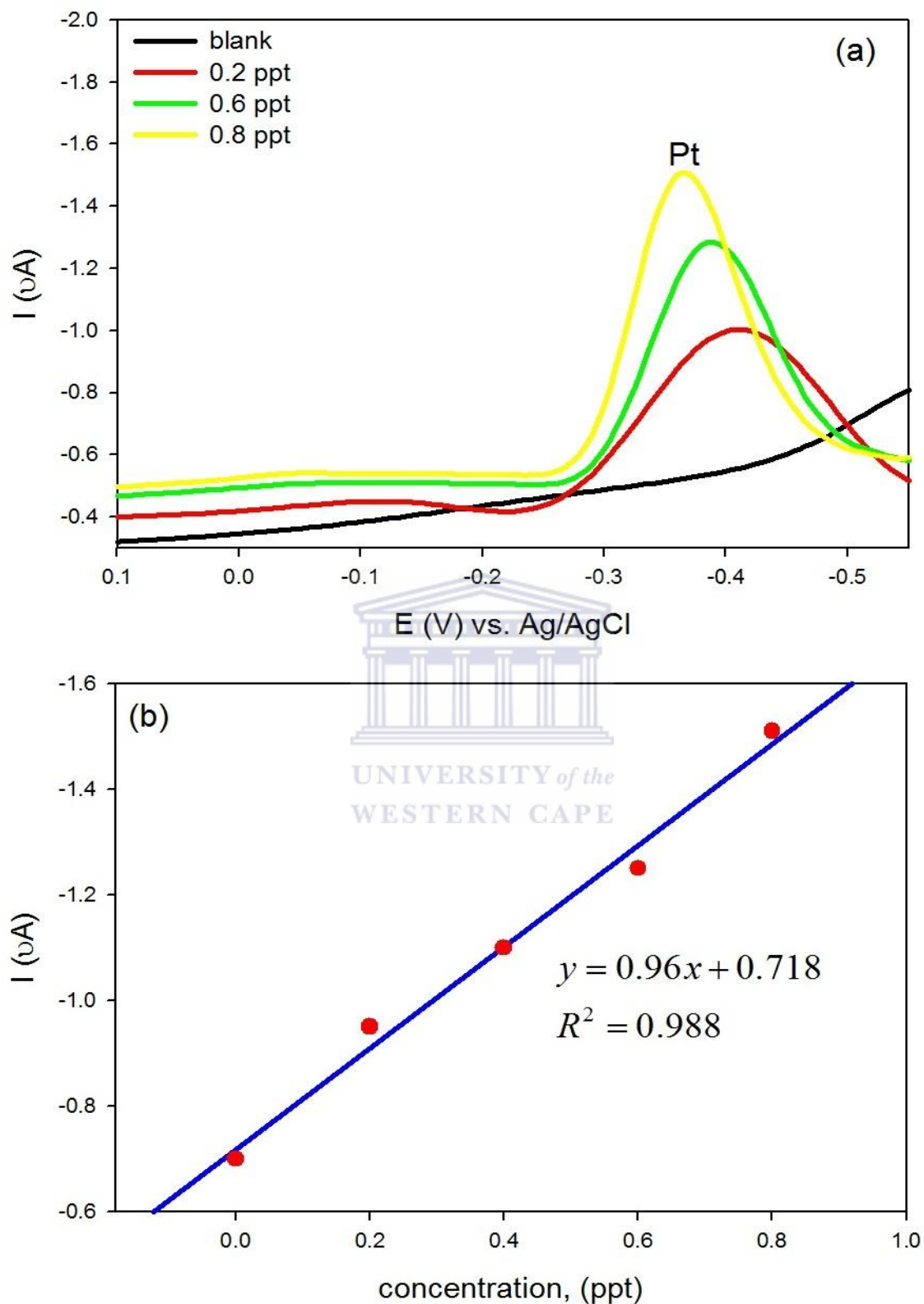
Figure 77. Differential pulse adsorptive stripping voltammetry results for increasing concentrations of Pt(II) at a bismuth-silver bimetallic nanosensor in (a). Corresponding calibration curve obtained for the Pt(II) analysis in (b). The electrolyte consisted of 0.2 M acetate buffer (pH = 4.7) solution containing 0.2 to 1 ppt Pt(II) with 1×10^{-5} M DMG; deposition potential was -0.9 V (vs. Ag/AgCl) and deposition time 120 s.

175

The determination of the Rh-(HDMG)$_3$ complex in 0.2 M acetate buffer (pH = 4.7) solution was performed by DPAdSV analysis under optimised working conditions and the voltammograms are shown in Figure 78(a). Well-defined stripping peaks were observed at the bismuth-silver bimetallic nanosensor in the concentration ranging from 0.2 to 0.8 ppt. The results indicated that dimethyglyoxime (DMG) can greatly promote the deposition of the Rh-(HDMG)$_3$ complex at the bismuth-silver bimetallic nanosensor and significantly increase the sensitivity of the determination of the Rh-(HDMG)$_3$ complex. In Figure 78(b) the results showed that the DPAdSV peak currents have a linear response for the five concentrations evaluated and the equation of the linear calibration curve is $y = 3.9527x + 0.5798$, with a correlation coefficient of 0.9703.
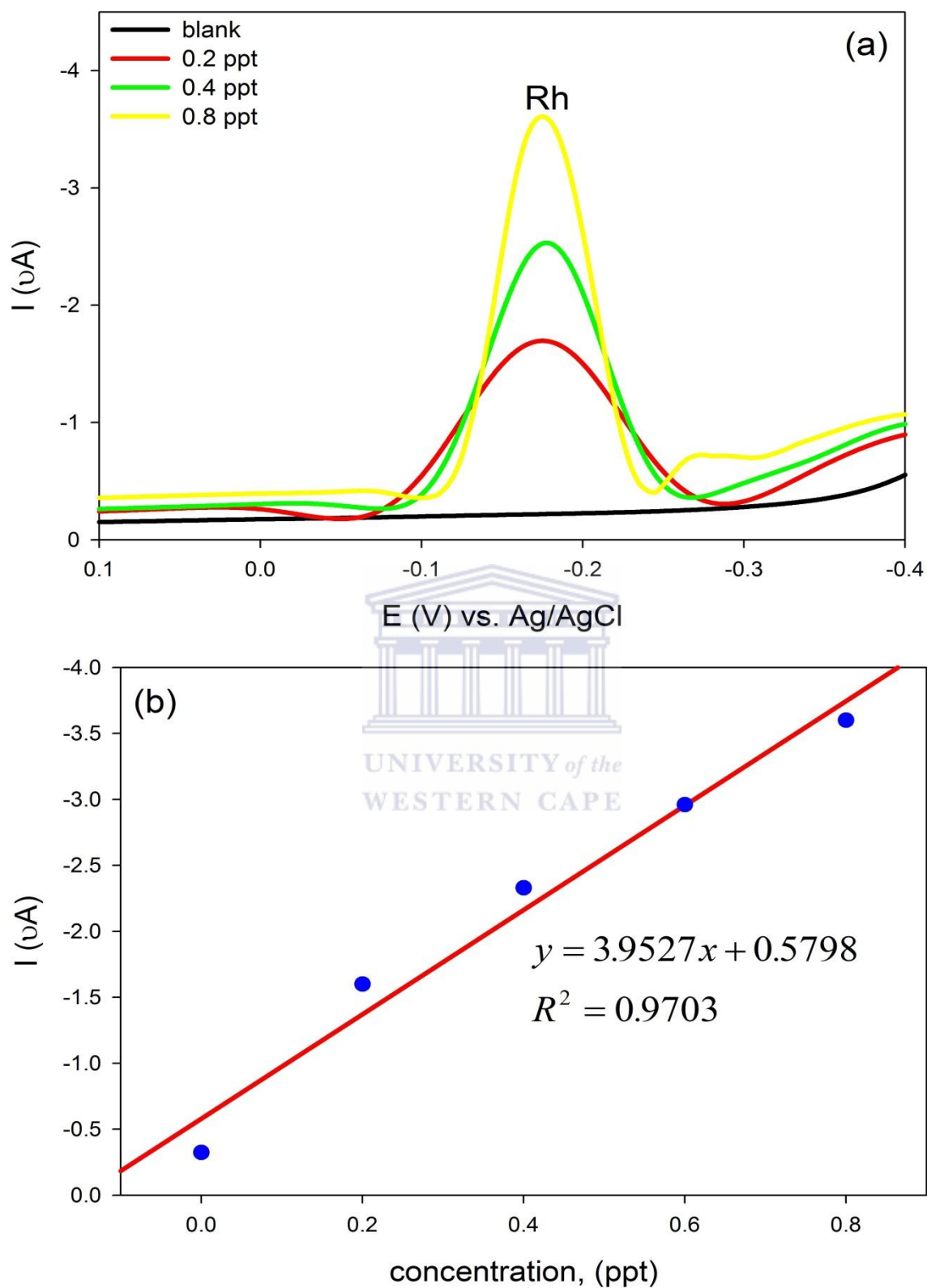
Figure 78. Differential pulse adsorptive stripping voltammetry results for increasing concentrations of Rh(III) at a bismuth-silver bimetallic nanosensor in (a). Corresponding calibration curve obtained for the Rh(III) analysis in (b). The electrolyte consisted of 0.2 M acetate buffer (pH = 4.7) solution containing 0.2 to 0.8 ppt Rh(III) with 1×10^{-5} M DMG; deposition potential was -0.7 V (vs. Ag/AgCl) and deposition time 30 s.

6.3.9. Interference studies

In differential pulse adsorptive stripping voltammetry (DPAdSV) several trace metals can interfere with the determination of platinum group metals (PGMs) absorbing competitively onto the bismuth-silver bimetallic film electrode (Bi-AgFE) surface or complexing competitively with DMG producing signals close to that of the different PGMs or completely suppress the peaks. In this study a number of metal ions that could potentially interfere with these PGMs were investigated such as Ni(II), Co(II), Fe(III), Na(I). The sulphates and phosphates were also investigated and 1 ppt of these interfering ions was added to the model solutions.

Figure 79 illustrates the behaviour of Pd(II), Pt(II) and Rh(III) at concentrations of 0.5 to 1.5 ppt in the presence of Ni(II) and Co(II) ions using the SPCE/Bi-AgF sensor. In Figure 79 (A) the ions of Ni(II) and Co(II) interferes minimally with Pd(II), but shows more interferences with Pt(II) and Rh(III) in Figure 79 (B) and (C) at the two higher concentrations investigated. It is observed in this investigation that DMG cannot be used as complexing agent in the presence of Ni(II) and Co(II) interfering ions.
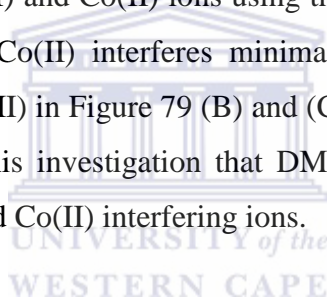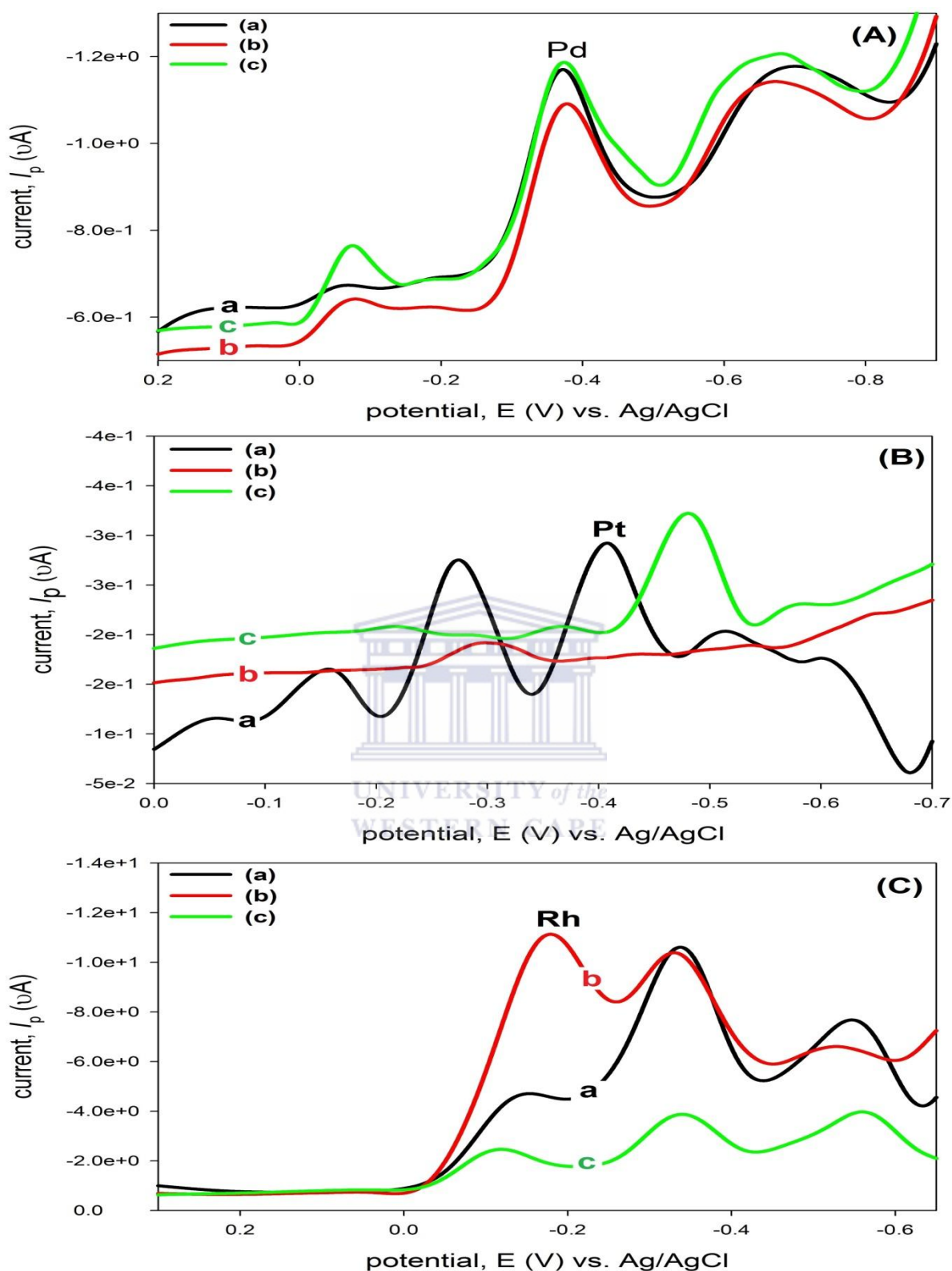
Figure 79. Effect of interfering ions on the peak current responses for Pd(II) in (A), Pt(II) in (B), and Rh(III) in (C) using the GCE/Bi-AgF sensor. The concentrations of Pd(II), Pt(II), and Rh(III) used were (0.5 ppt) in (a), 1 ppt in (b), and 1.5 ppt in (c), respectively. For Ni(II) and Co(II) the concentrations used were 1.0 ppt, with 0.2 M acetate buffer (pH = 4.7) solution containing 1×10^{-5} M DMG solution.

From the observed results illustrated in Figure 80 (A) it seems like Fe(III) and Na^+ interferes minimally with Pd(II) in all three solutions. Interferences of Pt(II) with the ions of Fe(III) and Na^+ were observed in Figure 80 (B) with minimum interferences of Rh(III) with the two interfering ions observed in Figure 80 (C).

The effect of SO_4^{2-} and PO_4^{3-} on the peak current of Pd(II), Pt(II) and Rh(III) were also studied and illustrated in Figure 81. From these observed results, the SO_4^{2-} and PO_4^{3-} ions interfered extensively with Pt(II) and Rh(III) but interfered minimally with Pd(II). This phenomenon shows that DMG cannot be used in the presence of these ions for the determination of Pt(II) and Rh(III).

This SPCE/Bi-AgF sensor shows favourable results for Pd(II) determination and it can be determined in the presence of these interfering ions with DMG as the chelating agent.

UNIVERSITY *of the*
WESTERN CAPE
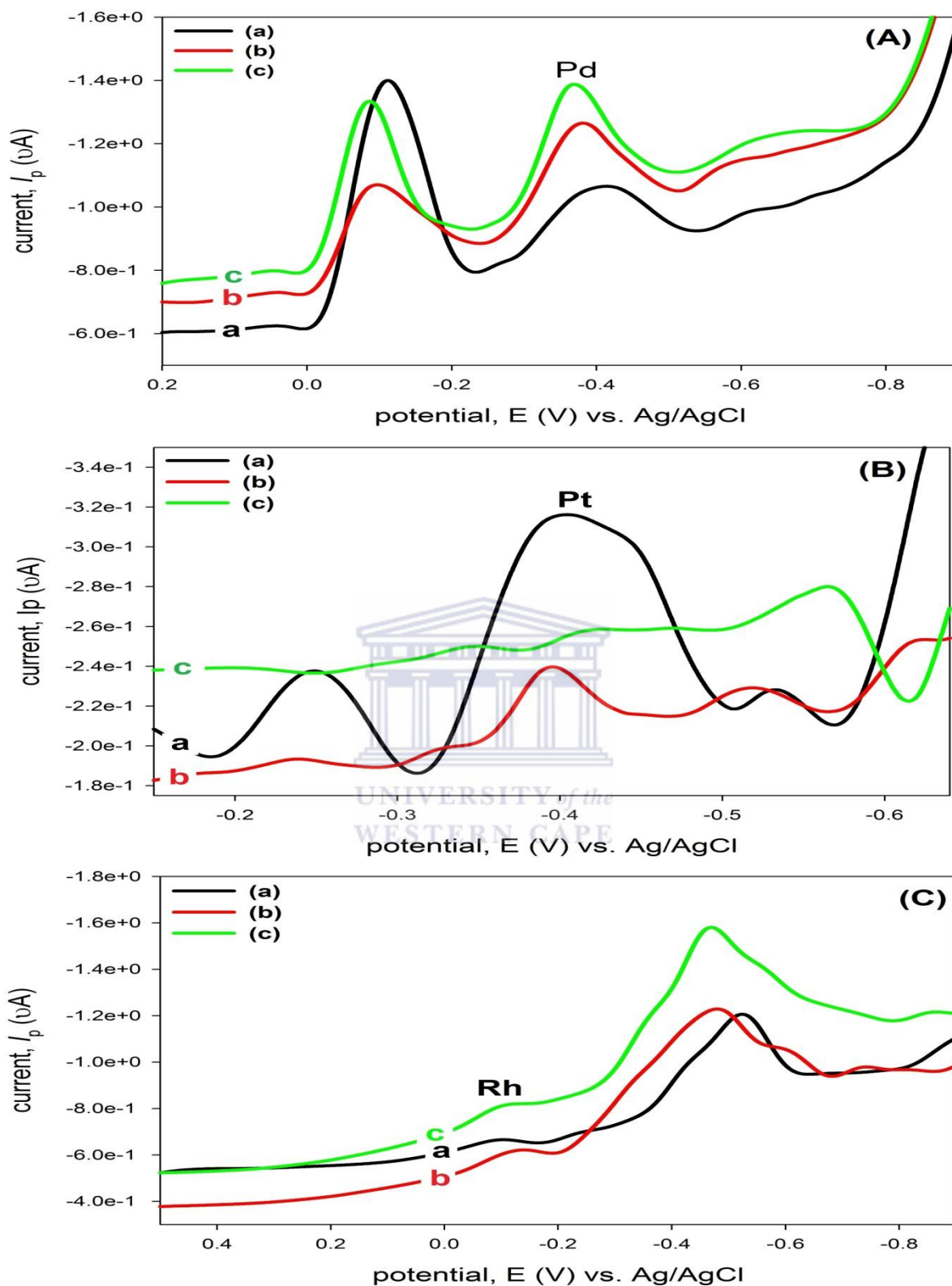
Figure 80. Effect of interfering ions on the peak current responses for Pd(II) in (A), Pt(II) in (B), and Rh(III) in (C) using the GCE/Bi-AgF sensor. The concentrations of Pd(II), Pt(II), and Rh(III) used were (0.5 ppt) in (a), 1 ppt in (b), and 1.5 ppt in (c), respectively. For Na(I) and Fe(III) the concentrations used were 1.0 ppt, with 0.2 M acetate buffer (pH = 4.7) solution containing 1×10^{-5} M DMG solution.
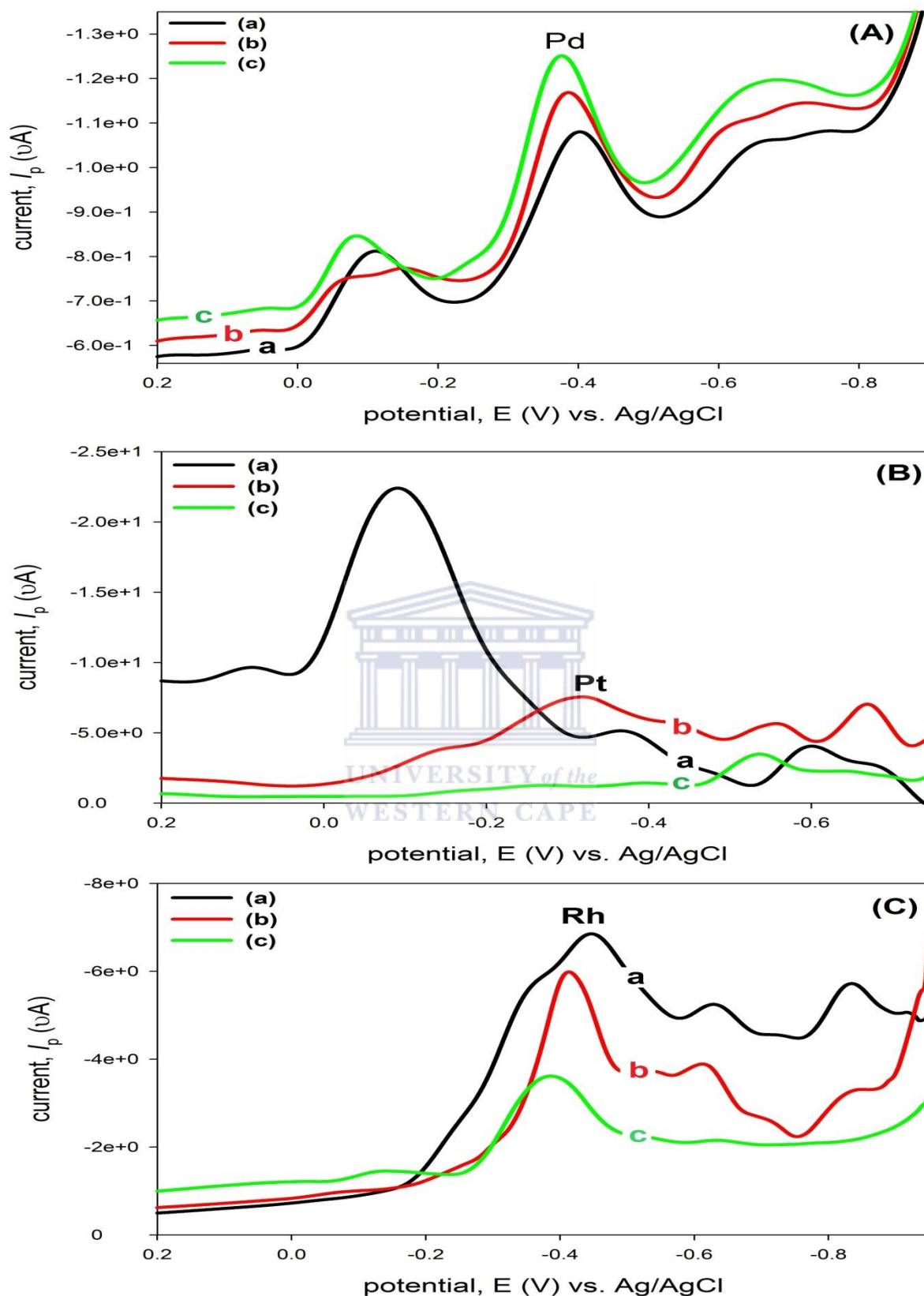
Figure 81. Effect of interfering ions on the peak current responses for Pd(II) in (A), Pt(II) in (B), and Rh(III) in (C) using the SPCE/Bi-AgF sensor. The concentrations of Pd(II), Pt(II), and Rh(III) used were (0.5 ppt) in (a), 1 ppt in (b), and 1.5 ppt in (c), respectively. For SO_4^{2-} and PO_4^{3-} the concentrations used were 1.0 ppt, with 0.2 M acetate buffer (pH = 4.7) solution containing 1×10^{-5} M DMG solution

6.3.10. Analysis of environmental samples

6.3.10.1. PGMs analysis in dust samples

In this study, different sensor platforms were used with the same analytical procedure and environmental samples as decribed in the above chapter. The determination of PGMs in dust samples using the SPC/Bi-AgFE sensor and ICP-MS analysis was performed and the two sets of results are shown in Table 13. The results for the dust samples have shown that the method was successfully applied using the SPC/Bi-AgFE sensor. Good recoveries were obtained for both DPAdSV and ICP-MS methods, respectively. These results indicate that the constructed SPC/Bi-AgFE sensor is more sensitive towards the determination of Pd(II), Pt(II) and Rh(III) in dust samples.

Table 13. **Results obtained for the determination of PGMs concentrations using a SPC/Bi-AgFE nanosensor and ICP-MS analysis in dust samples collected from roads near Stellenbosch, Western Cape Province.**

	DPAdSV			ICP-MS		
	Carbonate-bound	Organic-bound	Fe-Mn bound	Carbonate-bound	Organic-bound	Fe-Mn bound
Sample	Pd(II) (ng/L)	Rh(III) (ng/L)	Pt(II) (ng/L)	Pd (μg/L)	Rh (μg/L)	Pt (μg/L)
BOT1	4.33 ± 0.21	4.39 ± 0.28	1.68 ± 0.07	0.06	0.01	0.01
BOT2	3.68 ± 0.15	2.16 ± 0.27	0.90 ± 0.01	0.08	0.03	0.03
BOT3	3.85 ± 0.20	12.68 ± 0.31	1.28 ± 0.01	0.09	0.04	0.06
BOT4	4.25 ± 0.38	1.87 ± 0.38	0.56 ± 0.53	0.10	0.05	0.08
OP1	2.56 ± 0.04	0.71 ± 0.10	1.54 ± 0.14	0.04	0.004	0.02
OP2	3.05 ± 0.31	1.58 ± 0.08	2.39 ± 0.05	0.07	0.01	0.04
OP3	2.74 ± 0.06	0.78 ± 0.10	8.78 ± 0.61	0.09	0.03	0.06
OP4	4.29 ± 0.07	1.82 ± 0.32	2.96 ± 0.97	0.11	0.03	0.08

6.3.10.2. PGMs analysis in soil samples

The determination of PGMs in soil samples were performed by both DPAdSV and ICP-MS methods and the results are shown in Table 14. The DPAdSV results obtained for the soil samples have showed good recoveries for the SPC/Bi-AgFE sensor. The difference between the two sets of data is the sensor might be more sensitive than the ICP spectrophotometer.

Table 14. **Results obtained for the determination of PGMs concentrations using a SPC/Bi-AgFE nanosensor and ICP-MS analysis in roadside soil samples collected from roads near Stellenbosch, Western Cape Province.**

	DPAdSV			ICP-MS		
	Carbonate-bound	Organic-bound	Fe-Mn bound	Carbonate-bound	Organic-bound	Fe-Mn bound
Sample	Pd(II) (ng/L)	Rh(III) (ng/L)	Pt(II) (ng/L)	Pd (μg/L)	Rh (μg/L)	Pt (μg/L)
BOT1	4.87 ± 0.22	5.98 ± 0.26	1.84 ± 0.12	0.03	0.005	0.004
BOT2	3.68 ± 0.23	3.02 ± 0.29	1.18 ± 0.28	0.06	0.01	0.02
BOT3	3.55 ± 0.42	15.93 ± 0.76	2.35 ± 0.26	0.34	0.02	0.05
BOT4	4.55 ± 0.24	7.10 ± 0.45	1.23 ± 0.04	0.08	0.04	0.07
OP1	2.82 ± 0.08	1.12 ± 0.07	2.17 ± 0.03	0.02	0.002	0.01
OP2	3.87 ± 0.20	1.49 ± 0.15	2.57 ± 0.13	0.03	0.01	0.03
OP3	3.22 ± 0.37	1.40 ± 0.14	5.09 ± 0.55	0.04	0.02	0.04
OP4	4.53 ± 0.14	4.09 ± 0.54	1.08 ± 0.44	0.06	0.02	0.06

6.3.11. Comparison of calculated results for different sensor platforms

To calculate the limit of detection the formula 3σ/slope was employed, where σ is the standard deviation of the blank. The LODs of Pd(II), Pt(II) and Rh(III) obtained under the optimised conditions of these methods was 0.7 ng/L for Pd(II), 0.06 ng/L for Pt(II) and 0.2 ng/L for Rh(III) for the SPC/Bi-AgFE nanosensor. In this study the developed SPCE/Bi-AgF

nanosensor showed lower limit of detection than previously reported sensors based on the detection of PGMs in environmental samples. Table 15 is the comparison of obtained results in present work with other modified stripping procedures (Silwana *et al*., 2014; Van der Horst *et al*., 2012; Bobrowski *et al*., 2009). From the studies of modified electrodes this SPC/Bi-AgFE nanosensor revealed low limits of detection, high sensitivity and faster response time for PGMs analysis in the presence of DMG, using acetate buffer (pH = 4.7) solution as the supporting electrolyte.

Table 15. **Comparison of results obtained in present work with other modified stripping voltammetric procedures for the determination of PGMs in model standard solutions and environmental samples are listed.**

Electrode	Method	Linear range	LOD	References
SPC/Bi-AgFE	AdDPSV	Pd(II): 0.4 – 1.0 *ng*/L	Pd(II) – 0.07 *ng*/L	This work
		Pt(II): 0.2 – 0.8 *ng*/L	Pt(II) – 0.06 *ng*/L	
		Rh(III): 0.2 – 0.8 *ng*/L	Rh(III) – 0.2 *ng*/L	
GC/Bi-AgFE	AdDPSV	Pd(II): 0.2 – 1.0 *ng*/L	Pd(II) – 0.19 *ng*/L	This work
		Pt(II): 0.2 – 1.0 *ng*/L	Pt(II) – 0.20 *ng*/L	
		Rh(III): 0.4 – 1.0 *ng*/L	Rh(III) – 0.22 *ng*/L	
SPC/BiFE	AdDPSV	Pd(II): 0 – 0.1 μg/L	Pd(II) – 0.008 μg/L	Silwana *et al*., 2014
		Pt(II): 0.2 – 0.1 μg/L	Pt(II) – 0.006 μg/L	
		Rh(III): 0 – 0.08 μg/L	Rh(III) – 0.005 μg/L	
GC/BiFE	AdDPSV	Pd(II): 0 – 2. μg/L	Pd(II) – 0.19 μg/L	Van der Horst *et al*., 2012
		Pt(II): 0 – 3.5 μg/L	Pt(II) – 0.20 μg/L	
		Rh(III): 0 – 3.0 μg/L	Rh(III) – 0.22 μg/L	
Hg(Ag)FE	CSV	Pd(II): 1 – 50 μg/L	Pd(II) - 0.15 μg/L	Bobrowski *et al*., 2009

6.4. Summary

In conclusion, the construction, optimisation and practical application of the SPC/Bi-AgFE nanosensor, which was prepared by drop-coating onto an screen-printed carbon electrode have been presented. The important DPAdSV parameters were optimised and well-defined peaks were obtained for Pd(II), Pt(II) and Rh(III) in model standard solutions. To illustrate the practical application of the developed SPC/Bi-AgFE nanosensor, the sensor was tested for the detection of PGMs in roadside dust and soil samples, collected from the Bottelary and Old Paarl Roads near Stellenbosch in the Western Cape Province. The results obtained from DPAdSV and ICP-MS analysis were compared and it was found that the results obtained by DPAdSV analysis are lower than those obtained by ICP-MS analysis. The difference between the two sets of data have illustrated that the SPC/Bi-AgFE nanosensor is more sensitive than the ICP-MS spectrophotometer.

Chapter 7

Conclusion and Recommendations

7.1. Conclusions

The determination of ultra-traces of platinum group metals in standards and environmental samples was a huge challenge in this study. Chapter 1 presented the theme of the study, which included an introduction on electrochemical sensors, electrochemical characterisation of PGMs, a small introduction on nanoparticles, the research hypothesis, research design and the layout of the thesis.

In chapter 2, a review of the literature has summarised the roles that electrochemical sensors play in the determination of platinum group metals in standards and environmental samples. Most of the research on PGMs listed in this review was done by using a hanging mercury drop or mercury based electrodes. The bismuth film electrode was also used and shown good results but the major draw-back was the ability to operate only in highly alkaline media. In this study we observed that the application of metallic silver electrodes is not so common in the determination of PGMs in environmental samples.

In chapter 3, the experimental methods and analytical techniques were illustrated. In this chapter the important electroanalytical techniques such as cyclic voltammetry, differential pulse voltammetry and adsorptive stripping voltammetry were discussed. The microscopy techniques used for morphology studies such as scanning electron microscopy and transmission electron microscopy were also discussed. Finally, the spectroscopic techniques used for the characterisation of the chemically synthesised nanoparticles were also discussed.

In chapter 4 chemical syntheses of Ag, Bi, and Bi-Ag bimetallic NPs were successfully performed. The novel Bi-Ag bimetallic NPs was chemically synthesised by using $AgNO_3$, $Bi(NO_3)_3$ $5H_2O$ and the addition citric acid as reducing agent. Electrochemical characterisation in addition to spectroscopy and microscopy analysis was employed to study the properties of each of the Ag, Bi, and Bi-Ag bimetallic NPs. The UV-Vis, FT-IR and

Raman spectroscopy results confirmed the structural properties of the Bi-Ag bimetallic NPs. In addition the TEM and SAED morphological characterisation confirmed the nanoscale nature of the Bi-Ag NPs. The electrochemical results obtained have shown that the Bi-Ag bimetallic NPs exhibit good electro-catalytic activity that can be harnessed for sensor construction and related applications. The developed procedure presented in this study includes advantages of simplicity, high sensitivity, high selectivity, speed, and low cost. The novelty of this sensor lies in the fact that this type of nanosensor has not been applied for the determination of Pd(II), Pt(II) and Rh(III) in environmental samples before.

Chapters 5 and 6 demonstrated that DPAdSV analysis is an excellent method for the determination of PGMs in environmental samples. In conclusion, the above methods combined with bismuth-silver bimetallic nanosensors offered practical potential for the determination of trace amounts of platinum, palladium and rhodium. The developed procedures presented in these studies include the advantages of simplicity, high sensitivity, high selectivity, speed and low cost. The novelty of these methods lies in the fact that these types of nanosensors have not been applied for the determination of PGMs in environmental samples before. Besides obtaining sensitive LODs in the ng/L concentration range, these methods offers attractive analytical performance due to the capability to determine all three PGM-dimethylglyoxime complexes in both roadside dust and soil samples. The ability to detect PGMs in environmental samples makes this bismuth-silver bimetallic nanosensor an alternative replacement for bismuth films, toxic hanging mercury electrode and carbon paste electrodes.

7.2. Recommendation and Future work

The construction of bismuth-silver bimetallic sensors on glassy carbon and screen-printed electrodes has shown very good results. Only the simultaneous determination of Pd-Rh complex and Pt-Rh complex were possible. For future study the focus must be on the simultaneous determination of all three PGMs in one solution. The possible solution may be attainable by doing more optimisation of the parameters for adsorptive stripping voltammetric determination of PGMs. Future studies on the work presented in this thesis should also involve further optimisation of the detection limits obtained for the single and

simultaneous determination of Pt(II), Pd(II) and Rh(III). Studies should also include further optimisation of the interfering ions investigated in this work.

Chapter 8

References

8.1. References

Abdollah, Y. and Fatemeh, P. 2009. Highly selective sensing of mercury (II) by development and characterization of a PVC-based optical sensor. *Sensors and Actuators B*, 138: 467-473.

Abiman, P., Wildgoose, G.G., Xiao, L. and Compton, R.G. 2008. The convenient determination of palladium at a solid electrode via adsorptive stripping voltammetry at a glassy carbon electrode modified with a random array of mercury nanodroplets. *Electroanalysis*, 14: 1607-1609.

Abou El-Nour, K.M.M., Eftaiha, A., Al-Warthan, A. and Ammar, R.A.A. 2010. Review Article: Synthesis and application of silver nanoparticles. *Arabian Journal of Chemistry*, 3: 135-140.
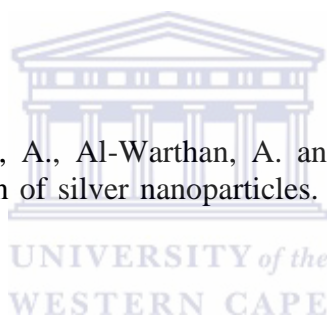
Aceto, M., Abollino, O., Bruzzoniti, M.C. Mentasti, E., Sarzanini, C. and Malandrino, M. 2002. Determination of metals in wine with atomic spectroscopy (flame-AAS, GF-AAS and ICP-AES), a review. *Food additives and contaminants*, 19(2): 126-133.

Adeloju, S.B., Bond, A.M. and Briggs, M.H. 1984. Assessment of Differential-Pulse Adsorption Voltammetry for the Simultaneous Determination of Nickel and Cobalt in Biological Materials. *Analytica Chimica Acta*, 164: 181-194.

Airey, L. 1947. The application of the cathode ray oscillograph to polarography-general lay-out and uses of the cathode ray polarograph. *Analyst*, 72: 304-307.

Al-roubaie, A.M. 1986. Condition of the periodontion of teeth with silver-palladium bridge. *Fogorvosi Szemle*, 79(7): 207-212.

Alt, F., Bambauer, A., Hoppstock, K., Mergler, B., Tölg, G. 1993. Platinum traces in airbourne particulate matter. Determination of whole content, particle size distribution and soluble platinum. *Journal of Analytical Chemistry*, 346: 693-696.

Alvarez, L.W., Alvarez, W., Asaro, F. and Michel, H.V. 1980. Extraterrestrial Cause for the Cretaceous-Tertiary Extinction. *Science*, 208(4448): 1095-1108.

Anshup, T.P. 2009. Noble metal nanoparticles for water purification: A critical review. *Thin Solid Films*, 517: 6441-6478.

Arrigan, D.W.M. 1994. Voltammetric determination of trace metals and organics after accumulation at modified electrodes. *Analyst*, 119: 1953-1966.

Ashmead, H.D. 1986. *Foliar Feeding of Plants with Amino Acid Chelates*, Noyes Publications, Park Ridge, N.J., U.S.A.

Aucelio, R.Q., Rubin, V.N., Smith, B.W. and Winefordner, J.D. 1998. Ultratrace determination of platinum in environmental and biological samples by electrothermal atomization laser-excited atomic fluorescence using a copper vapour laser pumped dye. *Journal of Analytical Atomic Spectrometry*, 13: 49-54.

Augthun, M., Lichtenstein, M. and Kammerer, G. 1990. Untersuchungen zur allergenen Potenz von Palladium-Legierungen. *Deutsche Zahnärztliche Zeitschrift*, 45(8): 480-482.

Balan, L. and Burget, D. 2006. Synthesis of metal/polymer nanocomposite by UV-radiation curing. *European Polymer Journal*, 42: 3180-3189.

Baleg, A., Jahed, N.M., Arotiba, O.A., Mailu, S.N., Hendricks, N.R., Baker, P.G. and Iwuoha, E.I. 2011. Synthesis and characterisation of poly (propylene imine) dendrimer-Polypyrrole conducting star copolymer. *Journal of Electroanalytical Chemistry*, 652: 18-25.

Bard, A.J. and Faulkner, L.R. 2000. Polarography and Pulse Voltammetry, Electrochemistry Methods: Fundamentals and Applications, 2nd Ed., Wiley: New Jersey, 261-304.

Bard, A.J. and Faulkner, L.R. 2000. Electrochemical methods: Fundamentals and applications. 2nd Ed., New York: Wiley.

Barefoot, R.R. 1997. Determination of platinum at trace levels in environmental and biological materials. *Environmental Science and Technology*, 31: 309-314.

Barefoot, R.R. and Van Loon, J.C. 1999. Recent advances in the determination of the platinum group elements and gold. *Talanta*, 49: 1-14.

Begerow, J., Turfeld, M. and Dunemann, L. 1997. Determination of physiological noble metals in human urine using liquid-liquid extraction and Zeeman electrothermal atomic absorption spectrometry. *Analytica Chimica Acta*, 340: 277-283.

Beinrohr, E., Lee, M.L., Tschopel, P. and Tölg, G. 1993. Determination of platinum in biotic and environmental samples by graphite furnace atomic spectroscopy after its electro-deposition into a graphite tube packed with reticulated vitreous carbon. *Fresenius Journal of Analytical Chemistry*, 346: 689-692.

Bieger, W.P. et al, 1996. "Immunotoxocolgy of metals", Zur Deutshcen Auszahe.

Bobrowski, A., Gawlicki, M., Kapturski, P., Mirceski, V., Spasovski, F. and Zarebski, J. 2009. The silver amalgam film electrode in adsorptive stripping voltammetric determination of palladium (II) as its dimethyldioxime complex. *Electroanalysis*, 21: 36-40.

Bonnig, K. et al, 1990. "Quantitative analysis of the corrosion rates of palladium alloys", *Dtsch Azhnarztl*, A 45(8): 508-510.

Brahim, S., Wilson, A.M., Narinesingh, D., Iwuoha, E. and Guiseppi-Elie, A. 2003. Chemical and Biological Sensors Based on Electrochemical Detection Using Conducting Electroactive Polymers. *Microchimica Acta*, 143: 123-137.

Brett, C.M.A. 1999. Electroanalytical techniques for the future – the challenges of miniaturization and of real-time measurements. *Electroanalysis*, 11: 1013-1016.

Briand, G.G. and Burford, N. 1999. Bismuth compounds and preparations with biological or medicinal relevance. *Chemical Reviews*, 99: 2601-2657.

Brihaye, C. and Dugckaerts, G. 1983. Determination of traces of metals by anodic stripping voltammetry at a rotating glassy carbon ring-disc electrode: Part 2. Comparison between linear anodic stripping voltammetry with ring collection and various other stripping techniques. *Analytica Chimica Acta*, 146: 37-43.

Buffle, J. and Tercier, M.L. 2000 In situ voltammetry: Consepts and practice for trace analysis and speciation, chapter 9 in: *"In situ monitoring of aquatic systems: Chemical analysis and speciation"*, Ed. J. Buffle, G. Horvai, Chichester, Wiley.

Buslaeva, T.M. 1999. Platinum group metals and their role in contemporary society. *Sorosovskiy Obrazovetelny Zhurnal*, 11: 45-49.

Butlerow, A. 1859. "Ueber einige Derivate des Jodmethylens". On some derivatives of methylene iodide. *Annalen der Chemie und Pharmacie*, 11: 242-252.

Buyanov, R.A. and Pakhomov, N.A. 2001. Catalysts and processes of dehydrogenation of paraffins and olefins. *Kinetika I Kataliz*, 42(1): 72-85.

Calamari, D., Bacci, E., Focardi, S., Gaggi, C., Morosini, M. and Vighi, M. 1991. Role of plant biomass in the global environmental partitioning of chlorinated hydrocarbons. *Environmental Science and Technology*, 25: 1489-1495.

Cardarelli, F. 1966. Materials Handbook: A Concise Desktop Reference, 2nd edition, Springer–Verlag, London, 411-413.

Carotenuto, G., Hison, C.L., Capezzuto, F., Palomba, M., Perlo, P. and Conte, P. 2009. Synthesis and thermoelectric characterisation of bismuth nanoparticles. *Journal of Nanoparticles Research*, 11: 1729-1738.

Castelain, P.Y. and Castelain, M. 1987. Contact dermatitis to palladium. *Contact Dermatitis*, 16(1): 46.

Cha, K.W., Park, C.I. and Park, S.H. 2000. Simultaneous determination of trace uranium(VI) and zinc(II) by adsorptive cathodic stripping voltammetry with aluminon ligand. *Talanta*, 52: 983-989.

Chimentao, R., Kirm, I., Medina, F., Rodriguez, X., Cesteros, Y., Salagre, P. and Sueiras, J. 2004. Different morphologies of silver nanoparticles as catalysts for the selective oxidation of styrene in the gas phase. *Chemical Communications*, 7: 846-847.

Choi, Y., Ho, N. and Tung, C. 2007. Sensing phosphatase activity by using gold nanoparticles. *Angewandte Chemie International Edition*, 46: 707-709.

Chou, K.S. and Lai, Y.S. 2004. Effect of Polyvinyl Pyrrolidone MolecularWeights on the Formation of Nanosized Silver Colloids. *Material Chemistry and Physics*, 83: 82-88.

Chou, K.S. and Lu, Y.C. 2005. Effect of Alkaline Ion on the Mechanism and Kinetics of Chemical Reduction of Silver. *Material Chemistry and Physics*, 94 (2-3): 429-433.

Chrimes, A.F., Khoshmanesh, K., Stoddart, P.R., Kayani, A.A., Mitchell, A., Daima, H., Bansal, V. and Kalantar-zadeh, K. 2012. Active Control of Silver Nanoparticles Spacing Using Dielectrophoresis for Surface-Enhanced Raman Scattering. *Analytical Chemistry*, 84: 4029-4035.

Colombo, C. 2008. The speciation and bioavailability of platinum, palladium and rhodium in the environment. PhD. Thesis. Imperial College London, UK.

Cordonna, G.W., Kosanovich, M. and Becker, E.R. 1989. Gas turbine emission control: Platinum and platinum-palladium catalysts for carbon monoxide and hydrocarbon oxidation. *Platinum Metals Review*, 33(2): 46-55.

Corr, S.J. 2011. Silver nanoparticles and thin films for strained-silicon surface enhanced Raman spectroscopy and capacitively-coupled radiofrequency heating. Published Ph.D Thesis, Dublin City University School of Electronic Engineering, Dublin, UK.

Creighton, J.A. and Desmond, G.E. 1991. Ultraviolet-visible absorption spectra of the colloidal metallic elements. *Journal of Chemical Society Faraday Trans*, 87(24): 3881-3891.

Cuenya, B.R. 2010. Synthesis and catalytic properties of metal nanoparticles: size, shape, support, composition, and oxidation state effects. *Thin Solid Films*, 518: 3127-3150.

Cui, F. and Zhang, X. 2012. Electrochemical sensor for epinephrine based on a glassy carbon electrode modified with graphene/gold nanocomposites. *Journal of Electroanalytical Chemistry*, 669: 35-41.

Cui, X.Y. and Martin, D.C. 2003. Fuzzy gold electrodes for lowering impedance and improving adhesion with electrodeposited conducting polymer films. *Sensors and Actuators A-Physical*, 103: 384-394.

Dalvi, A.A., Satpati, A.K. and Palrecha, M.M. 2008. Simultaneous determination of Pt and Rh by catalytic adsorptive stripping voltammetry, using hexamethylene tetramine (HMTA) as complexing agent. *Talanta*, 75: 1382-1387.

Daniel, S., Gladis, J.M. and Rao, T.P. 2003. Synthesis of imprinted polymer material with palladium ion nanopores and its analytical application. *Analytica Chimica Acta*, 488: 173-182.

Daniele, S., Baldo, M.A. and Bragato, C. 2008. Recent Developments in Stripping Analysis on Microelectrodes. *Current Analytical Chemistry*, 4: 215-228.

Débarre, A., Jaffiol, R., Julien, C., Tchénio, P. and Mostafavi, M. 2004. Raman scattering from single Ag aggregates in presence of EDTA. *Chemical and Physical Letters*, 386: 244-247.

Djingova, R., Heidenreich, H., Kovacheva, P. and Markert, B. 2003. On the determination of platinum group elements in environmental materials by inductively coupled plasma mass spectrometry and microwave digestion. *Analytica Chimica Acta*, 489: 245-251.

Do Carmo, D.R., Da Silva, R.M. and Stradiotto, N.R. 2003. Electrocatalytic and voltammetric determination of sulfhydryl compounds through iron nitroprusside modified graphite paste electrode. *Journal of the Brazilian Chemical Society*, 14(4): 616-620.

Doja, A. and Roberts, W. 2006. "Immunizations and autism: a review of the literature". *Canadian Journal of Neurological Sciences*, 33(4): 341-46.

Dong, Y.P., Huang, L., Zhang, J., Chu, X.F. and Zhang Q.F. 2012. Electro-oxidation of ascorbic acid at bismuth sulfide nanorod modified glassy carbon electrode. *Electrochimica Acta*, 74: 189-193.

Downey, D. 1989. Contact mucositis due to palladium. *Contact Dermatitis*, 21(1): 54-55.

Drake, K.F., Van Duyne, R.P. and Bond, A.M. 1978. Cyclic differential pulse voltammetry: A versatile instrumental approach using a computerized system. *Journal of Electroanalytical Chemistry and Interfacial Chemistry*, 89(2): 231-246.

Economou, A. and Fielden, P.R. 1998. Selective determination of Ni(II) and Co(II) by flow injection analysis and adsorptive cathodic stripping voltammetry on a wall jet mercury film electrode. *Talanta*, 46(10): 1137-1146.

Economou-Eliopoulos, M. 2010. Platinum-group elements (PGE) in various geotectonic settings: Opportunities and risks. *Hellenic Journal of Geosciences*, 45: 65-82.

Egorova, E. and Revina, A. 2000. Synthesis of metallic nanoparticles in reverse micelles in the presence of quercetin. Colloids and Surfaces A: *Physicochemical and Engineering Aspects*, 168: 87-96.

Ek, K.H., Morrison, G.M. and Rauch, S. 2004. Environmental routes for platinum group elements to biological materials–a review. *Science of the Total Environment*, 334/335: 21-38.

Elle, R., Alt, F., Tölg, G. and Tobschall, H.J. 1989. An efficient combined procedure for the extreme trace analysis of gold, platinum, palladium and rhodium with the aid of graphite furnace atomic absorption spectrometry and total reflection X-ray fluorescence analysis. *Fresenius Z. Analytical Chemistry*, 334: 723-739.

Eller, K., Henkes, E., Rossbacher, R. and Höke, H. 2005. Amines, Aliphatic in Ullmann's Encyclopedia of Industrial Chemistry, Wiley-VCH Verlag, Weinheim.

Fadrná, R. 2005. Polished Silver Solid Amalgam Electrode: Further Characterization and Applications in Voltammetric Measurements. *Analytical Letters*, 37(15): 3255-3270.

Fanjul-Bolado, P., Hernandez-Santos, D., Lamas-Ardisana, P.J., Martın-Pernia, A. and Costa-Garcia, A. 2008. Electrochemical characterization of screen-printed and conventional carbon paste electrodes. *Electrochimica Acta*, 53: 3635-3642.

Filipe, O.M.S. and Brett, C.M.A. 2004. Characterization of carbon film electrodes for electroanalysis by electrochemical impedance. *Electroanalysis*, 16: 994-1001.

Florence, M. 1970. Anodic stripping voltammetry with a glassy carbon electrode mercury-plated *in situ*. *Journal of Electroanalytical Chemistry and Interfacial Chemistry*, 27(2): 273-281.

Florence, T.M. 1984. Recent advances in stripping analysis. *Journal of Electroanalytical Chemistry*, 168: 207-218.

Forrester, J.S. and Ayres, G.H. 1959. Rhodium (III) in aqueous solutions. *Journal of Physical Chemistry*, 63: 1979-1981.

Fujii, K., Kumai, T., Takamuku, T., Umebayashi, Y. and Ishiguro, Y.S. 2006. Liquid Structure and Preferential Solvation of Metal Ions in Solvent Mixtures of *N,N*-Dimethylformamide and N-Methylformamide. *Journal of Physical Chemistry*, *A*. 110: 1798-1804.

Furia, T. 1964. "EDTA in Foods – A technical review". *Food Technology* 18(12): 1874-1882.

Gabbasova, Z.V., Kuzmin, M.D., Zvezdin, A.K., Dubenko, I.S., Murashov, V.A., Rakov, D.N. and Krynetsky, I.B. 1991. $Bi1-_xR_xFeO_3$ (R = Rare earth): A family of novel magnetoelectrics. *Physical Letters*, *A*. 158: 491-498.

Gaidau, C., Petica, A., Ciobanu, C. and Martinescu, T. 2009. Investigations on antimicrobial activity of collagen and keratin based materials doped with silver nanoparticles. *Biotechnology Letters*, 14(5): 4665-4672.

Galík, M., Michal Cholota, M., Ivan Švancara, I., Bobrowski, A. and Vytřas, K. 2006. A Study on Stripping Voltammetric Determination of Osmium(IV) at a Carbon Paste Electrode Modified In Situ with Cationic Surfactants. *Electroanalysis*, 18(22): 2218-2224.

Gardiner, D.J. 1989. *Practical Raman spectroscopy*. Springer-Verlag. ISBNº978-0-387-50254-0º.

Georgieva, M. 2002. Electrochemical Behavior of Pt(IV) on Mercury Electrode in the Presence of Dimethylglyoxime. *Portugaliae Electrochimica Acta*, 20: 179-189.

Georgieva, M and Pihlar, B. 1997. Determination of palladium by adsorptive stripping voltammetry. *Fresenius Journal of Analytical Chemistry*, 357: 874-880.

Georgieva, M. and Pihlar, B. 1996. Study of the Reduction of Palladium(II) on a Mercury Electrode in the Presence of Dimethylglyoxime. *Electroanalysis*, 8(12): 1155-1159.

Girolami, G.S., Rauchfuss, T.B. and Angelici, R.J. 1999. Synthesis and Technique in Inorganic Chemistry: A Laboratory Manual, 3rd Ed.: 213-215.

Goeken, M. and Kempf, M. 1999. Microstructural properties of superalloys investigated by nanoindentations in an atomic force microscope. *Acta Materialia*, 47(3): 1043-1052.

Goldstein, J.I., Yakowitz, H., Newbury, D.E., Lifshin, E., Colby, J.W. and Coleman, J.R. Pratical Scanning Electron Microscopy: Electron and Ion Microprobe Analysis, Pelnum Press. New York, N.Y., 1975.

Gómez, B., Gómez, G.M., Sanchez, J.L., Fernandez, L. and Palacios, M.A. 1998. Platinum and rhodium distribution in airborne particulate matter and road dust. *Science of the Total Environment*, 59: 215-222.

Gómez, B., Palacios, M.A., Gómez, M., Sanchez, J.L., Morrison, G., Rauch, S., McLeod, C., Ma, R., Caroli, S., Alimonti, A., Petrucci, F., Bocca, B., Schramel, P., Zischka, M., Petterson, C. and Wass, U. 2002. Levels and risk assessment for humans and ecosystems of platinum-group elements in the airborne particles and road dust of some European cities. *Science of the Total Environment*, 299: 1-19.

Gowda, H. Sänke and Ramappa, P.G. 1976. Trifluoperazine dihydrochloride as a new reagent for the spectrophotometric determination of osmium(VIII). *Analytical Chemistry*, 282: 141.

Gowda, H. Sänke and Thimmaiah, K.N. 1976. Spectrophotometric determination of Palladium by means of 2-Chlorophenothiazine. *Zeitschrift für Analytische Chemie*, 279: 208.

Gray, A.L. 1989. The Origins, Realization, and Performance of ICP-MS Systems, in: *Applications of Inductively Coupled Plasma Mass Spectroscopy*, Date, A.R. and Gray, A.L. editors, Blackie and Son Ltd.

Griffiths, P. and De Hasseth, J.A. 2007. *Fourier transform infrared spectrometry*, 2nd edition, Wiley-Blackwell, Inc., New York, USA.

Guo, O.H., Li, Y., Xiao, P. and He, N. 2005. "Determination of trace amount of bismuth(III) by adsorptive anodic stripping voltammetry at carbon paste electrode." *Analytica Chimica Acta*, 534: 143-147.

Gutiérrez, M. and Henglein, A. 1996. Nanometer-sized Bi particles in aqueous solution: absorption spectrum and some chemical properties. *Journal of Physical Chemistry*, 100: 7656-7661.

Guzmán, M.G., Dille, J. and Godet, S. 2008. Synthesis of silver nanoparticles by chemical reduction method and their antibacterial activity. *World Academy of Science, Engineering and Technology*, 43: 357-364.

Haes, A.J. and Van Duyne, R.P. 2003. Nanosensors Enable Portable Detectors for Environmental and Medical Applications. *Laser Focus World*, 39: 153-156.

Harmami, S.B., Sondari, D. and Haryono, A. 2008. The synthesis of silver nanoparticles produced by chemical reduction of silver salt solution. *Indonesian Journal of Materials Science*, 233-236.

Harris, D.C. 2007. *Quantitative Chemical Analysis*. 7th edition, W. H. Freeman and Compagny, New York, USA.

Hart, J.R. 2005. "Ethylenediaminetetraacetic Acid and Related Chelating Agents," in: *Ullmann's Encyclopedia of Industrial Chemistry*, Wiley-VCH, Weinheim.

Hartley, F.R. 1991. Chemistry of the Platinum Group Metals. *Elsevier*. Amsterdam, 60-74.

Hayama, K., Tanaka, H., Ju, M.J., Hayashi, K. and Toko, K. 2002. Fabrication of a Flow Cell for Electrochemical Impedance Measurements. *Sensors and Materials*, 14(8): 443-453.

He, B., Tan, J., Liew, K. and Liu, H. 2004. Synthesis of size controlled Ag nanoparticles. *Journal of Molecular Catalysis A: Chemical*, 221: 121-126.

Hees T, Wenclawiak B, Lustig S, Schramel P, Schwarzer M, Schuster M, Verstraete D, Dams R, Helmers E. 1998. Distribution of platinum group elements (Pt, Pd, Rh) in environmental and clinical matrices: Composition, analytical techniques and scientific outlook. *Environmental Science and Pollution Research*, 5(2):105-111.

Heinrich, E., Schmidt, G. and Kratz, K.L. 1996. Determination of platinum group elements (PGE) from catalytic converters in soil by means of docimasy and INAA. *Fresenius' Journal of Analytical Chemistry*, 354: 883-885.

Heitzmann, M., Basaez, L., Brovelli, F., Bucher, C., Limosin, D., Pereira, E., Rivas, B.L., Yal, G., Saint-Aman, E. and Moutet, J.C. 2005. Voltammetric Sensing of Trace Metals at a Poly (Pyrrole-Malonic Acid) Film Modified Electrode. *Electroanalysis*, 17(21): 1970-1976.

Hernandez-Delgadillo, R., Velasco-Arias, D., Diaz, D., Arevalo-Niño, K., Garza-nriquez, M., De la Garza-Ramos, M.A. and Cabral-Romero, C. 2012. Zerovalent bismuth nanoparticles inhibit Streptococcus mutans growth and formation of biofilm. *International Journal of Nanomedicine*, 7: 2109-2113.

Hernández-Santos D., González-García M.B. and García A.C. 2002. Review: Metal-nanoparticles based electroanalysis. *Electroanalysis*, 14: 1225-1235.

Hildebrandt, A., Bragos, R., Lacorte, S. and Marty, J.L. 2008. Performance of a portable biosensor for the analysis of organophosphorus and carbamate insecticides in water and food. *Sensors and Actuators B*, 133: 195-201.

Hocevar, S.B., Ogorevc, B., Wang, J. and Pihlar, B. 2002. A study on operational parameters for advanced use of bismuth film electrode in anodic stripping voltammetry. *Electroanalysis*. 14: 1707-1712.

Hodge, V.F. and Stallard, M.O. 1986. Platinum and Palladium in roadside dust. *Environmental Science and Technology*, 20: 1058-1060.

Hoffman, E.L., Naldrett, A.J., Van Loon, J.C., Hancock, R.G.V. and Manson, A. 1978. The determination of all the platinum group elements and gold in rocks and ores by neutron activation analysis after preconcentration by a nickel sulphide fire-assay techniques on large samples. *Analytica Chimica Acta*, 102: 157-166.

Honeychurch, K.C. and Hart, J.P. 2003. Screen-printed electrochemical sensors for monitoring metal pollutants. *Trends in Analytical Chemistry*, 22(7-8): 456-469.

Hong, T-G., Gwon, Y-S. and Czae, M.Z. 1997. Adsorptive Stripping Voltammetric Analysis of Ruthenium. *Analytical Science and Technology*, 10: 119-124.

http://www.lenntech.com/periodic/elements/rh.htm#ixzz1vEl3Zy3P

Hu, C., Wu, K., Dai, X. and Hu, S. 2003. Simultaneous determination of Lead(II) and Cadmium(II) at a diacetyldioxime modified carbon paste electrode by differential pulse stripping voltammetry. *Talanta*, 60: 17-24.

Hunter, D., Milton, R. and Perry, K.M.A. 1945. Asthma caused by the complex salts of platinum. *British Journal of Industrial Medicine*, 2: 92-98.

Huszal, S., Kowalska, J., Krzeminska, M. and Golimowski, J. 2005. Determination of Platinum with Thiosemicarbazide by Catalytic Adsorptive Stripping Voltammetry (AdSV). *Electroanalysis*, 17(4): 299-304.

Hutter, E. and Fendler, J.H. 2004. Exploitation of localized surface Plasmon Resonance. *Advance Materials*, 16(19): 1685-1706.

Hutton, E.A., Hocevar, S.B., Ogorevc, B. and Smith, M.R. 2003. Bismuth film electrode for simultaneous adsorptive stripping analysis of trace cobalt and nickel using constant current chronopotentiometric and voltammetric protocol. *Electrochemistry Communications*, 5: 765-769.

Hwang, G.H., Han, W.K., Park, J.S. and Kang, S.G. 2008. Determination of trace metals by anodic stripping voltammetry using a bismuth-modified carbon nanotube electrode. *Talanta*, 76: 301-308.

Hynes, W.A., Yanowski, L.K. and Ransford, J.E. 1950. Versene Used as a Spot Reagent for Gold. *Mikrochimica Acta*, 35: 160-163.

Ishiyama T. and Tanaka, T. 1996. Cathodic Stripping Voltammetry of Selenium(IV) at a Silver Disk Electrode. *Analytical Chemi*stry, 68: 3789-3792.

Jalili, N. and Laxminarayana, K. 2004. A review of atomic force microscopy imaging systems: application to molecular metrology and biological sciences. *Mechatronics*, 14: 907-945.

Jarvis, K.E., Gray, A.L. and Houk, R.S. *Handbook of Inductively Coupled Plasma Mass Spectrometry*, Blackie Academic and Professional, 1992.

Johnson Matthey: *Palladium*. Various issues. London, UK, 1996.

Jones, S. and Compton, R.G. 2008. Fabrication and applications of nanoparticle-modified electrodes in stripping analysis. *Current Analytical Chemistry*, 4: 177-182.

Jurgen, H. 1984. "Cyclic Voltammetry-Electrochemical Spectroscopy". New Analytical Methods (25)". *Angewandte Chemie International Edition in English*, 23(11): 831-847.

Kanitsar, K., Koellensperger, G., Hann, S., Limbeck, A., Puxbaum, H. and Stingeder, G. 2003. Determination of Pt, Pd and Rh by inductively coupled plasma sector field mass spectrometry (ICP-SFMS) in size-classified urban aerosol samples. *Journal of Analytical Atomic Spectrometry*, 18: 239-246.
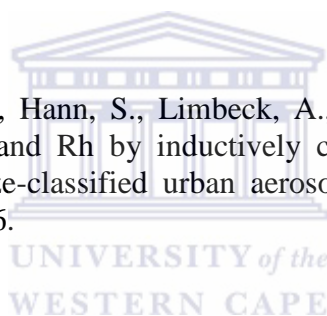
Kaowphong, S. 2012. Biomolecule-assisted hydrothermal synthesis of silver bismuth sulfide with nanostructures. *Journal of Solid State Chemistry*, 189: 108-111.

Kapturski, P. and Bobrowski, A. 2008. The silver amalgam film electrode in catalytic adsorptive stripping voltammetric determination of cobalt and nickel. *Journal of Electroanalytical Chemistry*, 617: 1-6.

Katz, E. and Willner, I. 2003. Probing biomolecular interactions at conductive and semiconductive surfaces by impedance spectroscopy: Routes to impedimetric immunosensors, DNA-sensors, and enzyme biosensors. *Electroanalysis*, 15: 913-947.

Kawata, Y., Shiota, M., Tsutsui, H., Yoshida, Y., Sasaki, H. and Kinouchi, Y. 1981. Cytotoxicity of Pd-Co dental alloys, *Journal of Dental Research*, 60(8): 1403-1409.

Kefala, G., Economou, A. and Sofoniou, M. 2006. Determination of trace aluminium by adsorptive stripping voltammetry on a preplated bismuth-film electrode in the presence of cupferron. *Talanta*, 68: 1013-1019.

Kempf, M., Göken, M. and Vehoff, H. 1998. Nanohardness measurements for studying local mechanical properties of metals. *Applied Physics A: Material Science and Processing*, 66: 843-846.

Khanna, R.K. 1981. "Raman-spectroscopy of oligomeric SiO species isolated in solid methane". *Journal of Chemical Physiscs*, 74(4): 2108.

Khezri, B., Amini, M.K. and Firooz, A.R. 2008. An optical chemical sensor for mercury ion based on 2-mercaptopyrimidine in PVC membrane. *Analytical and Bioanalytical Chemistry*, 390: 943-1950.

Khomutov, G. and Gubin, S. 2002. Interfacial synthesis of noble metal nanoparticles. *Material Science and Engineering C*, 22: 141-146.

Kim, S. and Cha, K. 2002. Determination of palladium(II) with α-(2-benzimidazolyl)-α',α"-(*N*-5-nitro-2-pyridiylhydrazone)-toluene by adsorptive cathodic stripping voltammetry. *Talanta*, 57: 675-679.

Kishi, Y. 1997. A Benchtop Inductively Coupled Plasma Mass Spectrometer. *Hewlett-Packard Journal*, 9: 1-10.

Kissinger, P.T. and Heineman, W.R. 1983. "Cyclic Voltammetry." *Journal of Chemical Education*, 60: 702.

Klüppel, D. 1997. Presented at: 4th Noble Metals Forum, Siegen.

Kolb, M. 1978. Physical and electrochemical properties of metal monolayers on metallic substrates. In Advances in Electrochemistry and Electrochemical Engineering; Gerischer, H., Tobias, C.W., Eds.; John Wiley & Sons: New York, Vol. 11: 125-271.

Kolesova, G.M., Zakharova, I.A., Raykhman, L.M. and Moshkovski, Y.S. 1979. Effect of Palladium compounds on mitrochondrial enzymatic systems. *Voprosy Meditsinskoi Khimii*, 25(5): 537-540.

Kominkova, M., Heger, Z., Zitka, O., Kynicky, J., Pohanka, M., Beklova, M., Adam, V. and Kizek, R. 2014. Flow Injection Analysis with Electrochemical Detection for Rapid Identification of Platinum-Based Cytostatics and Platinum Chlorides in Water. *International Journal of Environmental Research and Public Health*, 11: 1715-1724

Krachler, M., Alimonti, A., Petrucci, F., Irgolic, K.J., Forastiere, F. and Caroli, S.1998. Analytical problems in the determination of platinum group metals in urine by quadrupole and magnetic-sector field inductively coupled plasma-mass spectrometry. *Analytica Chimica Acta*, 363: 1-10.

Krastev, I., Valkova, T. and Zielonka, A. 2004. Structure and Properties of Electrodeposited Silver-Bismuth Alloys. *Journal of Applied Electrochemistry*, 34: 79-85.

Krolicka, A. and Bobrowski, A. 2004. Bismuth film electrode for adsorptive stripping voltammetry - electrochemical and microscopic study. *Electrochemistry Communications*, 6(2): 99-104.

Kshirsagar, P., Sangaru, S.S., Malvindi, M.A., Martiradonna, L., Cingolani, R. and Pompa P.P. 2011. Synthesis of highly stable silver nanoparticles by photoreduction and their size fractionation by phase transfer method. *Colloids Surfaces A: Physicochemical Engineering Aspects*, 392: 264-270.

Kubrakova, I.V., Kudinova, T.F., Kuzmin, N.M., Kovalev, I.A., Tsysin, G.I. and Zolotov, Y.A. 1996. Determination of low levels of platinum group metals – New solutions. *Analytica Chimica Acta*, 334: 167-175.

Lanigan, R.S. and Yamarik, T.A. 2002. "Final report on the safety assessment of EDTA, calcium disodium EDTA, diammonium EDTA, dipotassium EDTA, disodium EDTA, TEA-EDTA, tetrasodium EDTA, tripotassium EDTA, trisodium EDTA, HEDTA, and trisodium HEDTA". *International Journal of Toxicology*, 21(2): 95-142.

Lashka, D., Striebel, T., Daub J, Nachtwey M. 1996. Platin im Regenflußeiner Straße'. *Umweltwissenschaften Schadstoff-Forschung*, 8: 124-129.

Laviron, E. 1979. General expression of the linear potential sweep voltammogram in the case of diffusion less electrochemical systems. *Journal of Electroanalytical Chemistry and Interfacial Chemistry*, 100: 263-270.

Lee, G., Kim, C., Lee, M. and Rhee, C. 2010. A Study on Optimization of Nano-sized Bismuth Binding Technology Using a Nafion Solution. *Journal of the Korean Physical Society*, 57(6): 1667-1671.

Lee, M.L., Tolg, G., Beinrohr, E. and Tschopel, P. 1993. Preconcentration of palladium, platinum and rhodium by online sorbent extraction for graphite-furnace atomic-absorption spectrometry and inductively coupled plasma atomic emission-spectrometry. *Analytica Chimica Acta*, 272: 193-203.

Lesniewska, B.A., Messerschmidt, J., Jakubowski, N. and Hulanicki, A. 2004. Bioaccumulation of platinum group elements and characterization of their species in Lolium multiflorumby size-exclusion chromatography coupled with ICP-MS. *Science of the Total Environment*, 322: 95-108.

Li, L., Xu, Z., Wu, J. and Tian, G. 2010. Bioaccumulation of heavy metals in the earthworm Eisenia fetida in relation to bioavailable metal concentrations in pig manure. *Bioresource Technology*, 101: 3430-3436.

Li, M., Shang, Y., Gao, Y., Wang, G. and Fang, B. 2005. Preparation of novel mercury-doped silver nanoparticles film glassy carbon electrode and its application for electrochemical biosensor. *Analytical Biochemistry*, 341: 52-57.

Li, Y., Liu, X., Zeng, X., Liu, Y., Liu, X., Wei, W. and Luo, S. 2009. Simultaneous determination of ultra-trace lead and cadmium at a hydroxyapatite-modified carbon ionic liquid electrode by square-wave stripping voltammetry. *Sensors and Actuators B*, 139: 604-610.

Liang, H., Li, Z., Wang, W., Wu, Y. and Xu, H. 2009. Highly Surface-roughened ''Flower-like'' Silver Nanoparticles for Extremely Sensitive Substrates of Surface-enhanced Raman Scattering. *Advance Materials*, 21: 1-5.

Liu, Q.T., Diamond, M.E., Gingrich, S.E., Ondov, J.M., Maciejczyk, P. and Gary, A.S. 2003. Accumulation of metals, trace elements and semi volatile organic compounds on exterior windows surfaces in Baltimore. *Environmental Pollution*, 122: 51-61.

Liu, S., Yuan, L., Yue, X., Zheng, Z. and Tang, Z. 2008. Review paper. Recent Advances in Nanosensors for Organophosphate Pesticide Detection. *Advance Powder Technology*, 19: 419-441.

Liu, T.Z., Lin, T.F., Chiu, D.T., Tsai, K.J. and Stern, A. 1997. Palladium exacerbates hydroxyl radical mediated DNA damage. *Free Radical Biology & Medicine*, 23(1): 155-161.

Locatelli, C. 2007. Review: Voltammetric Analysis of Trace Levels of Platinum Group Metals – Principles and Applications. *Electroanalysis*, 19(21): 2167-2175.

Locatelli, C. 2006. Simultaneous square wave stripping voltammetric determination of platinum group metals (PGMs) and lead at trace and ultra trace concentration level, Application to surface water. *Analytica Chimica Acta*, 557: 70-77.

Locatelli, C. 2006. Possible interference in the sequential voltammetric determination at trace and ultratrace concentration level of platinum group metals (PGMs) and lead - Application to environmental matrices. *Electrochimica Acta*, 52: 614-622.

Locatelli, C., Melucci, D. and Torsi, G. 2005. Determination of platinum-group metals and lead in vegetable environmental bio-monitors by voltammetric and spectroscopic techniques: critical comparison. *Analytical Bioananlytical Chemistry*, 382: 1567-1573.

Loebenstein, J.R. 1988. Platinum group metals. *In: Minerals yearbook 1987, Vol. 1, Metals & Minerals*, Washington DC, US Department of the Interior, Bureau of Mines, 689-700.

Long, G.G., Freedman, L.D. and Doak, G.O. 1978. Bismuth and bismuth alloys. In: *Encyclopedia of Chemical Technology*, Wiley, New York, USA, 912-937.

Luo, X., Morrin, A., Killard, A.J. Smyth, M.R. 2006. Review Application of Nanoparticles in Electrochemical Sensors and Biosensors. *Electroanalysis*, 18(4): 319-326.

Lustig, S. Zang, S., Michalke, B., Schramel, P. and Beck, W. 1997. Platinum determination in nutrient plants by inductively coupled plasma mass spectrometry with special respect to the hafnium oxide interference. *Fresenius' Journal Analytical Chemistry*, 357: 1157-1163.

Lyman, C.E., Newbury, D.E., Goldstein, J.I., Williams, D.B., Romig, A.D., Armstrong, J.T., Echlin, P., Fiori, C.E., Joy, D.C., Lifshin, E. and Peters, K. 1990. Scanning Electron Microscopy, X-Ray Microanalysis and Analytical Electron Microscopy: A Laboratory Workbook, Plenum Press. New York, N.Y.

Magdassi, S., Bassa, A., Vinetsky, Y. and Kamyshny, A. 2003. Silver Nanoparticles as Pigments for Water-based Ink-Jet Inks. *Chemistry of Materials*, 15: 2208.

Maiti, J., Pokhrel, B., Boruah, R. and Dolui, S.K. 2009. Polythiophene based fluorescence sensors for acids and metal ions. *Sensors and Actuators B*, 141: 447-451.

Malakhova, N.A., Mysik, A.A., Saraeva, S.Y., Stozhko, N.Y., Uimin, M.A., Ermakov, A.E. and Brainina, K.Z. 2010. A Voltammetric Sensor on the Basis of Bismuth Nanoparticles Prepared by the Method of Gas Condensation. *Journal of Analytical Chemistry*, 65(6): 640-647.

Marcusson, J.A. 1996. Contact allergies to palladium chloride. *Contact Dermatitis*, 34(5): 320-323.

Mason, B. 1966. *Principles of geochemistry*, 3rd edition, New York, Wiley.

Maxwell, T.J. and Smyth, W.F. 1996. A Study of the Stripping Voltammetric Behavior of Selected Metal Chelates and its Application to Automated Analysis of River Waters. *Electroanalysis*, 8: 795-802.

McCreery, R.L. 1991. *Electroanalytical Chemistry*, Vol. 17 (Ed: A. J. Bard), Marcel Dekker, New York.
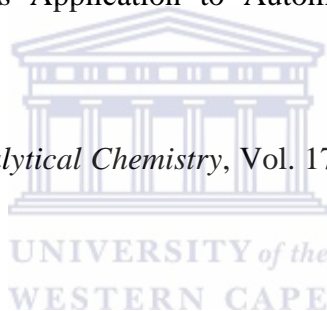
Meguro, K., Nakamura, Y., Hayashi, Y., Torizuka, M. and Esumi K. 1988. The preparation of colloidal precious metal particles using copolymers of vinyl alcohol-*N*-vinylpyrrolidone. *Bulletin of the Chemical Society of Japan*, 61(2): 347-350.

Melucci, D. and Locatelli, C. 2007. Platinum(II), Palladium(II), Rhodium(III) and Lead(II) voltammetric determination in sites differently influenced by vehicle traffic. *Annali di Chimica*, 97: 373-384.

Merget, R. 2000. Occupational platinum salt allergy. Diagnosis, prognosis, prevention and therapy, in: Zereini, F. and Alt, F. (Eds.), Antropogenic Platinum Group Element Emissions and Their Impact on Man and Environment, Springer-Verlag, Berlin, Heidelberg, 257-265, Chapter 5.2.

Merget, R. and Rosner, G. 2001. Evaluation of the health risk of platinum group metals emitted from automotive catalytic converters. *Science of the Total Environment*, 270: 165-173.

Merian, E. 1991. *Metals and their compounds in the environment − occurrence, Analysis and biological relevance*. VCH, Weinheim.

Merian, E., Anke, M., Ihnat, M. and Stoeppler, M. 2004. *Elements and Their Compounds in the Environment.* Wiley-VCH, Weinheim. Eds.

Methews, D.R., Brown, E., Watson, A., Holman, R.R., Steemson, J., Hughs, S. and Scott, D. 1987. Pen-sized digital 30-second blood glucose meter. *Lancet*, 1: 778-779.

Mikkelsen, O. and Schrøder, K.H. 2002. Voltammetry using a dental amalgam electrode for heavy metal monitoring of wines and spirits. *Analytica Chimica Acta*, 458: 249-256.

Mikkelsen, O. and Schroder, K. 2000. Dental amalgam in voltammetry some preliminary results. *Analytical Lettters*, 33: 3253-3269.

Mikkelsen, O., Schroder, K.H. and Aarhaug, T.A. 2001. Dental amalgam, an alternative electrode material for voltammetric analyses of pollutants. *Collection of Czechoslovak. Chemical Communications*, 66(3): 465-472.

Miva, T., Nishimura, Y. and Mizuike, A. 1982. Anodic stripping voltammetry of lead with microliter volumes of electrolytes and silver-plated glassy carbon electrodes. *Analytica Chimica Acta*, 140: 59-64.

Mojica, E-R.E. and Merca, F.E. 2005. Anodic stripping voltammetric determination of mercury (II) using lectin-modified carbon paste electrode. *Journal of Applied Science*, 5(8): 1461-1465.

Moldovani, M., Palacios, M.A., Gomez, M.M., Morrison, G., Rauch, S., McLeod, C., Ma, R., Caroli, S., Alimenti, A., Petrucci, F., Bocca, B., Schramel, P., Zischka, M., Pettersson, C., Wass, U., Luna, M., Saenz, J.C. and Santamaria, J. 2002. Environmental risk of particulate and soluble platinum group elements released from gasoline and diesel engine catalytic converters. *The Science of the Total Environment*, 296: 199-208.

Moldovani, M., Rauch, S., Gomez, M.M., Palacios, M.A. and Morrison, G. 2001. Bioaccumulation of palladium, platinum and rhodium from urban particulates and sediments by the freshwater isopod Asellus Aquaticus. *Water Research*, 35(17): 4175-4183.

Moore, B.A., Duncan, J.R. and Burgess, J.E. 2008. Fungal bioaccumulation of copper, nickel, gold and platinum. *Minerals Engineering*, 21: 55-60.

Morera, M.T., Echeverria, J.C., Mazkiaran, C. and Garrido, J.J. 2001. Isotherms and sequential extraction procedures for evaluating sorption and distribution of heavy metals in soils. *Environmental Pollution*, 113: 135-144.

Morfobos, M., Economou, A. and Voulgaropoulos, A. 2004. Simultaneous determination of nickel(II) and cobalt(II) by square wave adsorptive stripping voltammetry on a rotating-disc bismuth-film electrode. *Ananlytica Chimica Acta*, 519: 57-64.

Mukai, H., Ambe, Y. and Morita, M. 1990. Flow injection inductively coupled plasma mass spectrometry for the determination of platinum in airborne particulate matter. *Journal of Analytical & Atomic Spectrometry*, 5: 75-80.

Nagashima, N., Matsuoka, S. and Miyahara, K. 1996. Nanoscopic hardness measurement by atomic force microscope. *JSME International Journal, Series A: Mechanics and Material Engineering*, 39(3): 456-462.

Naldrett, A.J. 2010. Secular Variation of Magmatic Sulfide Deposits and Their Source Magmas. *Economic Geology*, 105: 669-688.

Navratil1, T. and Barek, J. 2009. Analytical Applications of Composite Solid Electrodes. *Critical Reviews in Analytical Chemistry*, 39:131-147.

Navrátil, T., Kopanica, M. and Krista, J. 2003. Anodic stripping voltammetry for arsenic determination of composite gold electrode. *Chemia Analityczna−Warsaw*, 48: 265-272.

Navratil, T. and Kopanica, M. 2002. Analytical application of silver composite electrode. *Critical Reviews in Analytical Chemistry*, 32: 153-166.

Navratil, T. and Kopanica, M. 2002. Lead determination on silver composite electrodes using the effect of underpotential deposition. *Chemicke Listy*, 96: 111-116.

Navratil, T., Šebková, S. and Kopanica, M. 2004. Voltammetry of lead cations on a new type of silver composite electrode in the presence of other cations. *Analytical and Bioanalytical Chemistry*, 379: 294-301.

Nersisyan, H.H., Lee, J.H., Son, H.T., Won, C.W., and Maeng, D.Y. 2003. A New and Effective Chemical Reduction Method for Preparation of Nanosized Silver Powder and Colloid Dispersion. *Materials Research Bulletin*, 38: 949-956.

Nie, S. and Emory, S.R. 1997. ''Probing Single Molecules and Single Nanoparticles by Surface-enhanced Raman Scattering''. *Science*, 275: 1102.

Noel, M. and Vasu K.I. 1990. Cyclic voltammetry and the frontiers of electrochemistry. Aspects Publications, London.

Noroozifar, M., Khorasani-Motlagh, M. and Taheri, A. 2011. Determination of cyanide in wastewaters using modified glassy carbon electrode with immobilized silver hexacyanoferrate nanoparticles on multiwall carbon nanotube. *Journal of Hazardous Material*, 185: 255-261.

Novotńy, L. and Yosypchuk, B. 2000. Solid silver amalgam electrodes. *Chemicke Listy*, 94, 1118-1120.

Ntsendwana, B., Mamba, B.B., Sampath, S. and Arotiba, O.A. 2012. Electrochemical Detection of Bisphenol A Using Graphene-Modified Glassy Carbon Electrode. *International Journal of Electrochemical Science*, 7: 3501-3512.

Oldham, K.B. and Myland, J.C. 1994. Fundamentals of electrochemical science. Academic Press, London.

Oliveira, M., Ugarte, D., Zanchet, D. and Zarbin, A. 2005. Influence of synthetic parameters on the size, structure, and stability of dodecanethiol-stabilized silver nanoparticles. *Journal of Colloid and Interface Science*, 292: 429-435.

Ordeig, O., Banks, C.E., Del Campo, F.J., Munoz, F.X. and Compton, R.G. 2006, Electroanalysis of Bromate, Iodate and Chlorate at Tungsten Oxide Modified Platinum Microelectrode Arrays. *Electroanalysis*, 18(17): 1672-1680.

Oymak, T. 2003. M.S. Thesis. Erciyes University, Kayseri, Turkey.

PACEPAC. Production and Certification of a Certified reference material (Road dust) for Platinum, Palladium used in Automotive Catalytic Converters 1998. SMT4-CT98-2225.

Palacios, M.A., Gomez, M., Moldovan, M. and Gomez, B. 2000. Assessment of environmental contamination risk by Pt, Rh and Pd from automobile catalyst. *Microchemical Journal*, 67:105-113.

Penn, S.G., He, L. and Natan, M.J. 2003. Nanoparticles for bioanalysis. *Current Opinion in Chemical Biology*, 7(5): 609-615.

Piech, R., Bas, B. and Władysław Kubiak, W. 2008. The cyclic renewable mercury film silver based electrode for determination of molybdenum (VI) traces using adsorptive stripping voltammetry. *Talanta*, 76: 295-300.

Pillai, C.K. et al, 1977. Interaction of palladium with DNA. *Biochimica et Biophysica Acta*, 474(1): 11-16.

Polaro-Sensors. 1997. Prague: Offer of accessories to the PC-controlled Eco-Tribo Polarograph, Prague.
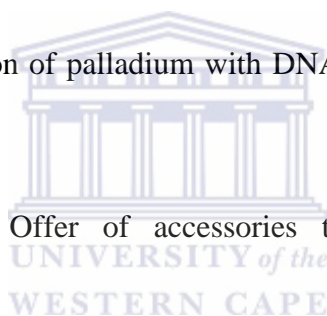
Postek, M.T., Howard, K.S., Johnson, A.H. and McMichael, K.L. 1980. Scanning Electron Microscopy: A Student's Handbook, Ladd Research Ind., Inc. Williston, VT.

Pradhan, N., Pal, A. and Pal, T. 2002. Silver Nanoparticle Catalyzed Reduction of Aromatic Nitro Compounds. *Colloids and Surfaces A: Physicochemical and Engineering Aspects*, 196(2): 247-257.

Prakash, S., Chakrabarty, T., Singh, A.K. and Shahi, V.K. 2012. Silver nanoparticles built-in chitosan modified glassy carbon electrode for anodic stripping analysis of As(III) and its removal from water. *Electrochimica Acta*, 72: 157-164.

Přibil, R., Dolezal, J. and Simon, V. 1953. *Chemické Listy*, 47: 88.

Pyrzyńska, K. 2000. Monitoring of platinum in the environment. *Journal of Environmental Monitoring*, (6)2: 99N-103N.

Qu, B. 1996. Recent developments in the determination of precious metals. A review. *Analyst*, 121: 139-161.

Ragoisha, G.A. and Bondarenko, A.S. 2003. Potentiodynamic electrochemical impedance spectroscopy for solid state chemistry. *Solid State Phenom*, 90-91: 103-108.

Raman, B., Meier, D.C., Evju, J.K. and Semancik, S. 2009. Designing and optimizing microsensor arrays for recognizing chemical hazards in complex environments. *Sensors and Actuators B*, 137: 617-629.

Ramírez, S.A. and Gordillo, G.J. 2009. Adsorption and reduction of palladium-dimethylglyoxime complex. *Journal of Electroanalytical Chemistry*, 629: 147-151.

Ramírez, S.A., Gordillo, G.J. and Posadas, D. 1996. The adsorption of nickel dimethylglyoxime complex on mercury. *Journal of Electroanalytical Chemistry*, 407: 219-225.

Rao, C.R.M. and Reddi, G.S. 2000. Platinum group metals (PGM); occurrence, use and recent trends in their determination. *Trends in Analytical Chemistry*, 19(9): 565-586.

Raoof, J-B., Ojani, R. and Beitollahi, H. 2007. Electrocatalytic determination of ascorbic acid at chemically modified carbon paste electrode with 2, 7-bis (Ferrocenyl ethynyl) fluoren-9-one. *International Journal of Electrochemical Science*, 2: 534-548.

Raub, C.J. 1994. ASM Metals Handbook: Surface Engineering, vol. 5. ASM International. 563-565.

Rauch, S. and Morrison, G.M. 2008. Environmental relevance of the platinum-group elements. *Elements*, 4(4): 259-263.

Rauch, S. and Morrison, G.M. 1999. Platinum uptake by the freshwater isopod *Asellus Aquaticus* in urban rivers. *The Science of the Total Environment*, 235: 261-268.

Ravindra, K., Bencs, L. and Van Grieken, R.N. 2004. Platinum group elements in the environment and their health risk. *Science of the Total Environment*, 318: 1-43.

Rena, X.L. Menga, X.W., Chena, D., Tanga, F. and Jiao, J. 2005. Using silver nanoparticles to enhance current response of biosensor. *Biosensors and Bioelectronics*, 21: 433.

Renner, H. and Schmuckler, G. 1991. Platinum-group metals. In: Merian E. (Ed.), Metals and Their Compounds in the Environment. VCH Verlagsgesellschaft, Weinheim: 1136-115.

Rico, M.G., Olivares-Marínb, M. and Gil, E.P. 2009. Modification of carbon screen-printed electrodes by adsorption of chemically synthesized Bi nanoparticles for the voltammetric stripping detection of Zn(II), Cd(II) and Pb(II). *Talanta*, 80: 631-635.

Rodilla, V., Miles, A.T., Jenner, W. and Hawksworth, G.M. 1998. Exposure of cultured human proximal tubular cells to cadmium, mercury, zinc and bismuth: toxicity and metallothionein induction. *Chemico-Biological Interactions*, 14: 71-83.

Ruska, E. and Knoll, M. 1931. Die magnetische Sammelspule für schnelle Elektronenstrahlen. *Zeitschrift fur Technische Physik*, 12: 389-400.

Safavi, A., Maleki, N. and Farjami, E. 2009. Electrodeposited Silver Nanoparticles on Carbon Ionic Liquid Electrode for Electrocatalytic Sensing of Hydrogen Peroxide. *Electroanalysis*, 21(13): 1533-1538.

Salazar-Pérez, A.J., Camacho-López, M.A., Morales-Luckie, R.A. and Sánchez-Mendieta, V. 2005. Structural evolution of Bi_2O_3 prepared by thermal oxidation of bismuth nano-particles. *Superficies y Vacío*, 18(3): 4-8.

Santosa, N.C., Castanhob, M.A.R.B. 2004. An overview of the biophysical applications of atomic force microscopy. *Biophysical Chemistry*, 107: 133-149.

Schafer, J. and Pulchet, H. 1998. Platinum group metals (PGMs) emitted from automobile catalytic converters and their distribution in roadside soil. *Journal of Geochemical Exploration*, 64: 307-314.

Schedle, A., Samorapoompichit, P., Rausch-Fan, X.H., Franz, A., Füreder, W., Sperr, W.R., Sperr, W., Ellinger, A., Slavicek, R., Boltz-Nitulescu, G. and Valent, P. 1995. Response of L-

929 fibroblasts, human gingival fibroblasts, and human tissue mast cells to variousmetal cations. *Journal of Dental Research*, 74(8): 1513-1520.

Schutyser, P., Govaerts, A., Dams, R. and Hoste, J. 1977. Neutron activation analysis of platinum metals in airborne particulate matter. *Journal of Radioanalytical Chemistry*, 37: 651-660.

Scribner, L.L. and Taylor, S.R. 1990. The measurement and corrections of electrolyte resistance in electrochemical test. ASTM Pub, STP1056, Philadelphia.

Šebková, S., Navrátil, T. and Kopanica, M. 2005. Graphite composite electrode voltammetry. *Analytical Letters*, 38(11): 1747-1758.

Šebková, S., Navrátil, T. and Kopanica, M. 2003. Comparison of Different Types of Silver Composite Electrodes to Varied Amount of Silver on Example of Determination of 2-Nitronaphtalene. *Analytical Letters*, 36(13): 2767-2782.

Selesovska-Fadrna, R., Fojta, M., Navratil, T. and Chylkova, J. 2007. Brdicka-type processes of cysteine and cysteine-containing peptides on silver amalgam electrodes. *Analytica Chimica Acta*, 582: 344-352.

Semon, W.L. and Damerell, V.R. 1943. Dimethylglyoxime, Organic Synthesis, Collective 2: 204.

Senthilkumar, S. and Saraswathi, R. 2009. Electrochemical sensing of cadmium and lead ions at zeolite-modified electrodes: Optimization and field measurements. *Sensors and Actuators B*, 141: 65-75.

Shain, I. and Perone, S.P. 1961. Application of stripping analysis to the determination of iodide with silver microelectrodes. *Analytical Chemistry*, 33: 325-329.

Shipway, A.N., Katz, E. and Willner, I. 2000. Nanoparticle Arrays on Surfaces for Electronic, Optical, and Sensor Applications. *Chemical Physics and Physical Chemistry*, 1: 18-52.

Shiraishi, Y. and Toshima, N. 1999. Colloidal silver catalysts for oxidation of ethylene. *Journal of Molecular Catalysis A: Chemical*, 141: 187-192.

Shukla, V.K., Yadava, R.S., Yadavc, P. and Pandeya, A.C. 2012. Green synthesis of nanosilver as a sensor for detection of hydrogen peroxide in Water. *Journal of Hazardous Materials*, 213-214: 161-166.

Shultz, M.D. et al, 1995. Palladium - a new inhibitor of cellulase enzyme activity. *Biochemical Biophysical Research Communications*, 209(3): 1046-1052.

Silwana, B., Van der Horst, C., Iwuoha, E., and Somerset, V. 2014a. Screen-printed electrodes modified with a bismuth film for stripping voltammetric analysis of platinum group metals in environmental samples. *Electrochimica Acta*, 128: 119-127.

Silwana, B., Van der Horst, C., Iwuoha, E., and Somerset, V. 2014b. Amperometric determination of cadmium, lead, and mercury metal ions using a novel polymer immobilised horseradish peroxidase biosensor system. *Journal of Environmental Science and Health*, *Part A*: *Toxic/Hazardous Substances and Environmental Engineering*, 49(13), 1501-1511.

Silwana, B., Van der Horst, C., Iwuoha, E. and Somerset, V. 2013. Inhibitive Determination of Metal Ions Using a Horseradish Peroxidase Amperometric Biosensor. *State of the Art in Biosensors - Environmental and Medical Application*: 105-119.

Simões, A.Z., Stojanovic, B.D., Ramirez, M.A., Cavalheiro, A.A., Longo, E. and Varela, J.A. 2008. Lanthanum-doped $Bi_4Ti_3O_{12}$ prepared by the soft chemical method: Rietveld analysis and piezoelectric properties. *Ceramic International*, 34: 257-261.

Skoog, D.A. 2007. *Principles of Instrumental Analysis*, 6th edition, Thomson Brooks/Cole, USA.

Sluyters-Rehbach, M. and Sluyters, J.H. 1986. in: Bamford, C.H., Compton, R.G. (Ed.). Comprehensive chemical kinetics. Vol. 26, *Elsevier*, Amsterdam, pp 203-345.

Sluyters-Rehbach, M. and Sluyters, J.H. 1984. in: Brockris, J.O.M. (Ed.). Comprehensive treatise of electrochemistry. Vol. 9, Plenum Press, New York, pp 174-292.

Smith, D.E. 1966. In: Bard, A.J. (Ed.). Electroanalytical Chemistry, vol. 1, Marcel Dekker, New York, 1-148.

Solomon, S.D., Bahadory, M., Jeyarajasingam, A.V., Rutkowsky, S.A., Boritz, C. and Mulfinger, L. 2007. Synthesis and Study of Silver Nanoparticles. *Journal of Chemical Education*, 84: 322-325.

Somerset, V.S., Hernandez, L.H. and Iwuoha, E.I. 2011. Stripping voltammetric measurement of trace metal ions using screen-printed carbon and modified carbon paste electrodes on river water from the Eerste-Kuils River System. *Journal of Environmental Science and Health*, *Part A*: *Toxic/Hazardous Substances and Environmental Engineering*, 46, 17-32.

Somerset, V., Leaner, J., Mason, R., Iwuoha, E. and Morrin, A. 2010. Development and application of a poly(2,2′-dithiodianiline) (PDTDA)-coated screen-printed carbon electrode in inorganic mercury determination. *Electrochimica Acta*, 55: 4240-4246.

Somerset, V., Van der Horst, C., Silwana, B., Walters, C. and Iwuoha, E. 2015. Biomonitoring and evaluation of metal concentrations in sediment and crab samples from the North-West Province of South Africa. *Water, Air, & Soil Pollution*. (Accepted).

Somerset, V., Van der Horst, C., Silwana, B., Walters, C., Iwuoha, E. and Le Roux, S. 2012. Development of Analytical Sensors for the Identification and Quantification of Metals in Environmental Samples. Water Research Commission (WRC). *Report Number: 2013/1/12.*

Sonthalia, P., McGaw, E., Show, Y. and Swain, G.M. 2004. Metal ion analysis in contaminated water samples using anodic stripping voltammetry and a nanocrystalline diamond thin-film electrode. *Analytica Chimica Acta*, 522(1): 35-44.

Sonune, A. and Ghate, R. 2004. Developments in wastewater treatment methods. *Desalination*, 167: 55-63.

Spikes, J.D. and Hodgson, C. 1969. Enzyme inhibition by palladium. *Biochemical Biophysical Research Communications*, 35(3): 420-422.

Staray, V. and Kopanica, M. 1984. Adsorptive stripping voltammetric determination of thiourea and thiourea derivatives. *Analytica Chimica Acta*, 159: 105-110.

Stefánsson, A., Gunnarsson, I. and Giroud, N. 2007. New methods for the direct determination of dissolved inorganic, organic and total carbon in natural waters by Reagent-Free Ion Chromatography and inductively coupled plasma atomic emission spectrometry. *Analitica Chimica Acta*, 582: 69-74.

Sternbeck, J., Sjodin, A. and Andreasson, K. 2002. Metal emissions from road traffic and the influence of resuspension − results from two tunnel studies. *Atmospheric Environment*, 36: 4735-4744.

Stetter, J.R., Penrose, W.R., Yao, S. 2003. Sensor, Chemical sensors, Electrochemical sensors, and ECS. *Journal of the Electrochemical Society*, 150(2): 11-16.

Stwertka, A. 2002. A guide to the Elements, 2nd edition, Oxford University Press, New York, p. 125.

Suhonen, R. and Kanerva, L. 2001. Allergic contact dermatitis caused by palladium on titanium spectacle frames. *Contact Dermatitis*, 44(4): 257-258.

Sujaritvanichpong, S., Aoki, K., Tokuda, K. and Matsuda, H. 1986. Voltammetry at microcylinder electrodes: Part IV. Normal and differential pulse voltammetry. *Journal of Electroanalytical Chemistry and Interfacial Chemistry*, 199: 271-283.

Sun, H., Li, H., Harvey, I. and Sadler, P.J. 1999. Interactions of bismuth complexes with metallothionein(II). *Journal of Biological Chemis*try, 247: 29094-29101.

Sun, S., Muray, C., Weller, D., Folks, L. and Moser, A. 2000. Monodisperse FePt nanoparticles and ferromagnetic FePt nanocrystal superlattices. *Science*, 287: 1989-1992.

Sun, Y. Xia, Y. 2002. Shape-controlled synthesis of gold and silver nanoparticles. *Science*, 298: 2176-2179.

Sures, B., Zimmermann, S., Messerschmidt, J., Von Bohlen, A., Thielen, F., and Baska, F. 2005. The intestinal parasite Pomphorhynchus laevis as a sensitive accumulation indicator for the platinum group metals Pt, Pd, and Rh. *Environmental Research*, 98: 83-88.

Sures, B., Zimmermann, S.A., Messerschmidt, J. and Von Bohlen, A. 2002. Relevance and analysis of traffic related platinum group metals (Pt, Pd, Rh) in the aquatic biosphere, with emphasis on Palladium. *Ecotoxicology*, 11: 385-392.

Švancara, I., Galík, M. and Vytřas, K. 2007. Stripping voltammetric determination of platinum metals at a carbon paste electrode modified with cationic surfactants. *Talanta*, 72: 512-518.

Švancara, I., Vytras, K., Barek, J., and Zima, J. 2001. Carbon paste electrodes in modern electroanalysis. *Critical Reviews in Analytical Chemistry*, 31: 311-345.

Ulakhowich, N.A., Budnikov, G.K. and Medyantseva, E.P. 1992. Concentration in the voltammetric analysis of platinum materials. *Journal of Analytical Chemistry.* 47(9): 1127-1144.

Usami, S., Fukami, T., Kinoshita, E., Puri, B.K. and Satake, M. 1990. Column chromatographic preconcentration of palladium with dimethyl glyoxime and acenaphthenequinone dioxime on naphthalene. *Analytica Chimica Acta*, 230: 17-22.

U.S. Centers for Disease Control, "Deaths Associated with Hypocalcemia from Chelation Therapy", 2006.
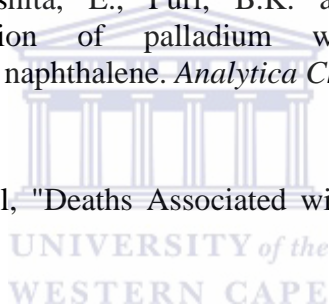
Vamnes, J.S., Lygre, G.B., Gronningsaeter, A.G. and Gjerdet, N.R. 2004. Four years of clinical experience with an adverse reaction unit for dental biomaterials. *Community Dentistry and Oral Epidemiology*, 32(2): 150-157.

Van der Horst, C., Silwana, B., Iwuoha, E. and Somerset, V. 2015. Synthesis and characterisation of bismuth-silver bimetallic nanoparticles for electrochemical sensor applications. *Analytical Letters*, 48(8). (Accepted)

Van der Horst, C., Silwana, B., Iwuoha, E. and Somerset, V. 2012. Stripping voltammetric determination of palladium, platinum and rhodium in South African water resources. *Journal of Environmental Science and Health*, *Part A*: *Toxic/Hazardous Substances and Environmental Engineering*, 47(13): 2084-2093.

Vilaplana, J., Romaguera, C. and Cornellana, F. 1994. Contact dermatitis and advers oral mucous membrane reactions related to the use of dental prostheses. *Contact Dermatitis*, 30: 80-84.

Vilchis-Nestor, A., Sánchez-Mendieta, V., Camacho-López, M., Gómez-Espinosa, R., Camacho-López, M. and Arenas-Alatorre, J. 2008. Solventless synthesis and optical properties of Au and Ag nanoparticles using *Camellia sinensis* extract. *Material Letters*, 62: 3103-3105.

Vlašánková, R., Otruba, V., Bendl, J., Fišera, M. and Kanický, V. 1999. Preconcentration of platinum group metals on modified silicagel and their determination by inductively coupled plasma atomic emission spectrometry and inductively coupled plasma mass spectrometry in airborne particulates. *Talanta*, 48: 839-846.

Voutou, B. and Stefanaki, E-C. 2008. Electron Microscopy: The Basics. Physics of Advanced Materials Winter School, 1-11.

Wang, D., Song, C., Hu, Z. and Zhou, X. 2005. Synthesis of silver nanoparticles with flake-like shapes. *Material Letters*, 59: 1760-1763.

Wang, J. 2006. *Analytical Electrochemistry*. Wiley-VCH, New York.

Wang, J. 2005. Stripping Analysis at Bismuth Electrodes: A Review. *Electroanalysis*, 17(15-16): 1341-1346.

Wang, J. 1994. *Analytical Electrochemistry*, Wiley-VCH, New York.

Wang, J. 1987. In: Bard, A.J. (Ed.), *Electroanalytical Chemistry*, vol. 16, Marcel Dekker, New York, 1-89.

Wang, J. 1985. *Stripping analysis: principles, instrumentation and applications*, VCH Publishers, Deerfield Beach.

Wang, J., Lu, D., Thongngamdee, S., Lin., Y. and Sadik, O.A. 2006. Catalytic Adsorptive Stripping Voltammetric Measurements of Trace Vanadium at Bismuth Film Electrodes. *Talanta*, 69(4): 914-917.

Wang, J., Lu, J.M., Hocevar, S.B., Farias, P.A.M. and Ogorevc, B. 2000. Bismuth-coated carbon electrodes for anodic stripping voltammetry. *Analytical Chemistry*, 72: 3218-3222.

Wang, J., Mahmoud, J. and J. Zadeii, J. 1989. Simultaneous Measurements of Trace Metals by Adsorptive Stripping Voltammetry. *Electroanalysis*, 1(3): 229-234.

Wang, J. and Varughese, K. 1987. Determination of traces of palladium by adsorptive stripping voltammetry of the dimethylglyoxime complex. *Analytica Chimica Acta*, 199: 185-189.

Watt, I.M. 1985. The Principles and Practice of Electron Microscopy. Cambridge University. Press. Cambridge, England.

Wayne, D.M. 1997. Direct Determination of Trace Noble Metals (Palladium, Platinum and Rhodium) in Automobile Catalysts by Glow Discharge Mass Spectrometry. *Journal of Analytical Atomic Spectrometry*, 12: 1195-1202.

Wei, C. and Morrison, G.M. 1994. Platinum in road dusts and urban river sediments. *Science of the Total Environment*, 146/147:169-174.

Welch, C.M., Banks, C.E., Simm, A.O. and Compton, R.G. 2005. Silver nanoparticle assemblies supported on glassy-carbon electrodes for the electro-analytical detection of hydrogen peroxide. *Analytical Bioanalytical Chemistry*, 382: 12-21.

Westra, K.L. and Thomson, D.J. 1995. Microstructure of thin films observed using atomic force microscopy. *Thin Solid Films*, 257(1): 15-21.

Whiteley, F. and Murray, 2003. Anthropogenic platinum group element (Pt, Pd and Rh) concentrations in road dusts and roadside soils from Perth, Western Australia. *Science of the Total Environment*, 17: 121-135.

WHO. 2002. Environmental Health Criteria 226-Palladium. International Programme on Chemical Safety. Geneva: World Health Organization.

Wichmann, H., Anquandah, G.A.K., Schmidt, C., Zachmann, D. and Muefit Bahadir, A. 2007. Increase of platinum group element concentrations in soils and airborne dust in an urban area in Germany. *Science of the Total Environment*, 388: 121-127.

Willemse, C. 2009. Determination of selected metals using electrochemical stripping analysis at thin metal films. BSc Honours Thesis, University of the Western Cape, Cape Town, South Africa.

www4.nau.edu.

Yamamoto, A., Watanabe, A., Tsubakino, H. and Fukumoto, S. 2000. AFM observations of microstructures of deposited magnesium on magnesium alloys. *Material Science Forum*, 350: 241-246.

Yantasee, W., Deibler, L.A., Fryxell, G.E., Timchalk, C. and Lin, Y.H. 2005. Screen-printed electrodes modified with functionalized mesoporous silica for voltammetric analysis of toxic metal ions. *Electrochemistry Communications*, 7(11): 1170-1176.

Ye, L., Lai, Z., Liu, J. and Tholen, A. 1999. ''Effect of Ag Particle Size on Electrical Conductivity of Isotropically Conductive Adhesives''. IEEE *Transaction on Electronics Packaging Manufacturing*, 22(4): 299-302.

Yeo, S., Lee, H. and Jeong, S. 2003. Preparation of nanocomposite fibers for permanent antibacterial effect. *Journal of Material Science*, 38: 2143-2147.

Yongming, H., Peixuan, D., Junji, C. and Posmentier, E. 2006. Multivariate analysis of heavy metal contamination in urban dust of Xi'an, Central China. *Science of the Total Environment*, 3555: 176-186.

Yoosaf, K., Ipe, B., Suresh, C.H. and Thomas, K.G. 2007. *In situ* synthesis of metal nanoparticles and selective naked-eye detection of lead ions from aqueous media. *The Journal of Physical Chemistry* C, 111(34): 12839-12847.

Yosypchuk, B. and Novotný, L. 2002. Nontoxic Electrodes of Solid Amalgams. *Critical Reviews in Analytical Chemistry*, 32(2):141-151.

Yosypchuk, B. and Novotný, L. 2001. *Proc. of the US-CZ Workshop on Electrochemical Sensors;* Prague, p. 26.

Zereini, F. 1997. Zur Analytik der Platingruppenelement (PGE) und ihren geochemischen Verteilungsprozessen in ausgewählten Sedimentsteinen und anthropogen beeinflussten Umweltkompartimenten Westdeutschlands; Shaker Verlag: Aachen, 175.

Zereini, F. Alt, F. (Eds.), 2000. Anthropogenic Platinum-Group Element Emissions. Their Impact on Man and Environment, Springer-Verlag, Berlin, Heidelberg, Germany.

Zimmermann, S., Baumann, U., Taraschewski, H. and Sures, B. 2004. Accumulation and distribution of platinum and rhodium in the European eel Anguilla Anguilla following aqueous exposure to metal salts. *Environmental Pollution*, 127: 195-202.

Zimmermann, S. and Sures, B. 2004. Significance of platinum group metals emitted from automobile exhaust gas converters for the biosphere. *Environmental Science and Pollution Research*, 11: 194-199.

Zhang, J., Chen, P., Sun, C. and Hu, X. 2004. Sonochemical synthesis of colloidal silver catalysts for reduction of complexing silver in DTR system. *Applied Catalysis A*, 266: 49-54.

Zhang, J., Song, S., Zhang, L., Wang, L., Wu, H., Pan, D. and Fan, C. 2006. Sequence−Specific Detection of Femtomolar DNA via a Chronocoulometric DNA Sensor (CDS): Effects of Nanoparticle−Mediated Amplification and Nanoscale Control of DNA Assembly at Electrodes. *Journal of the American Chemical Society*, 128: 8575-8580.

Zhang, W., Qiao, X., Chen, J. and Wang, H. 2006. Preparation of silver nanoparticles water-in-oil AOT reverse micelles. *Journal of Colloidal and Interface Science*, 302: 370-373.

Zhang, Z., Liu, H., Zhang, H. and Li, Y. 1996. Simultaneous cathodic stripping voltammetric determination of mercury, cobalt, nickel and palladium by mixed binder carbon paste electrode containing dimethylglyoxime. *Analytica Chimica Acta*, 333: 119-124.

Zhang, Z., Yu, K., Bai, D and Zhu, Z. 2010. Synthesis and Electrochemical Sensing toward Heavy Metals of Bunch−like Bismuth Nanostructures. *Nanoscale Research Letters*, 5: 398-402.

Zhao, Y., Zhang, Z. and Dang, H. 2004. A simple way to prepare bismuth nanoparticles. *Materials Letters*, 58: 790-793.